



**Effects of the Ruthenium(II) Arene Complexes with 1,3,5 -Triaza -7-  
Phosphaadamantane Ligand (RAPTA) on the Human Breast Cancer  
Suppressor Gene *BRCA1* and Its Encoded Protein**

**Pornvichai Temboot**

**A Thesis Submitted in Fulfillment of the Requirements for the  
Degree of Doctor of Philosophy in Pharmaceutical Sciences**

**Prince of Songkla University**

**2017**

**Copyright of Prince of Songkla University**

**Thesis Title** Effects of the Ruthenium(II) Arene Complexes with 1,3,5-Triaza-7-Phosphaadamantane Ligand (RAPTA) on the Human Breast Cancer Suppressor Gene *BRCA1* and Its Encoded Protein

**Author** Mr. Pornvichai Temboot

**Major Program** Pharmaceutical Sciences

---

**Major Advisor**

.....  
 (Assoc. Prof. Dr. Adisorn Ratanaphan)

**Examining Committee:**

.....Chairperson  
 (Assoc. Prof. Dr. Nongporn Towatana)

**Co-advisor**

.....  
 (Prof. Dr. Paul Joseph Dyson)

.....  
 (Assoc. Prof. Dr. Adisorn Ratanaphan)

.....  
 (Prof. Dr. Paul Joseph Dyson)

.....  
 (Asst. Prof. Dr. Bhutorn Canaryuk)

.....  
 (Asst. Prof. Dr. Apichart Atipairin)

The Graduate School, Prince of Songkla University, has approved this thesis as fulfillment of the requirements for the Doctor of Philosophy Degree in Pharmaceutical Sciences

.....  
 (Assoc. Prof. Dr. Teerapol Srichana)

Dean of Graduate School

This is to certify that the work here submitted is the result of the candidate's own investigations. Due acknowledgement has been made of any assistance received.

.....Signature  
(Assoc. Prof. Dr. Adisorn Ratanaphan)  
Major Advisor

.....Signature  
(Mr. Pornvichai Temboot)  
Candidate

I hereby certify that this work has not been accepted in substance for any degree, and is not being currently submitted in candidature for any degree.

.....Signature  
(Mr. Pornvichai Temboot)  
Candidate

<b>Thesis Title</b>	Effects of the Ruthenium(II) Arene Complexes with 1,3,5-Triaza-7-Phosphaadamantane Ligand (RAPTA) on the Human Breast Cancer Suppressor Gene <i>BRCA1</i> and Its Encoded Protein
<b>Author</b>	Mr. Pornvichai Temboot
<b>Major Program</b>	Pharmaceutical Sciences
<b>Academic Year</b>	2016

### ABSTRACT

The ruthenium(II) arene complexes with 1,3,5-triaza-7-phosphaadamantane ligand, namely RAPTA complexes (RAPTAs), have been reported to overcome drug resistance in cisplatin-resistant cancer cells. However, the exact mechanism of these complexes remains largely unknown. Here, we presented the effects of the RAPTAs on the human breast cancer suppressor gene *BRCA1* and its encoded protein. The RAPTAs induced the conformational change of the plasmid DNA in similar pattern. RAPTA-C formed *in vitro* interstrand Ru-*BRCA1* adducts more rapidly than carboRAPTA-C, preferentially attacked the base of A, C, and G (not T) in the order and consequently inhibited *BRCA1* amplification. The *in vitro* interactions of the RAPTAs with the *N*-terminal region of the BRCA1 RING domain proteins have been performed. The binding of the ruthenium compounds to the BRCA1 proteins resulted in change in protein conformation, a release of Zn<sup>2+</sup> ions in a dose- and time-dependent manner, as well as thermal alteration of ruthenated BRCA1 proteins, causing the inactivation of the BRCA1-mediated E3 ubiquitin ligase function, which plays an essential role in response to DNA damage repair. The D67Y BRCA1 reduced ubiquitination function and was more susceptible to RAPTAs treatment than the D67E BRCA1. In addition, other metal complexes including ruthenium(II) polypyridyl complexes (Ru-bpy and Ru-phen), and gold(III) complexes (Auphen and Auterpy) were used for comparison on metal-BRCA1 interaction. Surprisingly, Ru-bpy-, Ru-phen-, Auphen-, and Auterpy-treated BRCA1 showed strongly changes in protein conformation, the release of Zn<sup>2+</sup> ions in a dose- and time-dependent manner, resulting in the inactivation of the BRCA1-mediated E3 ubiquitin ligase, equivalent to RAPTA-EA1-treated BRCA1. HCC1937 cells appeared to be more sensitive against the RAPTAs or ruthenium(II) polypyridyl complexes than MCF-7 or MDA-MB-231 cells. The combination treatment of RAPTA-EA1 and olaparib exhibited a synergistic effect and showed a higher ability of inhibiting cell proliferation than RAPTA-EA1 or olaparib alone, with a 5-fold higher ability to inhibit E3 ligase activity than RAPTA-EA1 alone. These findings could provide insights into the underlying molecular mechanism by which the RAPTAs exerted on the *BRCA1* gene and its encoded protein. In addition, this could raise the possibility of utilizing the BRCA1, especially in mutant proteins, as a potentially molecular target for metal-based drugs in breast cancer chemotherapy.

ชื่อวิทยานิพนธ์	ผลของสารประกอบเชิงซ้อนรูเทเนียม(II)-เอรีนที่มี 1,3,5-ไตรเอซา-7-ฟอสฟาเอตาแมนเทนเป็นลิแกนด์ต่อยีนและโปรตีนกดมะเร็งเต้านมปีอาร์ซีเอวันของมนุษย์
ผู้เขียน	นายพรวิชัย เต็มบุตร
สาขาวิชา	เภสัชศาสตร์
ปีการศึกษา	2559

### บทคัดย่อ

มีรายงานว่าสารประกอบเชิงซ้อนรูเทเนียม(II)-เอรีนที่มี 1,3,5-ไตรเอซา-7-ฟอสฟาเอตาแมนเทนเป็นลิแกนด์ (สารประกอบเชิงซ้อน RAPTA, RAPTAs) มีฤทธิ์ต้านมะเร็งที่คือต่อยา cisplatin ได้ อย่างไรก็ตามกลไกการออกฤทธิ์ที่แท้จริงของสารประกอบเชิงซ้อนชนิดนี้ยังไม่ทราบแน่ชัด การศึกษานี้ได้แสดงผลของ RAPTAs ต่อยีนและโปรตีนกดมะเร็งเต้านมปีอาร์ซีเอวันของมนุษย์ พบว่า RAPTAs สามารถเหนี่ยวนำให้เกิดการเปลี่ยนแปลงโครงสร้างของพลาสมิดดีเอ็นเอในลักษณะที่คล้ายคลึงกัน RAPTA-C สามารถเกิดพันธะระหว่างอะตอมของรูเทเนียมกับสายดีเอ็นเอทั้งสองสายของยีนปีอาร์ซีเอวันได้เร็วกว่า carboRAPTA-C โดยที่พันธะดังกล่าวและมักจะเกิดขึ้นที่เบสอะดีนีน ไซโทซีน และกวีนีนตามลำดับ แต่ไม่เกิดกับเบสไทมีน ส่งผลให้ยับยั้งการสังเคราะห์ยีนปีอาร์ซีเอวันในหลอดทดลองได้ การศึกษาการเกิดอันตรกิริยาในหลอดทดลองระหว่าง RAPTAs และโปรตีนปีอาร์ซีเอวันบริเวณด้านปลายอะมิโนทั้งชนิดปกติและชนิดผ่าเหล่า (D67E และ D67Y) พบว่า RAPTAs สามารถจับกับโปรตีนปีอาร์ซีเอวันทำให้เกิดการเปลี่ยนแปลงโครงสร้างของโปรตีน การปลดปล่อยอะตอมของสังกะสีให้หลุดจากโปรตีนทั้งชนิดปกติและชนิดผ่าเหล่าซึ่งขึ้นอยู่กับปริมาณและเวลา ความคงตัวต่อความร้อนของโปรตีน ซึ่งมีผลทำให้ยับยั้งการทำงานของเอนไซม์ E3 ubiquitin ligase ของโปรตีนปีอาร์ซีเอวันซึ่งมีบทบาทสำคัญในการตอบสนองต่อการซ่อมแซมดีเอ็นเอที่เสียหายภายในเซลล์ RAPTAs สามารถยับยั้งการทำงานของเอนไซม์ของโปรตีนปีอาร์ซีเอวันชนิด D67Y ได้ดีกว่า D67E นอกจากนี้ได้ศึกษาเปรียบเทียบการเกิดอันตรกิริยาในหลอดทดลองระหว่างสารประกอบเชิงซ้อนรูเทเนียม(II)โพลีไพริดีล (Ru-bpy และ Ru-phen) และสารประกอบเชิงซ้อนทองคำ(III) (Auphen และ Auterpy) กับโปรตีนปีอาร์ซีเอวันบริเวณด้านปลายอะมิโนทั้งชนิดปกติและผ่าเหล่า พบว่าให้ผลที่สอดคล้องกันกับผลการทดลองระหว่าง RAPTA-EA1 กับโปรตีนปีอาร์ซีเอวัน สารประกอบเชิงซ้อนของโลหะดังกล่าวข้างต้นเป็นพิษต่อเซลล์มะเร็งเต้านมชนิด HCC1937 สูงกว่า MCF-7 และ MDA-MB-231 นอกจากนี้ RAPTA-EA1

จะเสริมฤทธิ์ความเป็นพิษต่อเซลล์มะเร็งเต้านมทั้งสามชนิดกับ olaparib และยังมีฤทธิ์เสริมกันในการยับยั้งการทำหน้าที่เป็นเอนไซม์ E3 ubiquitin ligase ของ โปรตีนปีอาร์ซีเอวันอีกด้วย ข้อมูลที่ได้จากการศึกษาในครั้งนี้จะทำให้เข้าใจถึงกลไกการออกฤทธิ์ของ RAPTAs ในระดับโมเลกุลต่อยีนและโปรตีนปีอาร์ซีเอวัน และความเป็นไปได้ที่โปรตีนปีอาร์ซีเอวัน โดยเฉพาะอย่างยิ่ง โปรตีนปีอาร์ซีเอวันที่ผ่าเหล่าเป็นเป้าหมายระดับโมเลกุลที่จำเพาะสำหรับยาประเภทสารประกอบเชิงซ้อนของโลหะในการรักษามะเร็งเต้านม

## ACKNOWLEDGEMENT

I would like to express my gratitude and sincere appreciation to my thesis advisor, Assoc. Prof. Dr. Adisorn Ratanaphan, for providing an important opportunity of Ph.D. degree study. I wish to thank him for valuable suggestions, comments, support, and constant encouragement throughout this work.

My sincere thanks are expressed to my thesis co-advisor, Prof. Dr. Paul Joseph Dyson, Director of Institut des Sciences et Ingénierie Chimiques, Ecole Polytechnique Fédérale de Lausanne (EPFL), CH-1015 Lausanne, Switzerland, for kindly providing me with the amazing opportunity of research experiences Laboratory of Organometallic and Medicinal Chemistry (LCOM) at EPFL, and kindly assistance during my research stay in Switzerland. I wish to thank him for providing the RAPTA complexes and valuable suggestions.

My sincere thanks are expressed to examining committee, Assoc. Prof. Dr. Nongporn Towatana, Asst. Prof. Dr. Bhutorn Canyuk, Asst. Prof. Dr. Apichart Atipairin for kindness, assistance, and valuable suggestions.

I would like to express my appreciation to the Thailand Research Fund under the Royal Golden Jubilee Ph.D. program (5.G.PS./49/F.2), the National Research Council of Thailand (PHA550011S, PHA560065S, PHA570058S and PHA580500S), Prince of Songkla University (PHA580926S), the Graduate School, Faculty of Pharmaceutical Sciences, Prince of Songkla University and the NCCR Chemical Biology, funded by the Swiss National Science Foundation for financial support.

I would like to thank Assoc. Prof. Dr. Chartchai Krittanai, Institute of Molecular Biosciences, Mahidol University, for kindly support and assistance in circular dichroism study, Asst. Prof. Dr. Supreeya Yuenyongsawad for kindly providing the human adenocarcinoma cell line (MCF-7), Asst. Prof. Dr. Kanidtha Hansongnern, Department of Chemistry, Faculty of Science, Prince of Songkla University and Prof. Dr. Angela Casini, Chair of Medicinal and Bioinorganic, Chemistry School of Chemistry, Cardiff University, Cardiff, Wales, United Kingdom, for kindly providing Ru-bpy and Ru-phen, and Auphen and Auterpy, respectively, and I also would like to extend my sincere thanks to the Pharmaceutical Laboratory Service Center, Faculty of Pharmaceutical Sciences, Prince of Songkla University for research facilities. I would like to thank Prof. Dr. Christian Heinis, Institut des Sciences et Ingénierie Chimiques, Ecole Polytechnique Fédérale de Lausanne (EPFL), CH-1015 Lausanne, Switzerland, for research facilities of protein purification during my research stay in Switzerland.

I would like to thank all my dear friends, the members and staff of BRCA1 Laboratory in PSU and Laboratory of Organometallic and Medicinal Chemistry at EPFL, especially Dr. Ronald F.S. Lee, for their helpful suggestions and friendship over the course of this study.



Finally, I would like to deeply express my sincere gratitude to my parents, especially my father and mother, and relatives for their love, understanding and supporting me through this journey.

*“It is strange that only extraordinary men make the discoveries, which later appear so easy and simple.” - Georg C. Lichtenberg-*

Pornvichai Temboot

## CONTENTS

	<b>Page</b>
CONTENTS	(x)
LIST OF TABLES	(xv)
LIST OF FIGURES	(xvi)
LIST OF ABBREVIATIONS AND SYMBOLS	(xxi)
 CHAPTER	
1. INTRODUCTION	1
1.1 Background and rationale	1
2. LITERATURE REVIEW	4
2.1 Breast cancer	4
2.1.1 Breast cancer incidence and mortality	4
2.1.2 Histopathological subtypes of breast cancer	5
2.1.3 Molecular subtypes of breast cancer	5
2.2 Risk factors for breast cancer	7
2.2.1 Gender	7
2.2.2 Age	8
2.2.3 Hormonal factors	8
2.2.4 Family history	9
2.2.5 Race	10
2.2.6 Lifestyle and environmental factors	10
2.2.7 Genetic risk factors	11
2.3 Breast cancer susceptibility gene 1 ( <i>BRCA1</i> )	11
2.3.1 Mutational spectrum of <i>BRCA1</i>	12
2.4 <i>BRCA1</i> protein	15
2.4.1 <i>BRCA1</i> RING finger domain	17
2.4.2 The large central segment of <i>BRCA1</i>	19
2.4.3 The <i>BRCA1</i> -C terminal domain	20
2.5 Functions of <i>BRCA1</i> protein	21
2.5.1 <i>BRCA1</i> and transcription	21
2.5.2 <i>BRCA1</i> and cell cycle control	23
2.5.3 <i>BRCA1</i> and apoptosis	24

## CONTENTS (Continued)

	<b>Page</b>
2.5.4 BRCA1 and chromatin modification	25
2.5.5 BRCA1 and centrosome dynamics	26
2.5.6 BRCA1 and DNA damage and repair	26
2.5.7 BRCA1 and protein ubiquitination	28
2.6 The ubiquitination systems in cancer therapy	32
2.6.1 Targeting E1 enzyme	32
2.6.2 Targeting E2 enzyme	34
2.6.3 Targeting E3 enzyme	34
2.7 Zinc finger proteins	38
2.7.1 Classification of zinc finger protein	38
2.7.2 Targeting zinc finger protein for therapeutic diseases	39
2.8 Classical anticancer drugs	43
2.8.1 Platinum-based drugs	43
2.9 Non-classical anticancer drugs	45
2.9.1 Ruthenium anticancer-based drug	45
2.9.2 Classification of ruthenium-based drugs	45
2.9.3 RAPTA complexes	47
2.9.3.1 DNA binding properties	47
2.9.3.2 Antitumor properties of RAPTA complexes	48
2.9.3.3 Protein binding properties	48
2.10 Therapeutic strategies for BRCA1-related breast cancer	50
2.10.1 Targeting homologous recombination repair (HR) pathway	50
2.10.2 Poly(ADP-ribose) polymerase inhibitors	51
2.11 Targeting dysfunctional BRCA1 by the metal-based drug for cancer therapy	55
3. MATERIALS AND METHODS	57
Materials	57
Methods	63
3.1 RAPTA complexes	63
3.2 Preparation of plasmid pBIND DNA by alkaline lysis	64
3.3 Amplification of the 3' terminal region of the 696-bp <i>BRCA1</i> gene fragment	65
3.4 <i>In vitro</i> ruthenation of plasmid DNA by RAPTA complexes	67
3.3.1 Conformation of RAPTA-treated plasmid DNA	67

## CONTENTS (Continued)

	<b>Page</b>
3.5 <i>In vitro</i> ruthenation of the <i>BRCA1</i> gene fragment by RAPTA complexes	67
3.5.1 Interstrand cross-linking assay	67
3.5.2 Restriction analysis of RAPTA- <i>BRCA1</i> adducts	67
3.5.3 Sequence preference of RAPTA- <i>BRCA1</i> adducts	68
3.6 <i>In vitro</i> inhibition of <i>BRCA1</i> amplification using a semi-quantitative polymerase chain reaction (QPCR)	69
3.7 Cell viability	69
3.7.1 Cell culture	69
3.7.2 Cell viability by a MTT assay (single complex treatment)	70
3.7.3 Cell viability by a MTT assay (combination treatment)	70
3.7.4 Cell viability by a Real-Time Cellular Analyzer	71
3.8 Plasmid construction and protein purification	72
3.8.1 Expression and purification of the <i>BRCA1</i> RING protein for CD analysis and gel shift assay	72
3.8.2 Expression and purification of the <i>BRCA1</i> RING protein for ICP-MS analysis, zinc ejection assay and <i>in vitro</i> ubiquitination assay	72
3.9 Preparation of metal- <i>BRCA1</i> complexes	74
3.10 Interaction of <i>BRCA1</i> RING protein with RAPTA complexes	74
3.10.1 Gel shift assay	74
3.10.2 ICP-MS analysis	74
3.10.3 Conformational study and thermal stability of the <i>BRCA1</i> RING protein	74
3.10.4 Zinc ejection assay	75
3.11 The effect of the metal complexes on the <i>in vitro</i> <i>BRCA1</i> / <i>BARD1</i> -mediated ubiquitination	76
3.11.1 <i>In vitro</i> ubiquitination assay	76
4. RESULTS	77
4.1 DNA binding study	77
4.1.1 <i>In vitro</i> ruthenation of plasmid DNA by RAPTA complexes	77
4.1.1.1 Conformational studies	77
4.1.2 Interstrand crosslinks assay	78
4.1.3 RAPTA- <i>BRCA1</i> adducts interfere restriction digestion	78
4.1.4 Preferential ruthenation site on the <i>BRCA1</i> gene fragment	79
4.1.5 Damage of <i>BRCA1</i> gene by RAPTA complexes	81

## CONTENTS (Continued)

	<b>Page</b>
4.2 Protein binding and functional consequence of RAPTA-induced wild type BRCA1 RING domain protein	82
4.2.1 Formation of Ru-wild type BRCA1 crosslinking	82
4.2.2 The effect of RAPTA complexes on secondary structure of wild type BRCA1 RING domain protein	84
4.2.3 Thermal stability of the ruthenated wild type BRCA1	88
4.2.4 RAPTAs dismissed the zinc ions from the zinc binding sites of BRCA1 RING domain protein	90
4.2.5 Inactivation of the wild-type BRCA1 E3 ligase activity by RAPTAs	92
4.3 Protein binding study and functional consequence of RAPTA-induced mutant BRCA1 RING domain protein	95
4.3.1 Formation of Ru-mutant BRCA1 crosslinking	95
4.3.2 The effect of RAPTA complexes on secondary structure of mutant BRCA1 proteins	96
4.3.3 Thermal stability of the ruthenated mutant BRCA1 adducts	100
4.3.4 RAPTAs dismissed the zinc ions from the zinc binding sites of mutant BRCA1 RING domain proteins	100
4.3.5 Inactivation of the mutant BRCA1 E3 ligase activity by RAPTAs	102
4.4 Cellular response to RAPTAs in human breast cancer cell lines	105
4.4.1 Antiproliferative effects of RAPTAs	105
4.5 The effect of RAPTA complexes on cells viability and protein function in the relation to the combination treatment with a PARP-1 inhibitors, olaparib	112
4.5.1 Synergistic effects of RAPTA-EA1/olaparib combination in <i>BRCA1</i> -associated breast cancer cell lines	112
4.5.2 Synergistic effects of RAPTA-EA1/olaparib combination on inhibition of BRCA1-mediated E3 ligase activity	114
5. DISCUSSION	116
5.1 DNA binding studies	116
5.1.1 <i>In vitro</i> ruthenation of plasmid DNA by RAPTA complexes	116
5.1.2 <i>In vitro</i> ruthenation of <i>BRCA1</i> gene fragment by RAPTA complexes	116
5.1.3 <i>In vitro</i> inhibition of <i>BRCA1</i> amplification by RAPTA Complexes	117

## CONTENTS (Continued)

	<b>Page</b>
5.2 Protein binding and functional consequence of RAPTA-induced wild type BRCA1 RING domain protein	118
5.2.1 Structural consequence of RAPTA-treated wild type BRCA1 RING domain protein	118
5.2.2 RAPTA complexes dismissed the zinc ions from the zinc binding sites of BRCA1 RING domain protein	120
5.2.3 Inactivation of the wild-type BRCA1 E3 ligase activity by the RAPTAs	120
5.3 Protein binding study and functional consequence of RAPTA-induced mutant BRCA1 RING domain protein	121
5.3.1 The structural consequence of RAPTA-treated mutant BRCA1 RING domain protein	121
5.3.2 RAPTA complexes dismissed the zinc ions from the zinc binding sites of mutant BRCA1 RING domain protein	121
5.3.3 Inactivation of the mutant BRCA1 E3 ligase activity by the RAPTAs	122
5.4 Cellular response to RAPTA complexes in human breast cancer cell lines	122
5.4.1 Antiproliferative effects of RAPTA complexes	122
5.5 Effect of RAPTA complexes on cells viability and protein function	123
5.5.1 The combination treatment of RAPTA-EA1 and olaparib exhibited a synergistic effect on cell growth inhibition in BRCA1-associated breast cancer cell lines	123
5.5.2 The combination treatment of RAPTA-EA1 and olaparib exhibited a synergistic effect on inhibition of BRCA1-mediated E3 ligase activity	124
6. CONCLUSION	125
REFERENCES	128
APPENDIX	166
VITAE	175

## LIST OF TABLES

<b>Table</b>	<b>Page</b>
2.1 Estimated breast cancer incidence and mortality by regions/country in 2012	4
2.2 Molecular subtypes of breast cancer	7
2.3 The clusters of triple-negative breast cancer	7
2.4 The cumulative incidences (standard error) of breast and ovarian cancers by age for <i>BRCA1</i> carries	12
2.5 Total number of mutations, polymorphisms, and variants of <i>BRCA1</i> from the Breast Cancer Information Core Database (BIC, 2017)	13
2.6 Frequent mutations of <i>BRCA1</i> according to the Breast Cancer Information Core Database (BIC, 2017)	14
2.7 Relative frequencies of <i>BRCA1</i> mutations in Thais	14
2.8 The BRCA1 domains and motifs	16
2.9 The mutations in RING domain and secondary structure effect	19
2.10 The list of compounds targeting E1 enzymes	33
2.11 The list of compounds targeting E2 enzymes	34
2.12 The list of compounds targeting E3 ligases	35
2.13 The list of compounds targeting zinc finger proteins	40
2.14 PARP1 inhibitors in clinical investigation	53
3.1 General properties of metal complexes used in this study	63
3.2 PCR reaction components for the amplification of the 3' terminal region of the 696-bp <i>BRCA1</i> gene fragment	66
3.3 Thermal cycle conditions for PCR for the amplification of the 3' terminal region of the 696-bp <i>BRCA1</i> gene fragment	66
3.4 Thermal cycle conditions for DNA sequencing	68

## LIST OF TABLES (Continued)

<b>Table</b>	<b>Page</b>	
3.5	Description and symbols of synergism or antagonism in drug combination studies analyzed with the combination index method	71
3.6	Reaction components for the <i>in vitro</i> E3 ubiquitin ligase	76
4.1	Thermodynamic parameters predicted by the CONTIN program on the binding of metal complexes with apo- or holo-form of BRCA1 RING domain (1-304)	88
4.2	Half inhibition of BRCA1/BARD1 E3 ligase activity was inactivated by metal complexes	94
4.3	Thermodynamic parameters predicted by the CONTIN program on the binding of metal complexes with holo-form of mutant BRCA1 RING domain (1-304)	97
4.4	Half inhibition of BRCA1/BARD1 E3 ligase activity was inactivated by RAPTA complexes	104
4.5	Comparison of 50% inhibition of cancer cell growth by metal complexes using a MTT assay (48 h after treatment) and RTCA system (24 h after treatment)	105
4.6	Comparison of 50 % inhibition of cancer cell growth by metal complexes using a MTT assay (48 h after treatment) and RTCA system (24 h after treatment)	112
4.7	The 50% inhibition of cancer cell growth by RAPTA-EA1, cisplatin, and olaparib on MCF-7, MDA-MB231 and HCC1937 cells after 48 h	113



## LIST OF FIGURES

<b>Figure</b>		<b>Page</b>
1.1	The RAPTA complexes and other metal complexes are used in this study	3
2.1	The histological types of breast cancer	5
2.2	Age-specific female breast cancer incidence and motility rates in US	8
2.3	The BRCA1 functional domain and its partners	17
2.4	Ribbon representation of the BRCA1/BARD1 heterodimer	18
2.5	The structure of the BRCT domain of BRCA1	20
2.6	Schematic of cellular function of BRCA1	21
2.7	BRCA1 transcriptional complexes	22
2.8	An overview of cell cycle regulation mediated by BRCA1 and its associated proteins	24
2.9	Proposed schematic overview of BRCA1-mediated homologous recombination repair (HR repair)	27
2.10	Overview of the ubiquitination pathway	28
2.11	Illustration of ubiquitin represents all seven lysines (K6, K11, K27, K29, K33, K48, and K63) and the amino-terminus (M1)	29
2.12	Different forms of ubiquitin modification	30
2.13	Cellular pathways associated with polyubiquitin chains of a specific topology	31
2.14	Potential inhibitors for E1, E2, or E3 enzymes	32
2.15	Zinc ions ( $Zn^{2+}$ ) have the ability to be chelated to cysteine residues within protein scaffolds	38
2.16	Structure of platinum-based anticancer drugs	44
2.17	Historical overview of the cytotoxic metal and metalloid complexes that have been approved or entered the clinical practice	44

## LIST OF FIGURES (Continued)

<b>Figure</b>	<b>Page</b>
2.18 Antitumor ruthenium complexes	46
2.19 Principle of synthetic lethality	52
3.1 Map of the plasmid pBIND DNA	64
3.2 Nucleotide alignment of the 696-bp <i>BRCA1</i> gene fragment (nucleotide 4,897-5,592) covering exon 16-24	65
3.3 Map of the plasmid pET-28a(+)	73
3.4 Map of the plasmid pGEX4T1	73
4.1 Effects of the RAPTA complexes on the conformation of pBIND plasmid	77
4.2 Interstrand cross-links formation induced by RAPTA complexes in 696-bp <i>BRCA1</i> gene fragment	78
4.3 Restriction digestion for ruthenation site of the 696-bp <i>BRCA1</i> gene fragment induced by RAPTA complexes	79
4.4 Schematic diagram showing base/sequence of <i>BRCA1</i> fragment gene used to monitor the inhibition of DNA synthesis on the template modified by RAPTA complexes	80
4.5 DNA amplification of the 696-bp <i>BRCA1</i> gene fragment induced by <b>A)</b> RAPTA-C and <b>B)</b> carboRAPTA-C	81
4.6 Amplification products obtained from Figure 4.5 were quantified using a Bio-Rad Molecular Imager	82
4.7 Concentration dependence of ruthenation of the 696-bp <i>BRCA1</i> gene fragment by RAPTA complexes.	82
4.8 Intermolecular cross-linking of metal-BRCA1 adducts	83
4.9 The binding affinity of the metal complexes to the BRCA1 proteins was evaluated by ICP-MS analysis	84
4.10 The CD spectra of the metal-induced secondary structure change of apo form of BRCA1 RING domain (residues 1-304)	85

## LIST OF FIGURES (Continued)

<b>Figure</b>	<b>Page</b>
4.11 The CD spectra of the metal-induced secondary structure change of holo form of BRCA1 RING domain (residues 1-304)	86
4.12 Relative structure of metal complexes binding to apo- and holo-form of BRCA1 proteins (without and with Zn <sup>2+</sup> , respectively)	87
4.13 Changes in ellipticity of protein at 208 nm	87
4.14 Thermal transition of metal-BRCA1 (1-304) adducts in the presence of ZnCl <sub>2</sub>	89
4.15 Thermal denaturation curves of the metal complexes-BRCA1 adduct	90
4.16 Concentration dependent zinc ejection assay on BRCA1 RING domain	91
4.17 Time dependent zinc ejection assay on holo form of BRCA1 RING domain protein were induced by RAPTA complexes	91
4.18 Concentration dependent zinc ejection assay on BRCA1 RING domain	92
4.19 <i>In vitro</i> E3 ubiquitin ligase activity	93
4.20 <i>In vitro</i> E3 ubiquitin ligase activity of the metal-treated BRCA1 protein	94
4.21 <i>In vitro</i> E3 ubiquitin ligase activity of the metal-treated BRCA1 protein	95
4.22 The binding affinity of the metal complexes to the mutant BRCA1 proteins, D67E and D67Y, were evaluated by ICP-MS analysis	96
4.23 CD spectra of metal-induced secondary structure change of holo-form mutant BRCA1 RING domain (residues 1-304)	98
4.24 Relative structure of metal-induced holo-form of mutant BRCA1 protein	99
4.25 Changes in ellipticity of mutant BRCA1 protein at 208 nm	99
4.26 Thermal denaturation curves of the RAPTA-treated mutant BRCA1 protein	100
4.27 Concentration dependent zinc ejection assay on mutant BRCA1 RING Domain	101

## LIST OF FIGURES (Continued)

<b>Figure</b>	<b>Page</b>
4.28 Time-dependent zinc ejection assay on mutant BRCA1 RING domain	102
4.29 <i>In vitro</i> E3 ubiquitin ligase activity of the ruthenated mutant BRCA1, D67E and D67Y	103
4.30 <i>In vitro</i> E3 ubiquitin ligase activity of the metal-treated BRCA1 protein	104
4.31 The effect of metal complexes on cell viability of MCF-7, HCC1937, and MDA-MB-231 cells	106
4.32 The dynamics of human breast cancer proliferation (MCF-7, HCC1937, and MDA-MB-231 cells) on the 96-wells E-plates	108
4.33 Real-time monitoring of metal complexes effect on human breast cancer cells using xCELLigence system	109
4.34 Real-time monitoring of metal complexes effect on human breast cancer cells using xCELLigence system (cont.)	111
4.35 The cell growth inhibitory effect of RAPTA-EA1 (A), olaparib (B), and RAPTA-EA1/olaparib combination (C) on human breast cancer cells using the MTT reduction assay	113
4.36 Effects of RAPTA-EA1/olaparib combination on <i>in vitro</i> E3 ubiquitin ligase activity	114
4.37 Effects of RAPTA-EA1/olaparib combination on <i>in vitro</i> E3 ubiquitin ligase activity	115
6.1 Following uptake RAPTA-EA1 interferes with the zinc finger motif of the BRCA1 RING domain protein resulting in zinc ion ejection and inactivation of the protein	127

## LIST OF ABBREVIATIONS AND SYMBOLS

$\alpha$	Alpha
$\beta$	Beta
$\eta$	Eta-
$\phi$	Unwinding angle
$\sigma$	Superhelical density
$^{\circ}\text{C}$	Degree celcius
$\mu\text{M}$	Micromolar
$\mu\text{l}$	Microliter
A	Adenine
A-20	Murine B cell lymphoma cell line
A2780	Human ovarian cancer cell line
A2780cisR	Cisplatin resistant human ovarian cancer cell line
ADP	adenosine diphosphate
AFt	Apo-ferritin
AJCC	American Joint Committee on Cancer
API	Asian/Pacific Islander
ATM	Ataxia telangiectasia-mutated gene
ATP	Adenosine triphosphate
ATR kinase	Ataxia telangiectasia and Rad3-related protein
Auphen	$\text{Au}(1,10\text{-phenanthrolineCl}_2)\text{Cl}$
Auterpy	$[\text{Au}(2,2':6,2''\text{ terpyridine})\text{Cl}]\text{Cl}_2$
BARD1	BRCA1-associated RING domain 1
Ben	Benzene
BER	Base excision repair
BIC	Breast Cancer Information Core Database
Bip	Biphenyl
BLBCs	Basal-like breast cancers
BMI	Body mass index
bp	Base pair
bpy	2,2'-bipyridine
BRCA1	Breast cancer susceptibility gene 1
BRCA2	Breast cancer susceptibility protein 2
BRCT	BRCA1 C-terminal domain
BRIP1	BRCA1-interacting protein 1
BSA	Bovine serum albumin
C	Cytosine
carboRAPTA-C	$\text{Ru}(\eta^6\text{-}p\text{-cymene})(\text{C}_6\text{H}_6\text{O}_4)(\text{PTA})$
CBDCA	Cyclobutane-dicarboxylic acid
CC0651	CDNB 1-chloro-2,4-dinitrobenzene
CD	Circular dichroism

## LIST OF ABBREVIATIONS AND SYMBOLS (Continued)

CC0651	CDNB 1-chloro-2,4-dinitrobenzene
CD	Circular dichroism
CHEK1	Checkpoint kinase 1
CHEK2	Checkpoint kinase 2
CI	Cell index
CK5/6	Cytokeratin 5/6
c-Myc	MYC proto-oncogene protein
CTD	Carboxyl terminal domain
Cym	p-cymene
Cys	Cysteines
Cyt-c	Cytochrome c
dATP	Deoxyadenosine triphosphate
dCTP	Deoxycytidine triphosphate
dGTP	Deoxyguanosine triphosphate
dTTP	Deoxythymidine triphosphate
DTPA	Diethylene-triaminepentaacetic acid
DUBs	Deubiquitylating enzymes
EA	Ethacrynic acid
EAC	Ehrlich Ascites Carcinoma
E1	Ubiquitin (Ub)-activating enzyme
E2	Ubiquitin conjugating enzyme
E3	Ubiquitin ligase
EDTA	Ethylenediaminetetraacetic acid disodium salt
EGFR	Epidermal growth factor receptor
EMA	European Medicines Agency
GSH	Glutathione
GST P1-1	Glutathione S-transferase P1-1
GST	Glutathione-S-transferase
H2Aub	Ubiquitylated histone H2A
HATs	Histone acetyltransferases
HBL-100	Human breast epithelial cell
HCl	Hydrochloric acid
HDAC	histone deacetylase
HER2	Human epidermal growth factor receptor 2
HIF-1 $\alpha$	Hypoxia inducible factor-1 $\alpha$
His	Histidine
HR	Homologous recombination
HRP	Horseradish Peroxidase
HRT	Hormone replacement therapy
ICLs	Interstrand cross links
IC <sub>50</sub>	Half maximal inhibitory concentration
ICP-MS	Inductively coupled plasma-mass spectrometer

## LIST OF ABBREVIATIONS AND SYMBOLS (Continued)

IL-2	Interleukin-2
Im	Imidazole
In	Indazole
in situ	Intraductal carcinoma with or without invasion
IR	Ionizing radiation
JNK	c-Jun N-terminal kinase
ki67	Antigen KI-67
LB	Luria-Bertani Broth medium
LSP1	Lymphocyte-Specific Protein 1
Lys	Lysine
MAP3K1	Mitogen-Activated Protein Kinase Kinase Kinase 1
MCa	Mammary carcinoma
MCF-7	Human breast adenocarcinoma cell line (an estrogen receptor positive (ER+) cell line)
Mdm2	Murine double minute 2
MED13	Mediator 13
MDA-MD-231	Human breast adenocarcinoma cell line (an estrogen receptor negative (ER-) cell line)
mg	Milligram
min	Minute
ml	Millilitre
mM	Millimolar
mTOR	Mammalian target of rapamycin
MT-2	metallothionein-2
MTT	3-(4,5-dimethylthiazol-2-yl)-2,5-diphenyltetrazolium bromide
NER	Nucleotide excision repair
ng	Nanogram
NHEJ	Non-homologous end-joining
NLS	Nuclear localization signal
nm	Nanometer
NMP1	Nucleoplasmin B23
NSCL	Non-small cell lung
<i>p</i> -	para-
p53	Tumor suppressor protein 53
PALB2	Partner and localizer of BRCA2
PAGE	Polyacrylamide gel electrophoresis
PARP1	poly(ADP-ribose) polymerase 1
PBS	Phosphate-buffered saline
PCR	Polymerase chain reaction

## LIST OF ABBREVIATIONS AND SYMBOLS (Continued)

phen	1,10-phenanthroline
PI3K	Phosphoinositide 3-kinase
PMSF	Phenylmethylsulfonyl fluoride
PRE	Progesterone responsive element
pSer	Phosphoserine
PTA	1,3,5-triaza-7-phosphaadamantane
pThr	Phosphothreonine
Pu	Purine base
PVDF membrane	Polyvinylidene fluoride membrane
QPCR	Quantitative polymerase chain reaction
$r_b$	Molar ratio
SOD	Superoxide dismutase
SSBs	single strand breaks
T	Thymine
TAD	Transactivation domain
TFIIIE	transcription factors at the promoter
terpy	2,2':6'2"-terpyridine
$T_m$	Melting temperature
TNBC	Triple-negative breast cancer
TRAF6	TNF receptor-associated factor 6
Trx-R	Thioredoxin reductase
TSQ	6-methoxy-8-p-toluenesulfonamido-quinoline
Ub	Ubiquitin
UV	Ultraviolet light
V	Volt
ZF	Zinc finger



## CHAPTER 1

### INTRODUCTION

#### 1.1 Background and rationale

Nowadays, metal-based drugs play an important role in medical application. Cisplatin, carboplatin and oxaliplatin are FDA approved platinum anticancer drugs that are used clinically worldwide for the treatment of various cancers (Ndagi *et al.*, 2017). They exert anticancer activity via covalent crosslinks with DNA. Pt-DNA adducts interfere with DNA replication, transcription, and finally lead to the programmed cell death (Ndagi *et al.*, 2017). However, an application of platinum-based drugs is restricted by their severe toxicity and drug resistance (Dilruba and Kalayda, 2016). Several anticancer drugs, based on transition metal, have been developed that mainly focused on the potential biomolecular target such as DNA and protein for overcoming problems associated with the platinum-based drugs. Ruthenium is one of the most promising metals which has some properties particular well suited for medical applications including relevant ligand exchange kinetics, redox potentials and the ability to mimic iron in the binding certain biological molecules (Allardyce and Dyson, 2001). Several ruthenium complexes have shown high *in vitro* and *in vivo* antitumor activity and exhibited a different mode of action compared with platinum-based drugs. Recently, some ruthenium complexes, such as NAMI-A ((ImH)[*trans*-Ru(III)Cl<sub>4</sub>Im(Me<sub>2</sub>SO)]); Im = imidazole), and KP1019, indazolium *trans*-[tetrachlorobis(1*H*-indazole)ruthenate(III)], are in advanced stages of phase I/II clinical trials (Leißen *et al.*, 2016). The ruthenium(II)-arene (PTA), (PTA = 1,3,5-triaza-7-phosphaadamantane), or RAPTA complexes have been shown to exhibit promising antitumor activities (Murray *et al.*, 2016). However, the mechanisms of action of these compounds are largely unknown. Several studies suggest that ruthenium compounds might directly interfere with the proteins in several processes but interact more weakly with DNA relative to platinum-based drugs (Adhireksan *et al.*, 2014; Bergamo *et al.*, 2008; Chatterjee and Mitra, 2009; Murray *et al.*, 2016; Nhugeaw *et al.*, 2014; Vergara *et al.*, 2013).

The breast cancer susceptibility gene 1, *BRCA1*, is an important tumor suppressor gene that plays a number of major roles in the maintenance of genome integrity such as transcriptional regulation, cell-cycle checkpoint, protein ubiquitination and DNA repair (Muggia and Safra, 2014; Starita *et al.*, 2015). The mutation and down-regulation of *BRCA1* expression can be abrogated *BRCA1* function, called '*BRCAness*', leading to tumorigenesis (Muggia and Safra, 2014; Tanino *et al.*, 2016). However, the application of *BRCA*-like functional abnormalities or dysfunctional of *BRCA1* raises the possibility of treatment regimens designed for familial *BRCA* tumors (Turner *et al.*, 2004). Recent studies have emphasized the potential of using *BRCA1* dysfunction to predict response to therapy. Exploitation of this knowledge in the treatment of *BRCA1* associated-breast cancer revealed varying degrees of success. Several clinical trial studies have demonstrated the utilization of the *BRCAness* as a clinically validated target by the platinum based-drugs to treat *BRCA1*-associated breast cancer (Byrski *et al.*, 2010; Tanino *et al.*, 2016). Several

studies have investigated the application of a dysfunctional BRCA1 as molecular targets for breast and ovarian cancer treatment (Audeh, 2010; Byrski *et al.*, 2010; Domagala *et al.*, 2016; Drost and Jonkers, 2014; Liu *et al.*, 2012; Price and Monteiro, 2010; Maksimenko *et al.*, 2014; Muggia and Safra, 2014; Sikov *et al.*, 2015; Tassone *et al.*, 2009). Therefore, targeting the BRCA1 gene and its encoded protein by the anticancer drugs are of interest for breast cancer treatment.

Ratanaphan and co-workers have studied the effect of the anticancer platinum drugs on the *BRCA1* gene and its encoded protein (Atipairin *et al.*, 2010; Atipairin *et al.*, 2011a; Atipairin *et al.*, 2011b; Chakree *et al.*, 2012; Ratanaphan *et al.*, 2005; Ratanaphan *et al.*, 2009; Ratanaphan and Canyuk, 2014; Ratanaphan *et al.*, 2017). The platinum drugs were found to reduce the amount of amplified DNA both in cells and cell-free system (Ratanaphan *et al.*, 2005). The cisplatin-modified *BRCA1* protected a cleavage by some restriction endonucleases, implying that cisplatin specially forms the 1,2-intrastrands d(GpG) crosslinks. The transcriptional transactivation activity of the BRCA1 protein is dramatically reduced in the presence of multiple cisplatin-damaged *BRCA1* sites. In addition, a repair-mediated transcriptional transactivation of cisplatin-damaged *BRCA1* appeared to be associated with increased DNA interstrand crosslinks and altered thermal stability (Ratanaphan *et al.*, 2009). Furthermore, it has been reported that intra- and inter-molecular of Pt-BRCA1 adducts was occurred with the preferential Pt-binding site on histidine 117, resulting in altered thermostability and conformation of the BRCA1 RING domain (Atipairin *et al.*, 2010; Atipairin *et al.*, 2011b). Moreover, the BRCA1-mediated E3 ubiquitin ligase activity was inhibited by the Pt-based drugs (Atipairin *et al.*, 2011b). These data suggest a possibility of the BRCA1 protein as a potentially molecular therapeutic target for metallodrug-based chemotherapy. However, the effects of RAPTA complexes on the human *BRCA1* gene and its encoded protein have not been studied.

In this work, the *BRCA1* gene and its respective protein are used as a model system for *in vitro* evaluation of the RAPTAs-induced response in comparison with cisplatin and some types of metal complexes, including two highly active gold(III) compounds, namely Auphen and Auperpy ([Auphen=Au(1,10-phenanthroline)Cl<sub>2</sub>]Cl and Auperpy = [Au(2,2':6,2'' terpyridine)Cl]Cl<sub>2</sub>), and two ruthenium(II) polypyridyl complexes, namely Ru-bpy and Ru-phen ([Ru-bpy=Ru(Clazpy)<sub>2</sub>bpy]Cl<sub>2</sub>.7H<sub>2</sub>O and [Ru-phen= Ru(Clazpy)<sub>2</sub>phen]Cl<sub>2</sub>.8H<sub>2</sub>O) (Fig.1.1). The investigation is focused on DNA interactions and protein binding as well as structural and functional consequences of the ruthenium-treated BRCA1. It is expected that resulting data provide insights into the molecular mechanism of action of the ruthenium compounds and the potential of using the BRCA1 protein as a molecular target in breast cancer chemotherapy.

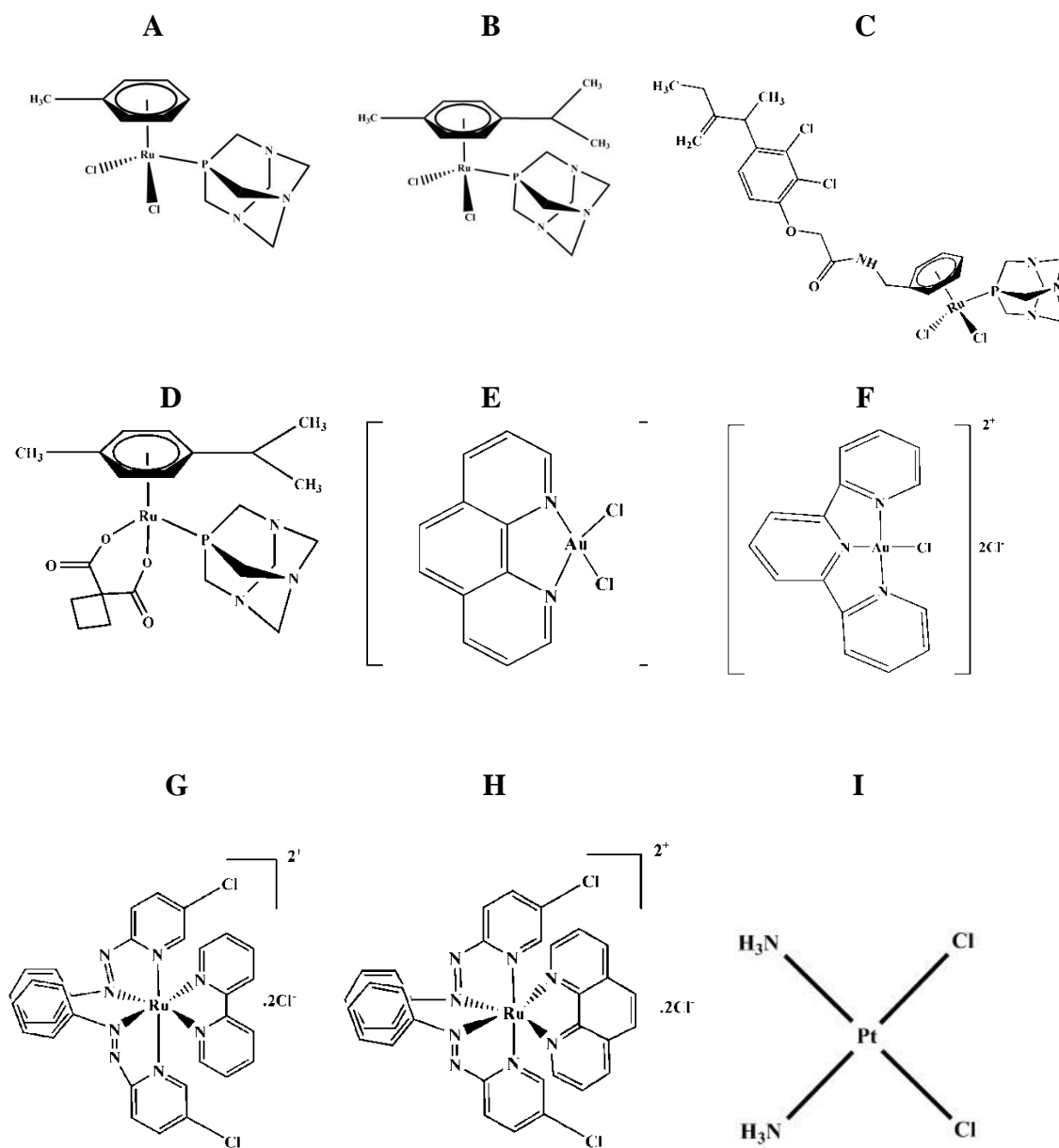


**Figure 1.1.** The ruthenium(II) arene (PTA) or RAPTA complexes and other metal complexes are used in this study. **A:**  $[\text{Ru}(\eta^6\text{-toluene})(\text{PTA})\text{Cl}_2]$ , RAPTA-T. **B:**  $[\text{Ru}(\eta^6\text{-}p\text{-cymene})(\text{PTA})\text{Cl}_2]$ , RAPTA-C. **C:**  $[\text{Ru}(\text{ethacrynic-}\eta^6\text{-benzylamide})(\text{PTA})\text{Cl}_2]$ , RAPTA-EA1. **D:**  $[\text{Ru}(\eta^6\text{-}p\text{-cymene})(\text{C}_6\text{H}_6\text{O}_4)(\text{PTA})]$ , carboRAPTA-C. **E:**  $[\text{Au}(1,10\text{-phenanthroline})\text{Cl}_2]\text{Cl}$ , Auphen. **F:**  $[\text{Au}(2,2'\text{-}6,2''\text{-terpyridine})\text{Cl}]\text{Cl}_2$ , Auterpy. **G:**  $[\text{Ru}(\text{Clazpy})_2\text{bpy}]\text{Cl}_2 \cdot 7\text{H}_2\text{O}$ , Ru-bpy. **H:**  $[\text{Ru}(\text{Clazpy})_2\text{phen}]\text{Cl}_2 \cdot 8\text{H}_2\text{O}$ , Ru-phen. **I:** cisplatin.

## CHAPTER 2

### LITERATURE REVIEW

#### 2.1 Breast cancer

##### 2.1.1 Breast cancer incidence and mortality

Breast cancer ranks as the second leading cause of cancer death in women and the third cause of death from cancer overall in 2017 (Siegel *et al.*, 2017). The estimated breast cancer incidence and mortality rates (Age standardized rate/100,000 population, ASR) are different by regions (Table 2.1) (Ferlay *et al.*, 2015; Siegel *et al.*, 2017; Youlden *et al.*, 2014; Zaguri *et al.*, 2014). The incidence is slightly less cases in more developed (794,000) than in less developed (883,000 cases) regions, where the predominant prevalence cause of cancer death in female is approximately 24.9% (198,000 deaths) and 36.7% (324,000 deaths) of total in more and less developed regions, respectively (Ferlay *et al.*, 2015). In Thailand, the incidence of breast cancer is lower than that in developing countries. The significant increase in breast cancer incidence in recent year was observed with incidence rates increasing by 3-4% per year (Fan *et al.*, 2015). However, it has become the most common cancer in women with the estimated incidence and mortality rates of 29.3 and 11.0, respectively, in 2012 (Youlden *et al.*, 2014).

**Table 2.1** Estimated breast cancer incidence and mortality by regions/country in 2012; ASR, Age standardized rate/100,000 population. (Ferlay *et al.*, 2015; Siegel *et al.*, 2017; Youlden *et al.*, 2014; Zaguri *et al.*, 2014).

Region/country	Incidence		Mortality	
	Case	ASR	Case	ASR
World	1,676,633	43.3	521,817	12.9
Europe	458,337	77.1	131,259	16.1
USA	255,180	123.3	41,070	21.1
Asia-Pacific	403,876	29.6	115,863	8.1
Eastern Asia	277,054	27.0	68,531	6.1
South-Eastern Asia	107,545	34.8	43,003	14.1
Oceania	19,277	79.2	4,329	15.6
Thailand	13,653	29.3	5,092	11.0

### 2.1.2 Histopathological subtypes of breast cancer

The main components of breast consist of three parts; lobules, ducts, and stromas. The lobules are mammary glands that produce milk. The ducts are tiny-tubes that carry the milk from the lobules to the nipple. The stromas are connective tissue, which consist of fibrous and fatty acids tissue, those surround and hold everything together (Fig. 2.1) (Pourteimoor *et al.*, 2016). Breast cancers are characterized into two major groups (Rubin *et al.*, 2005) as follows;

- Noninvasive carcinoma (*in situ*), are restricted to the ducts and do not invade surrounding fatty and connective tissues of the breast. It includes ductal carcinoma (*in situ*) (intraductal carcinoma with or without invasion) and lobular carcinoma (*in situ*).

- Invasive carcinoma, these cancer cells advance the duct and lobular walls and invade the surrounding fatty and connective tissues of the breast. It includes invasive ductal carcinoma, invasive lobular carcinoma and uncommon types of invasive breast cancer.

The American Joint Committee on Cancer (AJCC), has defined this group into three common histological types including invasive ductal carcinoma (about 55 %), ductal carcinoma (*in situ*) (about 13 %), and invasive lobular carcinoma (about 5 %) (Fig. 2.1) (Pourteimoor *et al.*, 2016).

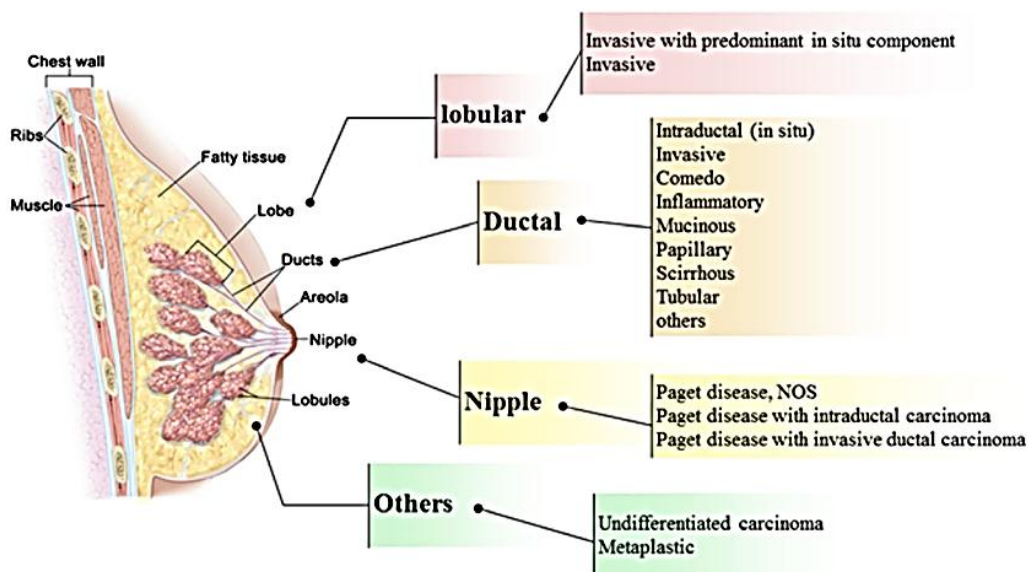


**Figure 2.1.** The histological types of breast cancer by the American Joint Committee on Cancer (AJCC) and National Comprehensive Cancer Network or National Cancer Institute (NCI) 2015 (Pourteimoor *et al.*, 2016).

### 2.1.3 Molecular subtypes of breast cancer

Breast cancer is classified into different molecular subtypes, in accordance with similarities in gene expression, pathological features and responsiveness to therapy. It is broadly divided into two groups: estrogen receptor

positive (ER+) and ER negative (ER-), leading to subdivisions into more biologically and clinically relevant subgroups as described in Table 2.2 (Prat and Perou, 2011; Sorlie *et al.*, 2001).

The ER positive tumor subgroups, due to their expression of genes that encode the characteristics of the proteins of luminal epithelial cells, are known as the luminal group. Luminal A is frequently characterized by the positive expression of progesterone receptor (PR) and negative expression of human epidermal growth factor receptor 2 (HER2), whereas luminal B is related to overexpression of HER2 and/or high proliferation status and devoid of PR expression (Sorlie *et al.*, 2001; Sotiriou *et al.*, 2003). Luminal A expresses a low Ki67, which is the marker for rapid cell division or the aggressive nature of cancer, while luminal B expresses a high ki67, and is very aggressive in behavior requiring more aggressive therapy (Naik *et al.*, 2015). Luminal B has a significantly worse prognosis than luminal A, and shows lower expression of ER and higher proliferation than luminal A (Sorlie *et al.*, 2006). Luminal A subtype is known to have good prognosis and is usually highly sensitive to hormonal therapy (Naik *et al.*, 2015).

The ER negative tumor subgroups are subdivided into HER2 positive, basal-like breast cancers, and triple-negative breast cancer (TNBC) (Brenton *et al.*, 2005). Approximately 10-20% of breast cancers are HER2 positive (overexpression of HER2). HER2 amplification plays a direct role in the pathogenesis of breast cancers, which has been targeted for doxorubicin and HER2-targeted therapies (trastuzumab, pertuzumab and lapatinib) (Biswas *et al.*, 2006; Rakha *et al.*, 2008). Approximately 15% of breast cancers are basal-like in origin and are associated with a higher histological grade, poor overall survival and younger patient age (Carey *et al.*, 2006; Cheang *et al.*, 2008). The basal-like breast cancers (BLBCs) are characterized by a lack of ER, PR, HER2 but positive in epidermal growth factor receptor (EGFR) and express normal basal epithelial cell markers such as CK5/6 (Naik *et al.*, 2015; Nielsen *et al.*, 2004). A key feature of BLBCs is the high frequency of point mutations in p53 (Naik *et al.*, 2015; Sorlie *et al.*, 2001). TNBC accounts for approximately 10–20% of all breast cancer. It is defined by the lack of ER-, PR- and HER2 (Naik *et al.*, 2015). Recently, TNBC has been classified into three clusters including cluster 1(C2), 2 (C2) and 3 (C3), respectively, as shown in Table 2.3 (Jézéquel *et al.*, 2015). In addition, the emerging data has revealed that 20-30% of TNBC patients harbor the germline breast cancer susceptibility gene 1 (*BRCA1*) mutation and these correlates with decreased *BRCA1* mRNA and protein expression (Lips *et al.*, 2013; Wong-Brown *et al.*, 2015). Recently, TNBCs and BLBCs have become a key topic of research interest, due to their aggressive behavior and lack of targeted therapy. Currently, no targeted treatment is available for patients harboring these cancer subtypes, and a standard chemotherapy remains a basic systemic treatment option with no optimal cytotoxic regimen recommended. Therefore, the development of a new targeted treatment to improve prognosis in TNBCs and BLBCs is necessary.

**Table 2.2** Molecular subtypes of breast cancer (Prat and Perou, 2011; Jézéquel *et al.*, 2015)

	Molecular subtypes				
	ER positive		ER negative		
	Luminal A	Luminal B	HER2 positive	Basal-like	TNBC
Genes status	ER+ PR+/ HER2– CK5/6–	ER+/- PR+ HER2– CK5/6–	ER– HER2+ PR– CK5/6+/-	ER– HER2– PR– CK5/6+	ER– PR– HER2– CK5/6+/-
p53 mutation	Low	Intermediate	High	High	High
Proliferation	Low	High	High	High	High
Histological grades	Low	High	High	High	High

**Table 2.3** The clusters of triple-negative breast cancer (Jézéquel *et al.*, 2015).

	Properties			
	Histological grade	Immune response	Clinical outcome	Remark
Cluster 1 (C1)	low	low	poor	this cluster was enriched by luminal subtypes and positive androgen receptor
Cluster 2 (C2)	high	low	poor	defined as a pure basal-like cluster with high M2-like macrophage activity*
Cluster 3 (C3)	high	high	better outcome than C1 and C2	low M2-like macrophage activity, generally known as a basal enriched subtype

\* M2 like macrophages = Macrophages that decrease inflammation and encourage tissue repair

## 2.2 Risk factors for breast cancer

There are several well-established factors that contribute to an increased risk of breast cancer. The possible factors can be divided into two groups. The first group includes intrinsic factors including age, sex, race, and genetic, while the second group includes extrinsic factors conditioned by lifestyle, diet or long-term medical intervention (Kamińska *et al.*, 2015).

### 2.2.1 Gender

Breast cancer is relatively uncommon in men whose the female-to-male breast cancer ratio is approximately 100:1. An estimated 246,660 and 2,600 new cases of breast cancers will be diagnosed among American women and men,

respectively in 2016, and about 40,450 women and 440 men will die from the disease (Siegel *et al.*, 2016). The higher risk in women is attributed to the responsiveness of breast tissues to ovarian hormones which are active from puberty to menopause (Evans and Lalloo, 2002).

### 2.2.2 Age

The age of a patient is highly related to the incidence of breast cancer. Eighty percent of these cancers are diagnosed in women aged 50 and more (Fig. 2.2). Moreover, according to epidemiological data, 50% of breast cancers occur in women aged from 50 to 69 years (DeSantis *et al.*, 2016). The risk doubles every 10 years up to the menopause (Key *et al.*, 2001). The disease is uncommon in women younger than 40 years of age which occur only 6.4% of all patients diagnosed with the first primary breast cancer while women, those are 40 years of age or older at time diagnosis, are accounted for 93.6% of all breast cancers (Gnerlich *et al.*, 2009). The characteristics of cancer in women under 40 years of age are significantly different from older women that had a poor prognosis, and this association was strongest among young women with axillary lymph node negative breast cancer (Brandt *et al.*, 2015).

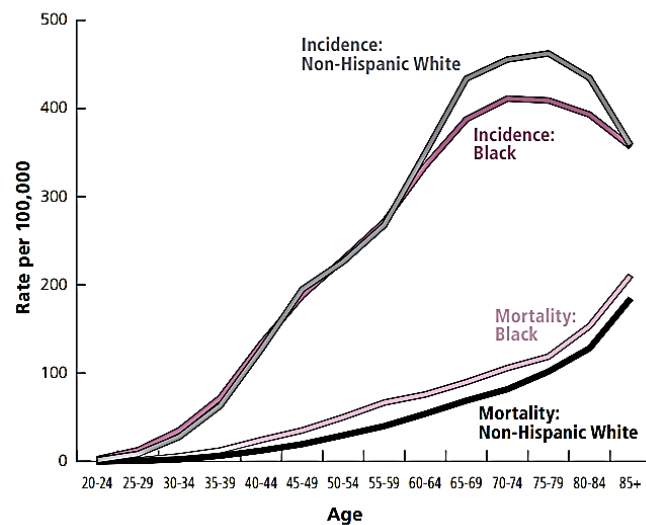


**Figure 2.2** Age-specific female breast cancer incidence and motility rates in US (US mortality data, National Center for Health Statistics, Centers for Disease Control and Prevention. American Cancer Society, Inc., Surveillance Research, 2015).

### 2.2.3 Hormonal factors

Hormonal and reproductive factors have long been recognized to be the important risk factors of breast cancer development. Women who have a bilateral oophorectomy before the age of five have only a 40% associated risk of breast cancer, compared to women who go through a normal menopause (Garcia-Closas *et al.*, 2006). The increased risk of women who experience normal menopause is thus due to



ER influence (Garcia-Closas *et al.*, 2006; Torres-Mejia *et al.*, 2005). Several groups have analyzed the relationship between lactation and the incidence of premenopausal breast cancer, with varying outcomes. Two independent studies have claimed an inverse association between lactation and the possibility of premenopausal or early-onset breast cancer (Lee *et al.*, 2003; Tryggvadóttir *et al.*, 2001). Hormone therapy using estrogen (often combined with progesterone) has been used for many years to help relieve symptoms of menopause and to help prevent osteoporosis. Recent epidemiological studies have inconsistently revealed a modestly-increased breast cancer risk associated with hormone replacement therapy (HRT) that showed a relative risk (RR) of 1.35 after 5 or more years of use (Chlebowski, *et al.*, 2009; Cibula *et al.*, 2010). No difference in relative risk was found, based on the use of estrogen plus progesterone that associated with a significantly increased risk (RR = 1.82), and the risk was higher (RR = 2.44) in women with prolonged use more than 10 years. Furthermore, women using only estrogen therapy showed a slightly increased risk (RR = 1.15) with no further evidence of increase seen for long durations of use (Brinton *et al.*, 2008). Several evidences indicated that a decreased mortality from breast cancer in women using hormone therapy more than 5 years of the disease diagnosis (Nichols *et al.*, 2013). Furthermore, the lower cardiovascular disease and osteoporosis risk was observed among women administering estrogen (Nichols *et al.*, 2013). Recently, several hormone-related factors (such as age at menarche, race, parity, age at first live birth, and number of live births) have been reported to be associated with the risk of ER positive breast cancer (Cui *et al.*, 2014).

#### 2.2.4 Family history

The family history is a well-established risk factor for breast cancer, however, its association with survival is still ambiguous. Several studies have reported an increased survival for females with a family history of breast cancer (Anderson and Badzioch, 2006; Thalib *et al.*, 2004) while other studies indicated slightly or no difference in survival rates (Chang *et al.*, 2009; Russo *et al.*, 2002). Susceptibility to breast cancer is usually inherited as an autosomal dominant, with limited penetrance. The overall relative risk of breast cancer in a woman with a positive family history in first-degree relative; mother, daughter, or sister, is  $> 5$  (Anderson and Badzioch, 2006). Moreover, it is believed that only about 25% of the occurrence of breast cancer in first-degree relatives of women affected by the disease may be implicated to mutations in well-known genes such as the high-penetrance susceptibility genes *BRCA1* and *BRCA2*. It has been reported that inherent deficiency of *BRCA1* and *BRCA2* in DNA repair function was a significant risk factor for breast cancer (Apostolou and Fostira, 2013). In addition, the reduced repair capacity was associated with certain clinical features that are indicative of poor prognosis (Fu *et al.*, 2015). Moreover, the low-penetrance genes, such as *MAP3K1*, *FGFR2*, *LSP1*, are presented with relative cancer risk around 1.5, whereas intermediate-penetrance genes, such as *ATM*, *CHEK2*, *BRIP1*, and *PALB2*, confer relative cancer risks from 1.5 to 5 (Apostolou and Fostira, 2013; Stratton and Rahman, 2007; Turnbull *et al.*, 2010). Recent advances in molecular biological techniques are useful for investigating certain inherited genes with the susceptibility to breast cancer.

### 2.2.5 Race

Race is a very important intrinsic factor elevating the risk of occurrence of breast cancer. Female breast cancer incidence rates vary considerably across racial and ethnic groups. The incidence in African-American women is lower than Caucasian women, the age-adjusted incidence of breast cancer is 120.8, 142.0 per 100,000, respectively (Siegel *et al.*, 2016). A proportion of African-American women with breast cancer are found in younger age groups than Caucasian women (Ries *et al.*, 2003). However, Asian/Pacific Islander (API) women have the lowest incidence and death rates (Howlader *et al.*, 2015). The incidence rate of breast cancer in white women, between the ages of 60 and 84, are markedly higher than black women, however, lower in women before age 45 (American Cancer Society, Inc., Surveillance Research, 2015). Incidence and death rates for breast cancer are lower among women of other racial and ethnic groups than among non-Hispanic white and black women (Howlader *et al.*, 2015).

### 2.2.6 Lifestyle and environmental factors

Alcohol is a well-established risk factor for breast cancer. Recent large prospective studies have confirmed a direct association between alcohol consumption and the occurrence of breast cancer. Higher alcohol consumption was associated with increased risk of breast cancer, compared to nondrinkers (Allen *et al.*, 2009; Chen *et al.*, 2011; Lew *et al.*, 2009). The increased breast cancer risk was varied between 13 to 35%, depending on the amount of alcohol intake (Ellison *et al.*, 2001; Manisto *et al.*, 2000). Recently, some evidences reported that women who started alcohol drinking after first pregnancy had increased risk by 9% per 10 g/day intake (Liu *et al.*, 2013). Furthermore, at relatively high intakes (>60 g/day) the cancer risk is approximately three-fold that of non-drinkers (Roswall and Weiderpass, 2015). A meta-analysis reported that alcohol consumption was associated with increased risks for ER+/PR+ and ER+/PR-, but not ER-/PR- tumor types (Chen *et al.*, 2011; Li *et al.*, 2010; Suzuki *et al.*, 2008). Several potential mechanisms for the consumption of alcohol might increase the risk of breast have been proposed (Park *et al.*, 2014; Roswall and Weiderpass, 2015). Alcohol could affect cellular response and differentiation of breast tissue by stimulating estrogen signaling, and by down-regulating the tumor suppressor BRCA1 (Fan *et al.*, 1999). By-products of alcohol metabolism such as acetaldehyde, reactive oxygen species, poor folate intake and its metabolites also led to DNA damage-induced carcinogenesis and decreased DNA repair efficiency or reduced intake of protective nutrients (Dumitrescu and Shields, 2005).

The relationship between body mass index (BMI) and breast cancer carcinogenesis has been reported. It revealed that women with a gain of 5 kg/m<sup>2</sup> in BMI is also associated with breast cancer risk, resulting in an 8% increase in disease risk, but only in postmenopausal women (<http://www.wcrf.org/int/researchwe-fund/continuous-update-project-cup/second-expert-report>). In contrast, some evidence

reported that excess weight is associated with a decrease in risk in premenopausal women (Travis and Key, 2003).

The relationship between smoking and the risk of breast cancer is still controversial. Recent cohort studies have suggested that increased breast cancer risks were associated with longer smoking duration or who smoke for a long time prior to their first pregnancy, while others reported the lack of an association among smoking intensively and the increased breast cancer risk (Catsburg *et al.*, 2015; Dossus *et al.*, 2014). However, there is no evidence of an association between either active smoking or passive smoking and risk of breast cancer (Roddam *et al.*, 2007). Chemical carcinogens in cigarette smoke, which can cause mammary tumors in animal, have been found in the circulation of smokers, including polycyclic aromatic hydrocarbons, aromatic amines and *N*-nitrosamines (Hecht, 2002). These compounds were metabolized and subsequently activated by mammary epithelial cells into electrophilic intermediates and form adducts with DNA resulting in DNA damage (Li *et al.*, 2002). To date, a number of environmental agents have been investigated in epidemiologic studies with respect to their potential influence on breast cancer risk (Brody *et al.*, 2007; Fenga, 2016; Weiderpass *et al.*, 2011). However, a few of these have been examined in terms of their specific relation to breast cancer risk. The organochlorines, including dichlorodiphenyl trichloroethane (DDT) and polychlorinated biphenyls (PCBs), can accumulate in the food chain, and may be found in human tissue, blood, and breast milk. Long term exposure to these chemicals showed a positive correlation with breast cancer risk (Fenga, 2016; Weiderpass *et al.*, 2011; Wolff *et al.*, 2003).

### 2.2.7 Genetic risk factors

Genetic predisposition is one of the most well-established factors associated with an increased breast cancer risk. Approximately 90-95% of all breast cancer cases are considered to be non-familial (sporadic), while the others 5-10% are related to a subset of hereditary (familial) breast cancers (Rich *et al.*, 2015). Recently, a better understanding of genetic predisposition to breast cancer has advanced significantly. The genetic factors associated with breast cancer risk are classified into three classes. Firstly, high penetrance mutations such as *BRCA1*, *BRCA2*, *TP53*, *PTEN*, *STK11*, and *CDH1* that are rare in the population but associated with very high risk; secondly, moderate penetrance variants, such as *ATM*, *CHEK2*, *BRIP1*, and *PALB2*, associated with moderate increases in risk, and thirdly, low penetrance mutations, such as *FGFR2*, *TOX3*, *CASP8*, *MAP3K1*, *RAD51L1*, and *LSP1*, which are common and associated with small increases in breast cancer risk (Mavaddata *et al.*, 2010; Rich *et al.*, 2015; Tan *et al.*, 2012; van Lier *et al.*, 2010).

## 2.3 Breast cancer susceptibility gene 1 (*BRCA1*)

Breast cancer susceptibility gene 1 (*BRCA1*) is a tumor suppressor gene and locates on chromosome 17q21. It was identified in 1990 (Hall *et al.*, 1990), and subsequently cloned (Miki *et al.*, 1994). The *BRCA1* gene consists of 24 exons and 22 of which encodes for 1863 amino acid with molecular weight of 220 kDa (Hall *et al.*, 1990; Miki *et al.*, 1994). The most common case of hereditary breast cancer is

an inherited germ line mutation in *BRCA1* gene that accounts for approximately 20-50% of hereditary breast cancer (Martin *et al.*, 2001), and at least 80% of both breast and ovarian cancers (Miki *et al.*, 1994). Female carriers of deleterious *BRCA1* mutations are also predisposed to high lifetime risks of breast and ovarian cancer. They are also at conferring an increased risk of other cancers, such as cervical, uterine and prostate cancers (Thompson and Easton, 2002). The cumulative incidence of breast cancer by age for *BRCA1* carriers is summarized in Table 2.4. Furthermore, approximately 4-14% of hereditary breast cancer was found in male breast cancer (Rich *et al.*, 2015).

**Table 2.4** The cumulative incidences (standard error) of breast and ovarian cancers by age for *BRCA1* carries (Eavans *et al.*, 2008).

Cancer risk to age	Breast cancer	Ovarian cancer
30	2%	0
40	16.5% (0.015)	3% (0.007)
50	48% (0.023)	21% (0.02)
60	55% (0.027)	40% (0.024)
70	68% (0.033)	60% (0.037)
80	79.5% (0.04)	65% (0.042)

### 2.3.1 Mutational spectrum of *BRCA1*

The Breast Cancer Information Core Database (BIC) reported that there are more 1700 distinct variants identified throughout the whole coding and non-coding regions of the *BRCA1* gene (Table 2.5). The type of mutations of the *BRCA1* gene includes frameshift, nonsense, missense, silent mutations, mutations in the non-coding regions, in-frame insertions or deletions, and splice altering mutations. The main groups of risk-associated mutations are frameshift or nonsense mutations that present in a premature stop codon and truncated protein product (NIH Breast Cancer Information Core, 2017).

The top three mutations are 185delAG, C61G, and 5382insC. Both 185delAG and C61G mutations are occurred in the RING domain of *BRCA1* (Mallery *et al.*, 2002). The 185delAG produces premature stop codons that mediated resistance to homologous recombination (HR) deficiency-targeted therapies (Drost *et al.*, 2016), while C61G mutation results in defective E3 ubiquitin ligase activity (Hashizume *et al.*, 2001). The 5382insC is missense mutation in exon 20 (*BRCA1* C terminus, BRCT, domain) that produces premature stop codons. This mutation mediated resistance to HR deficiency-targeted therapies (Drost *et al.*, 2016). Frequent mutations of the *BRCA1* gene are summarized in Table 2.6.

**Table 2.5.** Total number of mutations, polymorphisms, and variants of *BRCA1* from the Breast Cancer Information Core Database (BIC, 2017).

<b>Exon type</b>	<b>Total number of entries</b>	<b>Distinct mutations, polymorphisms, and variants</b>	<b>Alterations reported only once</b>
1	1	1	1
2	2197	53	35
3	187	47	26
4	8	2	1
5	445	49	27
6	198	30	19
7	164	36	19
8	360	36	19
9	349	19	9
10	54	17	12
11A	1251	224	115
11B	1982	223	123
11C	1835	235	124
11D	1678	221	116
12	118	47	28
13	655	51	28
14	111	28	18
15	241	47	24
16	790	88	52
17	578	50	25
18	466	55	26
19	123	32	18
20	1334	48	27
21	89	29	19
22	173	31	13
23	74	30	17
24	213	51	27
<b>Total</b>	<b>15674</b>	<b>1780</b>	<b>968</b>

**Table 2.6.** Frequent mutations of *BRCA1* gene according to the Breast Cancer Information Core Database (BIC, 2017) (F: frameshift, M: missense, N: non-sense; NT: nucleotide).

Exon	Designation	Type	NT	Codon	Count
2	185delAG	F	185	23	2038
20	5382insC	F	5382	1756	1093
5	C61G	M	300	61	239
11	R1347G	M	4158	1347	161
11	Q563X	N	1806	563	155
11	4184del4	F	4184	1355	144
13	R1443X	N	4446	1443	143
11	M1008I	M	3143	1008	139
11	3875del4	F	3875	1252	124
11	R841W	M	2640	841	119
11	E1250X	N	3867	1250	98
16	M1628T	M	5002	1628	96
18	A1708E	M	5242	1708	39

In Thai patients, the *BRCA1* mutations were analyzed (Patmasiriwat *et al.*, 2002; Ratanaphan *et al.*, 2011). Nine distinct variants and their frequencies are shown in Table 2.7. The T320G was a conservative missense mutation in exon 5 in which thymine at nucleotide 320 was changed to guanine. This mutation was identified in three unrelated Thai breast cancer patients, and no other mutations were found in the coding and non-coding regions of the *BRCA1* gene. This mutation is probably a founder mutation in Thais which resulted in the substitution of aspartic acid with glutamic acid at position 67 (D67E). It is in vicinity of Zn<sup>2+</sup>-binding site II (residues 58-68) that forms a recognition interface with a ubiquitin-conjugating enzyme (Brzovic *et al.*, 2003).

**Table 2.7.** Relative frequencies of *BRCA1* mutations in Thais.

Mutations	Relative frequencies	References
T320G	3/23 = 0.13	Patmasiriwat <i>et al.</i> , 2002
744ins20	1/23 = 0.04	Patmasiriwat <i>et al.</i> , 2002
3300delA	3/23 = 0.13	Patmasiriwat <i>et al.</i> , 2002
C3271G	2/23 = 0.08	Patmasiriwat <i>et al.</i> , 2002
IVS20+78 G>A	1/23 = 0.04	Patmasiriwat <i>et al.</i> , 2002
IVS7+34_47delTTCTTTTCTTTTTT	-	Ratanaphan <i>et al.</i> , 2011
IVS7+34_47delAAGAAAAGAAAAA	-	Ratanaphan <i>et al.</i> , 2011
IVS7+50_63delTTCTTTTCTTTTTT	-	Ratanaphan <i>et al.</i> , 2011
IVS7+38T>C	-	Ratanaphan <i>et al.</i> , 2011

The 744ins20 was a frameshift mutation in exon 10 as a result of insertion of AGGGATGAAATCAGGAGCCA. It provided a stop codon at nucleotide 839, resulting in a premature translational termination at codon 240. The 3300delA was a frameshift mutation in exon 11. It introduced a stop codon at nucleotide 3300, and resulted in a truncated BRCA1 protein of 1060 amino acids. The C3271G (cytosine was replaced by guanine) was a conservative missense mutation in exon 11. It caused the substitution of threonine with serine at residue 1051. The IVS20+78 G>G was a rare intronic mutation variant in which guanine was replaced by adenine at upstream position 70 in intron 20. In addition, the intronic *BRCA1* variants in a Thai hereditary breast cancer family were reported from a total of 50 Thai breast cancer patients (Ratanaphan *et al.*, 2011). A novel intronic *BRCA1* mutation (IVS7+34\_47delTTCTTTTCTTTTTT) was identified in one out of five breast cancer patients, with a family history of breast cancer cases. In addition, the unclassified mutations were also identified in the patient's healthy daughter, including two unclassified intronic *BRCA1* variations (IVS7+34\_47delAAGAAAAGAAAAAA and IVS7+50\_63delTTCTTTTTTTTTTTT) and one unclassified intronic point mutation (IVS7+38T>C). These alterations were not found in other family members or unrelated healthy volunteers.

## 2.4 BRCA1 protein

The full length (1863 amino acids) of human BRCA1 protein plays a vital role in genomic maintenance through multi-functional cellular processes including DNA damage repair, protein ubiquitination, cell cycle checkpoint, and transcriptional regulation (Brzovic *et al.*, 2003; Gudmundsdottir and Ashworth, 2006; Lane, 2004; Monteiro, 2000; O'Donovan and Livingston, 2010; Rosen *et al.*, 2006; Starita and Parvin, 2003; Yarden and Papa, 2006). The BRCA1 protein encompasses three major domains including the Zn<sup>2+</sup> finger RING domain (BRCA1 RING domain) at N-terminal region, the large central segment, and the BRCA1 C-terminal domain (BRCT domain). (Fig. 2.3). Nowadays, over 100 diverse BRCA1 interacting proteins have been identified. It is assumed that the ability of BRCA1 to act as a scaffold for the formation of multiple different protein complexes with different cellular functions through these interactions (Christou and Kyriacou, 2013; Savage and Harkin, 2014). The structure of the BRCA1 protein contains multiple conserved domains and motifs, which each of them associated with one or more specific function (Table 2.8).

**Table 2.8.** The BRCA1 domains and motifs

<b>Domains and Motifs</b>	<b>Amino acids</b>	<b>Function</b>	<b>Reference</b>
RING	1-101	E3-ubiquitin ligase	Miki <i>et al.</i> , 1994
NES	81-89	Nuclear export	Rodriguez and Henderson, 2000
Motif 1	123-130	unknown	Orelli <i>et al.</i> , 2001
Motif 2	178-189		Velkova <i>et al.</i> , 2010
Ser 308	308	Aurora A phosphorylation target site	Ouchi <i>et al.</i> , 2004
Motif 3	378-388	Unknown	Orelli <i>et al.</i> , 2001
Motif 4	458-467	Unknown	Orelli <i>et al.</i> , 2001
DNA binding region	452-1079	Binding to branched DNA	Paull <i>et al.</i> , 2001
NLS	503-508, 651-656	Nuclear import	Chen <i>et al.</i> , 1996
Motif 5	512-521	Unknown	Orelli <i>et al.</i> , 2001
Motif 6	845-869	Unknown	Velkova <i>et al.</i> , 2010
Ser 988	988	CHK2 phosphorylation target site	Lee <i>et al.</i> , 2000
Motif 7	1147-1153	Unknown	Orelli <i>et al.</i> , 2001
Ser 1189	1189	Cdk1 phosphorylation target site	Johnson <i>et al.</i> , 2009
Ser 1191	1191	Cdk1 phosphorylation target site	Johnson <i>et al.</i> , 2009
Motif 8	1208-1228	Unknown	Orelli <i>et al.</i> , 2001
Coiled-coil	1369-1418	PALB2 binding	Orelli <i>et al.</i> , 2001
Ser 1387	1387	ATM/ATR phosphorylation target site, intra-S-phase checkpoint	Xu, and Kastan, 2001
Ser 1423	1423	ATM/ATR phosphorylation target site, G2/M checkpoint	Xu, and Kastan, 2001
Ser 1497	1497	Cdk1/Cdk2 phosphorylation target site	Johnson <i>et al.</i> , 2009
Ser 1524	1524	ATM/ATR phosphorylation target site	Cortez <i>et al.</i> , 1999
Ser 1572	1572	CK2 phosphorylation target site	O'Brien <i>et al.</i> , 1999
BRCT 1	1650-1753	DNA damage signaling, transcription	Bork <i>et al.</i> , 1997
BRCT 2	1760-1855	DNA damage signaling, transcription	Bork <i>et al.</i> , 1997



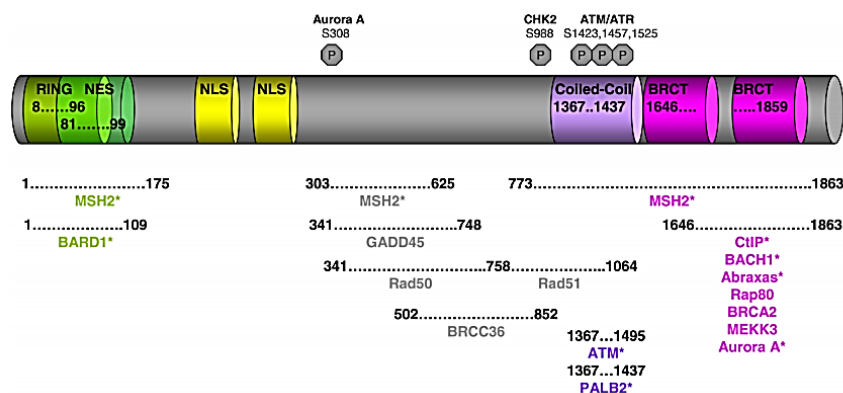


**Figure 2.3.** The BRCA1 functional domain and its partners. BRCA1 contains a RING domain at its *N*-terminus, two nuclear localization sequences (NLS) at the large central segment of BRCA1, two BRCT domains at the C-terminus and a coiled-coil domain upstream of BRCT domains. The interacting proteins are shown under the region of BRCA1 required for their association (Christou and Kyriacou, 2013).

#### 2.4.1 The BRCA1 RING finger domain

The BRCA1 RING finger domain locates on the *N*-terminal region covering 110 amino acid residues (Brzovic *et al.*, 2001). This domain contains zinc atom coordinated with a conservative pattern of cysteine and histidine residues, called a zinc-finger domain (residues 24-64), that is important for the specific coordination with two  $Zn^{2+}$  ions. The NMR solution structure of the BRCA1 RING domain reveals the existence of the antiparallel  $\alpha$ -helices at both ends, flanking the central RING motif characterized by a a central  $\alpha$ -helix, and a short antiparallel three-stranded  $\beta$ -sheets, two large  $Zn^{2+}$ -binding loops (Fig. 2.4) (Brzovic *et al.*, 2001). The two  $Zn^{2+}$ -binding sites are shaped in an interleaved fashion. The zinc binding site I is formed by the first and third pairs of cysteines (Cys24, Cys27, Cys44, and Cys47), and the zinc binding site II is formed by the second and fourth pairs of cysteines and a histidine (Cys39, His41, Cys61, and Cys64). The first residues 1-109 of the BRCA1 protein is a protease-resistance domain that is liable for homodimerization of BRCA1 and heterodimer formation of BRCA1/BARD1 (BRCA1-associated RING-domain protein) (Brzovic *et al.*, 2001; Irminger-Finger *et al.*, 1999). Structure of the BRCA1/BARD1 RING dimer (Fig. 2.4) reveals a 4 helix bundle, forming the binding interface, with residues 8-22 and 81-96 of BRCA1 and residues 36-48 and 101-116 of BARD1 which provide an extensive buried surface area of about 2200  $\text{\AA}^2$ . The BRCA1/BARD1 complex acquires to stabilize the proper conformation of the BRCA1 RING domain for significant exhibiting an E3 ubiquitin ligase activity that specifically transfers ubiquitin to protein substrate, in ubiquitination system (Hashizume *et al.*, 2001).

Approximately 15% of BRCA1 mutations are founded within the RING domain. The most frequent mutations is 185delAG, occurring more than 2000 times (Table 2.6). The finding of the adjacent 188del11 mutation leads to founding of C61G and C64G mutation of BRCA1 (Johannsson *et al.*, 1996). Some mutations in RING domain (Table 2.9) are critical binding sites giving rise to conformation or little structural effect. The BIC reported that mutations in zinc binding site II of RING domain arise ten times more frequently than in site I. The mutations in site II (residues Cys39, Cys61 and Cys64) in the second loop still allow for binding with BARD1 and less disruptive to BRCA1 function (Brzovic *et al.*, 2001), while the missense mutations in site I (residues Cys24, Cys44, or Cys47) affect erroneous protein folding resulting in revoke ubiquitin E3-ligase activity (Brzovic *et al.*, 2003). The two important areas for mutation in *N*-terminal region are the mutations found in RING domain of BRCA1 backbone that destabilize the BRCA1/BARD1 heterodimer and these mutation will impact ubiquitin E3 ligase activity (Morris *et al.*, 2006). These evidences supported a significance of  $Zn^{2+}$  as a structural component, playing critical roles in the stabilization and function of the BRCA1 RING domain.

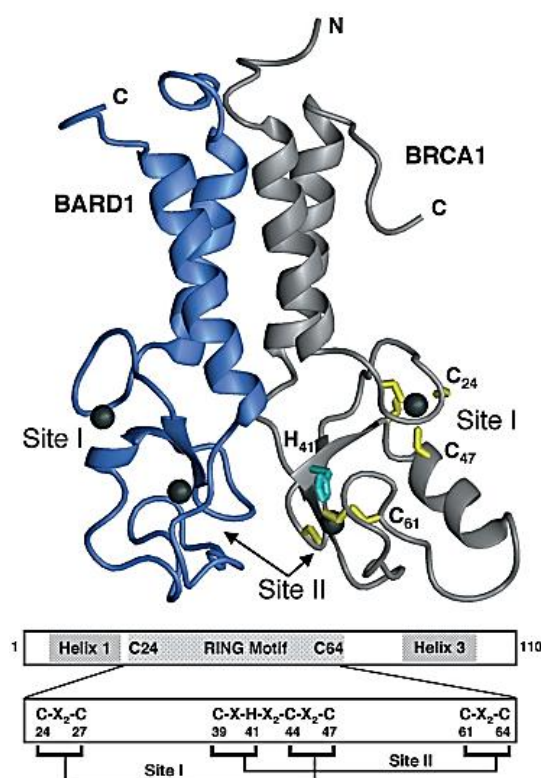


**Figure 2.4.** Top, ribbon representation of the BRCA1/BARD1 heterodimer. Bound  $Zn^{2+}$  ions were represented as spheres. The Cys (yellow) and His (cyan)  $Zn^{2+}$ -liganding residues of Sites I and II in BRCA1 are also shown. Below, the core BRCA1 RING motif (residues 24–64; boxed gray) and the N- and C-terminal helices are shown within the context of the first 110 residues that comprise the BRCA1 RING domain (Brzovic *et al.*, 2001).

**Table 2.9.** The mutations in RING domain and secondary structure effect; a1:  $\alpha$ -helix 1; a2:  $\alpha$ -helix 2; b1:  $\beta$ - sheet 1; b2:  $\beta$ - sheet 2.

<b>Mutation</b>	<b>Structure location</b>	<b>Predicted structure changes</b>	<b>Reference</b>
R7C	Adjacent to a1	Destroy salt bridge wild-type BARD1 Trp34	(Brzovic, 2001)
C24R	Adjacent a1	Alter folding	(Brzovic, 2001)
C44F	b2 surface	Alter folding	(Brzovic, 2001)
C47F	Adjacent to a2	Alter folding	(Brzovic, 2001)
C39S	Between b1-b2	Slight structure alteration	(Brzovic, 2001)
C39R	Between b1-b2	Slight structure alteration	(Brzovic, 2001)
C39Y	Between b1-b2	Slight structure alteration	(Brzovic, 2001)
L52F	a2 surface	Protein-protein interaction	(Brzovic, 2001)
L53F	a2 surface	Protein-protein interaction	(Brzovic, 2001)
C61G	Central motif	Slight structure alteration	(Brzovic, 1998)
C64G	Central motif	Slight structure alteration	(Brzovic, 2001)
C64Y	Central motif	Slight structure alteration	(Brzovic, 2001)
R71G	Central motif	-	(Diez <i>et al.</i> , 2003)

#### 2.4.2 The large central segment of BRCA1

The central region of the BRCA1 protein is present in vertebrates but not in lower eukaryotes (Savage and Harkin, 2014). This region of BRCA1 spans exons 11-13 covering approximately 1500 residues that lack any substantial conserved sequence motifs (Venkitaraman, 2014). No atomic level structures have been identified for this region, however, biophysical characterization showed that this region was intrinsically disordered or negatively unfolded at physical conditions (Mark *et al.*, 2005). This might potentially afford the central region of BRCA1 as a long flexible scaffold that interact with DNA and several proteins involved in a wide range of cellular pathways such as DNA damage response and repair, cell cycle progression, and transcription. The reported binding partners to the central region were RAD50, RAD51, retinoblastoma protein (Rb), c-Myc, p53, FANCA, JunB, PALB2, and BRCA2 (Deng *et al.*, 2000; Rosen *et al.*, 2006; Sy *et al.*, 2009). Exon 11 encodes nearly 60% of the BRCA1 protein that contains two nuclear localization sequences (NLS) (Li and Greenberg, 2012). The NLS sequences are situated in between amino acids 501–507 (NLS1) and 607–614 (NLS2) that interact with importin- $\alpha$ , which responsible for BRCA1 transports from the cytosol to the nucleus (Chen *et al.*, 1996). The L1407P and M1411P were mutations in BRCA1 proteins identified from breast cancer patients. These mutations have shown to interfere with the specific interaction between BRCA1 and PALB2, resulting in the defective HR repair (Sy *et al.*, 2009). In addition, the BIC reported that mutation at Ser1423 abolishes ATM ability to phosphorylate this site (Xu *et al.*, 2001). This suggested that defected HR repair was one of the causes for genomic integrity and tumorigenesis observed in patients, carrying *BRCA1*, *BRCA2*, or *PALB2* mutations.

### 2.4.3 The BRCA1 C-terminal domain

The BRCA1 C-terminal region spans exons 16-24 covering codons 1646-1863 with a tandem repeat of BRCT domain (BRCA1 carboxyl-terminal) (motif 1, amino acids 1653-1736; motif 2, amino acids 1760-1855). Two BRCA1-BRCT interact in a head-to-tail fashion, burying about 1600 Å<sup>2</sup> of hydrophobic, solvent accessible surface area in the interface with a 23-amino acid linker, connecting the two BRCT domains (Fig. 2.5) (Williams *et al.*, 2001). This domain serves as a phosphoprotein interaction module that binds to other BRCT repeats or other protein domains with apparently unrelated structure (Watts and Brissent, 2010). The BRCT domains can recognize pSer (phosphoserine) residues (class I BRCT) or recognize both pSer and pThr (phosphothreonine) residues (class II BRCT) (Yu *et al.*, 2003). In addition, the BRCA1-BRCT domain has been identified to bind the phosphorelated partners that recognize the pSer-X-X-Phe consensus sequence. The binding partners for the BRCT domain, include BACH1, CCDC98/abraxas and CtIP, involved mainly in the control of DNA damage response and the G2/M phase checkpoint (Kim *et al.*, 2007; Yamane *et al.*, 2000; Yu and Chen, 2004; Yu *et al.*, 2003).

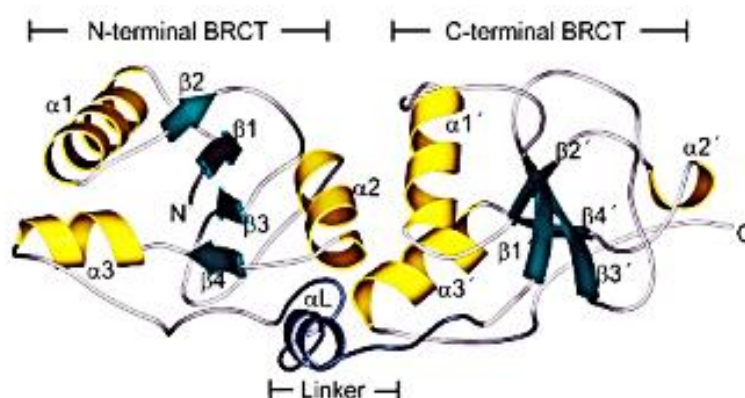


**Figure 2.5.** The structure of the BRCT domain of BRCA1 (Williams *et al.*, 2001).

Numerous novel cancer-predisposing mutations in the BRCT domain of BRCA1 proteins have been reported. These mutations caused the destabilization of the structural integrity at the BRCT active sites, and disrupt the recognition of phosphoprotein partners (Gough *et al.*, 2007; Rowling *et al.*, 2010). The most frequent mutation is 5382insC that is an insertion mutation at codon 1756 causing in a frameshift stop codon at 1829, and results in a premature protein. Furthermore, two cancer causing mutations in BRCT domain of BRCA1 protein (Phe1695Leu and Asp1733Gly) result BRCA1 to bind p53 with similar affinity to 53BP1 (Liu *et al.*, 2006). These evidences provide the better insight into the pathogenic BRCA1 mutations on function and tumorigenesis.

## 2.5 Function of BRCA1 protein

BRCA1 is a tumor susceptibility protein. It is essential to maintain genomic stability through several partner proteins to exert cellular processes including cell cycle checkpoint control, transcriptional regulation, DNA repair, and protein ubiquitination (Fig. 2.6) (O'Donovan and Livingston, 2010; Quinn *et al.*, 2009).

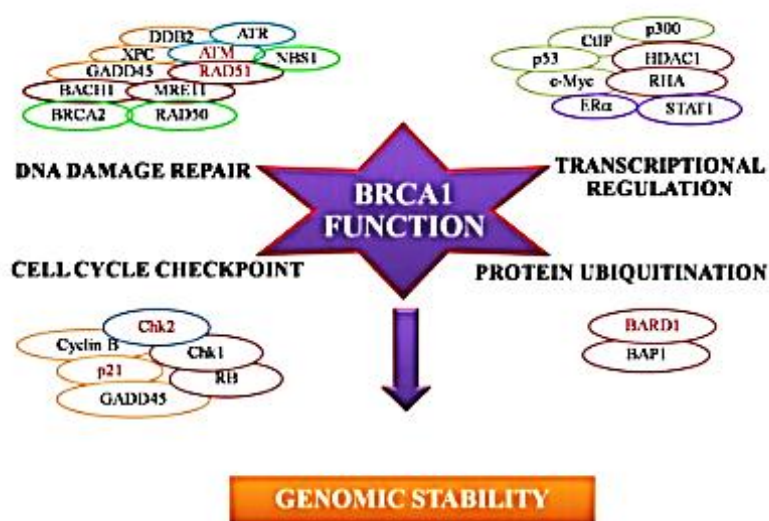


**Figure 2.6.** Schematic representative of cellular function of BRCA1 (Ratanaphan, 2012).

### 2.5.1 BRCA1 and transcription

BRCA1 protein contains transactivation domain (TAD) at its C-terminus that involved in the transcriptional regulation of several genes responsible for DNA damage (Fig.2.7) (Savage and Harkin, 2014). The BRCA1-TAD domain is a co-activator or a co-repressor of transcription that recruits the basal machinery of transcriptional and other proteins that have been involved in chromatin remodeling, such as RNA polymerase II (RNAPII) and histone deacetylase (HDAC) (Mullan *et al.*, 2006; Naseem *et al* 2006). The transcription function of BRCA1 was established by an association between BRCA1-TAD domain and RNAPII as a heterodimer with BARD1. This complex is necessary for ubiquitination and consequent proteasomal degradation of elongating form of RNAPII in a response to UV induced-stalled replication that inhibits transcription-coupled RNA processing and facilitates DNA repair (Kim *et al.*, 2006; Krum *et al.*, 2010). It has been reported that over expression of BRCA1 stimulates transcription of several stress-response factors including p21<sup>waf1/cip1</sup>, p27kip1, GADD45 which modulate transcription of target genes through protein-protein interactions with transcription factors, p53 (Harkin *et al.*, 1999; Kerr and Ashworth, 2001; MacLachlan *et al.*, 2000; Rosen *et al.*, 2006). In contrast, the transcription of an estrogen receptor  $\alpha$  (ER $\alpha$ ) and its downstream estrogen responsive genes could suppress by over expression of BRCA1 that occurs by the association of

BRCA1 (residues 1-300) with the AF2 of ER $\alpha$ . (Fan *et al.*, 1999; Fan *et al.*, 2001). Loss or mutations of the *BRCA1* gene in breast cancer were found to disturb its ability to inhibit ER $\alpha$  activity (Fan *et al.*, 2001). In addition, the p300-mediated ER acetylation, essential for its transactivation function, was inhibited by BRCA1 (Eakin *et al.*, 2007; Fan *et al.*, 1999; Fan *et al.*, 2002; Kim *et al.*, 2006; Ma *et al.*, 2010). Furthermore, BRCA1, together with the transcription factor Oct1 mediated transcription of ESR1 (Chandrasekharan *et al.*, 2013). It has also been described as a co-regulator of the estrogen responsive element (ERE) and AP1 promoters of ER $\alpha$  target genes (Zhou and Slingerland, 2014) and contributes to DNA repair mechanisms (Starita and Parvin, 2006; Saha *et al.*, 2010). Recently, some evidence have demonstrated that methylation within a CpG-rich 109 bp segment in the transactivation of the ER promoter may constitute an important mechanism of epigenetic control that affects the ability of BRCA1 to induce the endogenous ER gene's promoter activity (Archev and Arrick, 2017). Another study has reported that overexpression of BRCA1 also represses the recruitment of the co-activator, amplified breast cancer 1 (AIB1) and steroid receptor co-activator 1 (SRC1), and increased the recruitment of a co-repressor, histone deacetylase 1 (HDAC1), leading to the inhibition of PR activity by preventing PR from its binding to the c-Myc progesterone responsive element (PRE) and probably its mitogenic effect (Katiyar *et al.*, 2009; Ma *et al.*, 2006). Furthermore, the expression of BRCA1 is also required to finite the PI3K-AKT signaling in triple negative breast cancer cells that is a critical guardian factor for mitogenic pathways (Ibrahim *et al.*, 2012; Ma *et al.*, 2006).

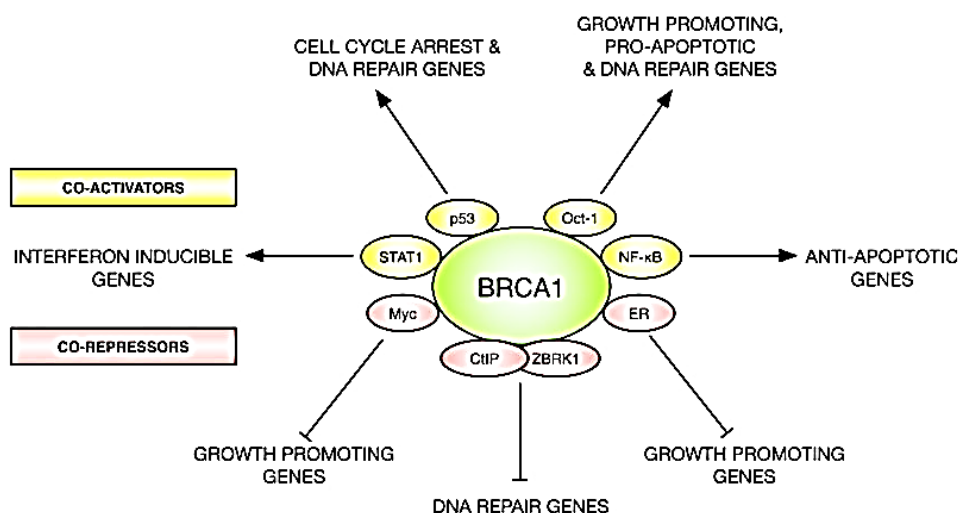


**Figure 2.7.** BRCA1 transcriptional complexes. BRCA1 forms co-repress and co-activate genes involved in diverse cellular processes (Savage and Harkin, 2014).

### 2.5.2 BRCA1 and cell cycle control

Cell cycle checkpoints play an essential role in cell survival by preventing the propagation of DNA damage through cell cycle progression before DNA repair. Failure of cell cycle checkpoints can lead to the acquisition and accumulation of genetic alterations and chromosomal abnormalities. It is well established BRCA1 is likely involved in all phases of the cell cycle progression and plays an important role in DNA damage sensing. BRCA1 has been shown to play numerous roles in cell growth control (Fig. 2.8) (Christou and Kyriacou, 2013). Overexpression of BRCA1 were reported to stimulate transcription of p21 gene, which resulted in cell cycle arrest at the G1/S phase (Li *et al.*, 1999). The BRCA1/BARD1 complex has been shown to be required for ATM/ATR-mediated phosphorylation of Chk2 and p53 at Ser15 after ionizing radiation-induced DNA damage which is required for G1/S-phase arrest via transcriptional induction of p21 (Fabbro *et al.*, 2004). In addition, BRCA1 has been shown to have a direct transcriptional role in the regulation of cyclin-dependent kinase inhibitor p27, leading to S phase arrest (Willimson *et al.*, 2002). Along with these roles in the activation and maintenance of G1/S-phase checkpoint, BRCA1 has also been demonstrated to be a transcriptional regulator of several genes associated with the regulation of the G2/M checkpoint (Xu *et al.*, 2001). As well, it has been reported to transcriptionally repress cyclin B that is responsible for activating cell division cycle 2 (*cdc2*) kinase and mitotic entry (MacLachlan *et al.*, 2000). Additionally, BRCA1 could transcriptionally stimulate a number of G2/M checkpoint regulatory genes such as growth arrest and DNA-damage-inducible protein 45 (GADD45), *wee1* kinase, or the chaperone protein 14-3-3 $\sigma$  which deters the *cdc2*-cyclinB mitotic kinase complexes by the deportation of *cdc2*, the inhibitory phosphorylation of *cdc2*, or by the deportation of *cdc25C* in the cytoplasm (Hutchins and Clarks, 2004; Mullan *et al.*, 2006; Yarden *et al.*, 2002). In addition, the BRCA1-A complex, (BRCA1/RAP80/BRCC36/45/ MERIT40/Abraxas), has been reported to inhibit DNA end resection and stabilize DNA damage signaling from the break site that promotes G2/M checkpoint arrest after DNA damage (Coleman and Greenberg, 2011; Hu *et al.*, 2011), while, the BRCA1-B complex (BRCA1/TopBP1/BACH1) has been reported to play a role in HR in S-phase (Xie *et al.*, 2012). The BRCA1-C complex consists of CtIP and the MRN (Mre11/Rad50/Nbs1). These complexes have been shown to triggering the initiation of double strand break (DSB) end resection, which is considered to help regulate the choice to repair DSBs via HR in S/G2 phase cells (Escribano-Diaz *et al.*, 2013).



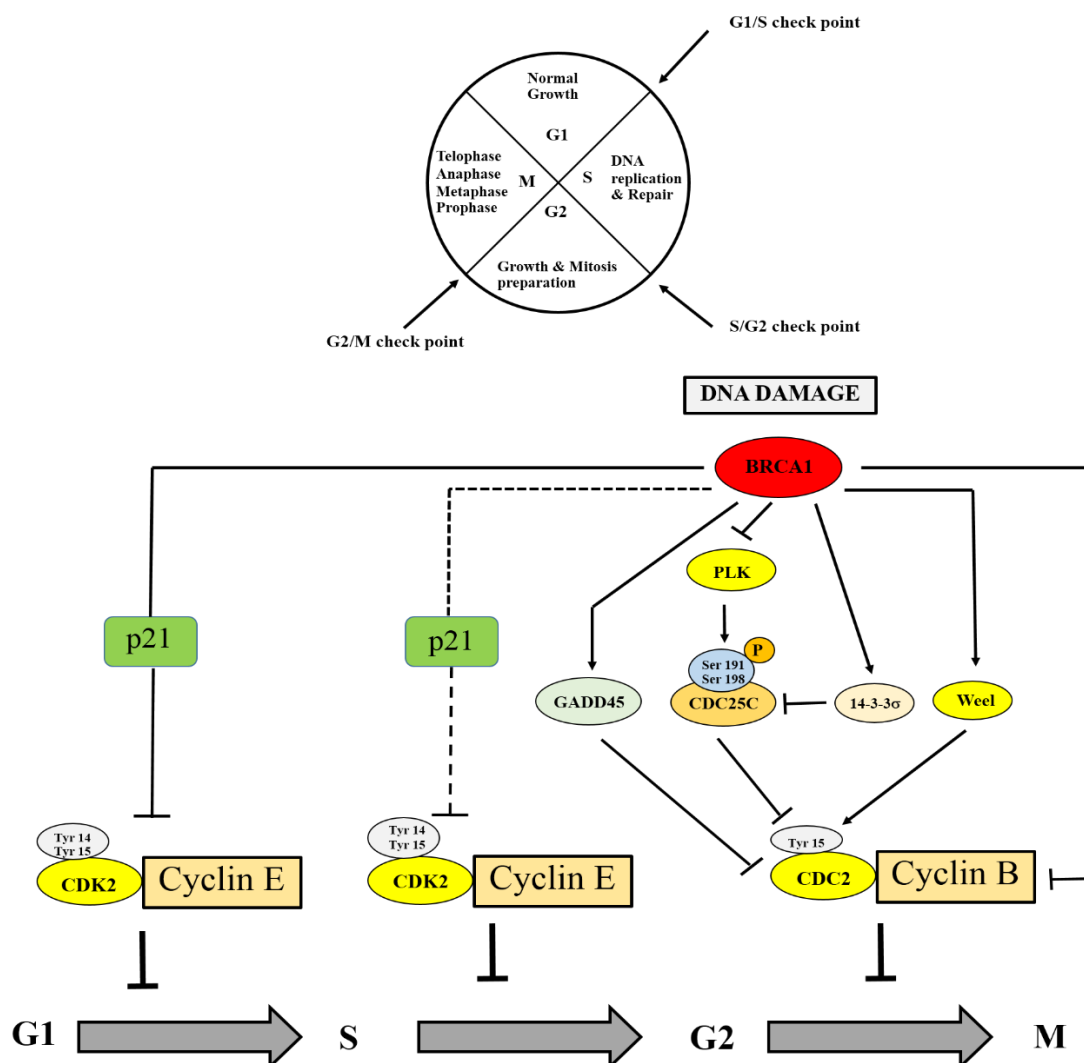


**Figure 2.8.** An overview of cell cycle regulation mediated by BRCA1 and its associated proteins (Christou and Kyriacou, 2013).

### 2.5.3. BRCA1 and apoptosis

Role of BRCA1 in apoptosis is intimately connected with its role in cell cycle regulation and DNA damage since apoptosis is a final outcome of prolonged cell cycle arrest as well as excessive DNA damage (Christou and Kyriacou, 2013). There has been demonstrated that BRCA1 is implicated in apoptosis both as a suppressor and an inducer. Some reports have suggested that BRCA1 is able to inhibit apoptosis (Irminger-Finger *et al.*, 2001; Quinn *et al.*, 2003). The status of BRCA1 and the regulation of apoptosis-related genes have been reported. For case in point, the expression of BRCA1 is positively-correlated with anti-apoptotic *Bcl-2* expression (Freneaux *et al.*, 2000; Wang *et al.*, 2011; Yang *et al.*, 2002), while, in some cancer cells, overexpression of wild type-BRCA1 was shown to down-regulate *Bax* expression (MacLachlan *et al.*, 2000). Overexpression of BRCA1 induced apoptosis through JNK/SAPK (c-Jun N-terminal Kinase/Stress-Activated Protein Kinase) as



well as Fas/Fas ligand-dependent apoptotic pathway (Harkin *et al.*, 1999; Quinn *et al.*, 2003). Recently, BRCA1 has shown to regulate the p53 inducible gene 3 (PIG3), which is a downstream target of p53 and is involved in p53-initiated apoptosis, mediated apoptosis in a p53-dependent manner (Zhang *et al.*, 2015). BRCA1/NF- $\kappa$ B (p65 subunit) has also been shown to inhibit apoptosis (Harte *et al.*, 2014). This complex constitutively binds to the promoters of a number anti-apoptotic NF- $\kappa$ B target genes, including *Bcl-2*. In addition, chemotherapy-induced apoptosis was also modulated by BRCA1. It facilitates resistance to a wide range of DNA-damaging agents, including cisplatin and etoposide, while sensitizing breast cancer cells to apoptosis induced by paclitaxel and vinorelbine (anti-microtubule agents) (Quinn *et al.*, 2003).

#### **2.5.4 BRCA1 and chromatin modification**

BRCA1 also plays a role in DNA decatenation through direct interaction with topoisomerase II $\alpha$  and regulates topoisomerase activity and distribution by ubiquitination (Pageau and Lawrance, 2006). Topoisomerase II $\alpha$  is essential for chromosome decatenation after DNA replication and its inhibition results in a defect in chromosome segregation. Similar defects are apparent after loss of BRCA1. Chromatin remodeling surrounding the sites of DSBs mediated by histone acetyltransferases (HATs) and other chromatin remodeling factors participates in DNA repair by dissolving higher order chromatin structure otherwise interfering with recruitment of DNA repair proteins to DSB sites. BRCA1 also interacts with HATs complex, paralogous histone acetyltransferases CBP and p300 (CBP and p300 are well known to function as transcriptional coactivators by producing “relaxed” chromatin accessible to transcription factors), which are key regulators of homologous recombination (Ogiwara and Kohno, 2012). In addition, BRCA1 has been linked to ubiquitin conjugates on chromatin at sites of DNA breaks. Recent evidence revealed that BRCA1/BARD1 ubiquitin ligase activity counteracts chromatin barriers to DNA resection (Densham *et al.*, 2016). BRCA1/BARD1 as a histone H2A-specific E3 ligase, helping to explain its localization and activities on chromatin in cells (Kalb *et al.*, 2014). Defects in BRCA1 E3 function are linked with a derepression of satellite DNA that is accompanied by decompaction of chromatin and reduced levels of ubiquitylated histone H2A (H2Aub) (Zhu *et al.*, 2011). BRCA1 may participate in DNA repair not only as a scaffold protein by orchestrating DNA repair proteins interactions but also by direct regulation of chromatin structure and its accessibility to DNA repair (Downey and Durocher, 2006; Yarden and Brody, 1999).

#### **2.5.5 BRCA1 and centrosome dynamics**

The centrosome functions as the principal microtubule-organizing center in animal cells. They are responsible for controlling the number, polarity, localization, shape, etc. of microtubules. Centrosomes normally controls cell motility and adhesion in interphase, and facilitate the organization of the spindle poles during mitosis (Bettencourt-Dias and Glover, 2007). Defects in the spindle pole-organization function of centrosomes arise in many cancers and are associated with genomic instability. Irregular centrosomes may provide increase to aberrant cell division.

Centrosomes were also reported to be a part of a signaling network connecting cell cycle arrest and repair signals in response to DNA damage. BRCA1 localizes to centrosome during mitosis (Lotti *et al.*, 2002) as well as interphase (Sankaran *et al.*, 2005). BRCA1 may control centrosome amplification in breast cells by preventing centrosome reduplication as HCC1937 breast cancer cells lacking functional BRCA1 have amplified centrosomes (Schlegel *et al.*, 2003). Depletion of BRCA1 resulted in centrosome amplification in human breast cells, but not in non-breast cells (Lingle *et al.*, 1998; Starita *et al.*, 2004; Xu *et al.*, 1999). This suggests that breast cells growing in culture are dependent on BRCA1 for centrosome regulation. BRCA1 binds to centrosomes in a  $\gamma$ -tubulin-dependent manner. Expression of the BRCA1  $\gamma$ -tubulin binding domain alone reduces BRCA1 at the centrosome and results in multipolar spindles. BRCA1 is phosphorylated in S-phase and in cells with DNA damage, and a reduction in BRCA1 phosphorylation results in reduced binding of BRCA1 to  $\gamma$ -tubulin and centrosomes and an induction of multipolar spindles (Xu *et al.*, 1999).

### 2.5.6 BRCA1 and DNA damage and repair

In eukaryotic cells, there are two primary mechanisms of DSBs repair. Homologous recombinant repair (HR) is the error-free process used in the cell cycle (during the S and G2 phases) when sister chromatids are available as templates. Non-homologous end-joining (NHEJ) is a process of ligating DSB ends together without a homologous template. It is the predominant mechanism in cells during G0, G1, and early S phases of the cell progression, and is considered as an error-prone process (Yang and Xia, 2010).

Several lines of evidences indicated that BRCA1 was involved in DNA damage response and DNA repair via HR pathway (Savage and Harkin, 2015; Venkitaraman, 2014) (Fig. 2.9). The significance of BRCA1 and HR was observed by the experiments that BRCA1-deficient mouse embryonic stem cells displayed a defective homologous repair of chromosomal DSBs, and an increased frequency of non-homologous recombination (Snouwaert *et al.*, 1999). This impairment could be corrected by the reconstruction of wild-type-BRCA1 (Snouwaert *et al.*, 1999). The BRCA1 forms stable complex with the BRCA2 and mediates HR repair. BRCA1/BRCA2 complex has a well-known role in HR through direct interaction with the mammalian homolog of the *Escherichia coli* RecA protein (RAD51) (Bhattacharyya *et al.*, 2000). RAD51, DNA recombinase, catalyzes strand exchange in an early step of HR (Baumann and West, 1997). Recently, PALB2 (the partner and localizer of BRCA2 protein) has been identified as the linking factor essential for the BRCA1/BRCA2 association (Rahman *et al.*, 2007). The BRCA1/PALB2 complex was conducted by interface of their individual coiled-coil domains that was founded to stimulate HR-mediated repair (Rahman *et al.*, 2007). Particularly, missense mutations of BRCA1 in the PALB2-binding region disturbed the specific BRCA1/PALB2 interaction, and decreased DNA repair (Sy *et al.*, 2009). However, a precise mechanism of the PALB2-BRCA2-RAD51 complex that promotes HR by BRCA1 remains largely unclear.

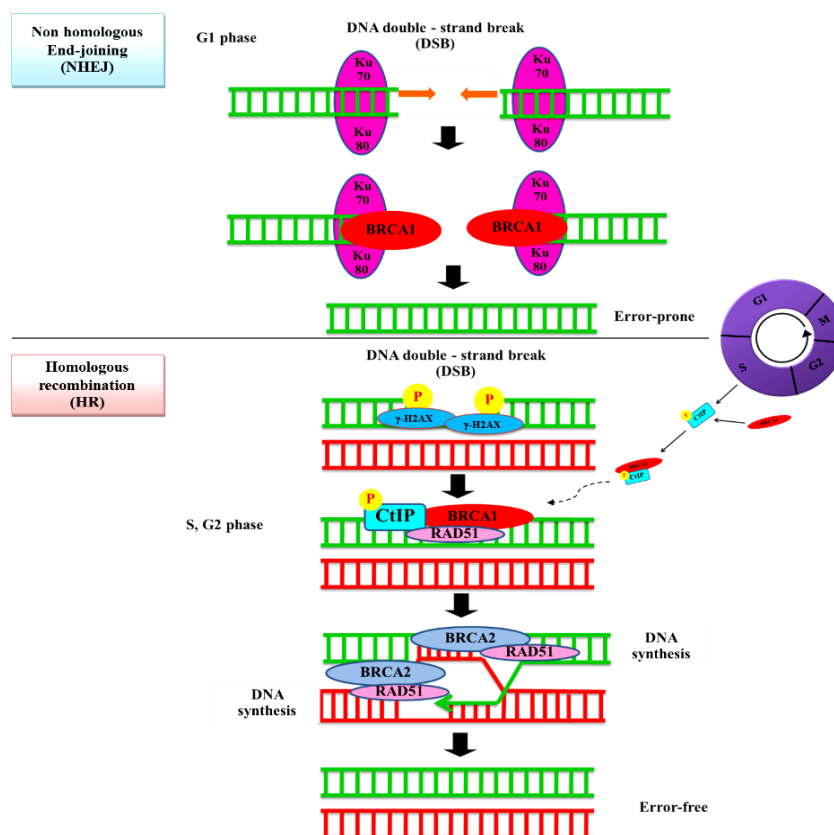


**Figure 2.9.** Proposed schematic overview of BRCA1-mediated homologous recombination (HR) repair (Hongthong and Ratanaphan, 2016).

Compared to relatively well-defined role of BRCA1 in HR, the role of BRCA1 in NHEJ is far less clear and often conflicting (Zhang and Powell, 2005). The main evidence for BRCA1 role in NHEJ comes from its interaction with MRN complex, which is known to play a role in both HR and NHEJ (Fu *et al.*, 2003). There is also evidence that HNEJ pathway is compromised in *BRCA1*<sup>-/-</sup> mouse embryonic fibroblast (Zhong *et al.*, 2002) and *BRCA1*-defective HCC1937 human breast cancer cell line (Bau *et al.*, 2004). However, some evidence suggest more prominent role of MRN complex in HR compared to NHEJ. Possible existence of HNEJ sub-pathways was suggested and BRCA1 may play role only in particular NHEJ sub-pathway, which repairs DNA damage with higher fidelity comparable to HR (Bau *et al.*, 2006). In addition, a *BRCA1* mutant (PI42H) failed to associate with a NHEJ factor Ku80 and to restore to irradiation in *BRCA1*-deficient cells (Chiba and Parvin, 2001; Wei *et al.*, 2008). These might be given a molecular basis of the involvement of BRCA1 in the NHEJ pathway of the DSBs repair process. Recently, a role for BRCA1 in base excision repair (BER) of oxidative DNA damage has been reported, finding that *Brcal*<sup>-/-</sup> mouse mammary epithelial cells (MMECs) exhibited greater sensitivity to methyl methanesulfonate (MMS) alkylating agent than isogenic *Brcal*<sup>+/+</sup> MMECs (Alli and Ford, 2015). These suggested that BRCA1 play a role beyond double-strand break repair.

### 2.5.7 BRCA1 and protein ubiquitination

The demonstration of BRCA1 RING domain function as an E3 is of particular significance given the crucial role of ubiquitination for eukaryotic cell viability. Failings in ubiquitination affect a host of cellular processes including cell-cycle progression, cell differentiation, apoptosis, the response to DNA damage, DNA repair, and transcription (Brzovic *et al.*, 2003). Ubiquitination is a one of post-translational modification process that it is responsible for conventionally targeting proteins for proteasome-dependent degradation and playing roles in various cellular processes, including protein transport, and DNA repair (Bergink and Jentsch, 2009). The biochemical steps in the ubiquitin pathway involves three steps (Fig. 2.10), generally requiring ubiquitin (Ub)-activating enzyme (E1), ubiquitin conjugating enzyme (E2) and ubiquitin ligase (E3). At the beginning, E1 stimulates Ub by a ATP dependent activation at the C-terminal glycine of Ub and cysteine residues of E1 which linked via a thioester bond resulting an E1–Ub intermediate. The Ub is then transferred to an E2 by transesterification. Then, the Ub moiety delivers to protein targets and specifically attached to the  $\epsilon$ -amino group of a lysine on its protein substrates, typically using an E3 as the catalyst (Vierstra, 2003). Upon completion, the deubiquitylating enzymes (DUBs) can eradicate ubiquitin molecules that are attached to proteins (Hochstrasser, 2009).

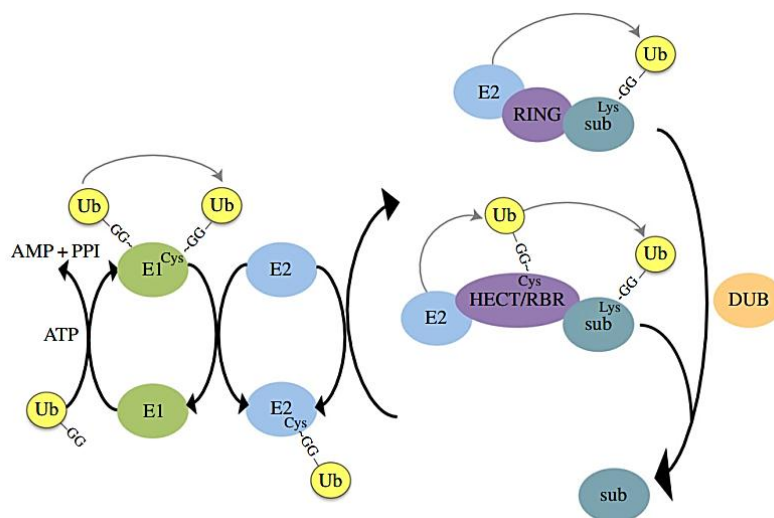


**Figure 2.10.** Overview of the ubiquitination pathway (Brown and Jackson, 2015)

The Ub is a small protein that contains 76 amino acids (~8.5 kDa) and is highly conserved among the eukaryotes. The function of Ub depends on the key features of the Ub protein include its C-terminal and the seven lysine (Lys) residues (located at positions 6, 11, 27, 29, 33, 48 and 63) which allow the formation of poly-Ub chains (Fig. 2.11). Notably, proteins labeled with different ubiquitin topologies or linkages between ubiquitin moieties are channeled to vastly different biological outcomes (Fig. 2.12) (Baer and Ludwig, 2002; Mersick and Greenberg, 2009; Sokratous *et al.*, 2014). Mono-ubiquitination is involved in different cellular processes such as endocytosis, DNA repair, histone regulation and protein transport.

Multi-ubiquitination is also implicated in endocytosis (Fig. 2.12) (Lub *et al.*, 2016). By contrast, the role for poly-ubiquitin chain varies widely, depending on the type of linkage (Fig. 2.13). For example, Lys48- and Lys29-linked poly-ubiquitin chains classically signal the target protein for proteasomal degradation (Chen *et al.*, 2002; Sokratous *et al.*, 2014), while Lys63 and Lys6-linked poly-ubiquitin chains act as a stimulation trigger in several pathways involving in DNA damage and repair (Ohta and Fukuda, 2004 Sokratous *et al.*, 2014), the inflammatory response (Sun and Chen, 2004), protein trafficking (Hicke and Dunn, 2003) and regulation of protein synthesis (Spence *et al.*, 2000). Some evidence has been reported that Lys11-linked chains function as potent regulator of cell division (Sokratous *et al.*, 2014). However, several evidences indicated that BRCA1-BARD1 predominantly catalyses K6-linked poly-ubiquitin chains could signal a process other than degradation, such a DNA repair pathway (Nishikawa *et al.*, 2004; Sokratous *et al.*, 2014; Wu-Baer *et al.*, 2003).

As mentioned earlier, the *N*-terminal region of BRCA1 RING domain has shown an E3 ubiquitin ligase activity, and this activity is enhanced when it heterodimerizes with the BARD1 RING domain (Xia *et al.*, 2003). Cancer-predisposing mutations in the BRCA1 RING domain are thought to lose an E3 ligase activity, and affect the other functions of BRCA1, such as ability to activate the G2-M checkpoint, and response to DNA damage (Ruffner *et al.*, 2001). However, the specified protein substrate of BRCA1 E3 ligase activity and biological significance to tumor suppression function are still unknown. The putative substrates for BRCA1 E3 ligase have been discovered from both *in vitro* and *in vivo* studies (Irminger-Finger *et al.*, 2016).

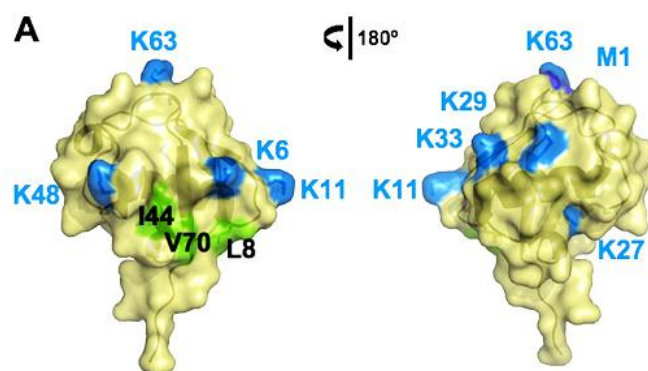


**Figure 2.11.** Illustration of ubiquitin represents all seven lysines (K6, K11, K27, K29, K33, K48, and K63) and the amino-terminus (M1). It can be conjugated to the carboxy-terminus of another protein substrate (PDB accession no. 1UBQ) (Messick and Greenberg, 2009).

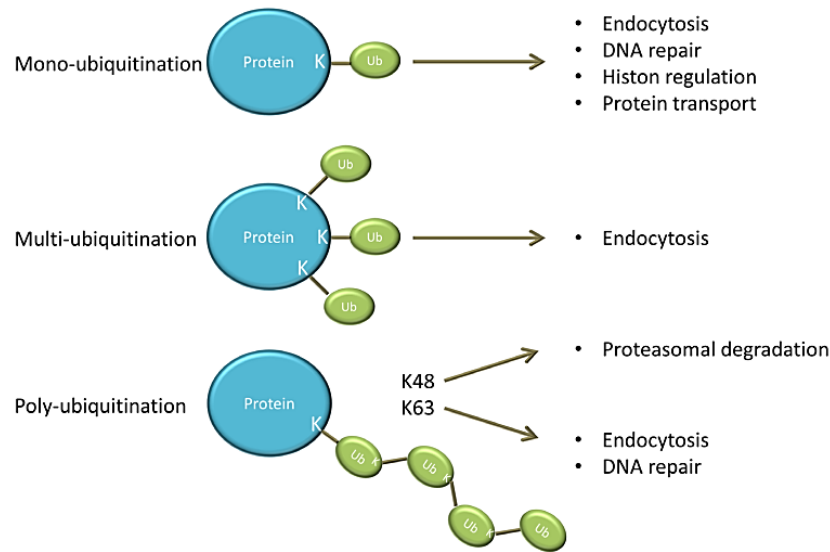


**Figure 2.12.** Different forms of ubiquitin modification (Lub *et al.*, 2016).

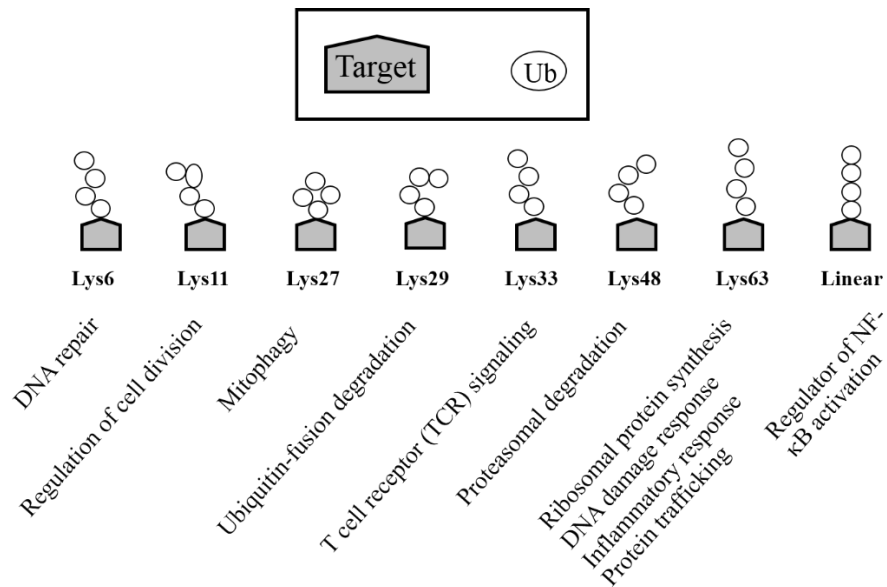


**Figure 2.13.** Cellular pathways associated with polyubiquitin chains of a specific topology (Sokratous *et al.*, 2014).

One of the well-known substrate of the BRCA1/BARD1 RING complexes is  $\gamma$ -tubulin (Joukov *et al.*, 2006; Parvin, 2009). The  $\gamma$ -tubulin was ubiquitinated by BRCA1/BARD1 E3 Ub-ligase required for proper organization of microtubules within centrosomes through targeting the protein TPX2 to spindle poles (Joukov *et al.*, 2006). In addition, nucleoplasmin B23 (NMP1) was found to be the candidate substrate of the BRCA1 E3 ligase activity *in vivo* (Sato *et al.*, 2004). These evidences suggested that ubiquitination of  $\gamma$ -tubulin and nucleoplasmin B23 played a

dynamic role in regulating the centrosome number and kept of genomic stability by unidentified mechanisms. Several evidences have been reported that histones H2A and its variant H2AX are mono-ubiquitinated by the BRCA1 E3 ligase (Chen *et al.*, 2002; Krum *et al.*, 2010; Malley *et al.*, 2002; Pan *et al.*, 2011). Furthermore, two RING finger E3 ubiquitin ligase activities (RNF8 and BRCA1) have recently been shown to sequentially recruit at the site of DNA damage (Foulkes, 2010). RNF8 catalyzes Lys63-linked poly-ubiquitin chains on H2AX (Wang and Elledge, 2007). Ubiquitinated H2AX recruits the BRCA1-Abraxas-RAP80 complexes through the RAP80 ubiquitin-interacting motif (UIM) (Sobhian *et al.*, 2007). BRCA1/BARD1 heterodimer exhibited E3 ligase that required for the recruitment of BRCA2 and RAD51 to damaged sites for HR repair (Ransburg *et al.*, 2010). This suggested that regulation of chromatin structure in the framework of transcriptional regulation and DNA repair was controlled by a BRCA1 function. Inactivation of BRCA1 E3 ligase decreased chromatin-bound claspin levels and weakened homology-directed DNA repair by disturbing signal transduction from the damage-activated ATR kinase to CHK1 (Sato *et al.*, 2012). This suggested that the BRCA1 E3 ligase selectively activated claspin-CHK1 activation and provided evidence for the BRCA1 E3 ligase-dependent mechanism in cellular responses to DNA damage. Specificity for RNAPII ubiquitination was determined by phosphorylation of YSPTSPS heptapeptide repeat motif in its carboxyl terminal domain (CTD) which involved in a response to UV irradiation. However, only hyper-phosphorylation of RNAPII on Ser5 within heptapeptide repeat is ubiquitinated by BRCA1/BARD1 (Starita *et al.*, 2005). The BRCA1-mediated ubiquitination of RNAPII also inhibited the assembly of basal transcription factors at the promoter (TFIIE and TFIIH) to form a stable transcriptional pre-initiation complex that disrupted the initiation of mRNA synthesis was established (Horwitz *et al.*, 2007). The BRCA1-mediated ER $\alpha$  E3 ligase ubiquitination and degradation that may represent the regulatory mechanism for repression of ER $\alpha$  transcriptional activity by BRCA1 (Dizin and Irminger-Finger, 2010; Eakin *et al.*, 2007). Furthermore, the BRCA1/BARD1 E3 ligase was also responsible for ubiquitination and degradation of progesterone receptor (PR) in the absence of hormone. These suggested that BRCA1 regulated progesterone and estrogen signaling. The phosphorylated CtIP binds to the BRCT domains of BRCA1. The BRCA1 mediated-CtIP ubiquitination is responsible for ionizing radiation causing the migration of CtIP to insoluble chromatin-containing fraction of cell lysates and does not resulting in proteasomal degradation. It indicated the role in cell cycle checkpoint in response to DNA damage (Yu *et al.*, 2006). In contrast, some evidence reported that BRCA1 autoubiquitination, and BRCA1 mediated-nucleophosmin/B23 ubiquitination were inhibited by BAP1 (BRCA1-associated protein 1), which is a deubiquitinating enzyme that can interact with the BRCA1 RING domain (Nishikawa *et al.*, 2009). The postponement of the S phase and ionizing hypersensitivity of irradiation in cells were resulted from down-regulation of BAP1. Furthermore, the regulation of ubiquitination during a DNA damage response and the cell cycle was controlled by corporation of the BRCA1-BARD1 complex and the BAP1 protein (Nishikawa *et al.*, 2009). However, further elucidations are required for a better understanding of these biological significances. Several BRCA1 RING domain mutations abolished the E3 ligase activity, the ability to accumulate at damaged sites and the HR repair required for tumor suppression (Morris *et al.*, 2006;

Ransburgh *et al.*, 2010). Consequently, the loss of the E3 ligase activity resulted in hypersensitive of cancerous cells to DNA-damaging agents, indicating an important role for ubiquitination in the DNA damage response and DNA repair activity (Ransburgh *et al.*, 2010; Ruffner *et al.*, 2001). Therefore, ubiquitination involved in the key steps that properly conduct the DNA repair after DSBs. Targeting the ubiquitin-proteasome system is potentially exploited for both molecular diagnosis and novel strategies in cancer therapy (Hoelloer and Dikic, 2009).

## 2.6 The ubiquitination systems in cancer therapy

Recently, the bortezomib is the most clinically successful ubiquitin proteasome system-active agent that is limited in application for the treatment of multiple myeloma and mantle (Chen *et al.*, 2011). However, the molecular targeting of specific ubiquitin system for cancer therapy has also emerged as a valid therapeutic strategy, and several targets are currently being explored. Several lines of evidence have implicated that some small molecules targeted general factors in the ubiquitin system including E1, E2, E3 enzymes that affect protein signaling or proteasome-mediated degradation (Fig. 2.13) (Bedford *et al.*, 2011; Liu *et al.*, 2015). Interestingly, several groups have been developing powerful inhibitors for E1 or E2 protein, but devoid of specificity hindered the use of these types of inhibitors in their clinical applications. Conversely, high selectivity to substrate proteins of E3 ligases protein are a more promising therapeutic target for cancer treatment with less effects to target. To date, small-molecule inhibitors of the p53-HDM2 E3 ligase has reached clinical trials (Patel and Player, 2008).

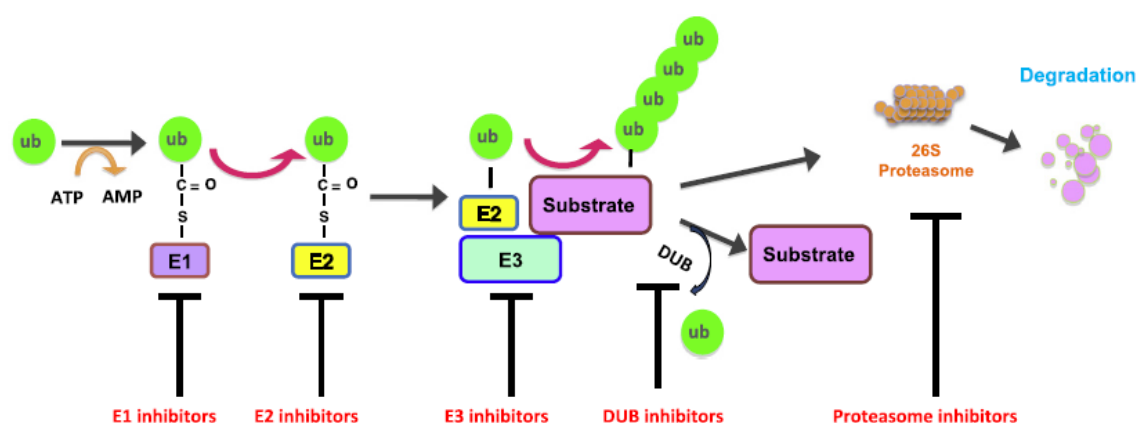


**Figure 2.14.** Potential inhibitors for E1, E2, or E3 enzymes have currently been developed for cancer therapy. (Liu *et al.*, 2015).

### 2.6.1 Targeting the E1 enzyme

Several inhibitors have been reported to target the Ub-activating enzyme E1 (Table 2.10). The E1-targeting compounds, panepophenanthrin and its derivatives, were reported to inhibit the ubiquitin-E1 interaction that did not affect cell growth (Lei *et al.*, 2003; Matsuzawa; *et al.*, 2006; Moses *et al.*, 2003; Sekizawa *et al.*,



2002). A marine fungal metabolite, Himeic acid A, also showed an inhibitory effect on E1 catalytic activity (Tsukamoto *et al.*, 2005). HDAC inhibitor, Largazole, exhibited the anti-proliferation in lung cancer cells (Wu *et al.*, 2013) and disrupted the ubiquitin-adenylate interaction (Ungermannova *et al.*, 2012). Hyrtioreticulins A and B, identified from sponge, exhibited the most potent E1 inhibitor (Yamanokuchi *et al.*, 2012). Several evidences have indicated that an adenosine sulfamate analog formed strongly adducts with ubiquitin molecules at the active site of the E1 enzyme and completely inhibited the ubiquitin activation process (Chen *et al.*, 2011). Recently, PYR41, a new cell permeable inhibitor of E1, has been reported to block the initiation of ubiquitination and inhibited the degradation of I $\kappa$ B $\alpha$  and p53 (Yang *et al.*, 2005; Yang *et al.*, 2007). However, more studies on these inhibitors are needed to establish it as a potential anticancer drug.

**Table 2.10** The list of compounds targeting E1 enzymes.

Compound	Target and function	Reference
Panepophenanthrin	Inhibits the ubiquitin/E1 binding, but inhibit cell growth	Sekizawa <i>et al.</i> , 2002; Moses <i>et al.</i> , 2003; Lei <i>et al.</i> , 2003; Li <i>et al.</i> , 2010
RKTS-80, -81, and -82	Cell-permeable E1 inhibitors	Matsuzawa <i>et al.</i> , 2006
Himeic acid A	Targeting on E1 catalytic activity	Tsukamoto <i>et al.</i> , 2005
Largazole	Histone deacetylase inhibitor; disturbs the ubiquitin-adenylate formation	Ungermannova <i>et al.</i> , 2012
Hyrtioreticulins A	inhibits E1 activity	Yamanokuchi <i>et al.</i> , 2012
Adenosine sulfamate analog	Targeted ubiquitin; binds at the active site of the E1 enzyme, and blocks the ubiquitin activation process	Chen <i>et al.</i> , 2011
PYR-41	Blocks the ubiquitination of TRAF6 and prevents the proteasomal degradation of I $\kappa$ B $\alpha$ and p53	Yang <i>et al.</i> , 2007
PYZD-4409	Inhibits the ATP-dependent activation of the E1 enzyme and induces cell death in hematologic malignant cell lines	Xu <i>et al.</i> , 2010
NSC624206	Prevents the I $\kappa$ B $\alpha$ and p53 proteasomal degradation	Yang <i>et al.</i> , 2007
E1 inhibitors	Block E1-dependent ATP-PP exchange activity, resulting in the loss of E1 thioester and inhibition of the E1-E2 transthioylation	Chen <i>et al.</i> , 2011

### 2.6.2 Targeting the E2 enzyme

Several studies have demonstrated the E2 inhibitors that suppress E2 catalytic activity (Table 2.11). The UBC13-UEV1A E2 complex is responsible for the K48- and K63-linkage poly-ubiquitination chain on a substrate protein through the addition of other ubiquitin molecules to the K63 and K48 residue of ubiquitin (Petroski *et al.*, 2007). A cyclic peptide, Leucettamol A, Manadosterols A and B, have been shown to interfere with the interaction of UBC13-UEV1A complex (Tsukamoto *et al.*, 2008). Recently, Cdc34, one of the E2 enzyme, has been reported as a target for CC0651 inhibitors that suppressed accumulation of Skp2 substrate p27 in human cancer cell lines and inhibited cell proliferation (Ceccarelli *et al.*, 2011; Harper *et al.*, 2011).

**Table 2.11** The list of compounds targeting E2 enzymes.

Compound	Target and function	Reference
CC0651	Cdc34 inhibitor, cell proliferation was suppressed, leading to accumulation of Skp2 substrate p27	Ceccarelli <i>et al.</i> , 2011; Harper <i>et al.</i> , 2011
NSC697923	Inhibitor of the Ubc13-Uev1A E2 enzyme blocks the formation of the E2-Ub thio-ester conjugate	Pulvino <i>et al.</i> , 2012
Leucettamol A	Targeted the interaction of UBC13-UEV1A complexes, inhibits the function of these complexes	Tsukamoto <i>et al.</i> , 2008
Manadosterols A and B	the UBC13-UEV1A complex inhibitors	Ushiyama <i>et al.</i> , 2012

### 2.6.3 Targeting E3 ligases

E3 ubiquitin ligases are a large family of proteins that engaged in the regulation of turnover and activity of many target proteins. There have been demonstrated that abnormal regulation of some E3 ligase involved in cancer development (Bielskienià *et al.*, 2015; Goka and Lippman, 2015; Kang and Sun, 2014). In addition, some E3 ubiquitin ligases are frequently overexpressed in human cancers that correlate well with increased chemo-resistance and poor clinic prognosis. Therefore, E3 ubiquitin ligase could be a better approach for developing anticancer with less side effect. Several E3 ligases inhibitors have been extensively studied (Table 2.12).

**Table 2.12** The list of compounds targeting E3 ligases.

Target	Compound	Target and function	Reference
Fbw7	Oridonin (diterpenoid compound)	It was extracted from medicinal plants. This compound induces cell cycle arrest and apoptosis in myeloid leukemia cells	Huang <i>et al.</i> , 2012
Fbw7	Genistein (A biplanar dicarboxylic acid compound)	It inhibits cell growth and invasion in pancreatic cancer cells via upregulates Fbw7 expression	Ma <i>et al.</i> , 2013
Fbw7	SCF-12 (A biplanar dicarboxylic acid compound)	It alters its substrate binding pocket and delay recognition of phosphodegron on substrates	Orlicky <i>et al.</i> , 2010
Skp2	Compound CpdA	Preventing p27 recruitment to form Skp2 ligase complex by increasing p27 levels in cancer cells	Chen <i>et al.</i> , 2008
Skp2	SMIP0004	Skp2 inhibitor	Rico-Bautista <i>et al.</i> , 2010
Skp2	Compound 25 (SZL-P1-41)	Skp2-mediated E3 ligase inhibitor	Chan <i>et al.</i> , 2013
Skp2	Curcumin, Vitamin D3, quercetin, silibinin, lycopene, epigallocatechin-3-gallate.	It inhibits the Skp2 expression in human cancers	Huang <i>et al.</i> , 2008; Huang <i>et al.</i> , 2013; Roy <i>et al.</i> , 2007; Yang and Burnstein, 2003;
$\beta$ -TrCP	Erioflorin (from <i>Eriophyllum lanatum</i> )	It inhibits the $\beta$ -TrCP/substrates interaction	Blees <i>et al.</i> , 2012
Fbx13	KL001	It blocks Fbx13 binding to pocket in CRY substrates	Nangle <i>et al.</i> , 2013
Fbxo3	BC-1215	Competitive inhibitor that inhibits the substrate binding to Fbxo3	Mallampalli <i>et al.</i> , 2013
Cdc20	Pro-TAME	It prevents APC activation by Cdc20 and Cdh1	Zeng, and King, 2012
Cdc20	Apcin	It inhibits the Cdc20-mediated ubiquitylation of D-box-containing substrates	Sackton <i>et al.</i> , 2014
Cdc20	Tosyl-L-arginine methyl ester	Blocks the APC/C-Cdc20 and APC/C-Cdh1 interaction	Sackton <i>et al.</i> , 2014
Cdc20	NAHA (a novel hydroxamic acid-derivative)	It down-regulates the Cdc20 expression in breast cancer cells	Jiang <i>et al.</i> , 2012
Cdc20	Medicinal mushroom blend	It suppresses the expression of Cdc20 in breast cancer cells	Jiang and Sliva, 2010

**Table 2.12** The list of compounds targeting E3 ligases (cont.).

<b>Target</b>	<b>Compound</b>	<b>Target and function</b>	<b>Reference</b>
Cdc20	Ganodermanontriol (GDNT) (a ganoderma alcohol from medicinal mushroom)	It inhibits the expression of Cdc20 in breast cancer cells	Jiang <i>et al.</i> , 2011
Mdm2	Nutlin-3	It specifically targets MDM2-p53 interaction	Voltan <i>et al.</i> , 2013
Mdm2	RITA	It specifically targets MDM2-p53 interaction	Vassilev <i>et al.</i> , 2004
Mdm2	MI-63	It specifically targets MDM2-p53 interaction	Lub <i>et al.</i> , 2015
Mdm2	Mel 23	It inhibit MDM2 autoubiquitination	Herman <i>et al.</i> , 2011
Mdm2	HL198	Inhibit MDM2 autoubiquitination	Yang <i>et al.</i> , 2005
Mdm2	Serdemetan	Inhibit MDM2 E3 ligase activity. Increases p53 levels and signaling, with cancer cell death	Khoury and Domling, 2012
Mdm2	MMRi6 and its analog MMRi64	Disrupting Mdm2–MdmX E3 ligase activity toward Mdm2 and p53 substrates in vitro and activating p53 in cells.	Wu <i>et al.</i> , 2015
BCA2	Disulfiram	Inhibited BCA2 mediated E3 ligase activity	Brahemi <i>et al.</i> , 2010
BRCA1/BARD1	Cisplatin, trans-platin, oxaliplatin, carboplatin	Inhibited BRCA1/BARD1 mediated E3 ligase activity	Atipairin <i>et al.</i> , 2011

The S-phase kinase associated protein (Skp2) plays a crucial role in the development and progression of human cancers (Wang *et al.*, 2012). It has been found that Skp2 targets and degrades its ubiquitination targets such as p27, p21, p57, FOXO1, and E-cadherin (Inuzuka *et al.*, 2012; Liu and Mallampalli, 2016; Wang *et al.*, 2014). Since Skp2 could be a vision target for cancer therapy, targeting Skp2 could take uses for various human cancers treatment with abnormal activation or Skp2 overexpression (Chan *et al.*, 2014). Therefore, selective small molecule inhibitors for Skp2 have been established which reported in Table 2.12.

Meanwhile, the NF- $\kappa$ B pathway, involved in inflammation and cell survival, was regulated by the RING E3 ligase TRAF6 (TNF receptor-associated factor 6) (Deng *et al.*, 2000). In addition, inhibition of TRAF6-mediated E3 ligase activity by benzoxadiazole derivatives could be appropriate to the treatment of inflammation and cancers (Chen, 2005). Furthermore, F-box and WD repeat domain-containing 7 (Fbw7) exhibited E3 ubiquitin ligase activity. Several onco-proteins have been reported to serve as the substrate of Fbw7 mediated-ubiquitin E3 ligase including c-Myc (Moberg *et al.*, 2004; Welcker *et al.*, 2004; Yada *et al.*, 2004), c-Jun (Nateri *et al.*, 2004; Wei *et al.*, 2005), NF- $\kappa$ B2 (Nuclear factor- $\kappa$ B2) (Fukushima *et al.*, 2012), Cyclin E (Koepp *et al.*, 2001), mTOR (mammalian target of rapamycin) (Mao *et al.*, 2008), Mcl-1 (Myeloid cell leukemia-1) (Inuzuka *et al.*, 2011), HIF-1 $\alpha$  (Hypoxia inducible factor-1 $\alpha$ ) (Flugel *et al.*, 2012), MED13 (Mediator 13) (Zhao *et al.*, 2010), and G-CSFR (Granulocyte colony stimulating factor receptor) (Lochab *et al.*, 2013). Fbw7 expression and activities are critical role in tumor suppression. Therefore, regulating Fbw7 E-3 ligase function could be a promising approach for treating cancers. Several Fbw7 inhibitors are summarized in Table 2.12.

An interesting validated target would be Mdm2 (murine double minute 2), a member of the RING E3 family. The p53-binding of Mdm2 or Hdm2 (human counterpart of Mdm2) binds to the tumors suppressor p53, whereas the RING domain acts as an E3 ubiquitin ligase to promote rapid degradation of p53 (Haupt *et al.*, 1997). It suggests that Mdm2 is a critical regulator of p53 stability (Wu *et al.*, 2001). Inhibition of MDM2-mediated p53 ubiquitination by E3 inhibitor, Nutlins and RITA, are reported that it directly targets the protein-protein interaction of p53-Mdm2 resulting in disrupt Mdm2-p53 complexes. The decreased p53 ubiquitination also results an increasing p53 levels and inhibit osteosarcoma and colon carcinoma cell lines proliferation in a p53-dependent manner (Issaeva *et al.*, 2004; Vassilev *et al.*, 2004). Some of these inhibitors, such as Ke-43, isoindolin-1-onebased inhibitors or 1,4-benzodiazepinedine derivatives, specifically inhibit the growth of a p53-positive prostate cancer cell line (Ding *et al.*, 2006; Grasberger *et al.*, 2005; Hardcastle *et al.*, 2005). Furthermore, HLI98, A family of 5-deazaflavin derivatives, has been documented as inhibiting Mdm2 ubiquitin ligase activity which stabilize p53 and Mdm2, and induce apoptosis (Yang *et al.*, 2005). In addition, several groups have reported that the small molecules specifically target Mdm2-p53 interaction that are summarized in Table 2.12. However, those compounds need to be verified as leading candidates for the development of anti-cancer drugs based on inhibition of Mdm2-mediated E3 ubiquitin ligase activity.

Several candidate substrates for the BRCA1/BARD1 RING complex have developed from *in vitro* studies, such as BRCA1 itself, histones,  $\gamma$ -tubulin, RNAPII, ER $\alpha$ , and CtIP (Chen *et al.*, 2002; Dizin and Irminger-Finger, 2010; Eakin *et al.*, 2007; Malley *et al.*, 2002; Starita *et al.*, 2005; Yu *et al.*, 2006; Wu-Bear *et al.*, 2010). Therefore, BRCA1-dependent ubiquitination is possibly accountable for modifying many cellular activities. Wide examinations have demonstrated the significance of the BRCA1-mediated E3 ubiquitin ligase activity to its tumor suppression function. It has been reported that the BRCA1-mediated E3-ubiquitin ligase activity is inactivated by platinum (Pt)-based drugs (Atipairin *et al.*, 2010; Atipairin *et al.*, 2011a; Atipairin *et al.*, 2011b). Pt -BRCA1 forms adducts was founded at His117 of BRCA1 protein, resulting in altered the conformation of this protein and inhibited the E3-ubiquitin ligase activity (Atipairin *et al.*, 2010; Atipairin *et al.*, 2011a). Similarly carboplatin, oxaliplatin as well as transplatin all inactivated the BRCA1-mediated E3 ligase activity at therapeutically appropriate concentrations (Atipairin *et al.*, 2011a). In addition, the mutation of the RING domain of the BRCA1 protein causes a loss of the E3 ubiquitin ligase activity, conferring hypersensitivity of the cancerous cells to DNA-damaging agents (Atipairin *et al.*, 2011b).

## 2.7 Zinc Finger proteins

### 2.7.1 Classification of Zinc Finger proteins

Approximately 10% of the human genome encodes zinc proteins. Zinc is an essential metal in biology of over 300 enzymes, being essential for growth and development (Pace and Weerapana, 2014). Zinc can bind to protein in different ways (Fig. 2.15) It can be categorized into two main classifications: i) Catalytic zinc in enzymes, which zinc ion functions as a Lewis acid; ii) Structural zinc in proteins, be important for maintaining protein structure and stability which it is an essential for protein function (Anzellotti and Farrell, 2008).

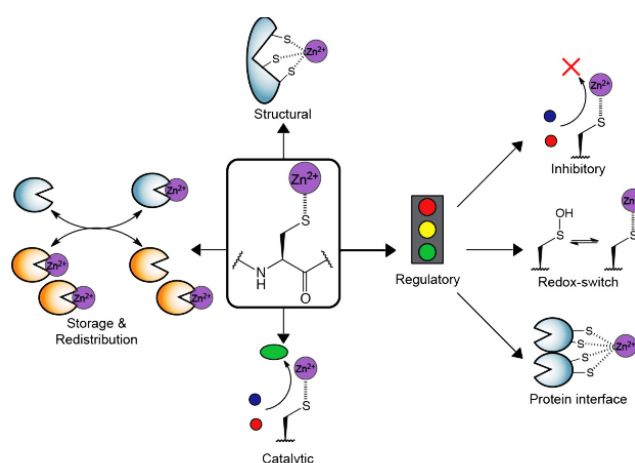


**Figure 2.15.** Zinc ions ( $\text{Zn}^{2+}$ ) have the ability to be chelated to cysteine residues within protein scaffolds. These resulting  $\text{Zn}^{2+}$ -cysteine complexes participate in a variety of functional roles, including structural, catalytic, regulatory and transport (Pace and Weerapana, 2014).

Zinc finger (ZF) proteins contribute in protein-nucleic acid and protein-protein interactions in various groups of proteins and show a various role in several cellular processes, such as transcriptional activation, DNA recognition and repair, RNA packaging, protein folding and assembly, cellular signaling and apoptosis, and lipid binding (de Almeida *et al.*, 2013). ZF proteins share several features as follows (Gamsjaeger *et al.*, 2007; Matthews and Sunde, 2002; Michalek *et al.* 2011):

- (i) The amino acids that serve as coordinating ligands are always four cysteine and/or histidine residues,
- (ii) The coordination number is always four
- (iii) The geometry at the Zn(II) center is always close to tetrahedral

In addition, ZF proteins contain multiple domains that bind zinc and fold individually, and in some cases even function individually (Andreini *et al.*, 2011). ZF proteins can be collective into at least 14 different classes of ZFs which is referred to as the “classical ZF” and at least 13 other classes of “non-classical” ZFs have been identified (Michalek *et al.*, 2011).

### **2.7.2 Targeting zinc finger protein for therapeutic diseases**

ZF proteins function in various cellular processes which are essential for cell growth and development. Substitution or coordination of zinc with another metal causes a loss of tertiary structure leading to impair or loss of protein function (Gaynor and Griffith, 2012; Levina and Lay, 2011; Pysz *et al.*, 2010). The most coordination compounds can incorporate into the active-site metal ion, interact with residues around the active site or interfere with the cysteine residues on the protein’s ZF motif, resulting in tertiary structure distortion, displacement of the Zn ion, and loss of functions (Fricker, 2006; Gaynor and Griffith, 2012; Wester, 2007; Weissleder and Pittet, 2008). Several evidences suggest that ZF proteins are recognized more frequently as possible medicinal targets for direct implications in health and disease such as HIV, cancer, and bacterial infection among which demonstrated targeting ZF motif in the several proteins such as, HIV nucleocapsid NCp7 protein, poly(ADP-ribose) polymerase 1 (PARP1), DNA polymerase  $\alpha$ , estrogen receptor-DNA binding domain (DBD), breast cancer-associated gene 2 (BCA2), and human papillomavirus (HPV) E6 protein which are summarized in Table 2.13.

**Table 2.13.** The list of compounds targeting zinc finger proteins.

Disease	Compound	Target	Reference
HIV	Phenyl-thiadiazolylidene-amine derivative (WDO-217)	NCp7	Vercruyssen <i>et al.</i> , 2012
	N,N-bis(1,2,3-thiadiazol-5-yl)benzene-1,2-diamine	NCp7	Pannecouque <i>et al.</i> , 2010
	3-nitrosobenzamide (NOBA)	NCp7	Rice <i>et al.</i> , 1993
	2,2-dithiobisbenzamide (DIBA)	NCp7	Rice <i>et al.</i> , 1995
	cyclic 2,2-dithiobisbenzamide	NCp7	Witvrouw <i>et al.</i> , 1997
	1,2-dithiane-4,5-diol-1,1-dioxide	NCp7	Rice <i>et al.</i> , 1997a
	Azadicarbonamide (ADA)	NCp7	Rice <i>et al.</i> , 1997b
	Pyridinioalkanoyl thioesters (PATEs)	NCp7	Turpin <i>et al.</i> , 1999
	S-acyl-2-mercaptobenzamide thioesters (SAMTs)	NCp7	Jenkins <i>et al.</i> , 2005
	Benzisothiazol-3-one derivatives	NCp7	Loo <i>et al.</i> , 1996
	Gold(I)-phosphine-N-peterocycles	NCp7	Abbehausen <i>et al.</i> , 2013; Abbehausen <i>et al.</i> , 2016
	<i>Cis</i> and <i>trans</i> -[PtCl <sub>2</sub> (NH <sub>3</sub> ) <sub>2</sub> ]	NCp7	Tsotsoros <i>et al.</i> , 2015
	[Au(dien)(N-heterocycle)] <sup>3+</sup>	NCp7	Spell and Farrell, 2015
	Auranofin	NCp7	Morelli <i>et al.</i> , 2016
	Platinum(II) and Gold(III) complexes containing tridentate ligands	NCp7	Bernardes <i>et al.</i> , 2016
	[Pt(dien)(nucleobase)] <sup>2+</sup>	NCp7	Tsotsoros <i>et al.</i> , 2017
	[MCl(dien)]Cl (M = Pt, Pd, Au; dien = diethylenetriamine)	NCp7	de Paula <i>et al.</i> , 2009 Tsotsoros <i>et al.</i> , 2014
Cisplatin	Retroviral nucleocapsid protein (PyrZf18)	Morelli <i>et al.</i> , 2013	



**Table 2.13.** The list of compounds targeting zinc finger proteins (cont.).

<b>Disease</b>	<b>Compound</b>	<b>Target</b>	<b>Reference</b>
Bacterial infection	Bismuth antiulcer drugs	chaperonin	Cun and Sun, 2010
	Selenium containing analogues	$\gamma$ -Butyrobetaine hydroxylase (BBOX)	Rydzic <i>et al.</i> , 2014
Cancer	Disulfiram (DSF)	breast cancer-associated protein 2 (BCA2)	Brahemi <i>et al.</i> , 2010
	Disulfiram (DSF)	histone demethylase JMJD2A	Sekirmik <i>et al.</i> , 2009
	2-thioxanthine	DNA glycosylases	Biela <i>et al.</i> , 2014
	Au(I) and Au(III) compounds	thioredoxin	Berners-Price, <i>et al.</i> , 2011 Bindoli <i>et al.</i> , 2009
	Au(I) and Au(III) compounds	glutathione peroxidase	De Luca <i>et al.</i> , 2013 Ilari <i>et al.</i> , 2012
	Au(I) and Au(III) compounds	trypanothione reductase	De Luca <i>et al.</i> , 2013 Ilari <i>et al.</i> , 2011
	Arsenite	PARP1 and XPA	Ding <i>et al.</i> , 2009; Hartwig, <i>et al.</i> , 2003; Qin <i>et al.</i> , 2012; Walter, <i>et al.</i> , 2007; Zhou <i>et al.</i> , 2011; Huestis <i>et al.</i> , 2016
	Arsenite	PARP1	Sun <i>et al.</i> , 2014; Zhou <i>et al.</i> , 2016
	Arsenite and Arsenic trioxide	PARP1	Zhou <i>et al.</i> , 2014
	Quinone and indandione	Transcriptional coactivators p300	Jayatunga <i>et al.</i> , 2015
	Cisplatin	ZF motif of BRCA1 protein	Atipairin <i>et al.</i> , 2010, Atipairin <i>et al.</i> , 2011a Atipairin <i>et al.</i> , 2011b
	Cisplatin	DNA polymerase I	Maurmann and Bose, 2010
	Cisplatin	DNA polymerase-alpha	Kelley <i>et al.</i> , 1993
	disulfide benzamide benzisothiazolone derivatives	estrogen receptor DNA-binding domain	Wang <i>et al.</i> , 2004

**Table 2.13.** The list of compounds targeting zinc finger proteins (cont.).

<b>Disease</b>	<b>Compound</b>	<b>Target</b>	<b>Reference</b>
Cancer	Divalent ions of barium, copper, iron, lead, manganese, nickel and tin	estrogen receptor DNA-binding domain	Deegan <i>et al.</i> , 2011
	Cadmium(II)	Metallothionein, the Zn-proteome of pig kidney LLC-PK <sub>1</sub> cells	Namdarghanbari <i>et al.</i> , 2016
	RAPTA-C and its analogues	PARP1	Wang <i>et al.</i> , 2013
	Gold(III) complex [Au <sup>III</sup> (terpy)Cl]Cl <sub>2</sub> (Auterpy)]	Cys <sub>4</sub> zinc finger domains	Jacques <i>et al.</i> , 2015
	Cisplatin and miR-128	zinc-finger E-box-binding homeobox 1	Sun <i>et al.</i> , 2015

## 2.8 Classical anticancer drugs

### 2.8.1 Platinum-based drugs

Cisplatin and its analogs, carboplatin and oxaliplatin, are the US-FDA approved Pt-based drugs and are widely used in the treatment of cancer (Fig. 2.16). Since the discovery of cisplatin in 1965, and its cytotoxic properties opened new avenue for the application of metal complexes in cancer therapy (Fig. 2.16, Fig.2.17) (Trudu *et al.*, 2015). In general, the drugs require an intracellular activation in which the leaving groups, surrounding the Pt center, are replaced by water molecules. The activated (aquated) of Pt-based drugs can interact with the biomolecules which contain nucleophilic groups such as, DNA and RNA proteins (Jordan and Carmo-Fonseca, 2000). Cisplatin and carboplatin form similar platinum-DNA cross-links, whereas oxaliplatin, containing the non-leaving group (1*R*,2*R*-diamminocyclohexane), exhibits different DNA cross-links and accounts for its different spectrum of activity (Dasari and Tchounwou,2014; Mehmood , 2014; Muggia, 2009; Sousa *et al.*, 2014; Woynarowski *et al.*, 2000). However, the application of platinum-based drugs is restricted by their severe toxicity and drug resistance (Jakupec *et al.*, 2008; Wong and Giandomenico, 1999). Hence, the search for new platinum-containing anticancer agents has continuously developed to overcome Pt-drug resistance and reduce the severe side effects with wider anticancer spectrum. Surprisingly, only nedaplatin [*cis*-diamineglycolatoplatinum(II)], lobaplatin [1,2-diaminomethylcyclobutaneplatinum(II) lactate] and heptaplatin [*cis*-malonato [(4*R*,5*R*)-4,5-bis (aminomethyl)-2-isopropyl-1,3- dioxolane] platinum(II)] (Fig. 2.16) have been permitted as the anticancer drugs restrictly used in Japan, China and South Korea, respectively (Hartinger *et al.*, 2006; Muhammad and Guo, 2014). However, limitation of their successful therapeutic use is severe side effects and activity in a limited spectrum of tumors as well as cellular resistance. As a result, the Pt(IV) complexes have been developed. The rationales behind the design of Pt(IV) complexes are the fine tuning of their redox potential, kinetic stability, hydrophilicity/lipophilicity to achieve desired reactivity and activity through selection of axial and equatorial ligands (Muhammad and Guo, 2014). The first introduction of orally administered Pt(IV) carboxylate complex, such as satraplatin (Fig. 2.16) has been evaluated in the preclinical phase (Wexselblatt and Gibson, 2012; Wheate *et al.*, 2010).

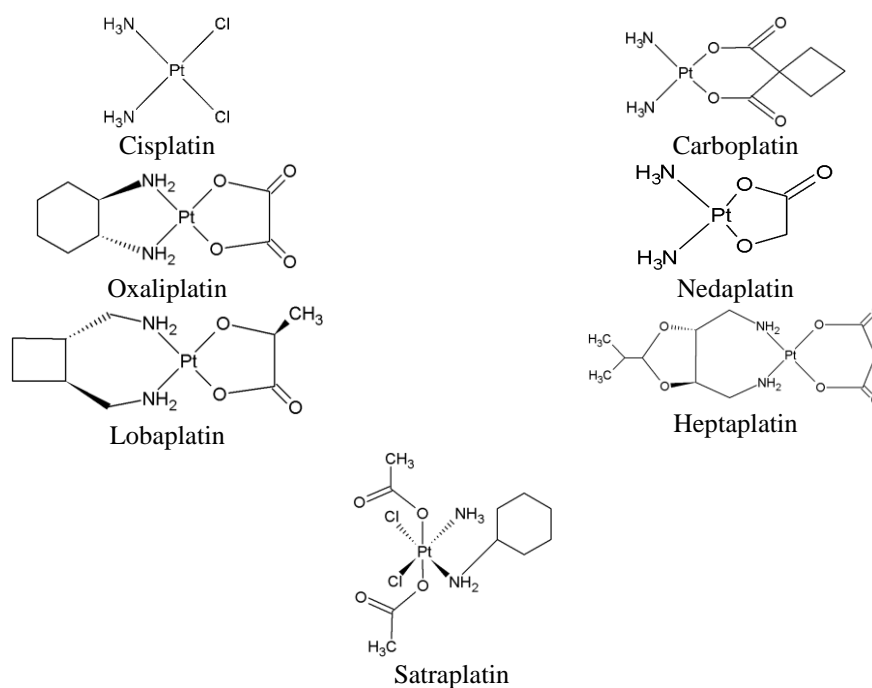


**Figure 2.16.** Structure of platinum-based anticancer drugs.

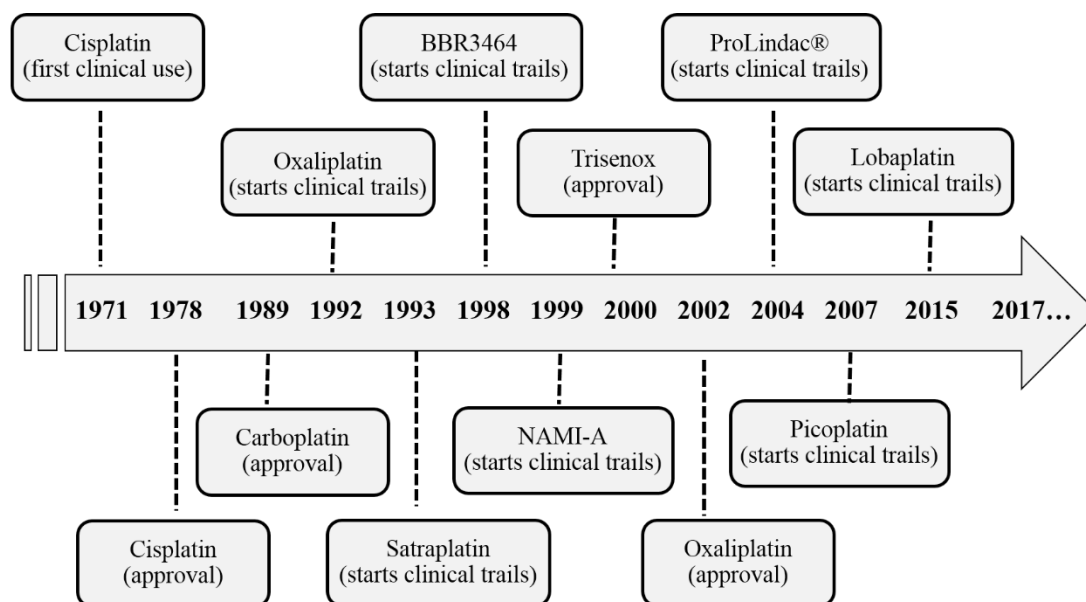


**Figure 2.17.** Historical overview of the cytotoxic metal and metalloids complexes that have been approved or entered the clinical practice (Trudu *et al.*, 2015).

## 2.9 Non-classical anticancer drugs

According to the previously mentioned problems in the limitation of clinical application of cisplatin and its analogs, the search for new anticancer drugs has extended beyond platinum species. The extensive investigations have examined the alternative metal centers such as rhodium, gold, iridium, osmium or ruthenium. Ruthenium complexes have been of significant prominence with several drug candidates underwent clinical trials.

### 2.9.1 Ruthenium-based drug

Ruthenium is a transition metal in the group VIIB and the fifth period of the periodic table. Its atomic number and atomic weight are 44 and 101.07. Ruthenium possesses three properties that make it theoretically suitable for medicinal use. These are (1) slow ligand exchange kinetics, (2) multiple accessible oxidation states, and (3) the ability to mimic iron in binding to certain biological molecules (Allardyce and Dyson, 2001). Ruthenium compounds offer the potential ability over the antitumor platinum(II) complexes such as reduced toxicity, a novel mechanism of action, no cross-resistance and different spectrum of activity, providing ruthenium compounds well suited for medicinal applications (Allardyce and Dyson, 2001). The low toxicity of ruthenium drugs results from similar ligand exchange kinetics to those of platinum(II) complexes, and different oxidation states under physiological conditions. Ruthenium is able to mimic iron in binding to carrier proteins such as transferrin, required for rapidly growing tumor cells for iron uptake (Allardyce and Dyson, 2001; Jakupc *et al.*, 2005; Wong *et al.*, 2014).

### 2.9.2 Classification of ruthenium-based drugs

Several ruthenium compounds (Fig. 2.18) have been shown to inhibit DNA replication, possess mutagenic activity, bind to nuclear DNA and reduce RNA synthesis, similar to cisplatin but they displayed lower *in vitro* anticancer activity (Brabec and Novakova, 2006). To date, two ruthenium(III) complexes have successfully completed phase I/II clinical trials; namely, NAMI-A ((ImH)[*trans*-Ru(III)Cl<sub>4</sub>Im(Me<sub>2</sub>SO)]]; Im = imidazole) (Leijen *et al.*, 2015), and KP1019, indazolium *trans*-[tetrachlorobis(1*H*-indazole)ruthenate(III)] (Groessler *et al.*, 2010; Hartinger *et al.*, 2006; Trondl *et al.*, 2014). Studies have shown that these drug candidates are efficiently taken up into the cells, probably via interactions with transferrin (Frasca *et al.*, 2001; Polec-Pawlak *et al.*, 2006; Pongratz *et al.*, 2004), where they induce a B-cell lymphoma 2 (*Bcl-2*)-mediated apoptosis (*Bcl-2* is a gene family that regulates mitochondrial permeability and has been linked to drug resistance) (Polec-Pawlak *et al.*, 2006). Thus, such compounds are highly valuable for overcoming the limitations of cisplatin in tumor with overexpression of *Bcl-2*. Some mechanisms of action of NAMI-A have been proposed as the following: interaction with the cell cycle regulation culminating in transient accumulation of cell in the G<sub>2</sub>/M phase (Bergamo *et al.*, 1999; Zorzet *et al.*, 2000), interaction with collagens of the extracellular matrix (Casarsa *et al.*, 2004; Gava *et al.*, 2006; Sava *et al.*, 2003; Sava *et al.*, 2004), inhibition of matrix metalloproteinase (Vacca *et al.*, 2002), and

coordination to nucleic acid (Pluim *et al.*, 2004). Unlike NAMI-A, KP1019 is thought to possess direct cytotoxic activity by promoting apoptosis in a number of cancer cell lines as well as in a range of tumor models, especially colorectal cancers (Galanski *et al.*, 2003; Kapitzka *et al.*, 2005).

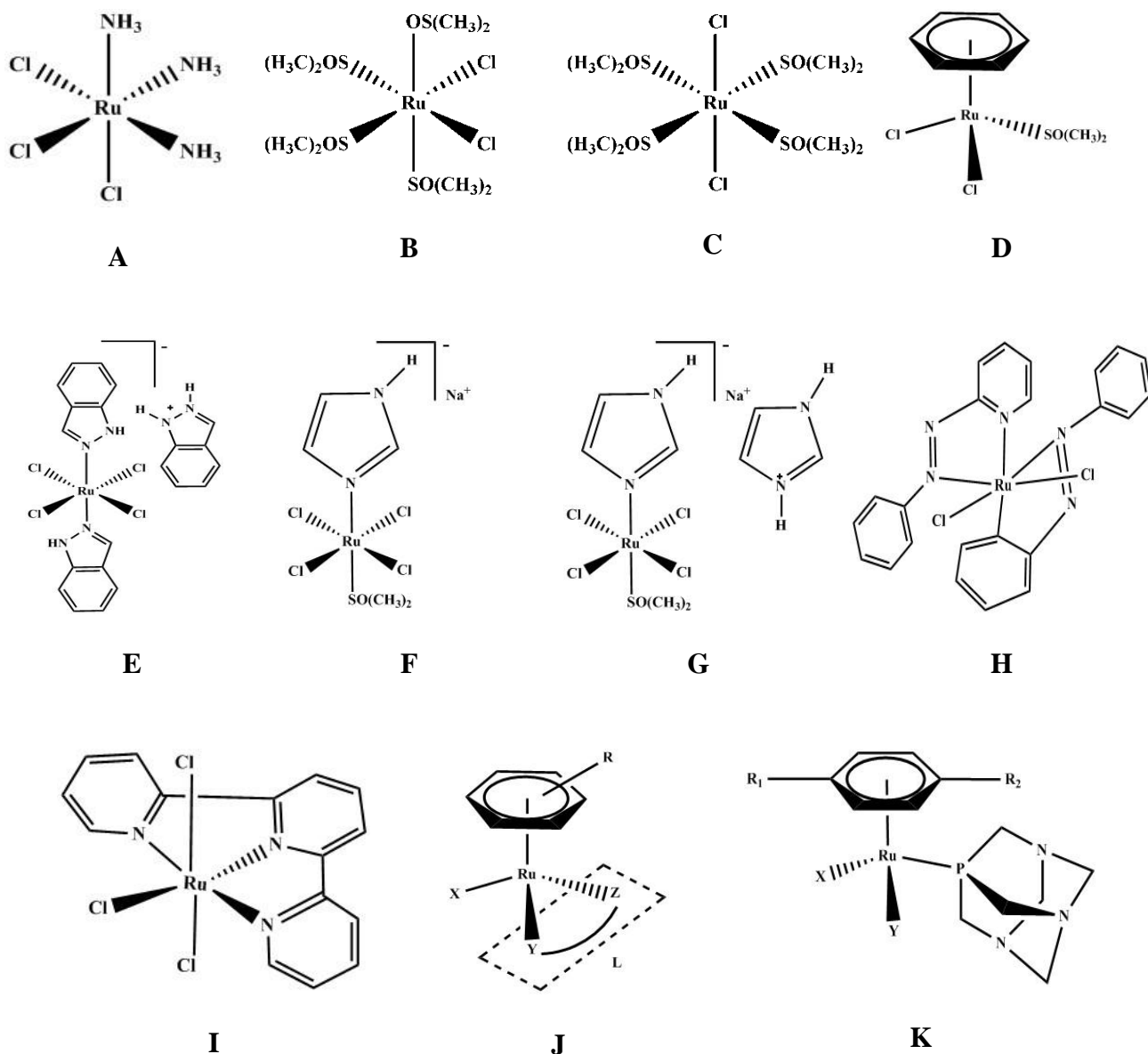


**Figure 2.18.** Antitumor ruthenium complexes. **A)** *fac*-[Ru(III)(NH<sub>3</sub>)<sub>3</sub>Cl<sub>3</sub>], **B)** *cis*-[Ru(II)Cl<sub>2</sub>(dmsO)<sub>4</sub>], **C)** *trans*-[Ru(II)Cl<sub>2</sub>(dmsO)<sub>4</sub>], **D)** ( $\eta^6$ -benzene)Ru(DMSO)Cl<sub>2</sub>, **E)** KP1019, **F)** NAMI, **G)** NAMI-A, **H)**  $\alpha$ -Ru(azpy)<sub>2</sub>Cl<sub>2</sub>, **I)** *mer*-[Ru(II)(tpy)Cl<sub>3</sub>], **J)** Ru(II)arene complexes “piano-stool”, **K)** Ru(II)arene (pta) complexes or “RAPTA types”. (Ang, 2007; Ang and Dyson, 2006; Ang *et al.*, 2006; Bergamo *et al.*, 2002; Dougan and Sadler, 2007; Dyson and Sava, 2006; Galanski *et al.*, 2003; Hartinger *et al.*, 2006; Kapitzka *et al.*, 2005; Peacock and Sadler, 2008; Rademaker-Lakhai *et al.*, 2004; Sava and Bergamo, 2000; Sava *et al.* 1999; Yan *et al.*, 2005).

### 2.9.3 RAPTA complexes

The success of ruthenium(II) arene-based anticancer drugs is favorably related to the amphiphilic properties of the arene-ruthenium system. This hydrophobic arene ligand is flanked by the hydrophilic metal center, as well as to the synthetic diversity of the arene moiety, which is an excellent scaffold for grafting organic segments to facilitate targeted chemotherapy (Medici *et al.*, 2015). The most numerous group of cytotoxic ruthenium compounds are organometallic ruthenium(II) arene complexes, (arene = *p*-cymene, toluene, benzene, benzo-15-crown, 1-ethybenzene-2,3-dimethylimidazolium tetrafluoroborate, ethyl benzoate, hexamethylbenzene) which were individually developed by Dyson and co-workers (Ang, 2007; Ang and Dyson, 2006; Ang *et al.*, 2006; Dyson and Sava, 2006; Guidi *et al.*, 2013; Murray *et al.*, 2016; Nazarov *et al.*, 2014; Scolaro *et al.*, 2005; Scolaro *et al.*, 2006; Scolaro *et al.*, 2007), Sadler and co-workers (Dougan and Sadler, 2007; Peacock and Sadler, 2008; Yan *et al.*, 2005), and other groups (Ramadevi *et al.*, 2017; Tabrizi and Chniforoshan, 2016). A typical structure of a half-sandwich, “piano-stool”, is  $[(\eta^6\text{-arene})\text{Ru}(\text{X})(\text{Y})(\text{Z})]$ , where the arene forms the seat of the piano stool and the ligands resemble the legs. Linking the ligands Y and Z to form a bidentate chelating ligand (L) seems to be advantageous for anticancer activity. The structure of Ru(II) half-sandwich complexes allows for variations of the three main building blocks, the monodentate ligand X, the bidentate ligand L and the arene, to fine-tune the pharmacological properties of these complexes (Melchart *et al.*, 2007; Ronconi and Sadler, 2007). The chelating ligand can help to control the stability and ligand-exchange kinetics of these complexes. The nature of the arene influences cellular uptake and interactions with potential targets. The leaving group, which typically is chloride and occupies the biomolecule binding site on the metal center, can be of importance to control the timing of activation of these complexes (Yan *et al.*, 2005). Dyson and co-workers have designed and developed the ruthenium(II) arene (PTA) complexes or RAPTA complexes, (PTA = 1,3,5-triaza-7-phosphaadamantane) (Ang and Dyson, 2006; Dyson and Sava, 2006; Guidi *et al.*, 2013; Murray *et al.*, 2016; Nazarov *et al.*, 2014; Scolaro *et al.*, 2007). Recently, Tabrizi and Chniforoshan have synthesized four ruthenium(II) *p*-cymene complexes of naphthoquinone-derived RAPTA complexes that showed anticancer activity against thioredoxin reductase (Trx-R) with lower IC<sub>50</sub> values in the nanomolar range (Tabrizi and Chniforoshan, 2016). Furthermore, the ruthenium(II) arene, named RAFcA complexes, have shown to inhibit the MCF-7 cells through interaction with DNA, the expression of apoptosis-related genes (*Bax* and *Bcl2*) (Ramadevi *et al.*, 2017). Interestingly, their IC<sub>50</sub> values are distinctly lower than those of NAMI-A and RAPTA complexes.

#### 2.9.3.1 DNA binding properties

A range of RAPTA compounds has shown to interact with DNA in a pH-dependent manner (Allardyce and Dyson, 2001; Chatterjee *et al.*, 2009; Dorcier *et al.*, 2005; Dorcier *et al.*, 2008; Egger *et al.*, 2010; Groessl *et al.*, 2008; Scolaro *et al.*, 2005; Scolaro *et al.*, 2006). However, the rates of interaction with DNA are significantly lower than those of cisplatin or NAMI-A (Groessl *et al.*, 2010). Ratanaphan and co-worker have reported that RAPTA-EA1, one of of RAPTA

derivatives, induced the DNA interstrand crosslinking and preferentially attacked at A, G, T and C, in the order, of the *BRCA1* gene fragment (Charkree *et al.*, 2012).

### 2.9.3.2 Antitumor properties of RAPTA complexes

Despite the lower affinity for DNA in *in vitro* studies, an *in vivo* effect of RAPTA compounds is strikingly different to most other anticancer compounds, both metal-based and organic drugs. RAPTA-C, [Ru( $\eta^6$ -*p*-cymene)Cl<sub>2</sub>(PTA)] and RAPTA-T, [Ru( $\eta^6$ -toluene)Cl<sub>2</sub>(PTA)], inhibited lung metastases in CBA mice bearing the MCA mammary carcinoma, reducing their weight and number, with only mild effects on the primary tumor being observed (Scolaro *et al.*, 2005). The patterns of protein alterations induced by NAMI-A and RAPTA-T are quite similar to each other while being deeply different from those of cisplatin (Dyson and Sava, 2006; Guidi *et al.*, 2013). RAPTA-T selectively reduced the number and weight of metastatic tumors have been undertaken on a series of breast cancer cells. It was found that RAPTA-T inhibited some steps of the metastatic process including detachment of cells from the primary tumor, migration, and the re-adhesion of cells to a new growth substrate (Scolaro *et al.*, 2005). It was also interesting to note that the effects of RAPTA-T were more pronounced in the highly invasive MDA-MD-231 breast cancer cells, compared with the non-invasive MCF-7 or the non-tumorigenic HBL-100 breast cells (Bergamo *et al.*, 2008). RAPTA-C also increased the survival of mice bearing Ehrlich Ascites Carcinoma (EAC), a highly proliferative and fluid tumor (Chatterjee *et al.*, 2008). Tumor cells extracted from the mice revealed that RAPTA-C inhibited cell growth by triggering G2/M phase arrest leading to apoptosis. RAPTA-C also up-regulated p53 via triggering the mitochondrial apoptotic pathway. Moreover, increased cytochrome *c* levels induced by RAPTA-C also activated pro-caspase-9, enhancing apoptosis and altering in the expression of key proteins involved in the regulation of the cell cycle and apoptosis. It is implied that RAPTA-C acts on various molecular pathways and does not bind to a single target (Chatterjee *et al.*, 2008). In addition, a series of RAPTA compounds with arene-tethered EA ligands (ethacrynic acid) has been shown to inhibit glutathione S-transferase (GST) activity which was comparable or better than free ethacrynic acid whereas RAPTA-C exhibited no inhibitory effect on GST P1-1, even at high concentrations. Moreover, RAPTA-EA1 is highly effective against the GST P1-1 positive A2780 and A2780cisR ovarian carcinoma cell lines (Ang *et al.*, 2007). Recently, several derivatized of RAPTAs have been developed by varying leaving ligands for improved anticancer activity (Bergamini *et al.*, 2012; Ganeshpandian *et al.*, 2014; Hajji *et al.*, 2017; Kaluđerović *et al.*, 2015; Montani *et al.*, 2016; Pettinari *et al.*, 2017; Serrano-Ruiz *et al.*, 2017). However, the exact mechanism of action is needed to be elucidated.

### 2.9.3.3 Protein binding properties

The exact mechanism of action of ruthenium complexes are, to date, still unknown. However, there have been demonstrated that RAPTAs exert on molecular targets other than DNA, implying a biochemical mode of action profoundly different to classical platinum anticancer drugs (Bergamo and Sava, 2007; Dyson and Sava, 2006). Indeed, RAPTAs have been shown to directly interfere with specific



proteins involved in signal transduction pathways and/or alter cell adhesion and migration process (Bergamo *et al.*, 2008). It is likely that the mechanism of action of RAPTAs may involve interaction with critical intracellular or extracellular proteins. Recent evidences have revealed that RAPTAs interacted with a number of cancer-related proteins (the cytokines midkine, pleiotrophin and fibroblast growth factor-binding protein 3), which may be responsible for the antiangiogenic and antimetastatic activity of these types of ruthenium complexes (Babak *et al.*, 2015). The preference for the protein binding of RAPTAs is also confirmed from *in vitro* studies (Ang *et al.*, 2011). The RAPTAs were found to bind mainly the serum proteins albumin and transferrin, which may prevent metallodrugs from being reduced and its subsequent activation in the blood. In addition, the RAPTA-T showed a marked preference for holo-form of transferrin, suggesting a cooperative iron-mediated metal binding mechanism (Groessler *et al.*, 2010). Moreover, the formation of ruthenium–protein adducts was clearly observed for ubiquitin (Ub), cytochrome c (Cyt-c), lysozyme (Lys), and superoxide dismutase (SOD), thioredoxin reductase, and cathepsin B (Casini *et al.*, 2007; Casini *et al.*, 2008; Casini *et al.*, 2009; Hartinger *et al.*, 2008; Michelucci *et al.*, 2017). Mass spectrometric analyses indicated that the RAPTA complexes have affinities for histidine, on protein binding (Casini *et al.*, 2008; Casini *et al.*, 2009). Under essentially equivalent conditions, cisplatin forms mono-, bis-, and tris-adducts whereas only mono- and bis-adducts are formed with the RAPTA complexes (Casini *et al.*, 2007). In addition, extensive spectroscopic studies were reported that preferential binding sites for the RAPTA complexes are histidines residues located on the protein surface (Casini *et al.*, 2007), similarly observed for NAMI-A (Messori *et al.*, 2000) and KP1019 (Piccioli *et al.*, 2004). Furthermore, the reactivity of RAPTA-C with a mixture containing ubiquitin, cytochrome c and superoxide dismutase showed that the ruthenium complex had a high affinity towards ubiquitin and cytochrome c, but not superoxide dismutase, indicating some degree of selectivity, which contrasts with the behavior of cisplatin (Casini *et al.*, 2009). The high reactivity towards protein molecules prompted the investigation of the RAPTA complexes towards clinically relevant enzyme targets, namely the seleno-enzyme thioredoxin and the cysteine protease cathepsin B (Ang *et al.*, 2011). RAPTA-T and RAPTA-C, were found to be good inhibitors of cathepsin B (Casini *et al.*, 2008). The reaction of RAPTA-C with metallothionein-2 (MT-2) was also investigated, demonstrating that it has higher affinity and selectivity for MT-2 binding with respect to cisplatin. This phenomenon may have important pharmacological and toxicological profiles of the compound (Casini *et al.*, 2009). In addition, similar binding affinity studies based on a mass spectrometric strategy showed that RAPTA-C can form several adducts with the tripeptide, glutathione (GSH), implying the possibility to overcome metallodrug resistance mechanisms as well as novel possible targets for RAPTA compounds (Hartinger *et al.*, 2008). The reactivity of RAPTA-T with poly-(adenosine diphosphate (ADP)-ribose) polymerase (PARP-1) was investigated. PARP-1 is an essential protein involved in cancer resistance to chemotherapies, and contains zinc-finger domains that might be altered by metal-based compounds. The results showed that RAPTA-T inhibits PARP-1 to a similar extent of the benchmark inhibitor 3-aminobenzamide (Mendes *et al.*, 2011).

However, the molecular mechanism and the signaling pathways remain to be elucidated. Recently, a systematic study on the interaction between two derivatives of RAPTA types compound, named RAED and RAED-C, and human transferrin has indicated that the ruthenium compounds preferentially coordinate with histidine residues, in contrast to cisplatin which binds beyond histidine residues (Guo *et al.*, 2013). In addition, several evidences reported that Ru(II)( $\eta^6$ -*p*-cymene) complexes interacted with several proteins such as apo-ferritin (AFt) nanocage, lysozymes, RNase A, ubiquitin, and nucleosome core particle histone protein preferentially coordinate with His residues of these proteins (Battistin *et al.*, 2016; Dubarle-Offner *et al.*, 2014; Egger *et al.*, 2010; Kilpina and Dyson, 2013). These data unambiguously demonstrate that, at least under the investigated experimental conditions the ruthenium center binds the imidazole of the histidine side chain adopting an octahedral geometry. The labile  $\eta^6$ -*p*-cymene and chlorido ligands are lost from ruthenium4 center, which experiences a change in the coordination number and in the geometry of its coordination sphere upon protein binding (Merlino, 2016). While many different RAPTA compounds have been developed, the prototype compound RAPTA-C remains the best anticancer compound of this series that has been characterized.

## 2.10 Therapeutic strategies for BRCA1-related breast cancer

### 2.10.1 Targeting homologous recombination repair (HR) pathway

In eukaryotic cells, there are two primary mechanisms of DSBs repair. HR is the error-free process used in the cells during the S and G2 phases of cell cycle when sister chromatids are available as templates. Non-homologous end-joining (NHEJ) is a process of ligating DSB ends together without a homologous template. It is the predominant mechanism in cells during G0, G1, and early S phases of the cell progression, and is considered as an error-prone process (Yang and Xia, 2010). Loss of function of the HR pathway is limited to the tumor, which makes it an ideal target for therapy by inhibition of the complementary HR pathway.

The currently three groups of DNA-targeting agents, involving in HR pathway, are used for the treatment of breast or ovarian cancer.

- i) The alkylating agents cause DNA interstrand cross links (ICLs), resulting in arrest of DNA replication forks and subsequently to DSBs.
- ii) The inhibitors of topoisomerase I and II, which stabilize the topoisomerase-DNA complex and thereby cause arrest of DNA replication forks and DSBs.
- iii) The platinum-based compounds, which induce DSBs by forming intra-strand and ICLs.

Since BRCA1 deficiency leads to the deregulation of DNA repair pathways, tumor cells with BRCA1 deficiency are more vulnerable to DNA damaging agents. The concept of 'BRCAness' was introduced by Ashworth and colleagues in

order to identify phenotypic changes in sporadic cancer that would lead to analogous treatment susceptibility to DNA damaging agents (Muggia and Safra, 2014).

### 2.10.2 Poly(ADP-ribose) polymerase inhibitors

The poly(ADP-ribose) polymerase 1 (PARP1) is an enzyme critical to the base excision repair (BER) pathway. PARP1 is a member of the PARP superfamily, which is responsible for the poly(ADP-ribosylation) (PAR-ylation) of nuclear proteins, a DNA damage-dependent posttranslational modification, that plays an important role in including DNA transcription, DNA damage response, genomic stability maintenance, cell cycle regulation, and cell death (Benafif and Hall, 2015). In cancer therapeutics, accumulation of single-strand DNA breaks (SSBs) with PARP inhibition leads to the development of double-strand DNA breaks (DSBs), which require competent HR repair to allow cell survival (Michels *et al.*, 2014). Loss of PARP1 protein function results in increased sensitivity to the DNA alkylating agents and  $\gamma$ -irradiation (Masutani *et al.*, 2000). Nowadays, the most advanced and promising drugs that target DNA repair is a PARP1 inhibitor that it has shown promising activity in patients with BRCA1 mutation-associated epithelial ovarian and breast cancers, based on the principle of synthetic lethality (Lord and Asworth, 2015). This lethality is a possible explanation by the cancer cells with defects in the *BRCA1* gene are defective in HR, as the wild-type *BRCA1* allele is absolutely lost. However, HR is intact in normal cells of the same patients who carry one wild-type *BRCA1* allele and one mutant *BRCA1* allele. Inhibition of PARP1 results in the accumulation of SSBs, which are converted to lethal DSBs that require HR for their repair (Fig. 2.19) (Hosoya and Miyagawa, 2014).

Recently, several PARP1 inhibitors, as single agents and/or in combination therapy, are currently in phase I, II or III clinical investigation (Table 2.14). In addition, this approach has led to the successful regulatory approval of olaparib, rucaparib, and niraparib for patients with advanced ovarian cancer (O'Sullivan Coyne *et al.*, 2017). However, understanding more about the molecular abnormalities involved in *BRCA*-like tumors will be critical to advance the field of PARP inhibition therapy and in improving patient selection and consequent clinical outcomes.

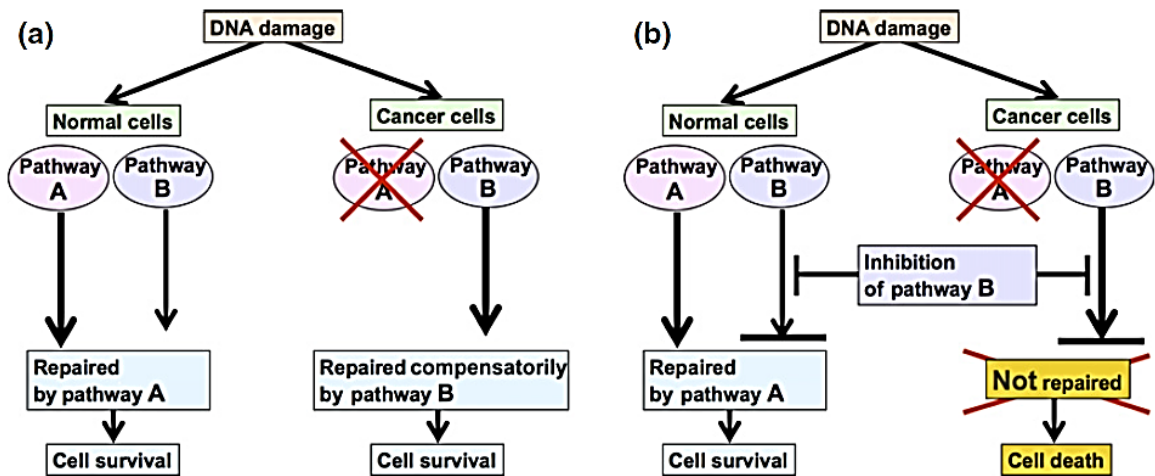


**Figure 2.19.** Principle of synthetic lethality. DNA damage is often processed by multiple DNA repair pathways. In the example shown here, pathways A and B are both intact in normal cells, whereas pathway A is defective in cancer cells. **(a)** In the absence of the pathway B inhibitor, cancer cells can survive, because the defect in pathway A is compensated by the alternative pathway B. **(b)** When the cells are treated with the pathway B inhibitor, both pathways will be blocked in cancer cells, which will result in cell death. However, normal cells will not be affected, because inhibition of pathway B will be compensated by pathway A (Hosoya and Miyagawa, 2014).

**Table 2.14.** PARP1 inhibitors (PARPi) in clinical investigation.

PARPi	Treatment	Cancer types	Phase	Ref.
Olaparib (AstraZeneca)	-Monotherapy -Combinations with cytotoxic chemotherapy -Combinations with targeted agents	- <i>BRCA1/2</i> mutation-associated breast cancer/ovarian cancer, <i>BRCA</i> -like tumors - Advanced hematologic malignancies and solid tumors - Maintenance study following remission in platinum sensitive ovarian cancer - FDA approves to treat advanced ovarian cancer in 2014	I/II/III	Fong <i>et al.</i> , 2009 Kaufman <i>et al.</i> , 2015 Gelmon <i>et al.</i> , 2011 Balmana <i>et al.</i> , 2014 Del Conte <i>et al.</i> , 2014 Ledermann <i>et al.</i> , 2014 Samol <i>et al.</i> , 2012 Lee <i>et al.</i> , 2014 Liu <i>et al.</i> , 2013 Liu <i>et al.</i> , 2014 Kaye <i>et al.</i> , 2012 Bang <i>et al.</i> , 2013 Oza <i>et al.</i> , 2015 van der Noll <i>et al.</i> , 2013 Rajan <i>et al.</i> , 2012 Khan <i>et al.</i> , 2011 Moore <i>et al.</i> , 2014 Tutt <i>et al.</i> , 2015 Dent <i>et al.</i> , 2013
Veliparib (Abbott)	-Monotherapy -Combinations with cytotoxic chemotherapy -Combinations with targeted agents	- <i>BRCA1/2</i> mutation-associated breast cancer/ovarian cancer, <i>BRCA</i> -like tumors - Advanced hematologic malignancies and solid tumors	I/II	Liu <i>et al.</i> , 2009 Lo Russo <i>et al.</i> , 2016 Villalona-Calero <i>et al.</i> , 2016 Hussain <i>et al.</i> , 2014 Kummar <i>et al.</i> , 2011 Kummar <i>et al.</i> , 2012 Isakoff <i>et al.</i> , 2011 Coleman <i>et al.</i> , 2015 Appleman <i>et al.</i> , 2012 Rugo <i>et al.</i> , 2013 Bell-McGuinn <i>et al.</i> , 2013 Wesolowski <i>et al.</i> , 2014 Pishvaian <i>et al.</i> , 2013 Puhalla <i>et al.</i> , 2014 Reiss <i>et al.</i> , 2015 Plummer <i>et al.</i> , 2013
Rucaparib (Clovis)	-Monotherapy -Combinations with cytotoxic chemotherapy	- Advanced solid tumors, recurrent ovarian cancer - <i>BRCA1/2</i> mutation-associated breast cancer/ ovarian cancer - Treatment of advanced <i>BRCA</i> -mutated (germline and/or somatic) ovarian cancer - FDA approves treatment of advanced ovarian cancer in 2016	I/II	Plummer <i>et al.</i> , 2008 Plummer <i>et al.</i> , 2013 Kristeleit <i>et al.</i> , 2014 Kristeleit <i>et al.</i> , 2015 Drew <i>et al.</i> , 2016 Dwadasi <i>et al.</i> , 2014 McNeish <i>et al.</i> , 2015 Molife <i>et al.</i> , 2013 Swisher <i>et al.</i> , 2017 Wilson <i>et al.</i> , 2017

**Table 2.14.** PARP1 inhibitors (PARPi) in clinical investigation (cont.)

PARPi	Treatment	Cancer types	Phase	Ref.
Iniparib	-Monotherapy -Combinations with cytotoxic chemotherapy	- Advanced in patients with metastatic triple-negative breast cancer - Patients with <i>BRCA1</i> or <i>BRCA2</i> associated advanced epithelial ovarian, fallopian tube, or primary peritoneal cancer	II/III	Bell-McGuinn <i>et al.</i> , 2016 Llombart-Cussac <i>et al.</i> , 2015 O'Shaughnessy <i>et al.</i> , 2011 O'Shaughnessy <i>et al.</i> , 2014 Mateo <i>et al.</i> , 2013 Telli <i>et al.</i> , 2015 Afghahi <i>et al.</i> , 2017
Talazoparib (BMN 673) (BioMarin)	- Monotherapy	- Advanced hematologic malignancies and solid tumors - Platinum sensitive <i>BRCA1/2</i> -mutant solid tumors - Metastatic breast cancer but not in ovarian cancer	I/II/III	de Bono <i>et al.</i> , 2013 BioMarin Pharmaceutical, 2015 Miller <i>et al.</i> , 2016 Wainberg <i>et al.</i> , 2014 Litton <i>et al.</i> , 2015
Niraparib (MK-4827) (TesarBio)	-Monotherapy -Combinations (temazolomide)	- Advanced hematologic malignancies and solid tumors - <i>BRCA1/2</i> mutation-associated and HER2 negative breast cancer - Maintenance study following remission in platinum sensitive ovarian cancer - FDA approves for treatment of adult patients with recurrent epithelial ovarian, fallopian tube, or primary peritoneal cancer	I/III	Sandhu <i>et al.</i> , 2013 Mirza <i>et al.</i> , 2016
CEP-9722 (Cephalon)	-Monotherapy -Combinations with cytotoxic chemotherapy	- Advanced solid tumors	I	Plummer <i>et al.</i> , 2014 Awada <i>et al.</i> , 2016

## 2.11 Targeting dysfunctional BRCA1 for the metal-based drug in cancer therapy

The DNA repair activity of the cell is an important determinant of cell sensitivity to the anticancer agents. In fact, it has been reported that resistance to DNA-damaging agents can be associated with the increased cellular repair activities, while defects in DNA repair pathways result in hypersensitivity to these agents (Kelley and Fishel, 2008; Quinn *et al.*, 2003; Quinn *et al.*, 2009). BRCA1 is implicated to play a crucial role in DNA interstrand crosslink repair through several mechanisms and is integral in HR, the less error-prone mechanism of repairing double strand DNA breaks (Ashworth, 2008). When cells lose all BRCA1 function, they become hypersensitive to DNA damage and develop gross chromosomal aberrations when challenged with DNA-damaging drugs or agents, such as cisplatin, carboplatin, or auranofin (Oommen *et al.*, 2016; Shen *et al.*, 1998). A woman with one inherited *BRCA1* mutation still has BRCA1 function from the other allele; however, there is usually somatic loss of the functional allele in her breast cancer, leading to complete tumoral inactivation of BRCA1 function and resultant hypersensitivity to DNA damage (Carey, 2010).

BRCA1-deficient mouse embryonic stem cells displayed defective DNA repair and a 100-fold increased sensitivity to the alkylating agents mitomycin C and cisplatin than those containing wild-type BRCA1 (Bhattacharyya *et al.*, 2000; Moynahan *et al.*, 2001). This sensitivity was reversed upon the correlation of BRCA1 mutation in mouse embryonic fibroblast cells with a disrupted BRCA1 with the decreased DNA repair and increased apoptosis (Fedier *et al.*, 2003; Ohta *et al.*, 2009; Quinn *et al.*, 2003). Recent studies have emphasized the potential of using BRCA1 dysfunction to predict response to therapy. Currently, chemotherapy, hormonal therapy and molecular targeted therapy are important strategies of breast cancer treatment. However, there are no specific chemotherapy guidelines for *BRCA1*-mutated breast cancer patients (Tanino *et al.*, 2016). As noted above, both mutation and down-regulation of expression of BRCA1 can be abrogated BRCA1 function, called '*BRCAness*', leading to tumorigenesis (Mugia and Safra, 2014; Tanino *et al.*, 2016). However, the application of BRCA-like functional abnormalities or dysfunctional of BRCA1 raises the possibility of treatment regimens designed for familial BRCA tumors (Turner *et al.*, 2004). Exploitation of this knowledge in the treatment of BRCA1 associated-breast cancer has varying degrees of success. Several clinical trial studies have demonstrated the utilization of the *BRCAness* as a clinically validated target by the platinum based-drugs to treated *BRCA1* associated-breast cancer (Byrski *et al.*, 2010; Tanino *et al.*, 2016). The clinical studies have recently gained much attention on taking advantage of the inherent weakness of the BRCA1 dysfunction in the cancer cells that increases their sensitivity to DNA-damaging agents such as platinum agents (Ashworth, 2008; Drost and Jonkers, 2014; Font *et al.*, 2011; Quinn *et al.*, 2009; Silver *et al.*, 2010; Sun *et al.*, 2014; Tassone *et al.*, 2009; Vencken *et al.*, 2011). In addition, the significant benefits of the pathological response and overall survival rate from cisplatin-based chemotherapy were extended to the several *BRCA1*-associated cancers, such as breast, bladder, ovarian, and non-small cell lung (NSCL) cancer patients (Byrski *et al.*, 2009; Byrski *et al.*, 2011; Domagala *et al.*, 2016; Font *et al.*, 2011; Isakoff *et al.*, 2015; Quinn *et al.*, 2007; Sikov *et al.*, 2015; Silver *et al.*, 2010; Taron *et al.*, 2004; Von Minckwitz *et al.*, 2015). Patients

with BRCA1 dysfunction gain more benefit from treatments causing DNA damage. Moreover, it was initially reported that overexpression of BRCA1 in human breast cancer resulted in an increased resistance to platinum based-drugs. As a result, cells lose all BRCA1 function, and they become hypersensitive to DNA damage and develop gross chromosomal aberrations in the presence of DNA-damaging drugs or agents (Busschots *et al.*, 2015; Husain *et al.*, 1998). It has been demonstrated that inhibition of PARP1 enzymatic activity could selectively target BRCA-mutant cells, sensitizing them to persistent DSBs and ultimately apoptosis (Choy *et al.*, 2016; Farmer *et al.*, 2005; Fong *et al.*, 2009). PARP1 is a key enzyme in the repair of DNA single strand breaks (SSBs) and its inhibition results in unrepaired SSBs, giving rise to DSBs when encountered by a replication fork during DNA replication. The inability of BRCA1-deficient cells to repair the indirectly induced DSBs results in a specific sensitivity to PARP inhibition (Audeh *et al.*, 2010; Benafif and Hall, 2015). Many BRCA1-mediated cancers are initially responsive to platinum-based therapy; however, resistance commonly develops (Choi *et al.*, 2016; Powell, 2016).

To date, several studies have been investigated targeting zinc finger protein for direct implications in disease. BRCA1 is a tumor suppressor protein involved in maintaining genomic integrity. The *N*-terminus of the BRCA1 protein contains two Zn<sup>2+</sup> binding loops. This domain is essential for tumor suppression functions. Many cancer-predisposing mutations in the BRCA1 RING domain are defective in DSB repair pathways, and render cancerous cells hypersensitive to ionizing radiations and alkylating agents. Therefore, approaching the BRCA1 RING domain as a potentially molecular target for a metal-based drug is of interest. The RAPTA complexes (RAPTAs) have been shown to exhibit promising antitumor properties. However, their mechanisms of action are largely unexplored. In this work, the *BRCA1* gene and its encoded protein are used as a model system for evaluation of the RAPTA-induced response. The investigation is focused on the *in vitro* interaction of RAPTAs with the plasmid DNA and the *BRCA1* gene fragment, including conformational study, interstrand cross-links, sequence preference of RAPTA-*BRCA1* adducts, and inhibition of *BRCA1* amplification. We have further investigated *in vitro* interaction of RAPTAs with the *N*-terminal region of the BRCA1 RING domain proteins, both wild-type and mutant proteins (D67E and D67Y), including protein binding, conformational study, zinc ejection, thermal stability and the functional assay of the ruthenated BRCA1 on BRCA1/BARD1-mediated ubiquitination. In addition, the antiproliferative effects of RAPTA complexes alone or in combination with PARP1 inhibitor in breast cancer cells is also investigated.



## CHAPTER 3

### MATERIALS AND METHODS

#### Materials

##### Cells

- *Escherichia coli* DH5 $\alpha$  (New England Biolab, USA)
- *Escherichia coli* BL21(DE3) (gift from Prof. Udo Heinemann, Max-Delbrück-Center for Molecular Medicine, Berlin, Germany)
- Human breast adenocarcinoma cell line [MCF-7 (BRCA1 wild-type, ER-, PR-, and HER2-positive)] (kindly provided from Asst. Prof. Supreeya Yuenyongsawad, Department of Pharmacognosy and Pharmaceutical Botany, Faculty of Pharmaceutical Sciences, Prince of Songkla University)
- Human breast adenocarcinoma cell line (ATCC<sup>®</sup> HTB-26<sup>™</sup>) [MDA-MB-231 (BRCA1 wild-type, Triple negative (ER-, PR-, and HER2-negative) breast cancer)] (ATCC, USA)
- Human breast adenocarcinoma cell line (ATCC<sup>®</sup> CRL-2336<sup>™</sup>) [HCC1937 (BRCA1 mutant, Triple negative (ER-, PR-, and HER2-negative) breast cancer)] (ATCC, USA)

##### Plasmids

- pET28a(+)\_BARD1 (plasmid 12646)
- pET28a(+)\_ubiquitin (plasmid 12647)
- pET28a(+)\_UbcH5c (plasmid 12643)
- pGEX-4T1 (gift from Prof. Udo Heinemann, Max-Delbrück-Center for Molecular Medicine, Berlin, Germany)
- pET28a(+) (gift from Prof. Udo Heinemann, Max-Delbrück-Center for Molecular Medicine, Berlin, Germany)
- pBIND (Promega, USA)

##### Chemicals

- 3-[4,5-dimethylthiazol-2-yl]-2,5 diphenyltetrazolium bromide (Sigma-Aldrich, USA)
- 6-Methoxy-8-*p*-toluenesulfonamido-quinoline (Enzo Life Sciences, USA)
- Absolute ethanol (Merck, Germany)
- Acetone (Roth, Germany)
- Acetic acid (Merck, Germany)
- Acrylamide (Viviantis, USA)

- Adenosine-5'-triphosphate disodium salt, trihydrate (Bio basic Inc, Canada)
- Agarose Molecular Biology Grade (Viviantis, USA)
- Ammonium persulfate (Sigma-Aldrich, USA)
- Ampicillin (Sigma-Aldrich, USA)
- Bacto™ agar (Becton, Dickinson and Company, USA)
- Bacto™ tryptone (Becton, Dickinson and Company, USA)
- Bacto™ yeast extract (Becton, Dickinson and Company, USA)
- Boric acid (Merck, Germany)
- Bovine serum albumin (BSA) (Sigma-Aldrich, USA)
- Bromocresol blue (Sigma-Aldrich, USA)
- Calcium chloride dihydrate (Merck, Germany)
- Cisplatin (Sigma-Aldrich, USA)
- Coomassie brilliant blue G-250 (Fluka, Switzerland)
- Coomassie brilliant blue R-250 (Fluka, Switzerland)
- dATP, dCTP, dGTP, and dTTP (INtRON Biotechnology, Korea)
- Dialysis bag (Sigma-Aldrich, USA)
- Difco™ LB Broth, Lennox (Becton, Dickinson and Company, USA)
- Dimethyl sulfoxide (Merck, Germany)
- Disodium hydrogen phosphate (Fluka, Switzerland)
- Dithiothreitol (DTT) (Fluka, Switzerland)
- Dulbecco's modified Eagle medium (DMEM) (Life Technologies, Paisley, UK)
- Ethidium bromide (Sigma-Aldrich, USA)
- Ethylenediaminetetraacetic acid disodium salt (EDTA) (BDH Laboratory Supplies, England)
- Fetal bovine serum standard quality (Invitrogen, USA)
- Formaldehyde (Merck, Germany)
- Glacial acetic acid (Merck, Germany)
- Glutathione-Reduced (USB, USA)
- Glycerol (BDH Laboratory Supplies, England)
- Guanidine hydrochloride (Fluka, Switzerland)
- HisPur™ Ni-NTA resin (Thermo scientific, USA)
- Hydrochloric acid (Merck, Germany)
- Imidazole (Fluka, Switzerland)
- Isopropanol (J.T. baker, USA)
- Isopropyl-1-thio-β-D-galactopyranoside (IPTG) (Sigma-Aldrich, USA)
- Kanamycin (Roth, Germany)
- Lysozyme (Viviantis, USA)
- Methanol (Labscan Asia, Thailand)
- Magnesium chloride (Merck, Germany)
- *N, N, N', N'*-Tetramethylethylenediamine (TEMED) (Sigma-Aldrich, USA)
- *N, N'*-Methylene-bis-acrylamide (Sigma-Aldrich, USA)
- Nonidet P-40 (NP40) (Bio Basic Inc., Canada)

- Phenylmethylsulfonyl fluoride (PMSF) (Sigma-Aldrich, USA)
- Potassium acetate (BDH Laboratory Supplies, England)
- Potassium chloride (Merck, Germany)
- Potassium dihydrogen phosphate (Merck, Germany)
- Proteinase K (Sigma-Aldrich, USA)
- Roswell Park Memorial Institute 1640 medium (RPMI 1640) (Life Technologies, Paisley, UK)
- Silver nitrate (Merck, Germany)
- Sodium acetate (APS Finechem, Australia)
- Sodium carbonate anhydrous (Ajax Finechem, Australia)
- Sodium chloride (Merck, Germany)
- Sodium hydrogen carbonate (Merck, Germany)
- Sodium dodecyl sulfate (Sigma-Aldrich, USA)
- Sodium hydroxide (Carlo Erba Reagenti, Italy)
- Sucrose (Sigma-Aldrich, USA)
- Trifluoroacetic acid (Fluka, Switzerland)
- Tris [hydroxymethyl] aminomethane hydrochloride (Tris-HCl) (Stratagene, USA)
- Tris [hydroxymethyl] aminomethane (Tris-Base) (Promega, USA)
- Triton X-100 (Sigma-Aldrich, USA)
- Xylene cyanol FF (Sigma-Aldrich, USA)
- Zinc(II) chloride (Fluka, Switzerland)

### Enzymes

- *Bam*HI (New England BioLabs, USA)
- E3 ubiquitin ligase (Enzo Life Sciences, USA)
- *i-Taq*<sup>TM</sup> DNA Polymerase (INtRON Biotechnology, Korea)
- Phusion<sup>TM</sup> Hot Start High-Fidelity DNA polymerase (FINNZYMES, Finland)
- *Eco*O109I (New England Biolabs, USA)
- *Pvu*II (New England Biolabs, USA)
- *Xho*I (New England BioLabs, USA)

### Solutions

- 0.25% Trypsin-EDTA (Invitrogen, USA)
- 100 bp DNA ladder (New England Biolabs, USA)
- 10x Alkaline agarose gel electrophoresis buffer (500 mM NaOH, 10 mM EDTA, pH 7.5)
- 10x PCR buffer, pH 7.4 (INtRON Biotechnology, Korea)
- 5x Phusion<sup>TM</sup> GC buffer, pH 7.4 (FINNZYMES, Finland)
- 5x TBE buffer (Tris-Base 54 g, Boric acid 27.5 g, 20 ml of 0.5 mM EDTA, pH 8.0)

- 6x Alkaline gel-loading buffer (300 mM NaOH, 6 mM EDTA, 18% (w/v) glycerol, 0.15% (w/v) bromocresol green, 0.25% (w/v) xylene cyanole FF)
- 6x Gel-loading buffers (0.25% (w/v) bromophenol blue, 0.25% (w/v) xylene cyanole FF, 30% (v/v) glycerol in distilled water)
- Alkaline lysis solution I (50 mM glucose, 25 mM Tris-HCl pH 8.0, 10 mM EDTA, pH 8.0)
- Alkaline lysis solution II [0.2 N NaOH (freshly diluted from a 10 N stock), 1% (w/v) SDS]
- Alkaline lysis solution III (5M potassium acetate 60 ml, glacial acetic acid 11.5 ml, and 28.5 ml of double distilled water)
- Anti-His<sub>6</sub> HRP (Horseradish Peroxidase) conjugated (QIAGEN, Germany)
- Calcium chloride solution (50 mM CaCl<sub>2</sub>)
- Cell lysis buffer (for bacterial cell) (10 mM Tris-HCl, 75 mM NaCl, 25 mM EDTA, pH 8.0)
- Super Signal West Pico Chemiluminescent Substrate (Thermo Fisher Scientific, USA)
- GST binding buffer (50 mM Tris (pH 7.6), 10 mM  $\beta$ -mercaptoethanol)
- GST eluting buffer (50 mM Tris (pH 7.6), 10 mM  $\beta$ -mercaptoethanol, 20 mM reduced glutathione)
- Gold standard for ICP (Sigma-Aldrich, USA)
- His<sub>6</sub> binding buffer [50 mM Tris (pH 7.4), 50 mM NaCl, and 10 mM imidazole]
- His<sub>6</sub> dialysis buffer [50 mM Tris (pH 7.0), 10 mM  $\beta$ -mercaptoethanol, and 10% glycerol]
- His<sub>6</sub> eluting buffer [50 mM Tris (pH 7.4), 50 mM NaCl, and 300 mM imidazole]
- E3 ligase buffer [50 mM Tris (pH 7.5), 0.5 mM DTT, 5 mM ATP, 2.5 mM MgCl<sub>2</sub>, and 5  $\mu$ M ZnCl<sub>2</sub>].
- Lambda DNA-*Hind*III Markers (New England Biolabs, USA)
- Loading buffer for DNA sequencing (deionized formamide (50 mM EDTA, pH 8.0)/ blue dextran 1:5)
- Lysis buffer (for mammalian cell) (50 mM Tris pH 7.6, 50 mM NaCl, 10 mM DTT, 1% Triton X-100, 0.5% NP-40 and 1 mM PMSF)
- Neutralizing solution for alkaline agarose gel electrophoresis (1 M Tris-HCl pH 7.6, 1.5 M NaCl)
- Penicillin/Streptomycin (100X) (PAA Laboratories GmbH, Austria)
- Phosphate buffered saline (PBS) (137 mM NaCl, 2.7 mM KCl, 10 mM Na<sub>2</sub>HPO<sub>4</sub>, 2 mM KH<sub>2</sub>PO<sub>4</sub>)
- Platinum standard for ICP (Sigma-Aldrich, USA)
- Sterile nonpyrogenic, Water for injections B.P. (Thai Otsuka Pharmaceutical, Thailand)
- Ruthenium standard for ICP (Sigma-Aldrich, USA)

- Trypsin EDTA 1X (Invitrogen, USA)
- Zinc ejection assay buffer (10% glycerol, 50 mM, Tris-HCl buffer, pH 7.6)

### Plasticware

- 25 cm<sup>2</sup> cell culture flask (Corning Incorporated, USA)
- 75 cm<sup>2</sup> cell culture flask (Corning Incorporated, USA)
- 96-well flat bottom cell culture cluster plates (Corning Incorporated, USA)
- Acrodisc<sup>®</sup> syringe filter (Pall Corporation, USA)
- Amicon<sup>®</sup> Ultra Centrifugal Filters (Merck Millipore, USA)
- Eppendorf tube 1.5 ml (Axygen Scientific Inc, USA)
- Polyvinylidene fluoride (PVDF) membrane (Millipore, Ireland)
- PCR tube (Axygen Scientific Inc, USA)
- Pipet tip T-1000-B (200-1000 µl) (Axygen Scientific Inc, USA)
- Pipet tip T-200-Y (20-200 µl) (Axygen Scientific Inc, USA)
- Pipet tip T-300-STK (0.2-10 µl) (Axygen Scientific Inc, USA)

### Instruments

- Agarose gel electrophoresis apparatus (BIO 101, USA)
- Allergra<sup>®</sup> X-15R centrifuge (Beckman Coulter)
- Autoclave (HD-3D, Hirayama Company, Japan)
- ABI PRISM<sup>™</sup> 337 DNA Sequencer (Applied Biosystem, USA)
- Bench top single UV transilluminator (Major Science, USA)
- Bio-Rad GS-700 imaging densitometer (BIO-Rad, USA)
- CO<sub>2</sub> incubator (ShellLab, Sheldon Manufacturing Inc, USA)
- Deep freezer (-86°C) (Forma Scientific, USA)
- Freezer (-20°C) (Hotpack, Forma Scientific, USA)
- Gel documentation equipment (1000, BIO-Rad, USA)
- Glutathione-agarose column (GSTrap-HP column) (GE Healthcare, Sweden)
- Hermle 2323K centrifuge (Hermle Labortechnik, Germany)
- Hot air oven (Mammert GmbH Co., Germany)
- Inductively coupled plasma-mass spectrometer (ICP-MS) (Agilent Technologies, USA)
- Inverted microscope (Ck2, Olympus, USA)
- Jasco J720 spectropolarimeter (Japan Spectroscopic Co., Ltd., Japan)
- Laboratory balance (Mettler Toledo AB204, USA)
- Laminar air flow, biosafety carbinet class II (Airstream<sup>®</sup>, ESCO, USA)
- Microplate spectrophotometer (Beckman Coulter, USA)
- Multichannel pipette (Eppendorf, Germany)
- Owl<sup>™</sup> Semi-Dry Electroblothing Systems, (Thermo Scientific, USA)

- pH meter (Mettler Toledo 320, USA)
- Polymerase chain reaction machine; Gene Amp PCR 9600 System (Perkin-Elmer, USA)
- Power supply (EC 135, E-C Apparatus Company, USA and AE-8150 my power 500, ATTO, Japan)
- xCELLigence<sup>®</sup> Real-Time Cellular Analyzer (RTCA) (Roche Applied Science, Germany)
- Shaking incubator (LabTech<sup>®</sup>, Korea)
- Spectrofluorometer FP 2600 (Japan Spectroscopic Co., Ltd., Japan)
- UV spectrophotometer (Genesis 5, Spectronic, USA)
- Vortex (VSM-3 mixer, Shelton Scientific, USA)
- Water bath (Mammert GmbH Co., Germany)

**Kits**

- *Big Dye Terminator Cycle Sequencing Ready Reaction Kit* (Applied Biosystem, USA)
- Ni<sup>2+</sup>-NTA bead (QIAGEN, Germany)

## Methods

### 3.1 RAPTA complexes

The RAPTA complexes, including RAPTA-C, CarboRAPTA-C, RAPTA-T and RAPTA-EA1 (Table 3.1) are kindly provided from Professor Dr. Paul Joseph Dyson, Institut des Sciences et Ingénierie Chimiques, Ecole Polytechnique Fédérale de Lausanne (EPFL), CH-1015 Lausanne, Switzerland. The RAPTA complexes were synthesized and prepared as described previously (Allardyce *et al.*, 2001; Ang, 2007; Scolaro *et al.*, 2005).

**Table 3. 1.** General properties of metal complexes used in this study (Allardyce *et al.*, 2001; Scolaro *et al.*, 2005).

Compound	MW	Formula	Appearance	Solubility
carboRAPTA-C Ru( $\eta^6$ - <i>p</i> -cymene) (C <sub>6</sub> H <sub>6</sub> O <sub>4</sub> )(PTA)	553.1	C <sub>22</sub> H <sub>32</sub> N <sub>3</sub> O <sub>4</sub> PRu ·(H <sub>2</sub> O)	Brown powder, yellow solution	Soluble in aqueous media up to 100-120 mM
RAPTA-C Ru( $\eta^6$ - <i>p</i> - cymene)Cl <sub>2</sub> (PTA)	463.3	C <sub>16</sub> H <sub>26</sub> Cl <sub>2</sub> N <sub>3</sub> PRu	Orange powder, dark orange solution	Soluble in aqueous media up to 20-40 mM
RAPTA-T Ru( $\eta^6$ - toluene)Cl <sub>2</sub> (PTA)	439.3	C <sub>13</sub> H <sub>20</sub> Cl <sub>2</sub> N <sub>3</sub> PRu ·(H <sub>2</sub> O)	Red-brown powder, orange solution	Soluble in aqueous media up to 20-40 mM
RAPTA-EA1 (ethacrynic- $\eta^6$ - benzylamide)RuCl <sub>2</sub> (PTA)	739.4	C <sub>26</sub> H <sub>31</sub> Cl <sub>4</sub> N <sub>4</sub> O <sub>3</sub> PRu ·(H <sub>2</sub> O)	Orange powder, light orange solution	Dissolve in 100% DMSO to 1 mM, dilute in aqueous media up to 100 $\mu$ M
Auphen [Au(1,10- phenanthrolineCl <sub>2</sub> )Cl]	483.46	C <sub>12</sub> H <sub>8</sub> Cl <sub>3</sub> N <sub>2</sub> Au	Orange powder	Soluble in H <sub>2</sub> O
Auterpy [Au(2,2':6,2'' terpyridine)Cl]Cl <sub>2</sub>	536.59	C <sub>12</sub> H <sub>11</sub> Cl <sub>3</sub> N <sub>3</sub> Au	Orange powder	Soluble in H <sub>2</sub> O
Ru-bpy [Ru(Clazpy) <sub>2</sub> bpyCl <sub>2</sub> .7H <sub>2</sub> O]	889.58	C <sub>32</sub> H <sub>24</sub> Cl <sub>4</sub> N <sub>8</sub> Ru ·7(H <sub>2</sub> O)	Dark-red power	Soluble in H <sub>2</sub> O
Ru-phen [Ru(Clazpy) <sub>2</sub> phenCl <sub>2</sub> .8H <sub>2</sub> O]	931.62	C <sub>34</sub> H <sub>24</sub> Cl <sub>4</sub> N <sub>8</sub> Ru ·8(H <sub>2</sub> O)	Dark-red power	Soluble in H <sub>2</sub> O

### 3.2 Preparation of plasmid pBIND DNA by alkaline lysis

A single colony of *Escherichia coli* DH5 $\alpha$  containing the plasmid pBIND DNA (Figure 3.1) was inoculated in 20 ml of rich Luria-Bertani Broth medium (LB Broth medium, containing 50  $\mu$ g/ml of ampicillin). The culture was incubated at 37°C for 12 h with vigorous shaking (150 rpm). One milliliter of the late-log-phase (OD<sub>600</sub> = ~0.6) culture was inoculated in 100 ml of LB Broth medium containing final concentration of ampicillin at 50  $\mu$ g/ml and further incubated at 37°C for 14-16 h with shaking or until the bacteria reached late log phase.

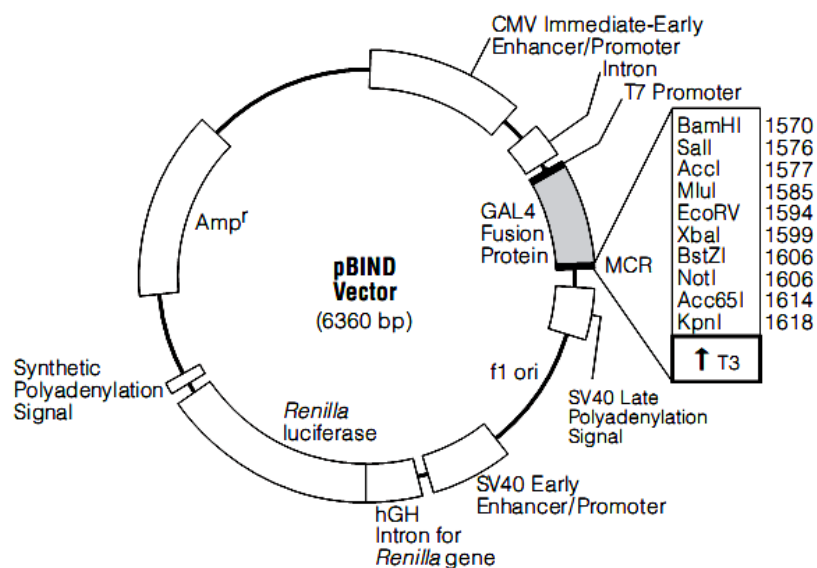


**Figure 3.1.** Map of the plasmid pBIND DNA.

One milliliter of the bacterial culture was pipetted and removed to a fresh microcentrifuge tube. The bacterial cells were harvested by centrifugation at 13,000g at 4°C for 5 min. The supernatant was discarded and the bacterial pellets were harvested and resuspended in 200  $\mu$ l of an ice-cold alkaline lysis solution I by vortexing. Four hundred microliter of alkaline lysis solution II (freshly prepared) was added to each bacterial suspension, then mixed by inverting rapidly for five times, and the tube was stored on ice for 10 min. Three hundred microliter of an ice-cold alkaline lysis solution III was added into the suspension, and the tube was stored on ice for 10 min. The bacterial cell lysates were harvested by centrifugation at 12,000g at 4°C for 10 min. The supernatant was transferred to a fresh microcentrifuge tube. Two volumes of cold absolute ethanol was added to precipitate DNA at -80°C for 3 h. After precipitation, the DNA pellets were collected by centrifugation at 12,000g at 4°C for 10 min, then washed with 1 ml of 70% ethanol and the supernatant was removed by centrifugation at 12,000g at 4°C for 10 min. The pellet of DNA was dried at room temperature and dissolved in 20  $\mu$ l of double distilled water and stored at -20°C.



### 3.3 Amplification of the 3' terminal region of the 696-bp *BRCA1* gene fragment

The 696-bp *BRCA1* fragment (3' terminal region of the *BRCA1* gene) (Figure 3.2) was amplified from the plasmid pBIND-BRCT (Ratanaphan *et al.*, 2009) by the polymerase chain reaction (PCR). The PCR reaction mixture was performed in the final volume of 100  $\mu$ l as described previously (Charkree *et al.*, 2012). Briefly, the PCR mixture contained 100 ng of DNA template, 1.5 units of *Taq* DNA polymerase, 0.5  $\mu$ M forward and reverse primers, 200  $\mu$ M dNTP, 2 mM MgCl<sub>2</sub>, 1x PCR buffer, and sterile water to make up 100  $\mu$ l (Table 3.2). The reaction mixture was thoroughly mixed. The thermal cycle was programmed according to the manufacturer's instructions (Table 3.3). The PCR product was electrophoresed on 1% agarose gel at 80 V for 60 min. The gel was stained with ethidium bromide and visualized under ultraviolet (UV) light.

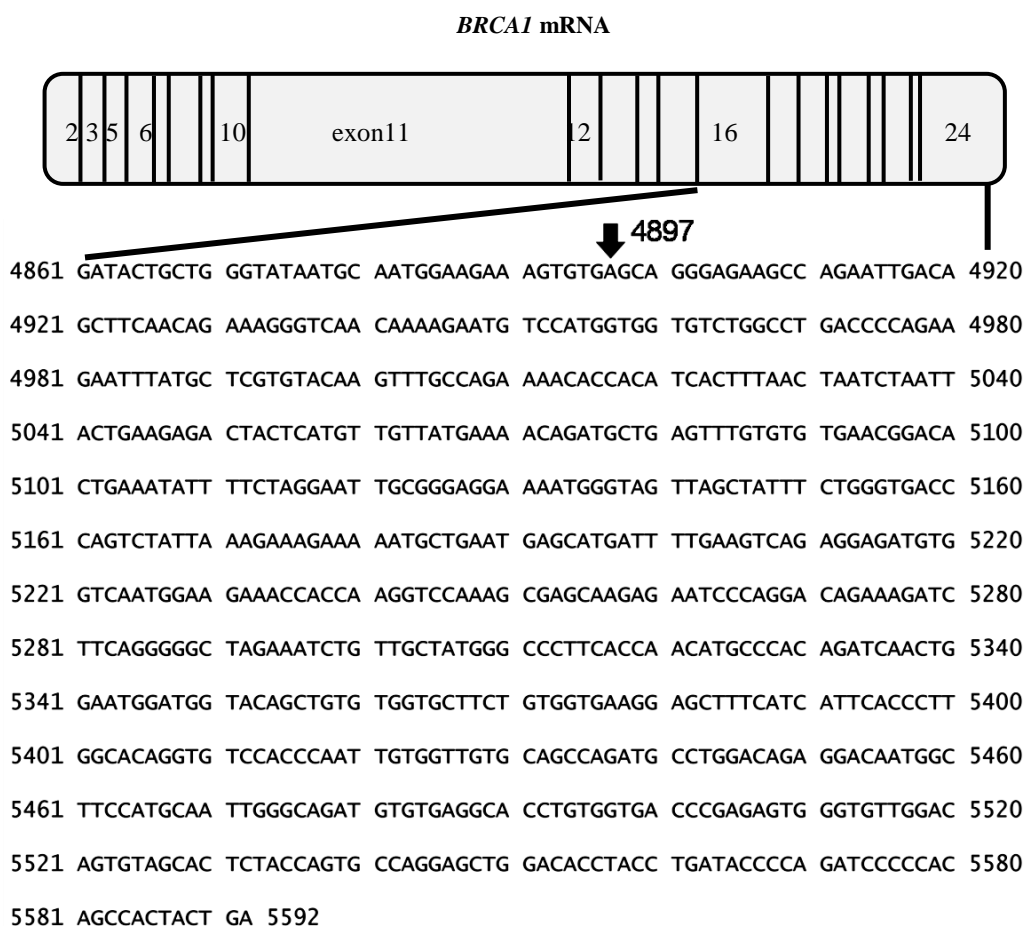


**Figure 3.2.** Nucleotide alignment of the 696-bp *BRCA1* gene fragment (nucleotide 4,897-5,592) covering exon 16-24.

**Table 3.2** PCR reaction components for the amplification of the 3' terminal region of the 696-bp *BRCA1* gene fragment.

Component	Final concentration
10x PCR buffer (contains 20 mM MgCl <sub>2</sub> )	1x
dNTP (10 mM of each)	200 μM
10 μM forward primer (5' ATAAAATCGACAGGGATCCTTAGCAGG GAGAAGCCAGAATTG 3')	0.5 μM
10 μM reverse primer (5' ACTTTGTGTTTCATTTCTAGATCAGTAG TGGCTGTGGGGGAT 3')	0.5 μM
<i>Taq</i> DNA polymerase	1.5 units
DNA template	100 ng
Steriled double distilled water	
<b>Total 50 μl</b>	

**Table 3.3** Thermal cycle conditions for the amplification of the 3' terminal region of the 696-bp *BRCA1* gene fragment.

Cycling condition	Temperature (°C)	Time
<b>Pre-denaturation</b>	94	3 min
Denaturation	94	30 sec
Annealing	60	45 sec
Extension	72	45 sec
<b>Number of cycles</b>	30 cycles	
<b>Final extension</b>	72	10 min

### 3.4 *In vitro* ruthenation of plasmid pBIND DNA by RAPTA complexes

#### 3.4.1 Conformational study of RAPTA-treated plasmid DNA

The pBIND plasmid (4 µg) was incubated with various molar ratios of RAPTA complexes per DNA nucleotide ( $rb$ ) at 37 °C for 24 h in the dark. The ruthenium-treated DNA was precipitated by absolute ethanol and subsequently centrifuged at 13,500g at 4°C for 30 min. The supernatant was removed and the DNA pellet was washed twice with 70% ethanol and centrifuged at 13,500g at 4°C for 30 min. The DNA pellet was dried at room temperature and redissolved in 20 µl of double distilled water. The samples were electrophoresed on 0.8% agarose gel at 80 V for 60 min. The gel was stained with ethidium bromide and visualized under UV light. The mean DNA supercoil unwinding angle ( $\Phi$ ) triggered by drug interactions was calculated from the equation:

$$\Phi = -18\sigma/rb(c)$$

Where  $\sigma$  is the superhelical density of the plasmid and  $r_b(c)$  is the drug concentration at which the supercoiled and open circular forms co-migrate (Ratanaphan *et al.*, 2005).

### 3.5 *In vitro* ruthenation of the *BRCA1* gene fragment by RAPTA complexes

#### 3.5.1 Interstrand cross-linking assay

The 696-bp *BRCA1* gene fragment was used for DNA template and incubated with various  $rb(s)$  at 37 °C for 24 h. The ruthenium-treated DNA was precipitated by absolute ethanol and subsequently centrifuged at 13,500g at 4°C for 30 min. The supernatant was removed and the DNA pellet was washed twice with 70% ethanol and centrifuged at 13,500g at 4°C for 30 min. The DNA pellet was dried at room temperature and redissolved in 20 µl of double distilled water. The amount of Ru-DNA cross-links was analyzed on 1% agarose gel under denaturing condition (Sambrook and Russell, 2001).

#### 3.5.2 Restriction analysis of Ru-*BRCA1* adducts

The 696-bp *BRCA1* gene fragment was used for DNA template and incubated with various  $rb(s)$  in 20 µl of reaction mixture at 37°C for 24 h in the dark. The ruthenium-treated DNA was precipitated by absolute ethanol and subsequently centrifuged at 13,500g at 4°C for 30 min. The supernatant was removed and the DNA pellet was washed twice with 70% ethanol and centrifuged at 13,500g at 4°C for 30 min. The DNA pellet was dried at room temperature and redissolved in 20 µl of double distilled water and further incubated at 37°C with 1 unit of *EcoO109I* (recognition sequence: PuG▼GNCCPy) and 1 unit of *PvuII* (recognition sequence: CAG▼CTG) for 5 and 6 h, respectively. The restricted samples were electrophoresed on 1% agarose gel. The gel was stained with ethidium bromide and visualized under UV light.

### 3.5.3 Sequence preference of RAPTA-*BRCA1* adducts

Localization of ruthenium-*BRCA1* adducts was determined based on premature termination of DNA synthesis on a ruthenium-modified *BRCA1* template, as described previously (Ratanaphan *et al.*, 2005). The 696-bp *BRCA1* gene fragment (4.25  $\mu$ g) was incubated with 500  $\mu$ M of RAPTAs at 37°C for 24 h in the dark. The ruthenium-treated or control (non-ruthenated) DNA was precipitated by absolute ethanol and subsequently centrifuged at 13,500g at 4°C for 20 min. The supernatant was removed and the DNA pellet was washed twice with 70% ethanol and centrifuged at 13,500g at 4°C for 30 min. The DNA pellet was dried at room temperature and redissolved in 20  $\mu$ l of double distilled water and the concentration of DNA was spectrophotometrically determined at 260 nm.

The 20  $\mu$ l of *BigDye* terminator was mixed with 200 ng of ruthenium-treated DNA in a PCR tube containing 5 pmol of forward primer (5'-GGAATTCCAT ATGAGCAGGGAGAAG-3') or reverse primer (5'-ATTGGTTCTGCAGRCAGT AGTGGCT-3'), 1 mM *Tris*-HCl (pH 8.3), 1.5 mM MgCl<sub>2</sub>, 200  $\mu$ M of each dNTP, and 1 unit of *Taq* DNA polymerase. The reaction mixtures were subjected to temperature cycling using a Perkin-Elmer Model 9600 cycle (Applied Biosystem, USA). The thermal cycle condition was programmed as shown in Table 3.4. Eighty microliter of 70% isopropanol was used to remove the unincorporated *BigDye* terminator (Applied Biosystem, USA). The sample was centrifuged at 14,000g at room temperature for 20 min. The supernatant was removed and the DNA pellet was washed twice with 70% ethanol and centrifuged at 14,000g for 5 min. The sample was dried in a heat block at 90°C for 1 min and redissolved in 6  $\mu$ l of loading buffer (deionized formamide (50 mM EDTA, pH 8.0)/ blue dextran 1:5) and was heated at 90°C for 2 min before incubation on ice. Aliquots of sample (1 ml) were loaded onto a 6% polyacrylamide/8 M urea DNA-sequencing gel using an automated DNA sequencer (ABI PRISM™ 377 DNA Sequencer, Applied Biosystem, USA). The DNA synthesis on the template containing the ruthenium adducts produced DNA fragments migrating on the sequencing gel as intense bands, which corresponded to the termination sites of DNA synthesis.

**Table 3.4** Thermal cycle conditions for DNA sequencing.

Cycling condition	Temperature (°C)	Time
<b>Pre-denaturation</b>	96	1 min
Denaturation	96	10 sec
Annealing	50	5 sec
Extension	60	4 min
<b>Number of cycles</b>	25 cycles	

### 3.6 *In vitro* inhibition of *BRCA1* amplification using a semi-quantitative polymerase chain reaction (QPCR)

A QPCR was used to determine the polymerase inhibiting effect of DNA ruthenation. RAPTA-C or carboRAPTA-C with various concentrations (0-1,000  $\mu\text{M}$ ) was incubated with the 696-bp *BRCA1* gene fragment (4.25  $\mu\text{g}$ ) at 37°C for 24 h in the dark. The ruthenium-treated DNA was precipitated by absolute ethanol and subsequently centrifuged at 13,500g at 4°C for 20 min. The supernatant was removed and the DNA pellet was washed twice with 70% ethanol and centrifuged at 13,500g at 4°C for 30 min. Then, the DNA pellet was dried at room temperature and redissolved in 20  $\mu\text{l}$  of double distilled water. The amount of DNA was spectrophotometrically determined at 260 nm. The PCR mixture contained Ru-treated DNA (100 ng), each forward and reverse primer (0.5  $\mu\text{M}$  of each), dNTP (200  $\mu\text{M}$  of each),  $\text{MgCl}_2$  (2 mM), and *Taq* DNA polymerase (1.5 units) and steriled water to make up to 50  $\mu\text{l}$ . The thermal cycle was programmed according to the Table 3.3. The PCR products were separated on 1% agarose gel electrophoresis at 80 V for 60 min. The gel was stained with ethidium bromide and visualized under UV light.

The amplification of PCR products from agarose gel was measured by a Bio-Rad Molecular Imager with ImageQuant Software (Molecular Dynamics). The amount of amplification was represented by the units of absorbance of the amplified products. Based on the assumption that the lesions distributed randomly as described previously (Ratanaphan *et al.*, 2005), the lesion frequency per strand was calculated by the Poisson equation as follows:

$$S = -\ln(A_d/A)$$

$S$	=	The lesion frequency/strand
$A$	=	The absorbance unit produced from a given amount of non-damaged DNA template
$A_d$	=	The absorbance unit produced from a given amount of damaged DNA template (damaged by a particular dose of RAPTA complexes)
$A_d/A$	=	The fraction of non-damaged template at a given dose

### 3.7 Cell viability study

#### 3.7.1 Cell culture

Human breast adenocarcinoma cell line, MCF-7 and MDA-MB-231 cells were grown in Dulbecco's modified Eagle's medium (DMEM) (Sigma-Aldrich, USA) without phenol red. HCC1937 cells were grown in Roswell Park Memorial Institute 1640 medium (RPMI 1640) (Sigma-Aldrich, USA) without phenol red. All media were supplemented with 1% penicillin-streptomycin and 10% fetal bovine serum (FBS). All cell lines were cultured at a constant temperature of 37°C in a 5% carbon dioxide ( $\text{CO}_2$ ) humidified atmosphere.

### 3.7.2 Cell viability by a MTT assay (single complex treatment)

The growth inhibitory effect towards breast cancer cell lines (MCF-7, MDA-MB-231 and HCC1937 cells) was evaluated by means of the tetrazolium salt MTT assay [MTT = 3-(4,5-dimethylthiazol-2-yl)-2,5-diphenyltetrazolium bromide]. About  $5 \times 10^4$  cells were seeded into each well of a 96-well flat bottom cell culture plate and grown at 37 °C in 5% CO<sub>2</sub> for 48 h. The medium was removed and replaced with 200 µl in the absence or presence of RAPTA complexes at various concentrations of the complexes, and then incubated at 37 °C in 5% CO<sub>2</sub> for 48 h. Each well was washed with 100 µl of phosphate buffered saline (PBS) and then 100 µl of 0.5 mg/ml of the 3-(4,5-dimethylthiazol-2-yl)-2,5-diphenyl tetrazolium bromide (MTT) solution was added and incubated at 37 °C in 5% CO<sub>2</sub> for 4 h. The MTT solution was gently removed and replaced with 200 µl of 100% dimethylsulfoxide solution (DMSO) to solubilize the purple formazan crystals. The optical density of each well was measured at wavelength of 570 nm using an automated microplate reader. The cell viability was calculated by the following equation:

$$\text{cell viability (\%)} = \frac{\text{abosorbance of the Ru – treated cells}}{\text{abosorbance of the control (Ru – untreated cells)}}$$

The percentage cell viability versus concentration was plotted. The 50% inhibitory concentration (IC<sub>50</sub>) for a particular drug was defined as the concentration producing 50% decrease in cell growth.

### 3.7.3 Cell viability by a MTT assay (combination treatment)

The effect of RAPTA-EA1 and olaparib combination treatment on cell proliferation was assessed in MCF-7, MDA-MB231 and HCC1937 cells using a MTT assay as previously described in Topic 3.7.1 and 3.7.2. Synergism, antagonistic or additive drug interactions were determined by combination index (CI) based on Chou-Talalay's Combination Index Theorem as follows (Chou and Talalay, 1984).

$$CI = \frac{(D)_1}{(Dx)_1} + \frac{(D)_2}{(Dx)_2}$$

$(Dx)_1$  = dose of drug 1 to produce 50% cell kill alone

$(D)_1$  = dose of drug 1 to produce 50% cell kill in combination of drug 2

$(Dx)_2$  = dose of drug 2 to produce 50% cell kill alone

$(D)_2$  = dose of drug 2 to produce 50% cell kill in combination of drug 1

The above equation provides the theoretical basis for the combination index (CI)-isobologram equation that allows quantitative determination of drug interactions, where CI is summarized in Table 3.5.

**Table 3.5** Description and symbols of synergism or antagonism in drug combination studies analyzed with the combination index method (Chou and Talalay, 1984)

Range of Combination Index	Description graded	Symbols
<0.1	Very strong synergism	+ + + + +
0.1–0.3	Strong synergism	+ + + +
0.3–0.7	Synergism	+ + +
0.7–0.85	Moderate synergism	+ +
0.85–0.90	Slight synergism	+
0.90–1.10	Nearly additive	±
1.10–1.20	Slight antagonism	-
1.20–1.45	Moderate antagonism	- -
1.45–3.3	Antagonism	- - -
3.3–10	Strong antagonism	- - - -
> 10	Very strong antagonism	- - - - -

#### 3.7.4 Cell viability by a Real-Time Cellular Analyzer

The Real-Time Cellular Analyzer (RTCA) (xCELLigence System, Roche Applied Science, Germany) was used for monitoring the growth kinetics of MCF-7, MDA-MB-231 and HCC1937 cells towards the RAPTAs treatments. Two additional ruthenium(II) complexes including Ru-bpy, {[Ru(Clazpy)<sub>2</sub>bpyCl<sub>2</sub>.7H<sub>2</sub>O]} and Ru-phen, {[Ru(Clazpy)<sub>2</sub>phenCl<sub>2</sub>.8H<sub>2</sub>O]} were used for comparison purpose. The RTCA system was performed according to the manufacturer's instructions as described previously (Nhukeaw *et al.*, 2014). For each experiment, the medium (100 µl) was added into 96-well E-plates for recorded the background. A cell density at  $5 \times 10^4$  cells/well of cell suspension (100 µl) was added to each well of the E-plate. The attachment, spreading and proliferation of the cells was monitored every 15 min until the cells entering their logarithmic growth phase (7 h for the MCF-7 cells and HCC1937 cells, 18 h for the MDA-MB-231 cells). Then, the plate was removed from the RTCA machine and the PBS was used for washing the cells to removing any cell debris. An either fresh medium (control) or fresh medium containing the metal complexes (at various concentrations) was added to each well. The proliferation of the cells was further assessed every 15 min interval for 24 h. Then, medium containing the metal complexes was removed after finished of incubation time, then the cells was washed twice with PBS to removing any cell debris and all wells was added fresh medium again. The degree of cellular recovery in the absence of the metal complexes was further measured for 24 h. Each experiments were performed in triplicate.

### 3.8 Plasmid construction and protein purification

#### 3.8.1 Expression and purification of the BRCA1 RING protein for CD analysis and gel shift assay

The BRCA1 RING proteins, both wild-type and variants (D67E and D67Y) containing the first 304 amino acid residues were prepared as described previously (Atiparin *et al.*, 2010). The D67E variant is the substitution of aspartic acid with glutamic acid at position 67, while D67Y variant is the substitution of aspartic acid with tyrosine at position 67. This variants is located in the second Zn<sup>2+</sup>-binding loop (residues 58-68) (Brzovic *et al.*, 2003). The PCR was used for amplified the desired *BRCA1* gene fragment. Primers used were synthesized to incorporate the 5' *Bam*HI and 3' *Xho*I endonuclease restriction sites on the PCR products. The digested of *Bam*HI and *Xho*I-treated PCR products was cloned into derivative of a plasmid pET28a(+), then subsequently verified by DNA sequencing. *E. coli* BL21 (DE3) were transformed with the recombinant plasmids for protein synthesis. Luria Broth medium with 30 µg/ml kanamycin was used for growing the transformed *E. coli* BL21(DE3) cells at 37°C. When the  $A_{600\text{ nm}}$  reached 0.5-0.6, the protein expression was induced by isopropyl-1-thio-β-D-galactopyranoside (IPTG) (at final concentration of 0.5 mM), then allowed cells growth for 5 h after induction and harvested by centrifugation. Lysis buffer (50 mM Tris pH 7.6, 50 mM NaCl, 10 mM DTT, 1% Triton X-100, 0.5% NP-40 and 1 mM PMSF) was used for cell lysis, then lysed by sonication (10 min with 60% amplitude, 9 s pulse on, and 4 s pulse off). The inclusion bodies were solubilized in guanidine HCl and then dialyzed against 0.1% acetic acid. Purified proteins were identified on 12% SDS-PAGE.

#### 3.8.2 Expression and purification of the BRCA1 RING protein for ICP-MS analysis, zinc ejection assay and *in vitro* ubiquitination assay

The BRCA1 RING proteins, both wild-type and variants (D67E and D67Y) containing the first 304 amino acid residues, the BARD1 protein (residues 26-327), the ubiquitin (full-length), and E2 (UbcH5c) were prepared as described previously (Atipirin *et al.*, 2011b). The BRCA1 protein (residues 1-304) and the BARD1 protein (residues 26-327) (Addgene plasmid 12646) were produced as a GST fusion by cloning the respective genes into the pGEX-4T1 (Amersham Biosciences). The ubiquitin (full-length) (Addgene plasmid 12647) and E2 (UbcH5c) (Addgene plasmid 12643) genes were inserted into a pET28a(+) derivative for expression of a His<sub>6</sub>-tagged protein. All recombinant plasmids were verified by DNA sequencing. *E. coli* BL21 (DE3) were transformed with the each recombinant plasmids. When the  $A_{600\text{ nm}}$  reached 0.5-0.6, the protein expression was induced by IPTG (0.5 mM) for 12 h at 25 °C. Lysis buffer (50 mM of Tris pH 7.6, 50 mM of NaCl, 10 mM of DTT, 1% of Triton X-100, 0.5% of NP-40 and 1 mM of PMSF) was used for cell lysis, then lysed by sonication (10 min with 60% amplitude, 9 s pulse on, and 4 s pulse off). A glutathione-agarose column was used for purified the GST-tagged proteins. The bound proteins were eluted with eluting buffer (50 mM of Tris (pH 7.4), 10 mM of β-mercaptoethanol, and 20 mM of reduced glutathione). A deionized water was used for extensively dialyzed purified proteins. Nickel beads was used for purified the His<sub>6</sub>-tagged proteins. The bound proteins were washed with a binding buffer [50 mM of



Tris (pH 7.4), 50 mM of NaCl, and 10 mM of imidazole], then His<sub>6</sub>-tagged proteins was eluted with the eluting buffer [50 mM of Tris (pH 7.4), 50 mM of NaCl, and 300 mM of imidazole]. The purified His<sub>6</sub>-Ub and His<sub>6</sub>-UbCH5c proteins were then dialyzed against a dialysis buffer [50 mM of Tris (pH 7.0), 10 mM of  $\beta$ -mercaptoethanol, and 10% of glycerol].

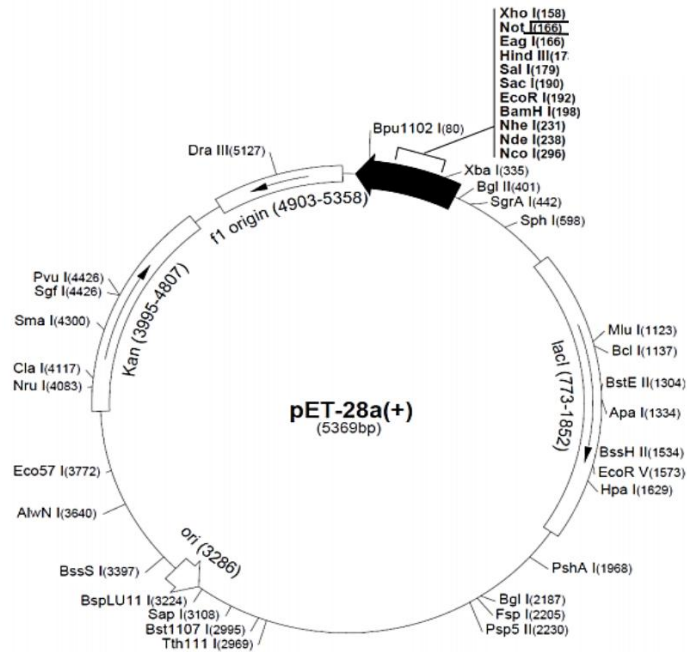


**Figure 3.3.** Map of the plasmid pET-28a(+).

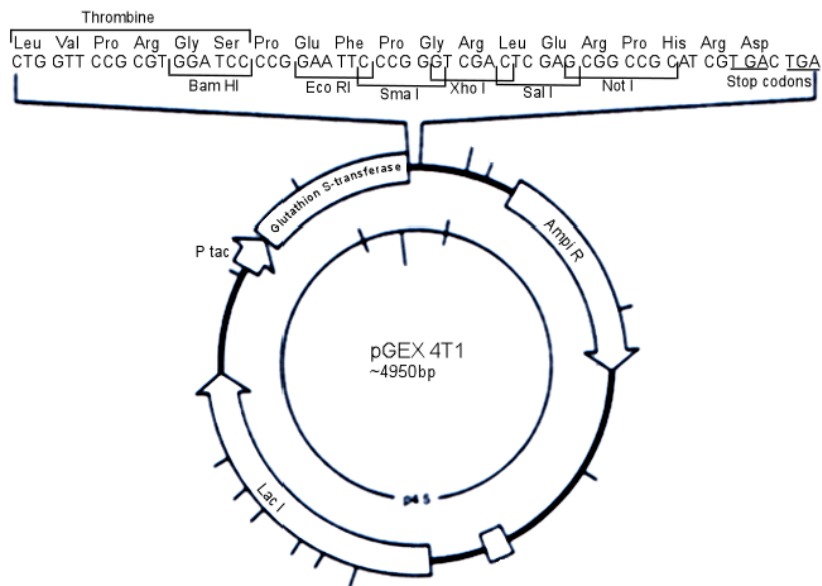


**Figure 3.4.** Map of the plasmid pGEX4T1.

### 3.9 Preparation of metal–BRCA1 complexes

Cisplatin, RAPTA complexes, two gold(III) compounds, namely Auphen ([Au(1,10-phenanthroline)Cl<sub>2</sub>]Cl) and Auterpy ([Au(2,2':6,2''-terpyridine)Cl]Cl<sub>2</sub>), and two ruthenium(II) polypyridyl complexes, namely Ru-bpy and Ru-phen were prepared as stock solutions in deionized water. The *N*-terminal BRCA1 (1-304) proteins, both wild-type and mutant (D67E and D67Y), were dissolved in deionized water. The holo-BRCA1 was prepared by pre-incubated with ZnCl<sub>2</sub> at the molar ratio of 1:3 (BRCA1: ZnCl<sub>2</sub>) at 4 °C for 8 h. The holo-BRCA1 proteins were treated with cisplatin, RAPTA complexes, gold(III) complexes or ruthenium(II) polypyridyl complexes at various concentrations at 4 °C for 24 h. Any unbound metal-complexes were removed by centrifugal devices. A Bradford assay, using BSA as standard, was used for determined the amount of protein.

### 3.10 Interaction of BRCA1 RING protein with RAPTA complexes

#### 3.10.1 Gel shift assay

The metal treated-holo-BRCA1 protein was prepared as described above (Topic 3.9). The interaction of metal-BRCA1 adducts was investigated by gel shift assay. BRCA1 protein (10 μM) was pre-incubated with ZnCl<sub>2</sub> (30 μM) at 4 °C for 8 h. Holo-BRCA1 was incubated with cisplatin, RAPTA-C, RAPTA-T or RAPTA-EA1 at various molar ratios of protein: drug at 4 °C for 24 h, and electrophoresed on 8% SDS/PAGE. The bands of protein were detected by silver staining.

#### 3.10.2 ICP-MS analysis

The metal treated-holo-BRCA1 proteins, both wild-type and variants (D67E and D67Y), were prepared as described in Topic 3.9. Ten μM of holo-BRCA1 proteins were incubated with 50 μM of cisplatin, RAPTA complexes or gold(III) complexes at 4 °C for 24 h. Any unbound metal complexes were removed by dialysis in deionized water. The amount of protein was then determined by a Bradford assay, using BSA as standard. Three microgram of metal-protein adducts were used for determination of the amount of metals binding to proteins. The amount of metal-BRCA1 adducts was analyzed by inductively coupled plasma-mass spectrometer (ICP-MS) (Agilent Technologies, USA) following the manufacturer's instructions. Each experiment was measured in triplicated.

#### 3.10.3 Conformational study and thermal stability of the BRCA1 RING domain protein

To study the conformational change and thermal denaturation of the metal-treated BRCA1, circular dichroism (CD) was used for determining the effect of ruthenium binding on the conformation and stability of the BRCA1 RING domain. Cisplatin, two gold(III) compound (Auphen and Auterpy) and two ruthenium(II) polypyridyl (Ru-bpy and Ru-phen) were used for comparison. Protein samples, both wild-type and variants (D67E and D67Y), (10 μM) were prepared as previously described in Topic 3.8.2. Acquiring CD spectra, 200-260 nm, was used for monitored

metal-dependent folding of the protein. Measurements of metal binding were carried out at 25°C using a 0.1 cm quartz cuvette. The average of five separate spectra with a step size of 0.1 nm, a 2 s response time and a 1 nm bandwidth was determined. The CD spectra of each ruthenium concentrations was measured for corrected baseline. The secondary structures of proteins were predicted by the CONTIN program (Greenfield, 2006; Provencher and Glockner, 1981). the thermal denaturation of metal-treated proteins were also performed in three separate scans in the range from 25°C to 95°C at 208 nm with a heat rate of 1°C/min. Thermal renaturation (25°C after being heated at 95°C) was also observed. The binding constant was determined as follows,

$$\theta_{obs} = \theta_{max} \left( \frac{(1 + (kC/n) + kP)/(2kP) - \sqrt{((1 + (kC/n) + kP)/(2kP))^2 - C/(nP)}}}{1} \right)$$

$\theta_{obs}$	=	The observed ellipticity change at any concentration of metal
$\theta_{max}$	=	The ellipticity change when all of the protein binds metal
k	=	The binding constant
P	=	The protein concentration.
C	=	The concentration of metal added
n	=	The number of binding sites

The free energy of binding was given by the following equation,  
 $\Delta G = -RT \ln k$

$\Delta G$	=	The free energy.
R	=	The gas constant of 1.987 cal mol <sup>-1</sup>
T	=	The temperature in Kelvin
k	=	The binding constant

### 3.10.4 Zinc ejection assay

The metal treated-BRCA1 proteins, both wild-type and variants (D67E and D67Y), were prepared as described in Topic 3.9. Two gold(III) complexes, Auphen and Auterpy, were used for comparison purpose. Purified BRCA1 proteins (10  $\mu$ M) were incubated with metal complexes at various molar ratio of protein: drug in zinc ejection assay buffer [10% of glycerol, 50 mM of Tris-HCl buffer (pH 7.6)]. The reaction mixtures were incubated at 4 °C in the dark for 8, 16, or 24 h. The ejection of zinc from the protein was monitored by the change in fluorescence of the zinc-selective fluorophore TSQ (6-methoxy-8-*p*-toluenesulfonamido-quinoline) in the assay buffer. The zinc ejection assay was initiated by the addition of 20  $\mu$ M (final concentration) of TSQ at room temperature. The TSQ fluorescence was immediately monitored at each concentration or time dependent (excitation filter, 360 nm; emission filter, 490 nm) by using a spectrofluorometer (FP 2600 Jasco Corporation). A ZnCl<sub>2</sub> standard curve was created under the same conditions in the absence of the BRCA1 protein. To control for fluorescence changes in the assay not due to the effect of metal complexes binding to TSQ, the results from above experiments were subtracted with fluorescence intensity of each compound in the presence of TSQ.

### 3.11 The effect of metal complexes on the *in vitro* BRCA1/BARD1-mediated ubiquitination

#### 3.11.1 *In vitro* ubiquitination assay

The metal treated-BRCA1 proteins, both wild-type and variants (D67E and D67Y), were prepared as described in Topic 3.9. Two ruthenium(II) polypyridyl complexes (Ru-bpy and Ru-phen) and two gold(III) complexes (Auphen and Auterpy) were used for comparison purpose. The ubiquitin ligase reactions were performed as previously described (Atipairin *et al.*, 2011a; Atipairin *et al.*, 2011b). The reaction mixture (20  $\mu$ l) was prepared according to Table 3.6. The reactions were incubated at 37 °C for 3 h. An equal volume of SDS-loading dye was used for terminated the reaction. The samples were electrophoresed on 8% SDS-PAGE. The separated protein was then transferred to the PVDF membrane. The membrane samples were incubated with anti-His<sub>6</sub> HRP (Horseradish Peroxidase) conjugated (at a dilution of 1:2000) (chemiluminescent method, QIAGEN). The blot was detected by chemiluminescence (SuperSignal<sup>TM</sup>, Pierce) on X-ray film. A densitometer (Bio-Rad GS-700 Imaging) was used for quantified the relative E3 ligase activity of the BRCA1 adducts. The experiment was performed in duplicate.

**Table 3.6.** Reaction components for the *in vitro* ubiquitination assay

Component	Final concentration
10X E3 ligase buffer	1X
Ub	20 $\mu$ M
E1	300 nM
UbcH5c	5 $\mu$ M
BRCA1 or a Ru-BRCA1 adduct	3 $\mu$ g
BARD1	3 $\mu$ g
<b>Total 20 <math>\mu</math>l</b>	

\* E3 ligase buffer [50 mM Tris (pH 7.6), 0.5 mM DTT, 5 mM ATP, 2.5 mM MgCl<sub>2</sub> and 5  $\mu$ M ZnCl<sub>2</sub>]

## CHAPTER 4

### RESULTS

#### 4.1 DNA binding study

##### 4.1.1 *In vitro* ruthenation of the plasmid DNA by RAPTA complexes

##### 4.1.1.1 Conformational study

The agarose gel electrophoresis method was used for determination of the RAPTA-mediated conformational change of the plasmid DNA. The pBIND plasmid was used as a model. The ruthenium-induced pBIND DNA exhibited two forms, i.e., Form I (supercoiled DNA, S) and Form II (open circular, O) (Fig. 4.1). The results revealed that the mobility of the RAPTA-treated plasmid DNA was reduced as the molar ratio of ruthenium/DNA nucleotide ( $r_b$ ) increased. This observation indicated that the DNA duplex unwinding of a complex causes the reducing of the number of supercoils in closed circular DNA, which in turn causes a decrease of migration through agarose gel. Furthermore, both RAPTA-C (Fig. 4.1A) and carboRAPTA-C (Fig. 4.1B) induce different degrees of DNA unwinding. The unwinding angle was about  $7^\circ$  per bound of RAPTA-C (calculated from the  $r_b$ , at 0.019). In contrast, the unwinding angle of carboRAPTA-C was about  $3^\circ$  (calculated from the  $r_b$  at 0.052).

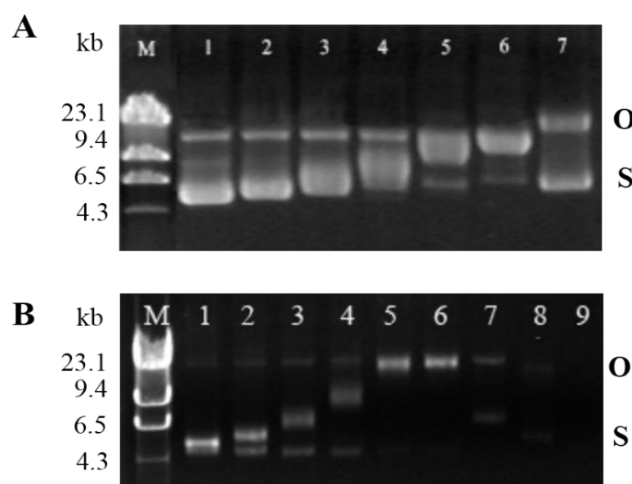


**Figure 4.1.** Effects of the RAPTA complexes on the conformation of the pBIND plasmid DNA. The top bands relate to the form of open circular DNA (O) and the bottom bands to supercoiled DNA (S). The DNA samples were incubated with complexes at the  $r_b$  of 0, 0.0026, 0.0065, 0.013, 0.016, 0.019 and 0.026 (lanes 1-7, respectively) for RAPTA-C (A), and that of 0, 0.0065, 0.013, 0.026, 0.039, 0.052, 0.065, 0.13 and 0.19 (lanes 1-9, respectively) for carboRAPTA-C (B). M stands for  $\lambda$ -HindIII digested marker.

### 4.1.2 Interstrand crosslinks assay

In this study, the effect of the RAPTA complexes on DNA interstrand crosslink was probed by alkaline gel electrophoresis method. Under alkaline condition double-strand DNAs is disrupted to a single strand. Both separated single-stranded DNAs, migrate faster (lower band) in the gel. The intensity of the interstrand crosslink increases as the  $r_b$  values increase in both complexes. The results showed that the intensity of the interstrand crosslink increases as the  $r_b$  values increase in the ruthenium complexes (Fig. 4.2). The interstrand crosslinks of RAPTA-C treated-DNA was observed at the  $r_b$  of 0.0016 and was completed at the  $r_b = 0.032$  (Fig. 4.2A). While carboRAPTA-C, the interstrand crosslink also occurred at the  $r_b$  of 0.0016 and increases as the  $r_b$  values increases, but more slowly compared to RAPTA-C (Fig. 4.2B).

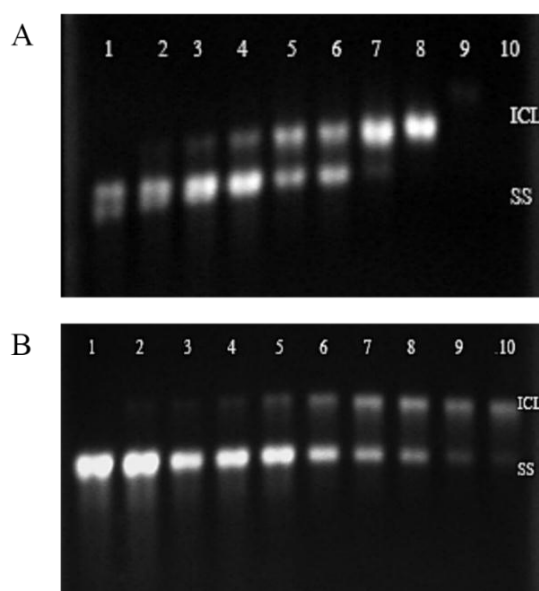


**Figure 4.2.** Interstrand cross-links formation induced by RAPTA complexes in the 696-bp *BRCA1* gene fragment. The top bands showed the migrating of interstrand cross-linked DNA (ICL) and the sigle-stranded DNA (SS) appears as the bottom bands. The DNA sample was incubated with RAPTA complexes at the  $r_b$  of 0 (control), 0.0016, 0.0033, 0.0066, 0.013, 0.020, 0.026, 0.032, 0.045 and 0.053 for RAPTA-C (lanes 1-10, respectively) (A), and at the  $r_b$  of 0 (control), 0.0016, 0.0033, 0.0066, 0.013, 0.033, 0.053, 0.066, 0.08 and 0.1 for carboRAPTA-C (lanes 1-10, respectively) (B).

### 4.1.3 RAPTA-*BRCA1* adducts interfere restriction digestion

The ruthenation sites on the specified *BRCA1* gene fragment can be inferred from restriction analysis using enzyme whose recognition sequence exist on the tested gene. Digested fragment of the *BRCA1* gene by *EcoO109I* (PuG/GNCCPy) generated two digested fragments (283-bp and 413-bp) and by *PvuII* (CAG/CTG) generated two digested fragments (237-bp and 459-bp) (Fig. 4.3). Production of

digested fragment from RAPTA-C-treated DNA and carboRAPTA-C-treated DNA in the presence of both enzymes were similar level of inhibition. These suggested that the ruthenation by RAPTA complexes does not show specificity between the two sites. In addition, the activity of these both restriction enzymes was affected about 2 fold less by carboRAPTA-C treatment compared to treatment with RAPTA-C. It suggested that either ruthenation by RAPTA-C occurs more rapidly than that of carboRAPTA-C or the former complex is more stable than the latter.

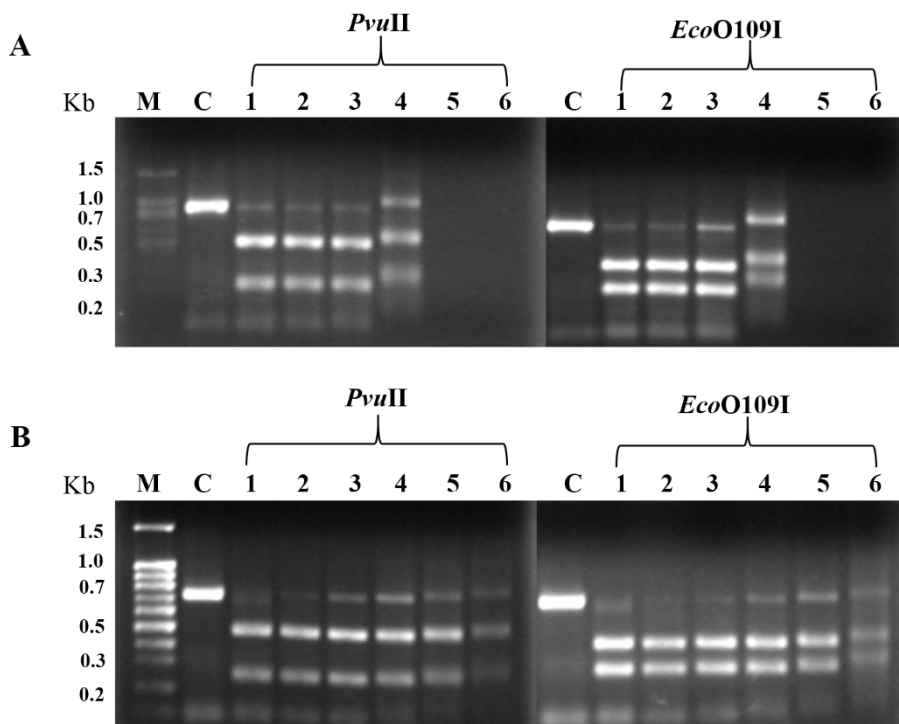


**Figure 4.3.** Restriction digestion for ruthenation site of the 696-bp *BRCA1* gene fragment induced by the RAPTA complexes. The 696-bp *BRCA1* gene fragment was incubated with the following various  $r_b$  values at 37°C for 24 h in the dark. The RAPTA-treated DNA was precipitated, washed, redissolved in doubly distilled H<sub>2</sub>O, and incubated with 1 unit of either *PvuII* or *EcoO109I* at 37 °C for 5 and 6 h, respectively. **A)** Lane 1-6 ( $r_b = 0, 0.013, 0.026, 0.052, 0.08, 0.093$ ) for RAPTA-C. **B)** Lane 1-6 ( $r_b = 0, 0.013, 0.026, 0.052, 0.1, 0.13$ ) for carboRAPTA-C. M is a 100-bp DNA ladder and C is the control untreated DNA.

#### 4.1.4 Preferential ruthenation site on the *BRCA1* gene fragment

The nucleotide sequence of the *BRCA1* gene fragment damaged by RAPTAs was determined (Fig. 4.4). Sequence analysis showed that the chain termination occurred most frequently at A, C and G (and not T). The dGpC site (star in Fig. 4.4) was a possible interstrand crosslinking between ruthenium atom and base/sequence of the *BRCA1* gene fragment. Both RAPTA-C- and carboRAPTA-C-*BRCA1* adducts were found at the cleavage site of *PvuII*, but not the cleavage site of *EcoO109I*, implying that the Ru-*BRCA1* adducts and nearby Ru-*BRCA1* adducts interfered the accessibility or function of these endonucleases.

A

DNA synthesis →

```

4861 GATACTGCTG GGTATAATGC AATGGAAGAA AGTGTGAGCA GGGAGAAGCC AGAATTGACA 4920
4921 GCTTCAACAG AAAGGGTCAA CAAAAGAATG TCCATGGTGG TGTCTGGCCT GACCCAGAA 4980
4981 GAATTTATGC TCGTGTACAA GTTTGCCAGA AAACACCACA TCACTTTAAC TAATCTAATT 5040
5041 ACTGAAGAGA CTACTCATGT TGTTATGAAA ACAGATGCTG AGTTTGTGTG TGAACGGACA 5100
5101 CTGAAATATT TTCTAGGAAT TGCGGGAGGA AAATGGGTAG TTAGCTATTT CTGGGTGACC 5160
5161 CAGTCTATTA AAGAAAGAAA AATGCTGAAT GAGCATGATT TTGAAGTCAG AGGAGATGTG 5220
5221 GTCAATGGAA GAAACCACCA AGGTCCAAAG CGAGCAAGAG AATCCCAGGA CAGAAAGATC 5280
5281 TTCAGGGGGC TAGAAATCTG TTGCTATGGG CCTTTCACCA ACATGCCAC AGATCAACTG 5340
5341 GAATGGATGG TACAGCTGTG TGTTGCTTCT GTGGTGAAGG AGCTTTCATC ATTCACCTT 5400
5401 GGCACAGTG TCCACCCAAT TGTGTTGTG CAGCCAGATG CCTGGACAGA GGACAATGGC 5460
5461 TTCCATGCAA TTGGGCAGAT GTGTGAGGCA CCTGTGGTGA CCCGAGAGTG GGTGTTGGAC 5520
5521 AGTGTAGCAC TCTACCAGTG CCAGGAGCTG GACACCTACC TGATACCCCA GATCCCCCAC 5580
5581 AGCCACTACT GA 5592
DNA synthesis ←

```

B

DNA synthesis →

```

4861 GATACTGCTG GGTATAATGC AATGGAAGAA AGTGTGAGCA GGGAGAAGCC AGAATTGACA 4920
4921 GCTTCAACAG AAAGGGTCAA CAAAAGAATG TCCATGGTGG TGTCTGGCCT GACCCAGAA 4980
4981 GAATTTATGC TCGTGTACAA GTTTGCCAGA AAACACCACA TCACTTTAAC TAATCTAATT 5040
5041 ACTGAAGAGA CTACTCATGT TGTTATGAAA ACAGATGCTG AGTTTGTGTG TGAACGGACA 5100
5101 CTGAAATATT TTCTAGGAAT TGCGGGAGGA AAATGGGTAG TTAGCTATTT CTGGGTGACC 5160
5161 CAGTCTATTA AAGAAAGAAA AATGCTGAAT GAGCATGATT TTGAAGTCAG AGGAGATGTG 5220
5221 GTCAATGGAA GAAACCACCA AGGTCCAAAG CGAGCAAGAG AATCCCAGGA CAGAAAGATC 5280
5281 TTCAGGGGGC TAGAAATCTG TTGCTATGGG CCTTTCACCA ACATGCCAC AGATCAACTG 5340
5341 GAATGGATGG TACAGCTGTG TGTTGCTTCT GTGGTGAAGG AGCTTTCATC ATTCACCTT 5400
5401 GGCACAGTG TCCACCCAAT TGTGTTGTG CAGCCAGATG CCTGGACAGA GGACAATGGC 5460
5461 TTCCATGCAA TTGGGCAGAT GTGTGAGGCA CCTGTGGTGA CCCGAGAGTG GGTGTTGGAC 5520
5521 AGTGTAGCAC TCTACCAGTG CCAGGAGCTG GACACCTACC TGATACCCCA GATCCCCCAC 5580
5581 AGCCACTACT GA 5592
DNA synthesis ←

```

**Figure 4.4.** The nucleotide sequence of cDNA of the *BRCA1* gene fragment (exon 16-24) damaged by RAPTAs. The start site and the direction of DNA synthesis was indicated by arrow. The possible monofunctional crosslinks were represented by bars. TGGGCC is a recognition sequence of *Eco0019I* and CAGCTG is a recognition sequence of *PvuII*.



#### 4.1.5 Damage of *BRCA1* gene by RAPTAs

The semi-quantitative polymerase chain reaction (semi-QPCR) was used to monitor the degree of DNA damage after induced by RAPTAs. The PCR was performed at the experimental conditions giving the exponential amplification that any DNA adducts within the specified DNA fragment will decrease a total amount of each amplified PCR product. The results revealed that the amount of amplified DNA was reduced in the presence of RAPTAs that compared to the DNA control as a concentration dependent manner (Fig. 4.5). RAPTA-C exhibited completely preventing DNA amplification at a concentration of 600  $\mu\text{M}$ , while the amplification of carboRAPTA-C-treated *BRCA1* gene fragments was still observed at concentrations exceeding 1000  $\mu\text{M}$ . It is consistent with the restriction analysis indicating a ca. 2-fold ruthenation by RAPTA-C compared to carboRAPTA-C. As seen in Figure 4.6, RAPTA-C (600  $\mu\text{M}$ ) completely diminished the amount of DNA amplification, while carboRAPTA-C reduced by half at approximately 600  $\mu\text{M}$ .

A random (Poisson) distribution of damage was used for semi-quantified of lesion induction with the 696-bp *BRCA1* gene fragment (Ratanaphan *et al.*, 2005). The results demonstrated that the amount of lesions are 4 lesion/*BRCA1* gene fragment for RAPTA-C, while 1 lesion/*BRCA1* gene fragment for carboRAPTA-C, suggesting an approximately 3 to 4 fold higher rate of ruthenation by RAPTA-C compared to carboRAPTA-C under equivalent experimental conditions (Fig. 4.7).

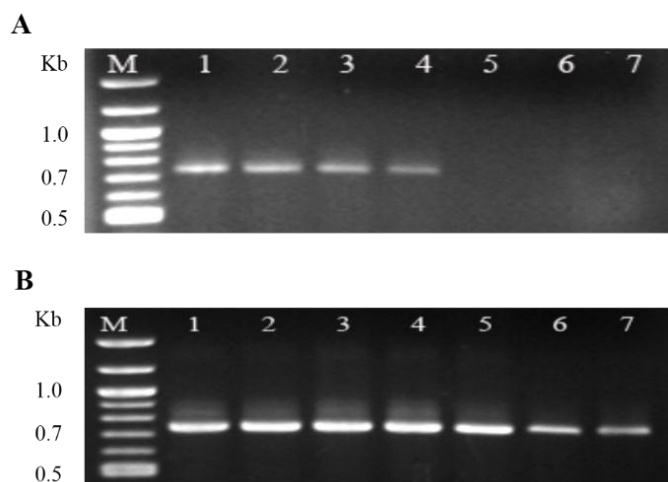


**Figure 4.5.** DNA amplification of the 696-bp *BRCA1* gene fragment induced by RAPTA-C (A) or carboRAPTA-C (B). The 696-bp *BRCA1* gene fragment was incubated with various concentrations of the RAPTA complexes: 0, 100, 200, 400, 600, 800, and 1000  $\mu\text{M}$  (lanes 1-7, respectively, and M is 100-bp ladder) at 37  $^{\circ}\text{C}$  for 24 h in the dark. The RAPTA-treated 696-bp *BRCA1* gene fragment was then amplified by PCR. PCR products were electrophoresed on 1.5% agarose gel, stained with ethidium bromide and visualized under UV illumination.

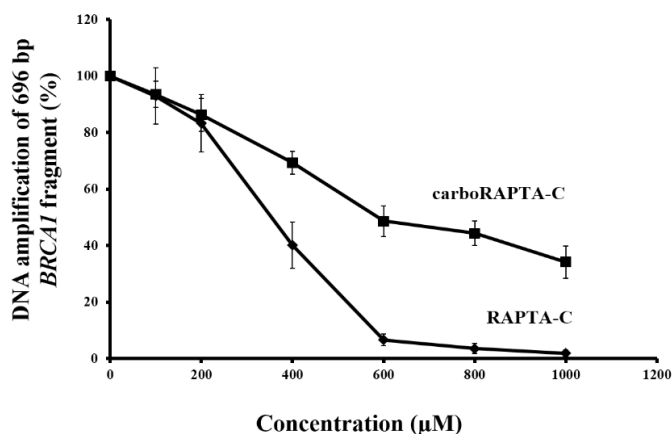


**Figure 4.6.** Amplification products obtained from Figure 4.5 were measured by a Bio-Rad Molecular Imager. An amount DNA amplification (%) was plotted as a function of concentration.

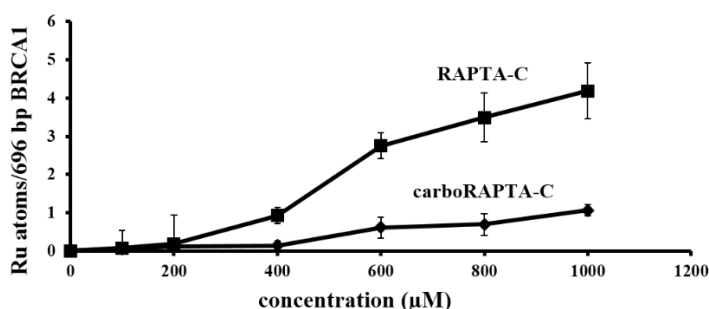


**Figure 4.7.** Concentration dependence of ruthenation of the 696-bp *BRCA1* gene fragment by RAPTAs. Absorbance units from the amplification products were applied to the Poisson equation. The number of lesions (Ru atoms) per the 696-bp *BRCA1* fragment was plotted as a function of the concentration of the RAPTAs.

## 4.2 Protein binding and functional consequence of RAPTA-induced wild type BRCA1 RING domain protein

### 4.2.1 Formation of Ru-wild type BRCA1 crosslinking

Adducts formation between RAPTAs and the BRCA1 protein were initially investigated by gel shift assays. The results showed that the RAPTA complexes induce intermolecular crosslinks as a concentration-dependent manner, resulting in dimers or larger aggregates (Fig. 4.8). The binding affinity of ruthenium to protein was further investigated using ICP-MS. Cisplatin and two highly active gold(III) compounds (Auphen and Auterpy) were used for comparison. RAPTA-EA1 exhibited a similar binding affinity to the wild type BRCA1 RING domain, which was ca. 5-fold higher than RAPTAC and RAPTA-T, and more thousand-fold than both gold(III) complexes, however similar to cisplatin. (Fig. 4.9).

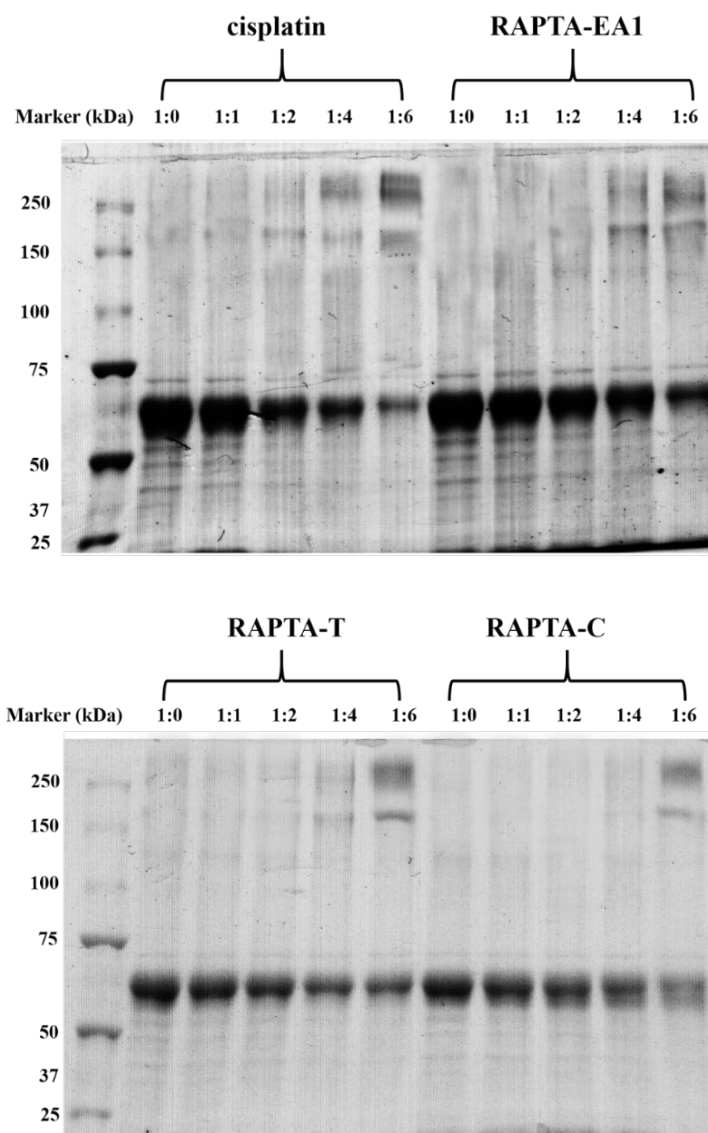


**Figure 4.8.** Intermolecular cross-linking of the metal-BRCA1 adducts. Ten  $\mu\text{M}$  of the BRCA1 protein was pre-incubated with 30  $\mu\text{M}$  of  $\text{ZnCl}_2$  at 4  $^\circ\text{C}$  for 8 h. the holo-BRCA1 was incubated with cisplatin or RAPTA complexes at various molar ratios (protein: drug) of 1:0, 1:1, 1:2, 1:4, and 1:6, at 4  $^\circ\text{C}$  for 24 h, and electrophoresed on 8 % SDS/PAGE. The bands of protein were detected by silver staining. The electrophoretic mobility of standard protein markers was indicated (kDa) on the left-handed side.

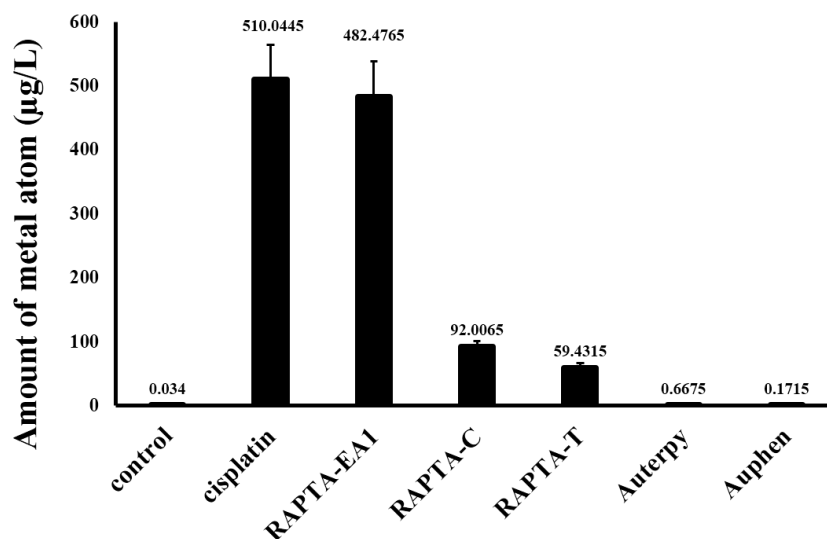


**Figure 4.9.** The binding affinity of metal complexes to the BRCA1 proteins evaluated by ICP-MS analysis. Each experiment was performed in triplicate.

#### 4.2.2 The effect of RAPTA complexes on secondary structure of wild-type BRCA1 RING domain protein

Circular dichroism (CD) was used to verify whether the metal complexes alter the conformation of the *N*-terminal BRCA1 RING domain proteins. Cisplatin, two gold(III) compound (Auphen and Auferpy) and two ruthenium(II) polypyridyl {Ru-bpy; ([Ru(Clazpy)<sub>2</sub>bpy]Cl<sub>2</sub>·7H<sub>2</sub>O and Ru-phen; [Ru(Clazpy)<sub>2</sub>phen]Cl<sub>2</sub>·8H<sub>2</sub>O)} were used for comparison. CD Spectra of apo- and holo-form of BRCA1 RING domain proteins (without and with Zn<sup>2+</sup> bound, respectively) changed upon metal binding in a concentration dependent manner (Fig. 4.10, Fig. 4.11). However, cisplatin-, RAPTA-C-, and RAPTA-T- induced the apo-form of BRCA1 RING domain showed more increase in their amplitudes than those-induced holo-form of BRCA1 RING domain (Fig. 4.10, Fig. 4.11). This indicated that a potential pre-formation of the BRCA1 structure in the absence of Zn<sup>2+</sup> (apo-form of BRCA1), and the BRCA1 RING increased additionally folded structure in the holo-form of BRCA1 after Zn<sup>2+</sup> binding. Surprisingly, RAPTA-EA1-induced BRCA1 RING protein, both apo- and holo-form, showed a similar profile in shape and their amplitudes (Fig. 4.10, Fig. 4.11). This indicated that RAPTA-EA1 has high proficiency in binding to the BRCA1 structure in the absence and presence of Zn<sup>2+</sup> ions. Changes in the secondary structure of the apo- and holo-form of the proteins were predicted based on the CONTIN program (Fig. 4.12, Fig. 4.13). All of these complexes increased  $\alpha$ -helical content and decreased  $\beta$ -sheets in the apo- and holo-form of BRCA1 RING proteins. This indicated that both forms of the BRCA1 proteins was altered the secondary structure of BRCA1 proteins by the binding of metal complexes. The extent of increase in  $\alpha$ -helical structure was almost the same for all the complexes. The binding constant (*k*) and the free energy of binding ( $\Delta G$ ) of the metal complexes-induced apo- and holo-form of BRCA1 (1:5; protein to metal) were summarized in Table 4.1. The metal-induced apo-form of BRCA1 had a higher

binding constant and gave lower the free energy. In contrast, cisplatin, RAPTA-C, or RAPTA-T-induced holo-form of BRCA1 had a lower binding constant and gave a higher the free energy (summarized in table 4.1). Surprisingly, RAPTA-EA1-induced holo-form showed strongly change in CD profiles, and gave a higher binding constant and a lower free energy at the same level to the apo-form of BRCA1.

Furthermore, two ruthenium(II) polypyridyl complexes, Ru-bpy and Ru-phen, and two gold(III) complexes, Auphen and Auterpy, were used for comparison. The results showed that the CD spectra of the holo-form of BRCA1 RING domain proteins change upon metal binding in a concentration dependent manner (Fig. 4.11), characterized by a large increase in negative ellipticity at 208 and 220 nm that showed a similarly profile and effected overall of protein structure in similar way of RAPTA complexes (Fig. 4.12, Fig. 4.13). Furthermore, the binding constant ( $K$ ) and free energy ( $\Delta G$ ) of the ruthenium(II) polypyridyl- and gold(III)-BRCA1 complexes (1:100; metal to protein) were predicted, and summarized in Table 4.1. Surprisingly, Ru-bpy - Ru-phen-, Auphen- and Auterpy-treated holo-form of BRCA1 proteins showed strongly change in CD profiles (Fig. 4.11), and gave the binding constant and the free energy at the same level to both RAPTA-EA1-treated apo- and holo-form of BRCA1 proteins. In contrast, cisplatin, RAPTA-C and RAPTA-T showed strongly change in CD profiles, and had a higher the binding constant and lower the free energy, only apo form, not holo form, of BRCA1 proteins.

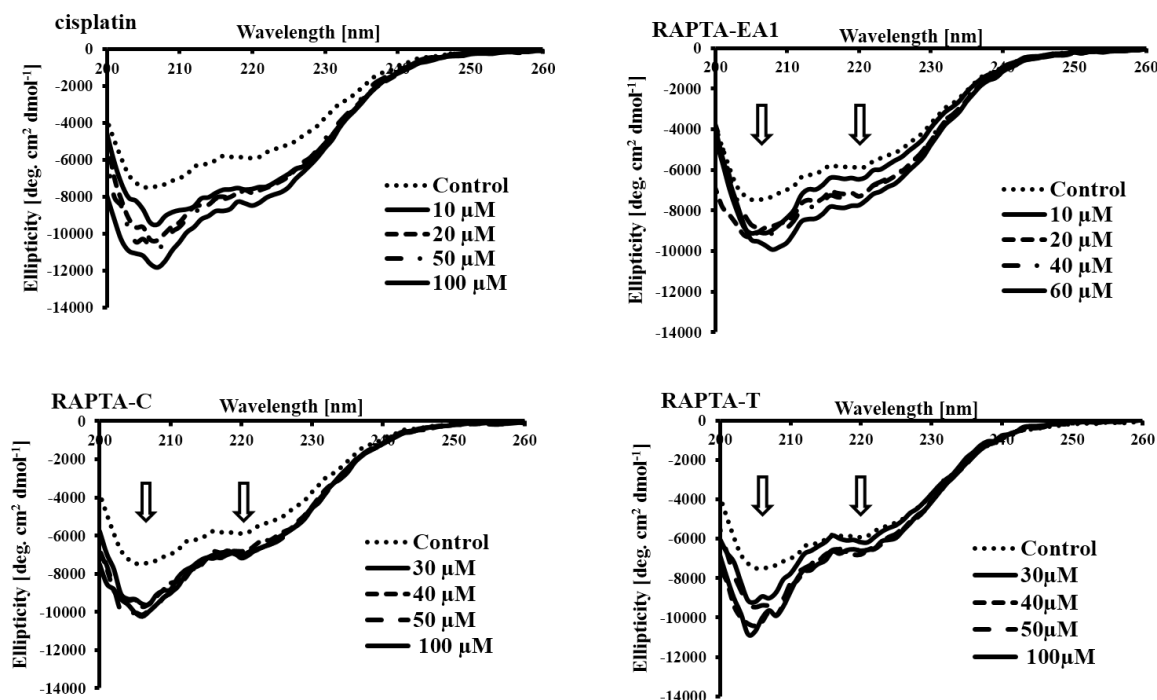


**Figure 4.10.** The CD spectra of the metal-induced secondary structure change of the apo-form of BRCA1 RING domain (residues 1-304).

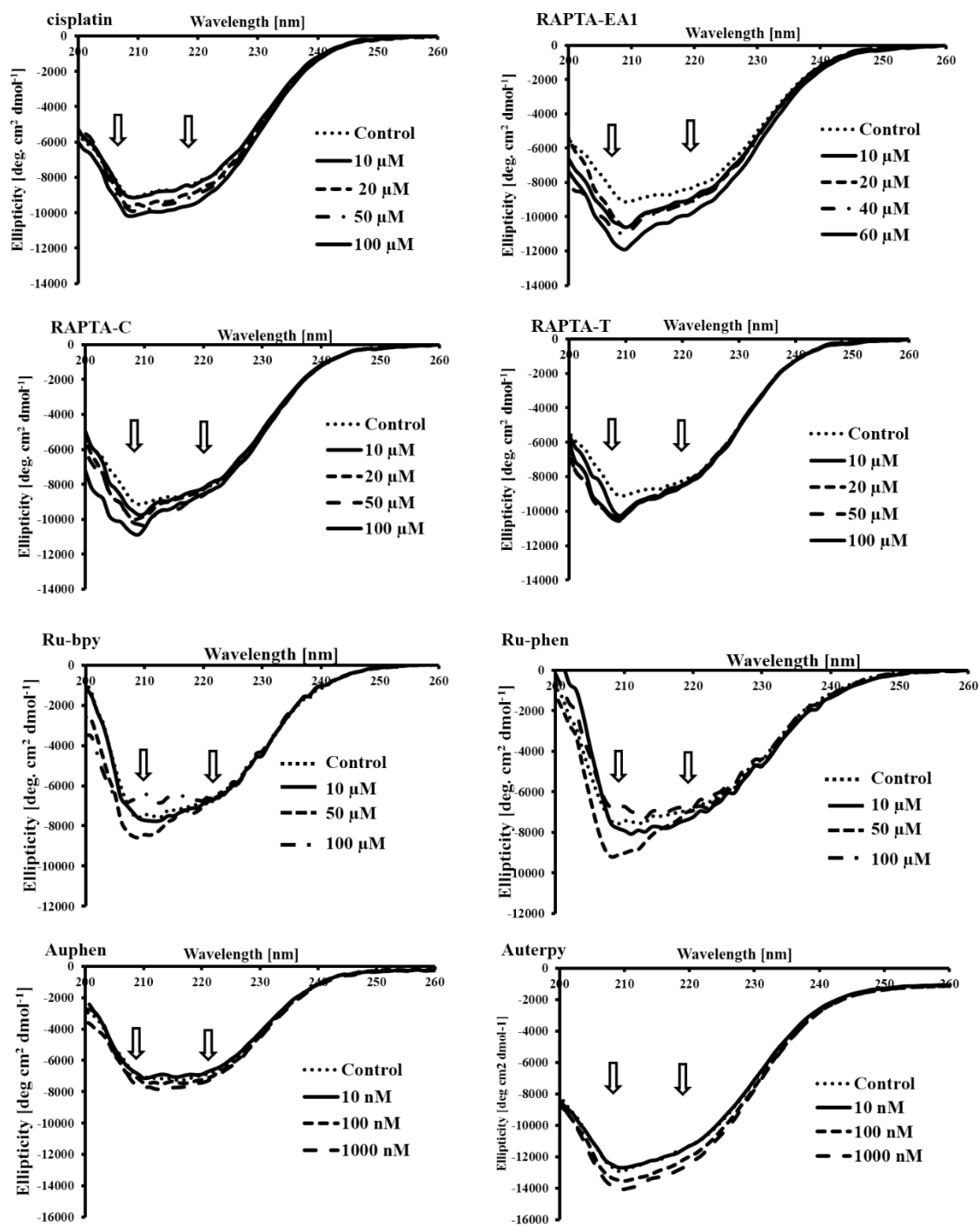


**Figure 4.11.** The CD spectra of the metal-induced secondary structure change of the holo-form of BRCA1 RING domain (residues 1-304).

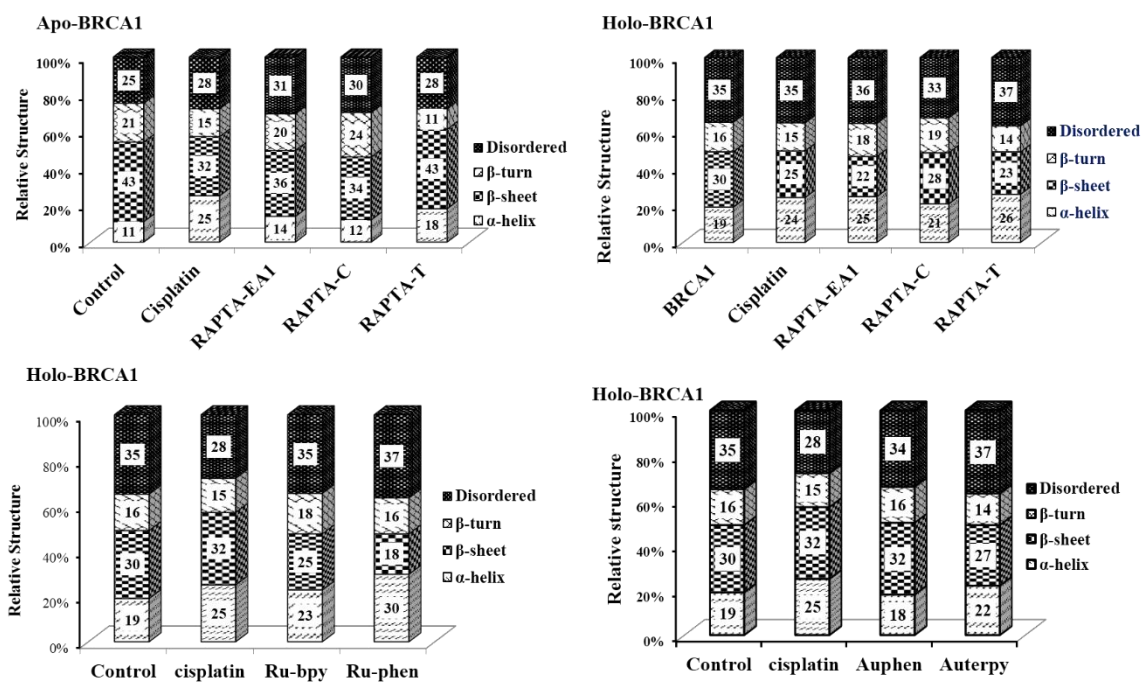


**Figure 4.12.** Relative secondary structure of metal complexes binding to the apo- and holo-form of BRCA1 proteins (without and with  $Zn^{2+}$ , respectively), estimated by the CONTIN program.

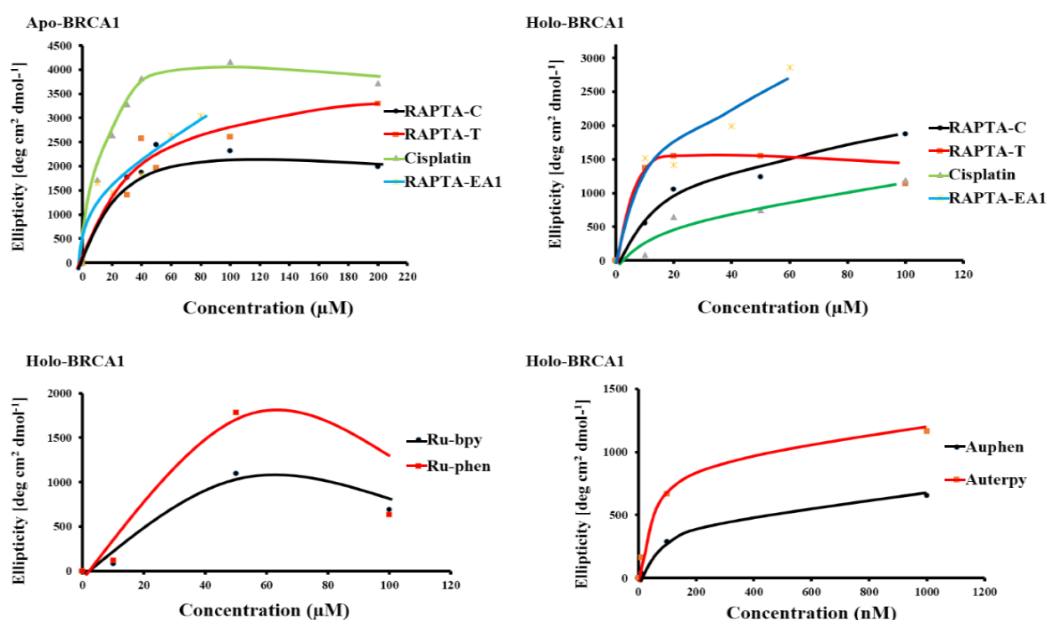


**Figure 4.13.** Changes in ellipticity of protein at 208 nm were plotted against increasing metal complexes concentrations.

**Table 4.1.** Thermodynamic parameters predicted by the CONTIN program on the binding of metal complexes with the apo- or holo-form of BRCA1 RING domain (1-304).

complexes	Apo-form		Holo-form	
	Binding constant (K) M <sup>-1</sup>	Free energy (ΔG) cal mol <sup>-1</sup>	Binding constant (K) M <sup>-1</sup>	Free energy (ΔG) cal mol <sup>-1</sup>
cisplatin	3.00 ± 0.33 x 10 <sup>6</sup>	-650.84	4.85 ± 0.23 x 10 <sup>4</sup>	1792.64
RAPTA-C	2.82 ± 0.51 x 10 <sup>6</sup>	-613.39	2.03 ± 0.02 x 10 <sup>5</sup>	945.44
RAPTA-T	2.93 ± 0.28 x 10 <sup>6</sup>	-637.00	5.13 ± 0.07 x 10 <sup>5</sup>	395.55
RAPTA-EA1	2.73 ± 0.61 x 10 <sup>6</sup>	-596.00	2.72 ± 0.65 x 10 <sup>6</sup>	-594.32
Ru-phen	-	-	6.53 ± 0.09 × 10 <sup>5</sup>	-252.95
Ru-bpy	-	-	3.18 ± 0.05 × 10 <sup>5</sup>	679.22
Auphen	-	-	2.99 ± 0.014 x 10 <sup>6</sup>	-650.83
Auterpy	-	-	2.99 ± 0.563 x 10 <sup>6</sup>	-649.79

#### 4.2.3 Thermal stability of the ruthenated-wild type BRCA1

The thermal stability of the BRCA1 RING proteins induced by the metal complexes was also determined by CD. The BRCA1 protein in the presence of Zn<sup>2+</sup> ions was incubated with metal complexes, and CD spectra revealed the similar changes with an increase in the ellipticity when the temperature was increased from 25 °C to 95 °C (Fig. 4.14). This suggested that the folded proteins showed slowly loss of their ordered structures upon thermal denaturation. In addition, the thermal denaturation curves were plotted for comparison of metal-induced proteins stabilities, and the melting temperatures (*T<sub>m</sub>*) were collected (Fig. 4.15). The RAPTA complexes stabilize the wild type of BRCA1 protein structure with an associated increase in *T<sub>m</sub>*. The *T<sub>m</sub>* of the BRCA1 RING domains are >95 °C, >95 °C, 83.1 °C, and 85.2 °C after treatment with cisplatin, RAPTA-EA1, RAPTA-C and RAPTA-T, respectively (Fig 4.15). It is likely that the metal-bound proteins are more thermostable by about 4 °C and 7 °C for RAPTA-T and RAPTA-C and > 19 °C for cisplatin and RAPTA-EA1, respectively.



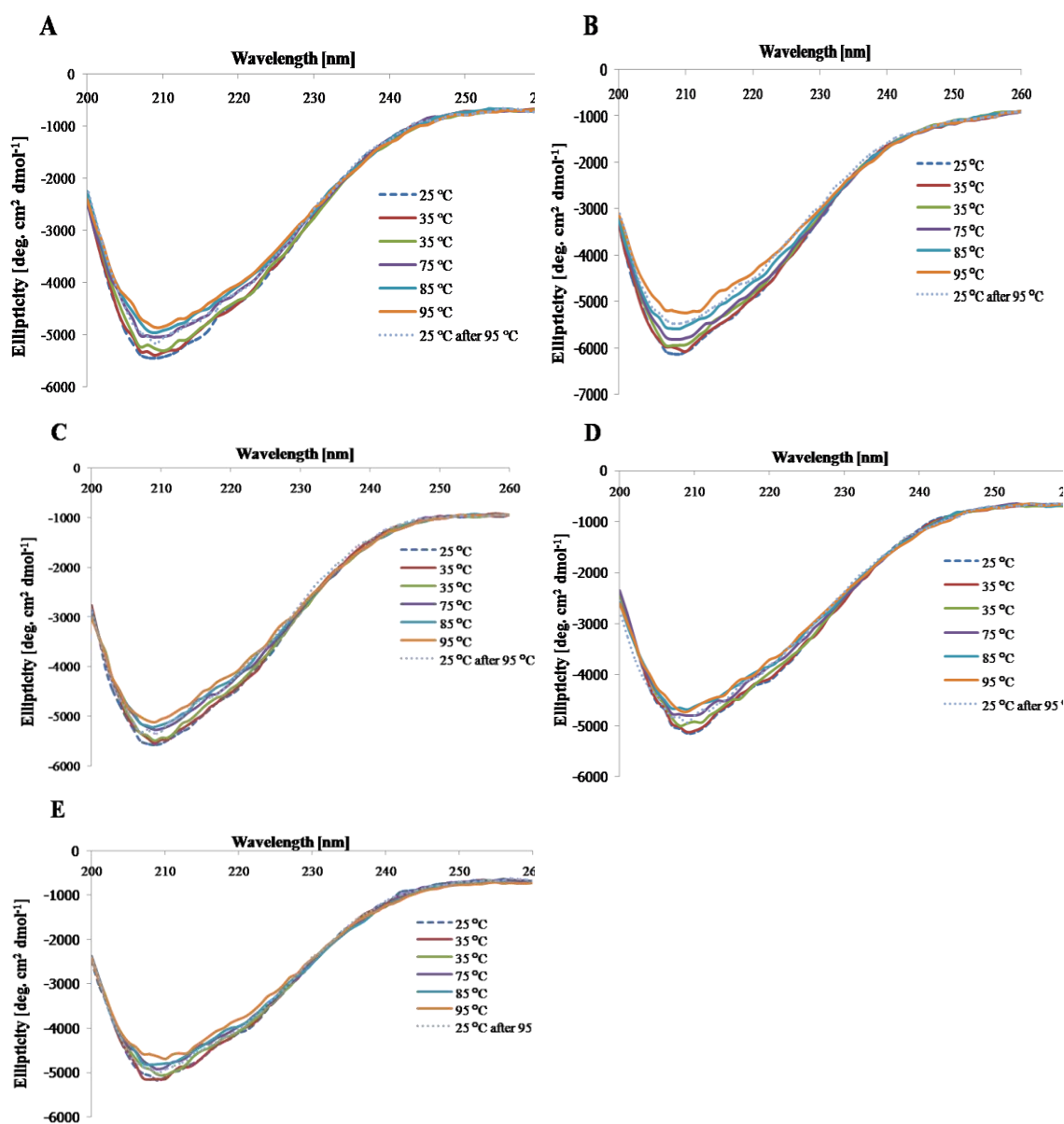


**Figure 4.14.** Thermal transition of metal-BRCA1 (1-304) adducts in the presence of  $\text{ZnCl}_2$ . Samples were incubated with no complexes (A), cisplatin (B), RAPTA-C (C), RAPTA-T (D), and RAPTA-EA1 (E) in the dark at ambient temperature for 16 h. The measurements were performed from 25 °C to 95 °C. The measurement at 25 °C was also performed after heating at 95 °C. The CD spectra were plotted between mean residues ellipticity and wavelength.

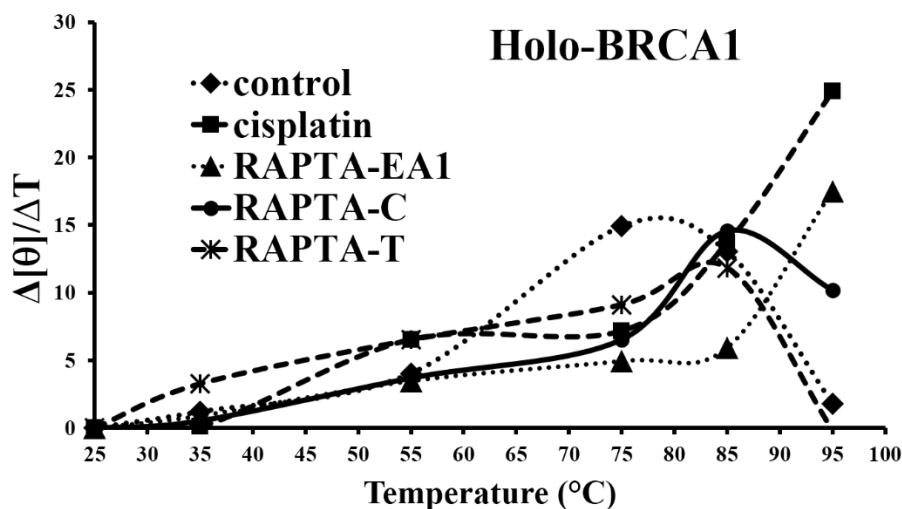


**Figure 4.15.** Thermal denaturation curves of the metal complexes-BRCA1 adduct. The denaturation curves of the metal complexes-BRCA1 adducts were plotted against  $\Delta[\theta]_{208\text{ nm}}/\Delta T$ .

#### 4.2.4 RAPTAs dismissed the zinc ions from the zinc binding sites of BRCA1 RING domain protein

The previous data showed that the RAPTA complexes interacted and interfered the conformation of BRCA1 protein. The zinc ejection assay was subsequently used to verify whether the complexes disrupt the conformation of the BRCA1 RING domain protein sufficiently to dislodge the zinc ion from its binding sites (Fig. 4.16, Fig. 4.17). The results showed that the binding of RAPTAs and cisplatin to BRCA1 proteins released the  $\text{Zn}^{2+}$  ion in a dose-dependent manner (Fig. 4.16). In addition, the rate of zinc ion ejection by RAPTA-EA1 is markedly higher than that induced by the other compounds (Fig. 4.17). Furthermore, two gold(III) complexes, Auphen and Auterpy, were used for comparison. The binding of both gold(III) complexes to the BRCA1 protein released the  $\text{Zn}^{2+}$  ion in a dose-dependent manner (Fig. 4.18). Interestingly, zinc ejection by both gold(III) complexes and RAPTA-EA1 were similarly and slightly greater than that estimated for the RAPTA-C and RAPTA-T. These results suggested that metal, such as Ru, Au and Pt, could affect the conformation of this protein and interfered with the zinc binding sites, leading to a release of  $\text{Zn}^{2+}$  ion from the binding sites.

### Wild-type BRCA1

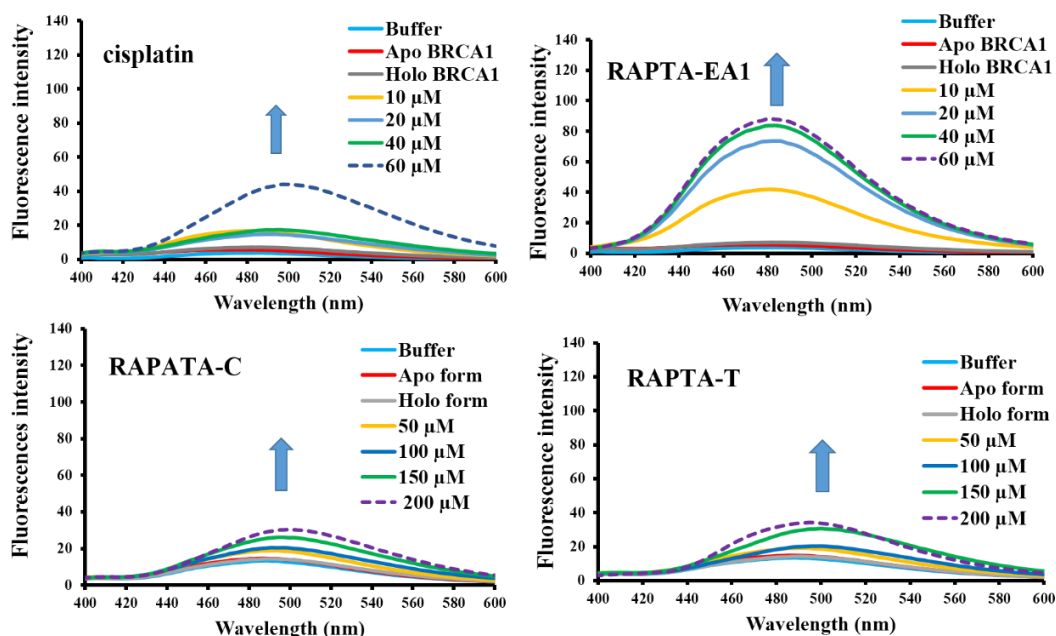


**Figure 4.16.** Concentration-dependent zinc ejection assay on BRCA1 RING domain. The holo-form of BRCA1 proteins were induced by the metal complexes. Reactions were performed in zinc ejection buffer (10% glycerol, 50 mM Tris-HCl buffer, pH 7.6). Three microgram of holo-proteins was incubated with the metal complexes at various concentrations. The change in fluorescence of the zinc-selective fluorophore TSQ (6-methoxy-8-*p*-toluenesulfonamido-quinoline) was used for monitoring the ejection of zinc from the protein, at each concentration or time interval (excitation filter, 360 nm; emission filter, 490 nm).

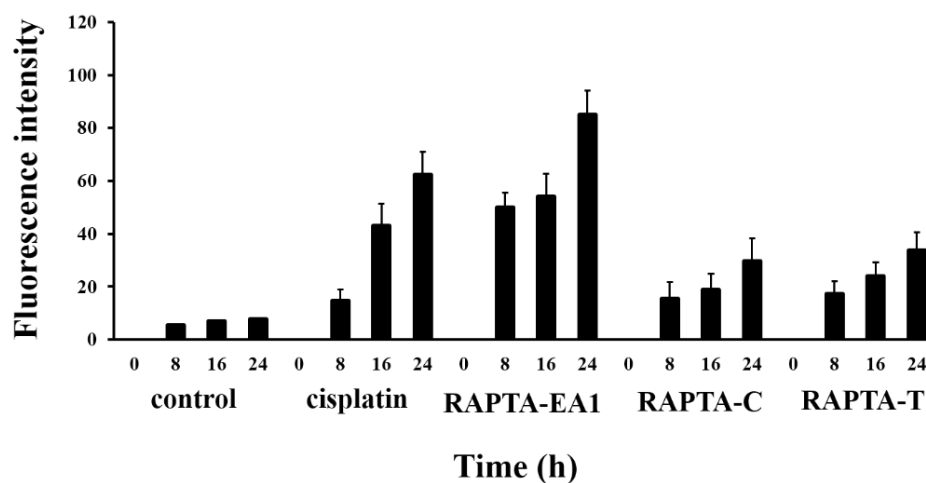


**Figure 4.17.** Time-dependent zinc ejection assay on the holo-form of BRCA1 RING domain protein induced by the metal complexes. Each experiment was performed in triplicate.

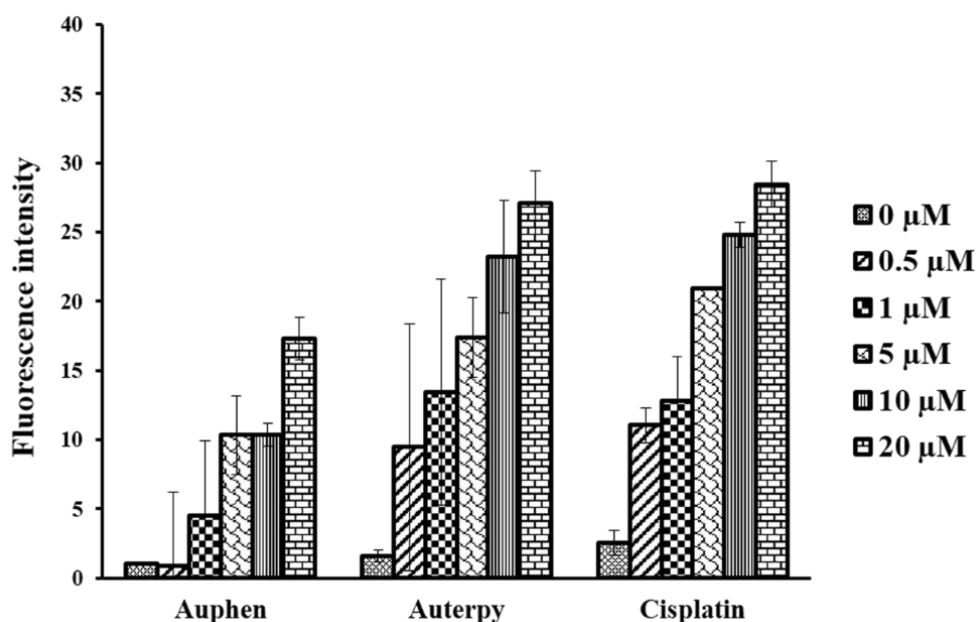


**Figure 4.18.** Concentration-dependent zinc ejection assay on the holo-form of BRCA1 RING domain induced by the gold(III) complexes. Each experiment was performed in triplicate.

#### 4.2.5 Inactivation of the wild-type BRCA1 E3 ligase activity by RAPTAs

The results from secondary structure, thermostability, binding affinity, gel shift assay, and zinc ejection assay showed that the RAPTA complexes greatly disturbed the physical properties of wild-type BRCA1 protein. The effect of RAPTAs on E3 ubiquitin ligase activity of the BRCA1 protein was further investigated. The BRCA1/BARD1 complexes promoted the formation of high molecular weight polyubiquitin species in the presence of ATP (Fig. 4.19). The E3 ubiquitin ligase activity of the ruthenium-treated BRCA1/BARD1 protein decreased in a dose-dependent manner of the complexes in all cases (Fig. 4.20), implying that all the RAPTA complexes are promising agents that can inhibit the E3 ligase activity. However, RAPT-EA1 exhibited a 6-fold and 2-fold higher ability to inhibit E3 ligase activity than RAPT-A-C and RAPT-A-T, respectively. The  $IC_{50}$  value for inactivation of an E3 ubiquitin ligase activity by RAPT-EA1 is markedly lower than that for RAPT-A-C, RAPT-A-T and cisplatin (Table 4.2, Fig. 4.21). In addition, the E3 ligase activity of both ruthenium(II) polypyridyl complexes was reduced by half at concentrations at the same levels of the RAPTA complexes (50  $\mu$ M for Ru-phen, and 70  $\mu$ M for Ru-bpy, respectively). However, the E3 ligase activity was reduced in a nanomolar levels that by half at concentrations of 63 nM and 8 nM for Auphen and Auterpy, respectively (Fig. 4.20, Fig. 4.21, Table 4.2).

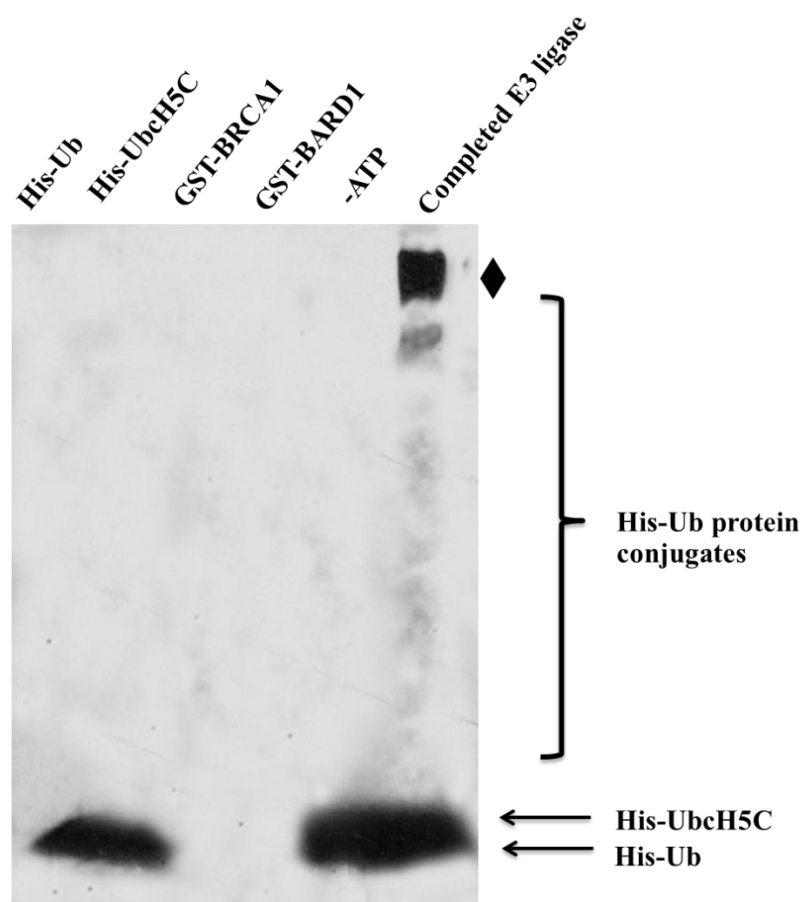


**Figure 4.19.** *In vitro* E3 ubiquitin ligase activity. Complete E3 ubiquitin ligase reaction mixtures, containing Ub (20  $\mu$ M), E1 (300 nM), UbcH5c (5  $\mu$ M), BRCA1 (residues 1-304) (3  $\mu$ g), and BARD1 (residues 26-327) (3  $\mu$ g), were incubated at 37°C for 3 h. The control reactions (without ATP or incomplete E3 ubiquitin ligase reaction) were carried out under the same conditions. Samples were then separated on 8% SDS-PAGE and subjected to Western blotting with anti-6-His-HRP conjugated antibody. A filled diamond indicated an apparent ubiquitinated product.

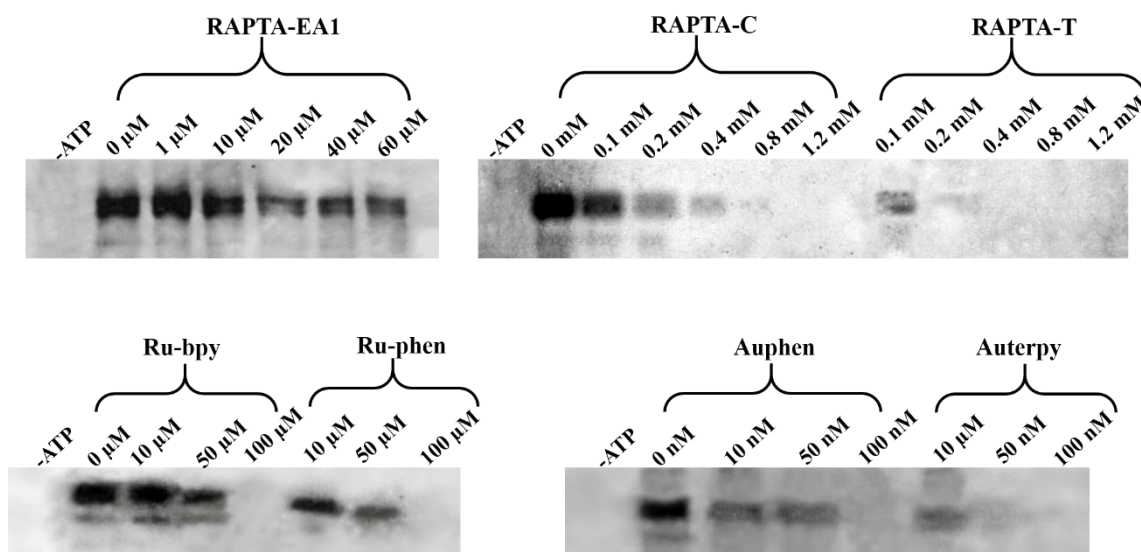


**Figure 4.20.** *In vitro* E3 ubiquitin ligase activity of the metal-treated BRCA1 protein. The wild-type BRCA1 RING protein (3  $\mu\text{g}$ ) was incubated with a number of metal complexes at various concentrations between 0–60  $\mu\text{M}$  (RAPTA-EA1), 0–1200  $\mu\text{M}$  (RAPTA-C and RAPTA-T), 0–100  $\mu\text{M}$  (Ru-bpy and Ru-phen), 0–100 nM (Au-phen and Au-terpy), and assayed for the E3 ubiquitin ligase activity.

**Table 4.2.** Half inhibition of BRCA1/BARD1 E3 ligase activity inactivated by metal complexes.

Complexes	IC <sub>50</sub>
RAPTA-EA1	55 $\mu\text{M}$
RAPTA-C	167 $\mu\text{M}$
RAPTA-T	95 $\mu\text{M}$
Ru-bpy	70 $\mu\text{M}$
Ru-phen	50 $\mu\text{M}$
Au-phen	63 nM
Au-terpy	8 nM
Cisplatin*	60 $\mu\text{M}$ *

\* A. Atipairin, A. Ratanaphan, Breast Cancer: Basic and Clinical Research, 2011, 5, 201-208.

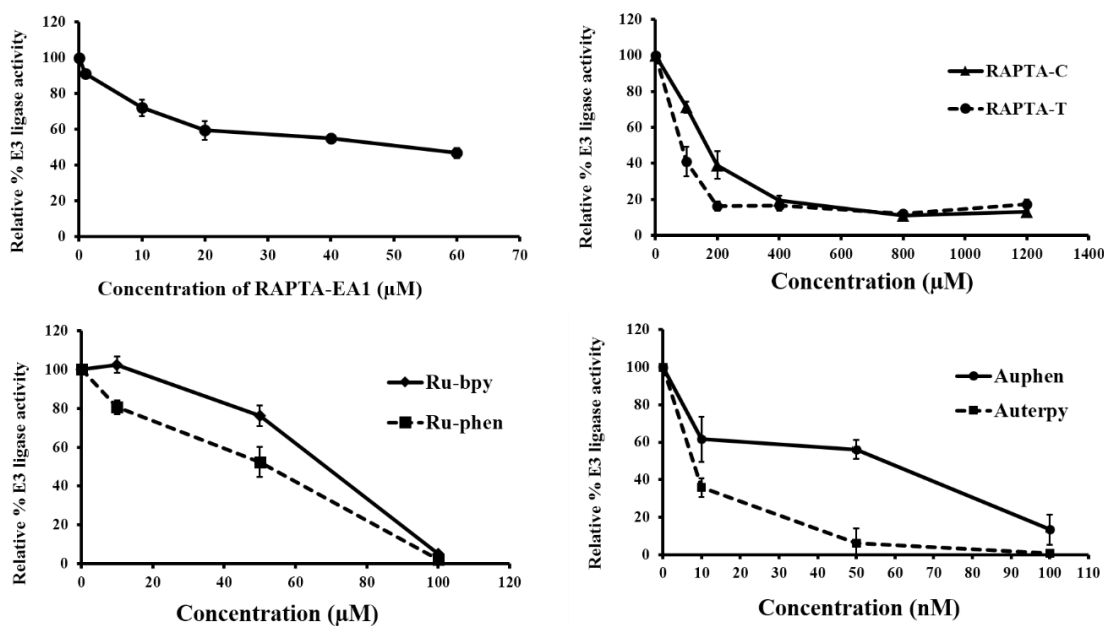


**Figure 4.21.** *In vitro* E3 ubiquitin ligase activity of the metal-treated BRCA1 protein. The apparent ubiquitinated products shown in Fig. 4.20 were quantified by densitometer (Bio-Rad GS-700 Imaging). The relative (%) E3 ligase activity of the ruthenated-BRCA1 was plotted as a function of the concentration of metal complexes. Each experiment was performed in duplicate.

### 4.3 Protein binding and functional consequence of RAPTA-induced mutant BRCA1 RING domain protein

#### 4.3.1 Formation of Ru-mutant BRCA1 crosslinking

The binding affinity of the RAPTA complexes to the mutant proteins, D67E and D67Y, was further investigated using ICP-MS. Cisplatin was used for comparison. The ruthenated-D67E BRCA1 exhibited a similar binding profiling as to the ruthenated-D67Y BRCA1. RAPTA-EA1 exhibited a 5-fold higher binding affinity to both mutant BRCA1 protein than RAPTA-C and RAPTA-T (Fig. 4.22).

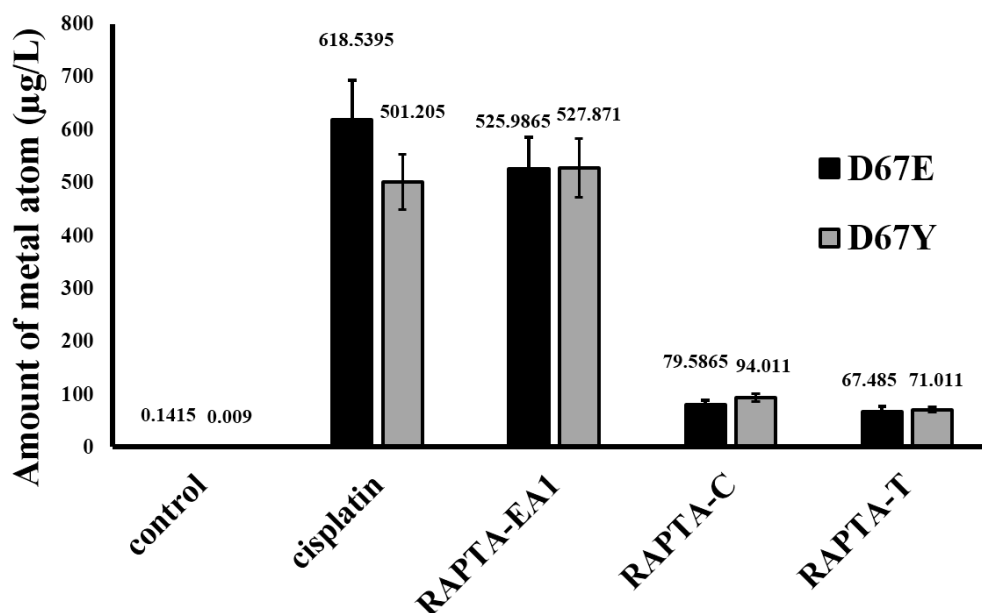


**Figure 4.22.** The binding affinity of the metal complexes to the mutant BRCA1 proteins, D67E and D67Y, were evaluated by ICP-MS analysis. Each experiment was performed in triplicate.

#### 4.3.2 The effect of the RAPTA complexes on secondary structure of mutant BRCA1 proteins

CD spectra of the holo-form of both mutant BRCA1 showed some different profiles in shape and amplitudes after exposure to RAPTA-EA1 (Fig. 4.23). After increasing the concentrations of metal complexes, the D67Y protein was continued and underwent more folded structural reorganization, whereas, the D67E protein was slightly change in secondary structure, implying that the RAPTA complexes perturbs the secondary structure of the D67Y protein more than the D67E protein.

All of tested RAPTAs showed an increase in  $\alpha$ -helical content and decrease in  $\beta$ -sheets content in the holo-form of both mutant BRCA1, indicative of the binding of metal complexes to both BRCA1 proteins alters the secondary structure of these BRCA1 proteins (Fig. 4.24). The binding constant ( $k$ ) and the free energy of binding ( $\Delta G$ ) of the metal-induced holo-form of the mutant BRCA1 (1:5; protein to metal) were summarized in Table 4.3 and Figure 4.25. RAPTA-EA1-induced holo-form of D67Y had a higher binding constant and gave lower the free energy. In contrast, all metal complexes-induced holo-form of D67E had a lower binding constant and gave a higher the free energy, compared with D67Y.



**Table 4.3.** Thermodynamic parameters predicted by the CONTIN program on the binding of metal complexes with the holo-form of the mutant BRCA1 RING domain (1-304).

complexes	D67E		D67Y	
	Binding constant (K) M <sup>-1</sup>	Free energy (ΔG) cal mol <sup>-1</sup>	Binding constant (K) M <sup>-1</sup>	Free energy (ΔG) cal mol <sup>-1</sup>
Cisplatin	6.11±0.44 x 10 <sup>5</sup>	291.46	2.46±0.46 x 10 <sup>5</sup>	831.12
RAPTA-EA1	5.85±0.68 x 10 <sup>5</sup>	317.71	2.99±0.015 x 10 <sup>6</sup>	-650.81
RAPTA-C	2.99±0.04 x 10 <sup>5</sup>	714.81	3.69±0.02 x 10 <sup>5</sup>	589.68
RAPTA-T	2.89±0.03 x 10 <sup>5</sup>	735.57	3.73±0.07 x 10 <sup>5</sup>	582.65

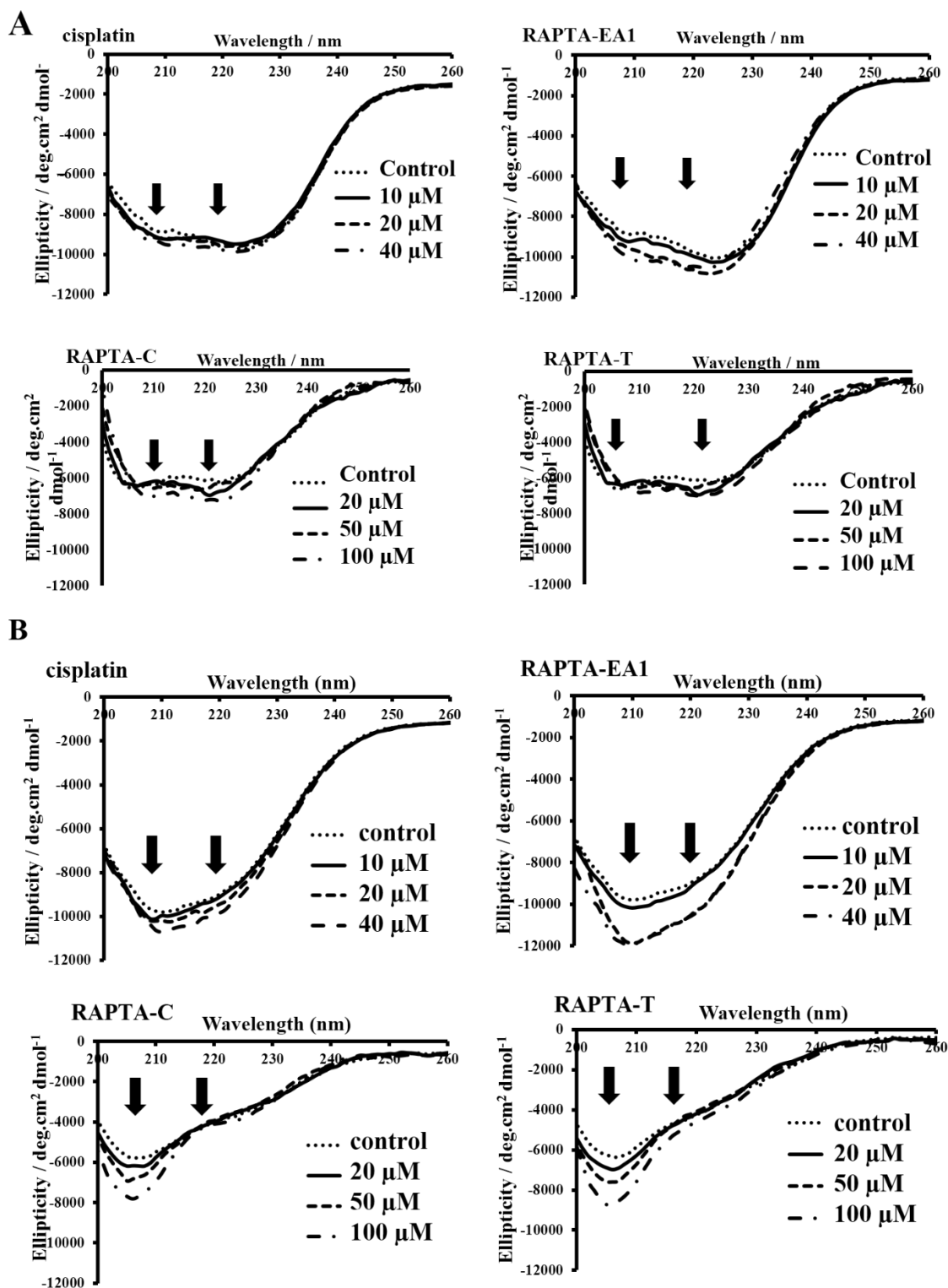


**Figure 4.23.** CD spectra of metal-induced secondary structure change of the holo-form of the mutant BRCA1 (residues 1-304). (A) D67E BRCA1, (B) D67Y BRCA1.

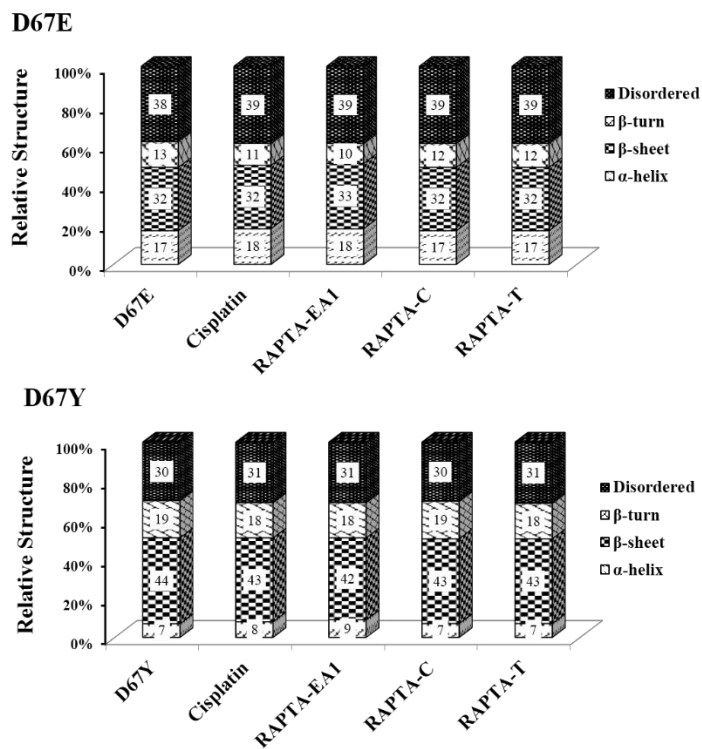


**Figure 4.24.** Relative secondary structure of metal (50  $\mu\text{M}$ )-induced holo-form of mutant BRCA1 proteins (10  $\mu\text{M}$ ), D67E and D67Y. The CONTIN program was used for predicting the extent of secondary structures of proteins.

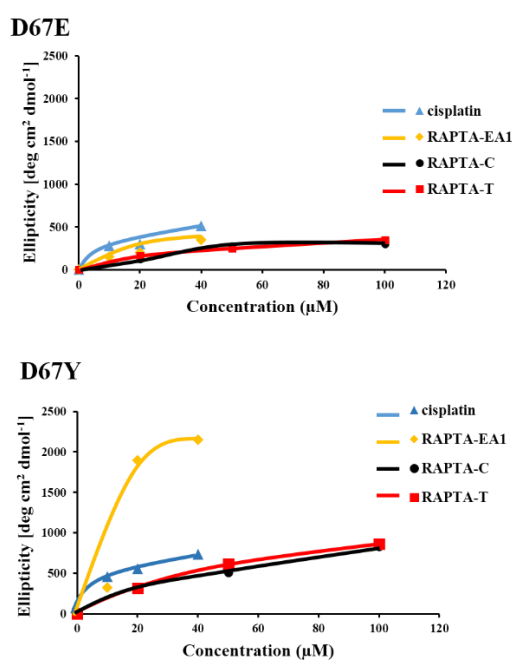


**Figure 4.25.** Changes in ellipticity of the mutant BRCA1 protein at 208 nm versus increasing concentrations of metal complexes were plotted.

### 4.3.3 Thermal stability of the ruthenated-mutant BRCA1

From the previous experiment, RAPTAs stabilize the wild-type protein structure with an associated increase in melting temperatures ( $T_m$ ) (Fig. 4.15). In contrast, the  $T_m$  of both the D67Y and D67E proteins decreased as a result of RAPTAs binding to cisplatin, RAPTA-EA1, RAPTA-C and RAPTA-T with the  $T_m$  of 65 °C, 60 °C, 65 °C, and 63 °C for the D67E BRCA1, and that of 65 °C, 65 °C, 65 °C, and 65 °C for the D67Y BRCA1, respectively (Fig 4.26).

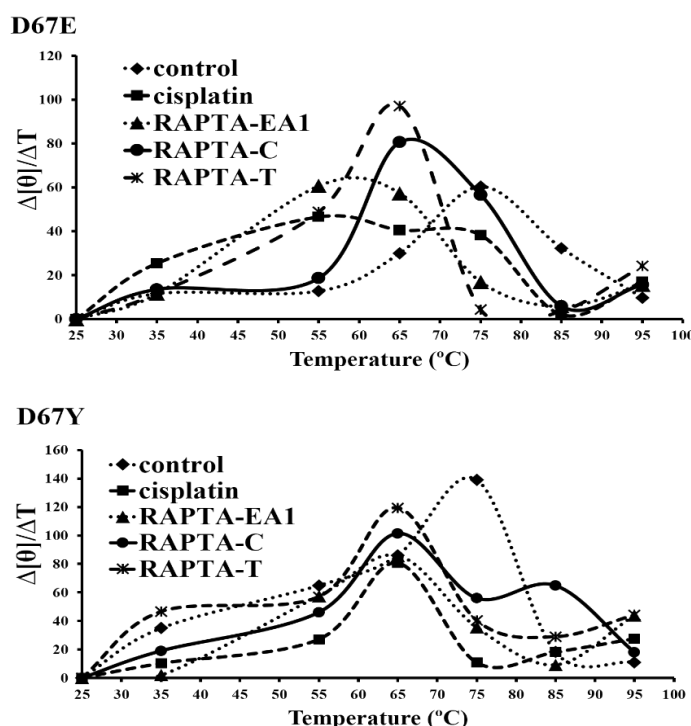
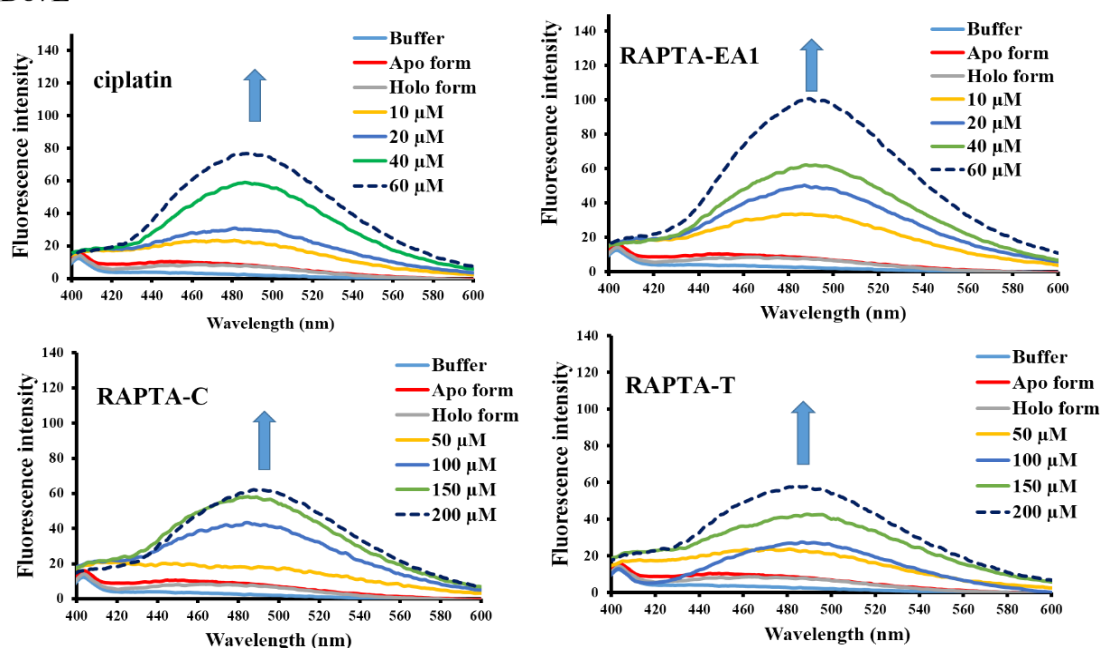


**Figure 4.26.** Thermal denaturation curves of the RAPTA-treated mutant BRCA1 protein. The denaturation curves of the ruthenated-mutant BRCA1 were plotted in term of  $\Delta[\Theta]_{208 \text{ nm}} / \Delta T$ .

### 4.3.4 RAPTAs dismissed the zinc ions from the zinc binding sites of mutant BRCA1 proteins

To confirm whether the RAPTA complexes disrupt the conformation of the mutant BRCA1 RING domain protein sufficiently to dislodge the zinc ion from binding site, the zinc ejection assay was used. As seen in Fig. 4.27, it revealed that the binding of RAPTAs and cisplatin to both mutant BRCA1 proteins released the  $\text{Zn}^{2+}$  ion in a dose-dependent manner. Furthermore, the rate of zinc ejection by RAPTA-EA1 was markedly greater than that estimated for the other compounds (Fig. 4.28). These results agree very well with a previous experiment that the tested metal complexes interacted with the wild-type BRCA1 RING protein, resulting in a release of  $\text{Zn}^{2+}$  ions from the zinc binding site of the BRCA1 RING domain protein.

## D67E



## D67Y

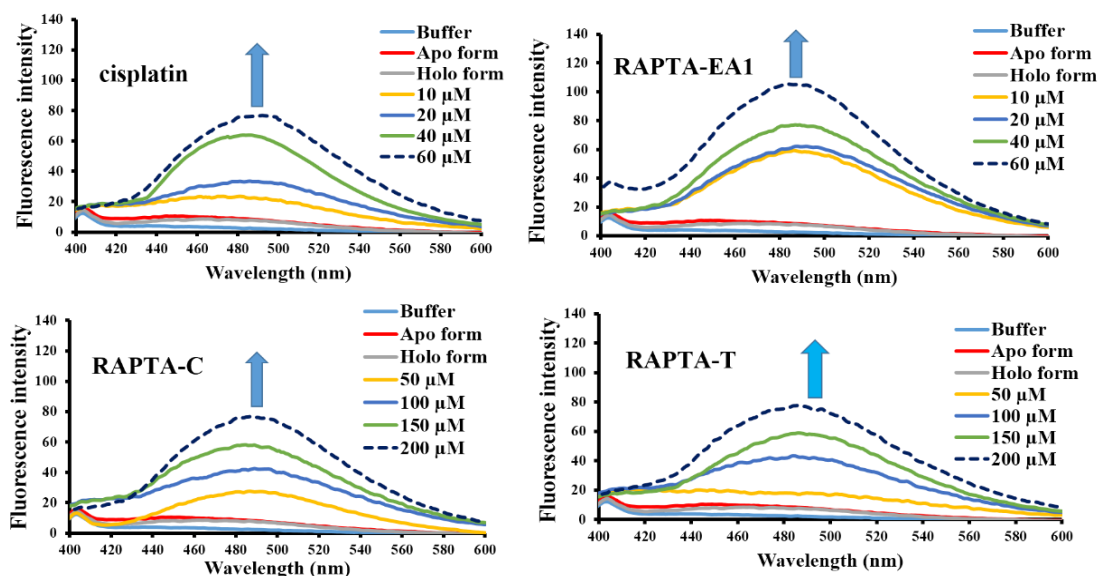


**Figure 4.27.** Concentration-dependent zinc ejection assay on mutant BRCA1 RING domain protein. Both mutant, D67E and D67Y, BRCA1 proteins were induced by the metal complexes. Reactions were performed in zinc ejection buffer (10% glycerol, 50 mM Tris-HCl buffer, pH 7.6). Three microgram of holo-proteins was incubated with the metal complexes at various concentrations. The change in fluorescence of the zinc-selective fluorophore TSQ (6-methoxy-8-*p*-toluenesulfonamido-quinoline) was used for monitoring the ejection of zinc from the protein, at each concentration or time interval (excitation filter, 360 nm; emission filter, 490 nm).

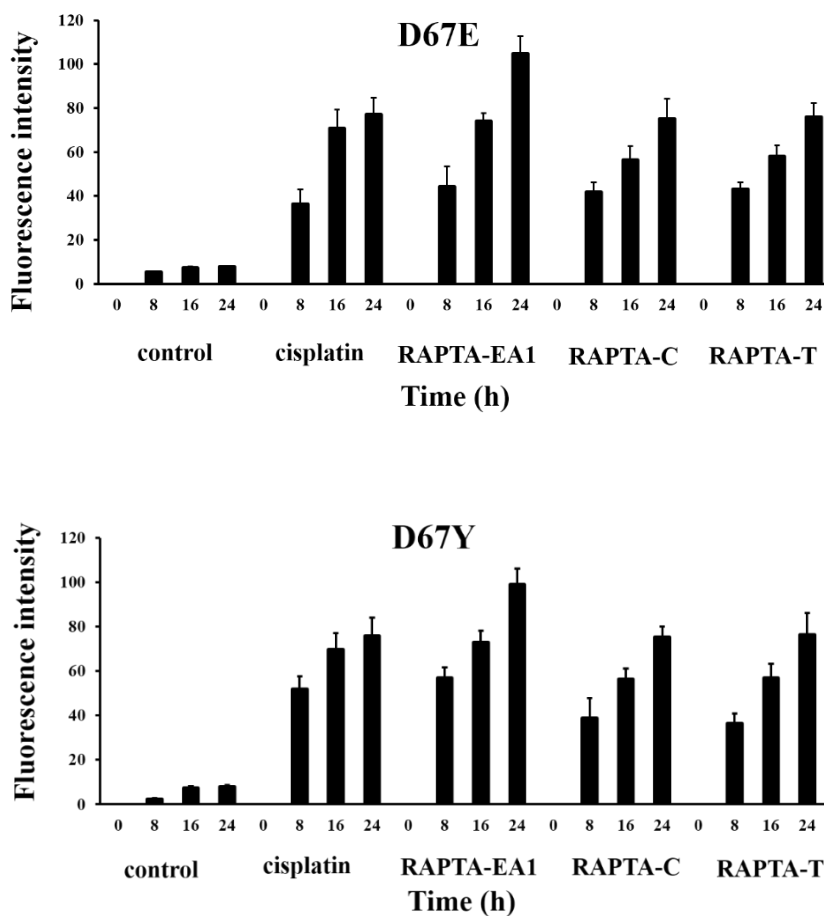


**Figure 4.28.** Time-dependent zinc ejection assay on the mutant BRCA1 RING domain proteins. Both mutant proteins (D67E and D67Y) were incubated with the metal complexes at time intervals prior to fluorescence measurement as previously described in Fig. 4.27. Each experiment was performed in triplicate.

#### 4.3.5 Inactivation of the mutant BRCA1 E3 ligase activity by RAPTAs

The D67E and D67Y BRCA1 proteins were treated with various concentrations of RAPTAs at 4 °C for 24 h prior to assaying the E3 ligase activity. The results revealed that the E3 ligase activity decreased in a dose-dependent manner in both mutant proteins (Fig. 4.29). Surprisingly, the D67E and D67Y proteins showed hypersensitivity to RAPTAs, especially the D67Y protein (Fig. 4.29, Table 4.4). RAPTA-EA1 exhibited a 10-fold and 25-fold higher ability to inhibit the D67E- and D67Y-mediated E3 ligase activities, respectively, than the wild-type BRCA1-mediated E3 ligase activity. The  $IC_{50}$  values for inactivation of E3 ubiquitin ligase activity by RAPTA-EA1 were markedly lower than those for RAPTA-C, RAPTA-T and cisplatin (Fig. 4.30, Table 4.4).

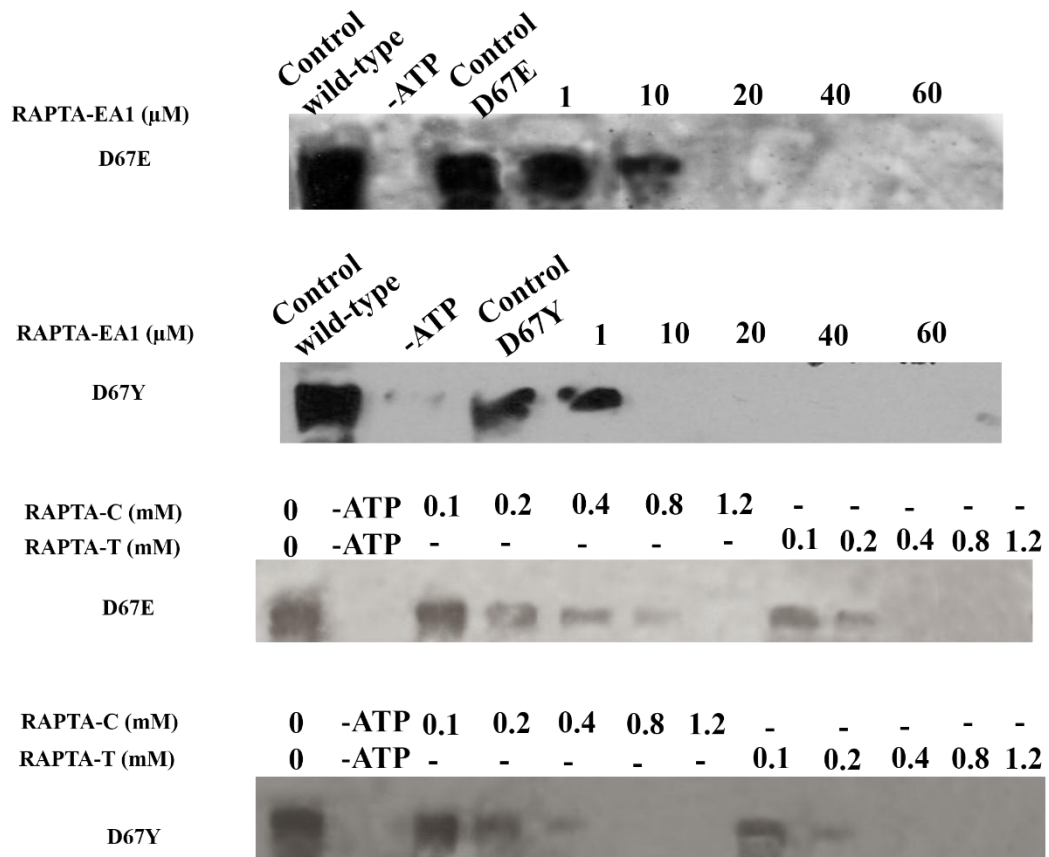


**Figure 4.29.** *In vitro* E3 ubiquitin ligase activity of the ruthenated mutant BRCA1, D67E and D67Y. Three  $\mu\text{g}$  of the mutant BRCA1 RING domain protein was incubated with the RAPTA complexes at various concentrations, and then assayed for the E3 ubiquitin ligase activity.

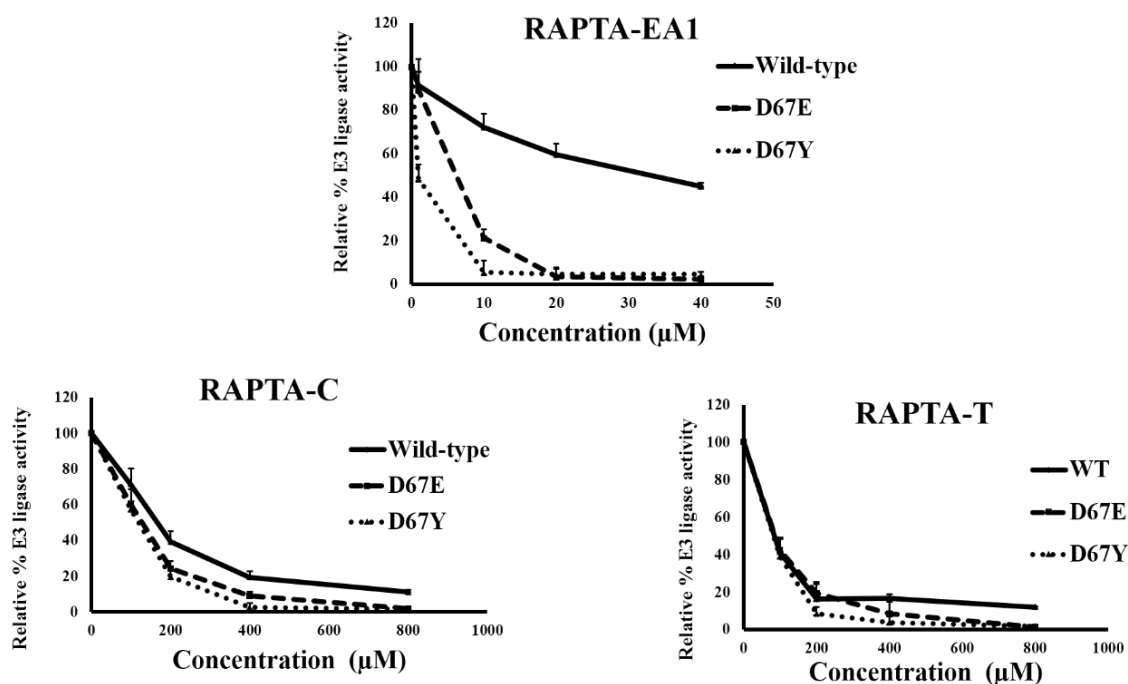


**Figure 4.30.** *In vitro* E3 ubiquitin ligase activity of the metal-treated BRCA1 protein. The apparent ubiquitinated products shown in Fig. 4.29 were quantified by densitometer (Bio-Rad GS-700 Imaging). The relative E3 ligase activity of the ruthenated BRCA1 (%) was plotted as a function of the concentration of metal complexes. Each experiment was performed in duplicate.

**Table 4.4.** Half inhibition of BRCA1/BARD1 E3 ligase activity was inactivated by RAPTA complexes.

	WT ( $\mu\text{M}$ )	D67E( $\mu\text{M}$ )	D67Y( $\mu\text{M}$ )
<b>RAPTA-EA1</b>	55	6	3
<b>RAPTA-C</b>	168	148	126
<b>RAPTA-T</b>	95	79	74
<b>Cisplatin*</b>	60*	60*	32*

\* A. Atipairin, A. Ratanaphan, Breast Cancer: Basic and Clinical Research, 2011, 5, 201-208.





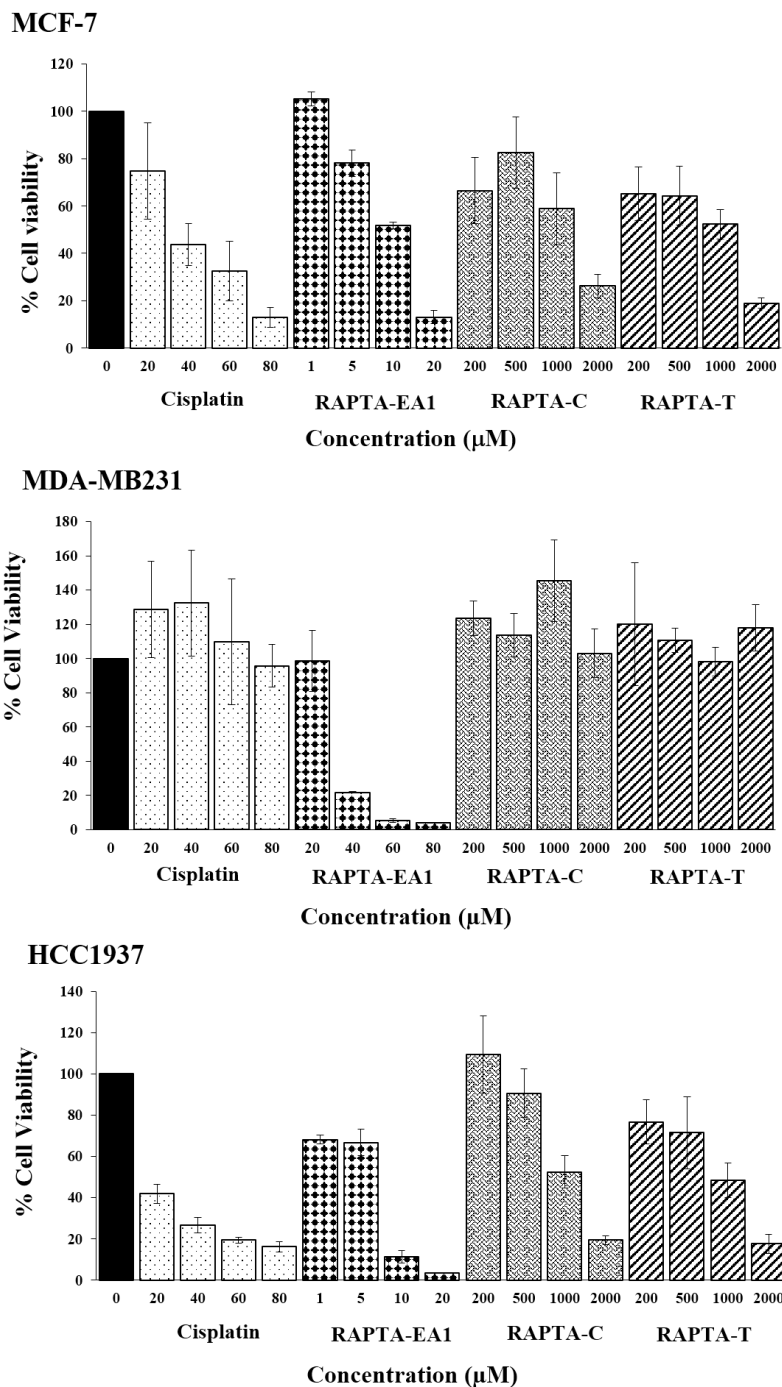


**Figure 4.31.** The effect of metal complexes on cell viability of MCF-7, HCC1937, and MDA-MB231 cells. Cells were treated with various concentration of metal complexes for 48 h and cell proliferation was measured using a MTT assay. Each value represents the mean  $\pm$ SD of two independents, performed in triplicate.

Real time monitoring the dynamics evaluation of human breast cancer (MCF-7, HCC1937 and MDA-MB-231 cells) proliferation on the 96-wells E-plates was monitored by RTCA system at every 15 min interval from the time of plating until the cells entered the logarithmic growth phase. The results showed that at  $5 \times 10^4$  cell/well of MCF-7 and HCC1937 cells rapidly entered the logarithmic growth phase within 9 h after seeding cells into the plate, whereas MDA-MB-231 cells slowly entered this phase at this time interval (Fig. 4.32). After treatment, the CI values were read at 15 min intervals for 24 h. For the MCF-7 cells, it was observed that there was a rapid decrease in the CI value that occurred as early as a few hours after treatment with 40, and 20  $\mu\text{M}$  of RAPTA-EA1 and 80, and 60  $\mu\text{M}$  of cisplatin, but a slow decrease in CI value after treatment with all concentrations of RAPTA-C and RAPTA-T (Fig. 4.33), suggesting that MCF-7 cells were more sensitive to RAPTA-EA1 > cisplatin > RAPTA-C and RAPTA-T. For the HCC1937 cells, it was observed that a rapid decrease in CI value occurred as early as a few hours after treatment with 80, and 60  $\mu\text{M}$  of cisplatin and 40, and 20  $\mu\text{M}$  of RAPTA-EA1 and a rapid decrease in CI value occurred at 5 h after treatment with high concentration of RAPTA-C and RAPTA-T (Fig. 4.33). However, the CI value of HCC1937 was more rapidly decreased than that of MCF-7 cells, suggesting all complexes appears to be more active against the HCC1937 cells than MCF-7 cells. Additionally, RAPTA-EA1-treated MDA-MB-231 cells rapidly decreased in CI value as early as an hour after treatment with 40  $\mu\text{M}$  and rapidly decreased in CI value at 7 h after treatment with all concentration of RAPTA-C and RAPTA-T (0.2-2.0 mM) and slowly decreased in CI value after treatment with all concentrations of cisplatin (20-120  $\mu\text{M}$ ) (Fig. 4.33). Moreover, in all experiments observed the transient increase of CI value, indicating a change in cell interactions in response to treatment before induction of cell death. The  $\text{IC}_{50}$  values, 24 h post-treatment with metal complexes, for MCF-7, HCC1937 and MDA-MB-231 cells were summarized in Table 4.5. Considering the  $\text{IC}_{50}$  of cisplatin, RAPTA-EA1, RAPTA-C and RAPTA-T, the results showed that RAPTA-EA1 exhibited a 5-fold, 2-fold, and 10-fold greater cytotoxicity than cisplatin in MCF-7, HCC1937, and MDA-MB-231 cells, respectively. In contrast, RAPTA-EA1 exhibited >10-fold greater cytotoxicity than RAPTA-C and RAPTA-T in all cell lines. It is notable that HCC1937 cells were more sensitive to all of these complexes than the other breast cancer cell lines (Table 4.5).

Whether metal complexes had a sustained effect on MCF-7, HCC1937 or MDA-MB-231 cells after removal of the complexes, the results showed that MCF-7, HCC1937 or MDA-MB231 cell lines recovered from the suppressive effects of both RAPTA-C and RAPTA-T. However, MCF-7 cell recovered from the suppressive effects of both cisplatin and RAPTA-EA1. Furthermore, a greater recovery of cell growth was observed for RAPTA-C and RAPTA-T than for cisplatin or RAPTA-EA1 in all cells, being drug dose-dependent. In addition, HCC1937 and MDA-MB-231 cells showed ongoing cells death when cisplatin or RAPTA-EA1 was removed after 24 h, indicating continued cellular damage (Fig. 4.33).

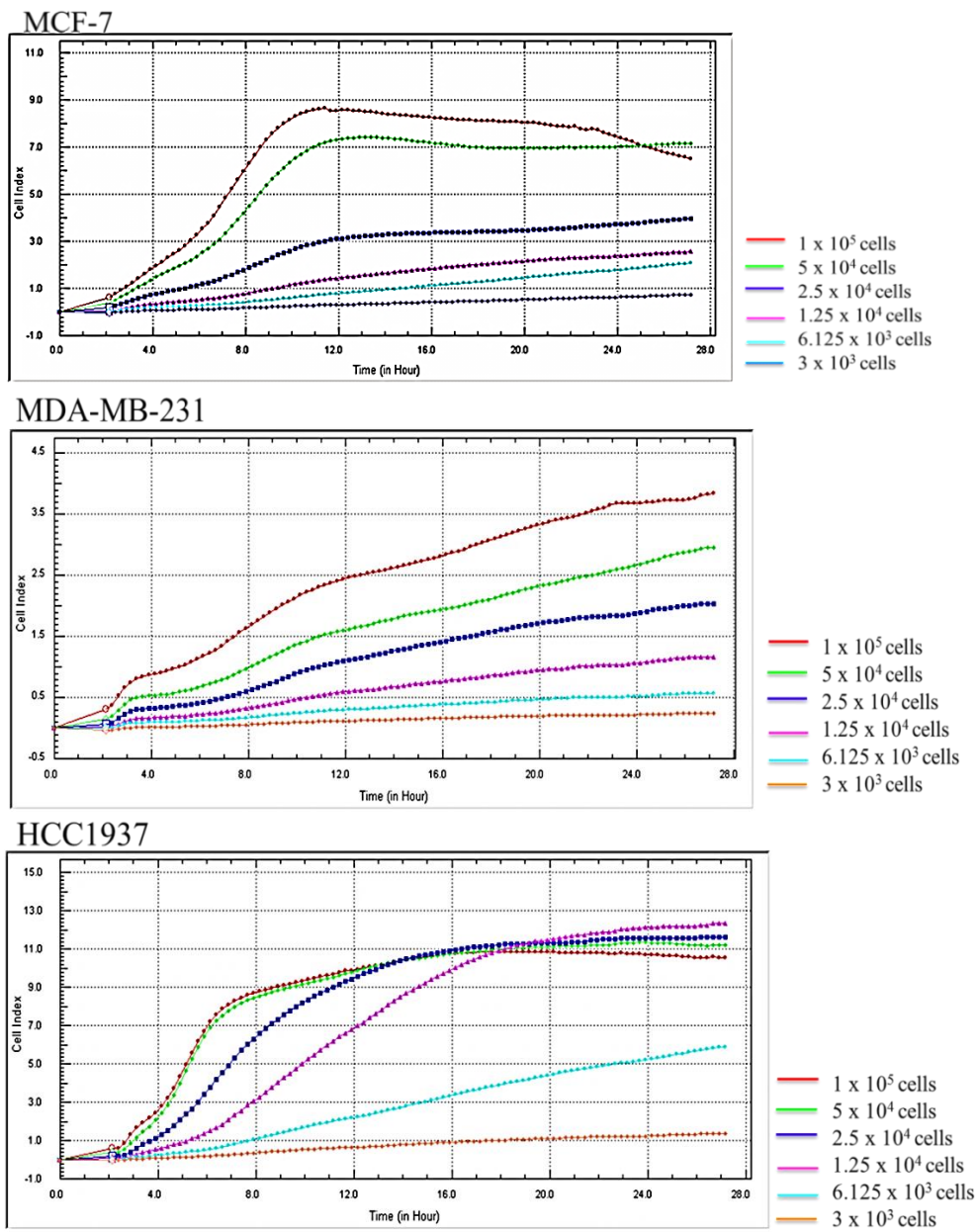
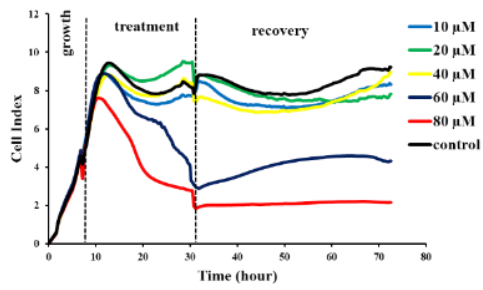


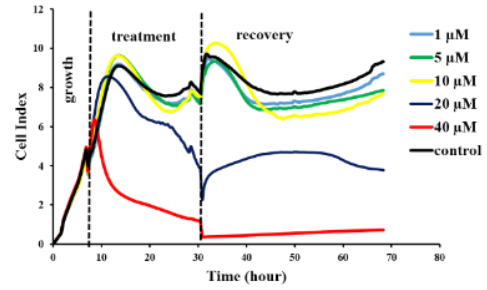
**Figure 4.32.** The dynamics of human breast cancer proliferation (MCF-7, MDA-MB-231 and HCC1937 cells) on the 96-wells E-plates.

## MCF-7

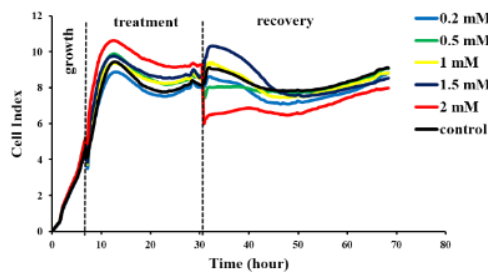
## Cisplatin



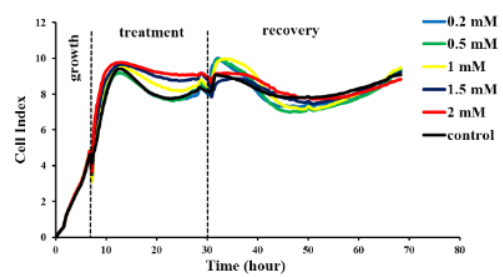
## RAPTA-EA1



## RAPTA-C

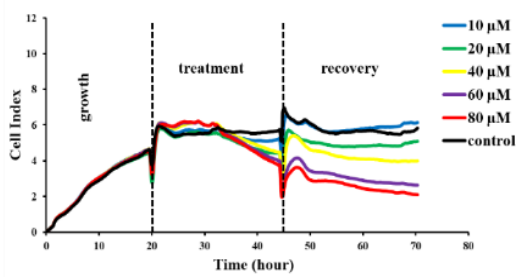


## RAPTA-T

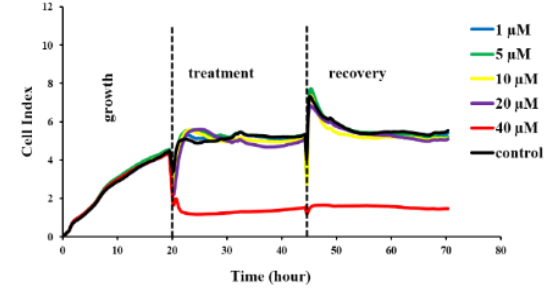


## MDA-MB231

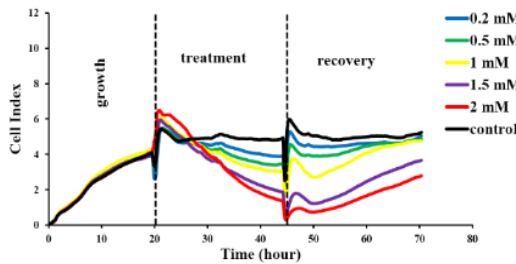
## Cisplatin



## RAPTA-EA1



## RAPTA-C



## RAPTA-T

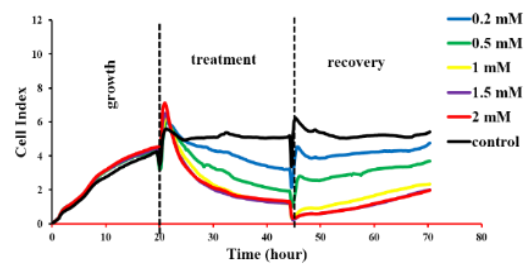
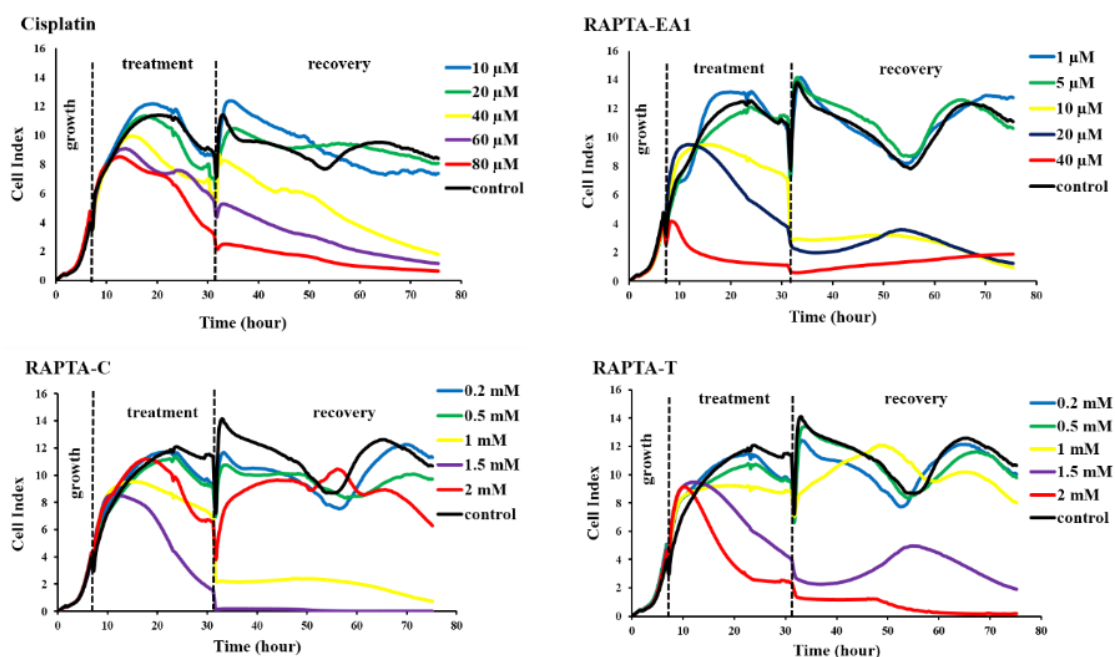


Figure 4.33. (To be continued).

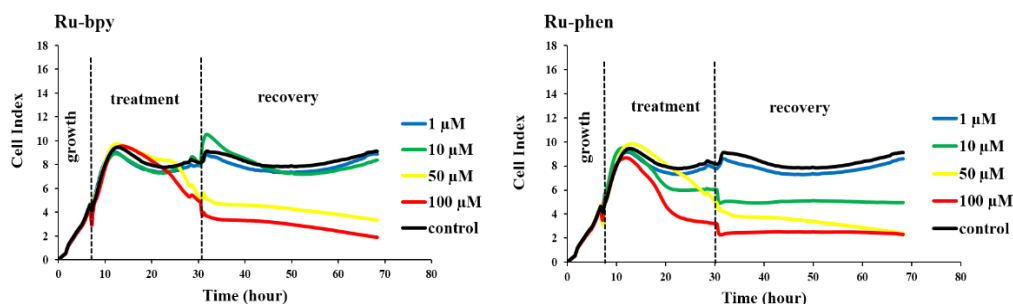
## HCC1937



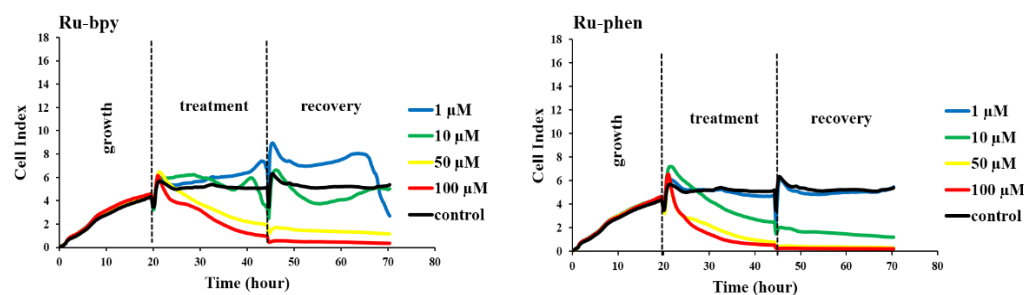
**Figure 4.33.** Real-time monitoring of the effect of metal complexes on human breast cancer cells using xCELLigence system. Cells were seeded onto the E-plate and allowed to grow prior, then incubated with various concentration of metal complexes. 24 h later, the complexes were removed and fresh media was added, then cells were allowed to grow for 24 h to assess the recovery cell proliferation after drugs treatments. Cell Index (CI) was recorded every 15 min. Each concentration was performed in triplicate.

In addition, the real time growth profiling of two ruthenium(II) polypyridyl complexes-treated breast cancer cell lines exhibited a similar growth profiling of RAPTAs-treated breast cancer cell lines in all cases (Fig. 4.34). The  $IC_{50}$  values at 24 h post-treatment with ruthenium(II) polypyridyl complexes on breast cancer cells were reported in Table 4.6.

### MCF-7



### MDA-MB231



### HCC1937

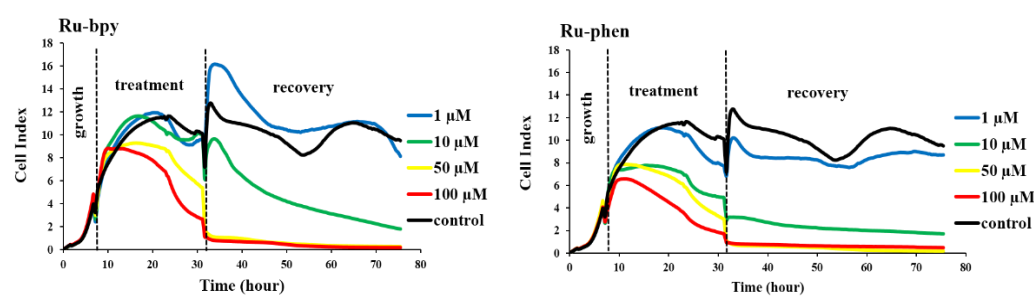


**Figure 4.34.** Real-time monitoring of the effect of metal complexes on human breast cancer cells using xCELLigence system. Cells were seeded onto the E-plate and allowed to grow prior, then incubated with various concentration of metal complexes. 24 h later, the complexes were removed and fresh media was added, then cells were allowed to grow for 24 h to assess the recovery cell proliferation after drugs treatments. Cell Index (CI) was recorded every 15 min. Each concentration was performed in triplicate.

**Table 4.6.** Comparison of 50 % inhibition of cancer cell growth by metal complexes using a MTT assay (48 h after treatment) and RTCA system (24 h after treatment).

Complex	MCF-7		MDA-MB-231		HCC1937	
	MTT ( $\mu\text{M}$ )	RTCA ( $\mu\text{M}$ )	MTT ( $\mu\text{M}$ )	RTCA ( $\mu\text{M}$ )	MTT ( $\mu\text{M}$ )	RTCA ( $\mu\text{M}$ )
Ru-bpy	18 $\pm$ 2	11 $\pm$ 1	39 $\pm$ 4	14 $\pm$ 0.5	6 $\pm$ 2	9 $\pm$ 0.1
Ru-phen	15 $\pm$ 1	8 $\pm$ 0.1	36 $\pm$ 1	13 $\pm$ 0.3	4 $\pm$ 1	2 $\pm$ 0.1

#### 4.5 The effect of RAPTA complexes on cells viability and protein function in the relation to the combination treatment with a PARP-1 inhibitor, olaparib

##### 4.5.1 Synergistic effect of RAPTA-EA1/olaparib combination in *BRCA1*-associated breast cancer cell lines

Combined therapies using several drugs with different molecular targets are effective in treating heterogeneous cancers, but require complicated treatments. From previous experiments, breast cancer cell treated with RAPTA-EA1 showed a dose-dependent inhibition of cell growth and cell viability in all tested cell lines. In the present study, RAPTA-EA1 and olaparib alone showed a dose-dependent inhibition of cell viability in all tested cell lines (Figure 4.35A, 4.35B). The combination treatment of RAPTA-EA1 and olaparib (Fig. 4.35C, Table 4.7) showed a 40-, 14- 120-fold higher ability of inhibiting cell proliferation than RAPTA-EA1 alone and a 36-, 42-, 77-fold higher ability of inhibiting cell proliferation than olaparib alone in MCF-7, MDA-MB-231, and HCC1937 cell, respectively. Indeed, it is an order of magnitude more effective in *BRCA1*-deficient (HCC1937) than *BRCA1*-proficient (MCF-7 and MDA-MB-231) cells. Furthermore, the combination treatment of RAPTA-EA1 with olaparib exhibited a synergistic effect in these cell lines in a dose-dependent manner (Figure 4.35C). The combination index (CI) of RAPTA-EA1 and olaparib is 0.28 (strong synergism), 0.693 (synergism), and 0.911 (nearly additive) in MCF-7, HCC1937 and MDA-MB-231, respectively.



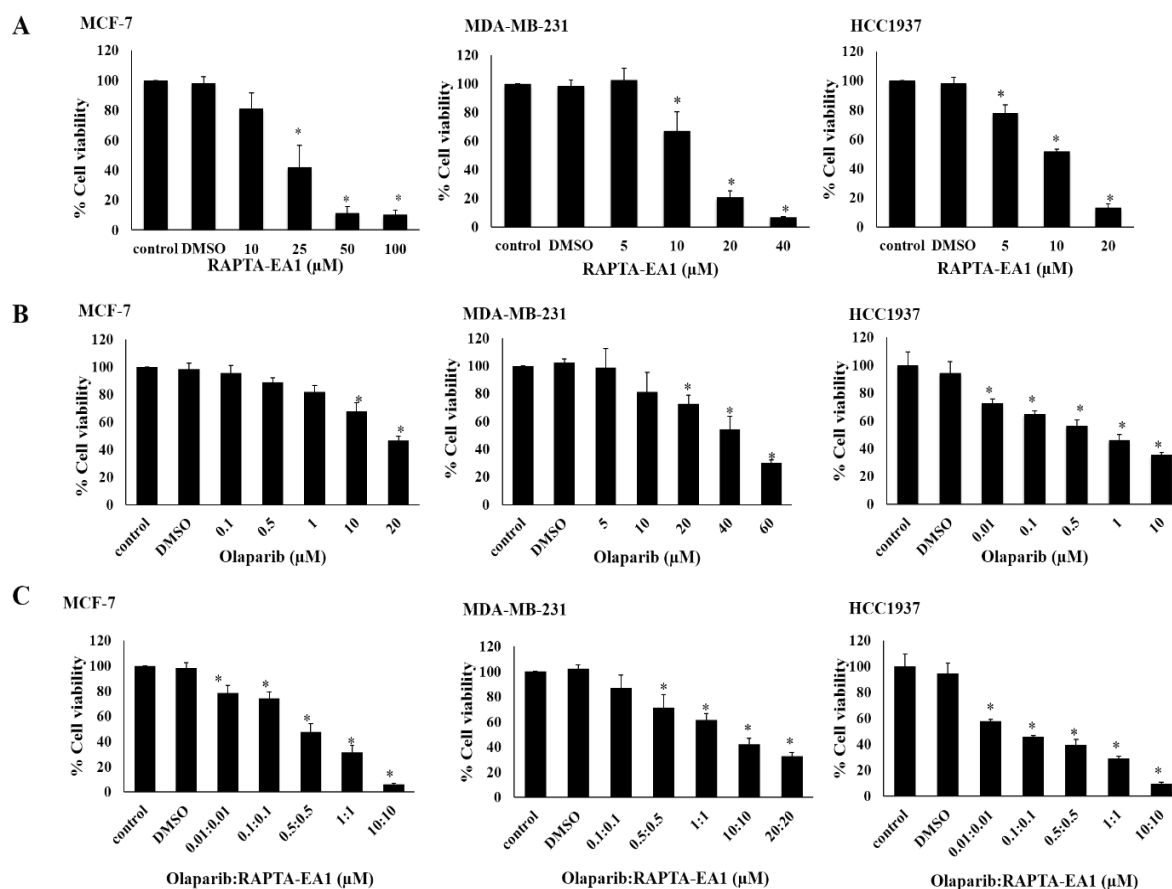


**Figure 4.35.** The effect of RAPTA-EA1 (A), olaparib (B), and RAPTA-EA1/olaparib combination (C) on cell viability of human breast cancer MCF-7, HCC1937, and MDA-MB231 cells using the MTT assay. MCF-7, MDA-MB-231 and HCC1937 cells were treated with various concentrations of drugs at 37 °C for 48 h. The experiments were performed in triplicate. Following notation was used throughout: \*  $p < 0.01$ , relative to control.

**Table 4.7.** The 50% inhibition of cancer cell growth by RAPTA-EA1, cisplatin, and olaparib on MCF-7, MDA-MB-231 and HCC1937 cells after 48 h.

Complex	IC <sub>50</sub> (μM)		
	MCF-7	MDA-MB-231	HCC1937
Cisplatin	42.2 ± 8	128.2 ± 7	23.4 ± 3
RAPTA-EA1	20 ± 5	15 ± 2	12 ± 5
Olaparib	18 ± 2	43 ± 2	8 ± 0.8

#### 4.5.2 Synergistic effect of RAPTA-EA1/olaparib combination on inhibition of BRCA1-mediated E3 ligase activity

To address whether the inhibition of the E3 ligase activity resulted from the combination treatment with the ruthenium compound and the PARP1 inhibitor, olaparib was used in combination with RAPTA-EA1. The E3 ligase activity decreased as the ratio of concentration between RAPTA-EA1/olaparib increased (Fig. 4.36). The E3 ligase activity was reduced by half at concentration ratio of RAPTA-EA1/olaparib at 10:10  $\mu\text{M}$ . Surprisingly, the combination treatment of RAPTA-EA1/olaparib exhibited a 5-fold (Fig. 4.37) higher ability to inhibit E3 ligase activity than RAPTA-EA1 alone at the same concentration (Fig. 4.20). It suggests that the combination treatment of RAPTA-EA1 and the PARP1 inhibitor has a synergistic effect.

##### RAPTA-EA1



##### RAPTA-EA1/olaparib

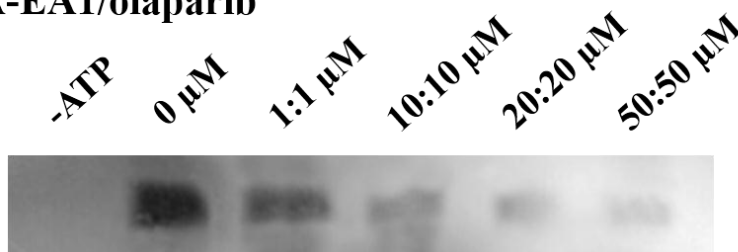


**Figure 4.36.** Effects of RAPTA-EA1/olaparib combination on an *in vitro* E3 ubiquitin ligase activity. The wild-type BRCA1 RING protein (3  $\mu\text{g}$ ) was treated with RAPTA-EA1 and olaparib (1:1 to 50:50  $\mu\text{M}$ ), then assayed for the E3 ubiquitin ligase activity. An apparent ubiquitinated product was markedly reduced as the RAPTA-EA1/olaparib concentration increased.

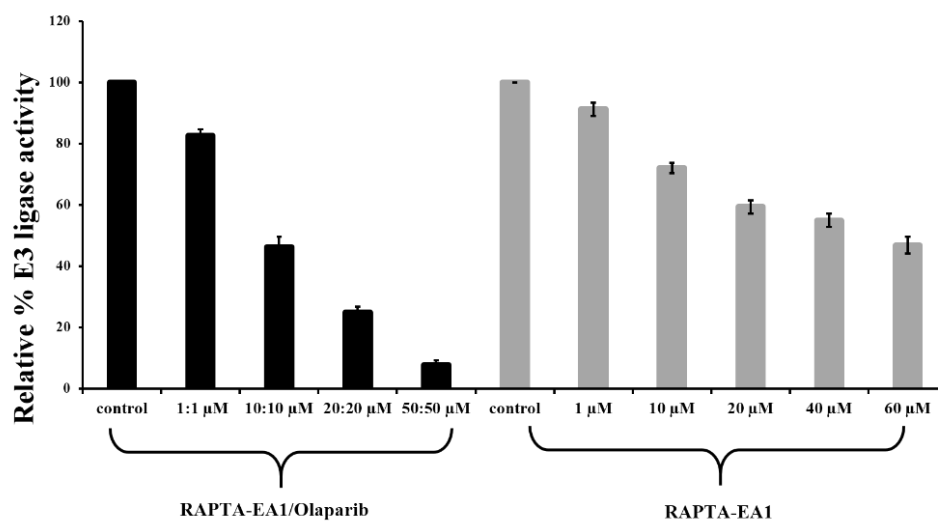


**Figure 4.37.** Effects of RAPTA-EA1/olaparib combination on an *in vitro* E3 ubiquitin ligase activity. The relative E3 ligase activity of the ruthenated BRCA1 (%) was plotted as a function of the RAPTA-EA1/olaparib concentrations. Each experiment was performed in duplicate.

## CHAPTER 5

### DISCUSSION

#### 5.1 DNA binding study

##### 5.1.1 *In vitro* ruthenation of the plasmid DNA by RAPTA complexes

In general, there are three plasmid DNA conformations, namely, a covalently closed circular DNA form (supercoiled DNA or Form I), a circular relax DNA (Form II), and a linear DNA (Form III), respectively (Travers and Muskhelishvili, 2005). The supercoiled plasmid DNA migrates the fastest on agarose gel. After ruthenium treatment, the RAPTA complexes can induce the change in conformation of the plasmid DNA as evidenced by the electrophoretic mobility of the ruthenium-treated plasmid DNA, i.e., the supercoiled form is changed into the circular relax form as the molar ratio of ruthenium/DNA nucleotide (*rb*) increased (Fig. 1). At the higher *rb* ratios, however, the circular relax form is changed into the supercoiled form. Both RAPTA-C and carboRAPTA-C induced different degrees of DNA unwinding. The unwinding angle was about 7° per bound of RAPTA-C. In contrast, the unwinding angle of carboRAPTA-C was about 3.0°. This unwinding angle is smaller than that of cisplatin (about 13° per bound of cisplatin) but is similar to that of RAPTA-EA1 (about 8.1° per bound of RAPTA-EA1) or  $[(\eta^6\text{-arene})\text{Ru}(\text{en})\text{Cl}]^+$  (about 7° per bound of complex) (Chakree *et al.*, 2012; Novakova *et al.*, 2003). Therefore, both RAPTA-C and carboRAPTA-C cause the conformational alteration of the plasmid DNA.

##### 5.1.2 *In vitro* ruthenation of the *BRCA1* gene fragment by RAPTA complexes

The interstrand DNA crosslinking induced by both complexes was similar to that by RAPTA-EA1 (Chakree *et al.*, 2012). However, RAPTA-C showed more rapidly crosslinking than carboRAPTA-C. Difference in cross-linking capability of these ruthenium complexes may be attributable to their different rates of hydration (Groessl *et al.*, 2008; Scolaro *et al.*, 2005). This binding may be facilitated by hydrophobic interactions with the arene while the ligand provides an additional site for binding (Beckford *et al.*, 2011).

The ruthenation sites on the specified *BRCA1* gene fragment can be deduced from restriction analysis using enzyme whose recognition sequence exists on the tested gene. *PvuII* and *EcoO109I* enzymes were inhibited in a dose-dependent manner. RAPATA-C at a concentration of 600  $\mu\text{M}$  completely interfered with the enzyme activity. In contrast, the enzymatic activity persisted at a concentration of 1000  $\mu\text{M}$  of carboRAPTA-C. Production of digested fragment from RAPTA-C-treated DNA and carboRAPTA-C-treated DNA in the presence of both enzymes were

similar level of inhibition. These suggested that ruthenation of RAPTAs does not show specificity between the two sites. CarboRAPTA-C was required approximately 2-fold higher concentrations to inhibit these enzyme activities, compared with RAPTA-C. It suggested that either ruthenation by RAPTA-C occurs more rapidly than that of carboRAPTA-C or the former complex is more stable than the latter. Due to the similarity in the nature of the resultant hydration product of both ruthenium compounds, it is likely that the observed effects are a consequence of the reaction rate rather than the nature of the product. It was reported that the inhibition of two restriction enzymes by RAPTA-EA1 was about two-fold more effective than that by carboRAPTA-C, but similar to RAPTA-C (Chakree *et al.*, 2012). It indicates that the large bulky group of ruthenium center may hinder accessibility by the enzymes to their restriction sites on the DNA molecules.

Data from sequence analysis showed that RAPTA-C and carboRAPTA-C showed a preferential attack at A, C and G (and not T) of *BRCA1* gene. It has been shown that ruthenated DNA adducts at the thymine sites are not thermodynamically stable, so the ruthenium atom migrates to the thermodynamically favored guanine sites (Wu *et al.*, 2013a; Wu *et al.*, 2013b). This statement consists with the hydration study of RAPTA-C. It demonstrated that the mono-aqua species of RAPTA-C was found to be the most abundant hydration product (Gossens *et al.*, 2007; Scolaro *et al.*, 2008). In contrast, RAPTA-EA1 showed a preferential attack at A, G, T and C of the *BRCA1* gene fragment (Charkree *et al.*, 2012). These cross-links can be anticipated based on their different properties of ruthenium complexes (Hartinger *et al.*, 2003). However, the preferential ruthenation sites differ from the preferential platination sites (Ratanaphan *et al.*, 2009). Several evidences reported that the affinity of some ruthenium arene complexes decreases in the order  $G > T \gg C > A$  (Aird *et al.*, 2002; Chen *et al.*, 2003). These complexes seemed to bind to guanine bases only in native DNA in cell-free media and single/double-stranded oligonucleotides in aqueous solutions (Liu *et al.*, 2010; Novakova *et al.*, 2003).

### 5.1.3 *In vitro* inhibition of *BRCA1* amplification by RAPTA complexes

Previous documents revealed that the quantitative polymerase chain reaction (QPCR) method can be used to study the effect of cisplatin on cellular DNA damage and repair after (Ratanaphan *et al.*, 2005), nitrogen mustards (Kalinowski *et al.*, 1992; Jennerwein and Eastman, 1991), 2-chloro-2-deoxyadenosine (Yuh *et al.*, 1998), chlorambucil, alkylbenzylguanine (Honma *et al.*, 1997), ruthenium(II) polypyridyl complexes (Ratanaphan *et al.*, 2012), and RAPTA-EA1 (Chakree *et al.*, 2012). When compared with RAPTA-EA1 under the same experimental conditions, RAPTA-C and carboRAPTA-C were considerable less effective at blocking replication but more effective than ruthenium(II) polypyridyl complexes (Chakree *et al.*, 2012; Ratanaphan *et al.*, 2012). A complete inhibition of *BRCA1* amplification induced by cisplatin and carboplatin was observed at 50 and 400  $\mu\text{M}$ , respectively (Ratanaphan *et al.*, 2005). Therefore, the inhibition concentrations of carboplatin and RAPTA-C are in the same range. The ruthenation level of the *BRCA1* gene fragment by RAPTA-C is also very similar to the platination value observed for carboplatin.

Nevertheless, RAPTA-C and carboplatin show very different *in vitro* cytotoxicity and *in vivo* profiles. The replacement of the labile chloride ligands in the prototype, cisplatin, by the more tardily hydrating cyclobutane-1,1-dicarboxylate ligand present in carboplatin reduces the rate by which the platinum center hydrolyzes, a necessity to DNA damage, as well as toxicity of this compound. Therefore, the replacement of the two labile chloride ligands in the RAPTA-C prototype by a dicarboxylate ligand may be observed a similar change in activity in the RAPTAs series. A comparable effect of ligand substitution on the DNA-binding screens between the Pt and Ru pairs, suggesting the substitution results in a parallel change in properties. These results support the recent report that the redox potential of the drugs was strongly affected by subtle changes of the ligand spheres with direct impact on the nature of the most likely metabolite species available, and as a result in the biodistribution and biological activity of the compounds (Palermo *et al.*, 2016).

## **5.2 Protein binding and functional consequence of RAPTA-induced wild type BRCA1 RING domain protein**

### **5.2.1 Structural consequence of RAPTA-treated wild type BRCA1 RING domain protein**

It revealed that the RAPTA complexes, including RAPTA-EA1, RAPTA-C and RAPTA-T, induce intermolecular crosslinks, resulting in dimers or larger aggregates. The binding affinity of each complex, in parallel with other metal complexes including Auphen and Auterpy, cisplatin, to the proteins was further investigated. The RAPT-EA1 complex bound efficiently to the BRCA1 protein in the absence and presence of  $Zn^{2+}$  and had a higher binding constant and gave rise to a lower free energy than other complexes. Moreover, the RAPTAs had a higher binding constant and gave rise to a lower free energy than cisplatin, it might be that the affinity of cisplatin affected only the apo-form of the BRCA1 RING protein (Atipairin *et al.*, 2010). These results agree with a previous study that cisplatin affects the conformation of the apo-form more than the holo-form of the BRCA1 RING finger domain, forming intra- and intermolecular Pt-BRCA1 adducts, where a preferential platinum-binding site was found at His-117 (Atipairin *et al.*, 2010). It is implied that RAPTAs have a highly effective binding to the BRCA1 protein and consequently affect the overall conformation of the protein than cisplatin. In addition, the interaction of some metal complexes, including ruthenium(II) polypyridyl complexes (Ru-bpy and Ru-phen,) and two gold(III) complexes (Auphen and Auterpy), with the holo-form of BRCA1 RING domain proteins was investigated. The binding of the compounds to the holo form of BRCA1 proteins induced conformational alteration of the BRCA1 protein, similar to that observed for the RAPTAs. The differences in the binding constants and free energies may be attributed to the differences in the structure of the metal complexes that the ligand of Ru-bpy, Ru-phen, Auphen, Auterpy, or RAPTA-EA1 is more hydrophobic than that cisplatin (Atipairin *et al.*, 2010). It has been revealed that the binding of the KP1019 to cytochrome c altered the conformation of the protein, affecting its capability to encourage cell apoptosis (Trynda-Lemiesz, 2004). Furthermore, some evidences reported that RAPTA-T showed a marked preference for transferrin binding. The

ruthenium complex exhibited a higher affinity to the holo-transferrin than that for the apo-form. It suggested that a cooperative iron-mediated metal binding mechanism was observed (Groessler *et al.*, 2010).

The thermal stability of the ruthenated BRCA1 was also observed. RAPTAs stabilized the BRCA1 protein structure with an associated increase in melting temperatures. The results are consistent with previous studies, showing that the drug-protein interaction forms the thermostable structure (Atipairin *et al.*, 2010; Atipairin *et al.*, 2011). The increased thermal stability of the ruthenated BRCA1 is possibly, in part, due to thermodynamically stabilizing contribution of the intra molecular and intermolecular crosslinks (Byrne and Stites, 1995). Notably, the melting temperature of the BRCA1 protein was considerably high and far from physical condition (76 °C), consistent with the previous studies. It showed that the Zn<sup>2+</sup> finger domain could form the thermostable structure (Arnold and Zhang, 1994; Frankel *et al.*, 1987; Mathhews *et al.*, 2000).

Several evidences suggested that ruthenium compounds might directly affect with proteins in signal transduction pathways (Bergamo *et al.*, 2008; Chatterjee and Mitra, 2009; Gaiddon *et al.*, 2005). There has been reported that RAPTAs have high affinities for cysteine-rich proteins involved in DNA replication and transcription as well as in epigenetic pathways (Ang *et al.*, 2009). RAPTAs were found to bind the serum proteins albumin and transferrin, which may prevent metallodrugs from being reduced and its subsequent activation in the blood (Ang *et al.*, 2011). Mass spectrometric analyses indicated that RAPTAs have affinities for histidine, on protein binding (Casini *et al.*, 2008; Casini *et al.*, 2009), similarly observed for NAMI-A (Messori *et al.*, 2000) and KP1019 (Piccioli *et al.*, 2004). Under essentially equivalent conditions, cisplatin forms mono-, bis-, and tris-adducts whereas only mono- and bis-adducts are formed with the RAPTA complexes (Casini *et al.*, 2007). Subsequent reactivity of RAPTA-C with a mixture containing superoxide dismutase, cytochrome c and ubiquitin showed that RAPTA-C had a high affinity towards both cytochrome c and ubiquitin, but not superoxide dismutase, showing a selectivity, which differences with the behavior of cisplatin (Casini *et al.*, 2009). The high reactivity towards protein molecules provoked the search of clinically relevant enzyme targeting by the RAPTAs, namely, cysteine protease cathepsin B and seleno-enzyme thioredoxin (Ang *et al.*, 2011). RAPTA-T and RAPTA-C were found to be promising inhibitors of cathepsin B (Casini *et al.*, 2008). RAPTA-C has been shown a higher affinity and a selectivity for metallothionein (MT-2) binding than cisplatin. This feature may have important pharmacological consequences, at least in part, for the different toxicological and pharmacological profiles of these two compounds (Casini *et al.*, 2009). In addition, similar binding affinity studies based on a mass spectrometric method showed that RAPTA-C can form adducts with the glutathione (GSH), tripeptide (Hartinger *et al.*, 2008). Furthermore, the reactivity of RAPTA-T with PARP-1 was examined. PARP-1 is an important protein involved in drug resistance of cancer. It contains zinc-finger domains that might be altered by metal-based compounds. Preliminary results showed that RAPTA-T inhibits PARP-1 to a similar level of inhibition by 3-aminobenzamide (Mendes *et al.*, 2011). These observations could reveal the possibility of both compound to overcome drug resistance

mechanisms and to identify novel possible targets for RAPTA compounds. Recently, it has been reported that the RAPTA complexes bind preferentially to proteins through coordination, in which their scaffold was found predominantly at the histone proteins (Adhireksan *et al.*, 2014; Wu *et al.*, 2011).

### **5.2.2 RAPTA complexes dismissed the zinc ions from the zinc binding sites of BRCA1 RING domain protein**

Previous studies reported that platinum- and ruthenium-based agents interacted with the zinc finger proteins and disturbed their conformation, resulting in displacement of zinc ions from the zinc finger protein and reducing their enzyme/protein activity (de Paula *et al.*, 2009). Our experiments revealed that the binding of the RAPTA complexes, gold(III) complexes, and cisplatin to the BRCA1 proteins releases the  $Zn^{2+}$  ion in a dose- and time-dependent manner. Furthermore, zinc ejection by gold(III) complexes, cisplatin and RAPTA-EA1 was similar and slightly greater than that estimated for RAPTA-C and RAPTA-T. The results suggest that metal, such as Ru, Au and Pt, could affect the conformation of this protein and interfered with its zinc binding sites, leading to a release of zinc ions from the binding sites. These results agree very well with previous studies that cisplatin, NAMI-A and RAPTA-T interact with PARP-1, leading to a reduction in PARP1 activity (Mendes *et al.*, 2011). Moreover, platinum-based complexes have been reported to interact with the C-terminus of the HIV nucleocapsid (NCp7) zinc finger leading to zinc ejection (de Paula *et al.*, 2009). Furthermore, targeting the zinc finger motif in BCA2 protein by a coordinated compound resulted in zinc atom release from the binding site, causing a reduction in E3 ligase activity (Brahemi *et al.*, 2010). Importantly, the extent and rate of displacement of the zinc ion by metal complexes depend on the nature (metal, ligand) of the complex (Quintal *et al.*, 2011).

### **5.2.3 Inactivation of the wild-type BRCA1 E3 ligase activity by the RAPTAs**

The reactivity of metal complexes towards the BRCA1 RING domain was reduced in the following order: AuTerpy > AuPhen > Ru-phen > RAPTA-EA1 > cisplatin > Ru-bpy > RAPTA-T > RAPTA-C. The results revealed that the BRCA1-mediated ubiquitin E3 ligase activity was contrariwise proportional to the concentration of RAPTAs, ruthenium(II) polypyridyl, and gold(III) complexes. It is consistent with a previous study, that the relative E3 ligase activity was contrariwise proportional to the concentration of the platinum-based drugs (Atipairin *et al.*, 2010a; Atipairin *et al.*, 2011b). A decrease in BRCA1 E3 ligase activity by these metal complexes could be due to an altered interaction between the RING heterodimer domains of BRCA1 and BARD1 that disturbed protein conformation, ultimately resulting in the displacement of zinc ion from the zinc finger domain. The vital roles in controlling of metal complexes reactivity towards the BRCA1 protein might depend on the properties and the geometry of these metal center, the leaving and the non-leaving groups of the metal complexes. The activation of the metal complexes



emerges when the chloride is substituted by water before interacting with the nucleophilic groups of biomolecules (Allardyce *et al.*, 2003).

### **5.3 Protein binding study and functional consequence of RAPTA-induced mutant BRCA1 RING domain protein**

#### **5.3.1 The structural consequence of RAPTA-treated mutant BRCA1 RING domain protein**

The interaction of the RAPTA complexes with the mutant BRCA1 RING protein was investigated in a similar manner to that with the wild-type BRCA1 protein. The ruthenated mutant BRCA1 exhibited a similar binding affinity to the ruthenated wild-type BRCA1. RAPTA-EA1 predominantly exhibited a higher binding affinity to the mutant proteins than RAPTA-C and RAPTA-T. It is notable that the secondary structure of the D67Y is more susceptible towards the binding of the RAPTA complexes than the D67E or wild-type, consistent with previous studies which showed that cisplatin strongly perturbs the secondary structure of the D67Y protein, but barely perturbs the secondary structure of the D67E protein (Atipairin *et al.*, 2010; Atipairin *et al.*, 2011a). In addition, the RAPTA complexes and cisplatin have higher binding constants and lower free energies in the D67Y protein than in the D67E or wild-type proteins. This suggests that RAPTAs interact with the Zn<sup>2+</sup> binding sites and other residues rather than the Zn<sup>2+</sup> binding sites of the protein alone, and affect the overall conformation of the BRCA1 protein. The differences in the binding constants and free energies may be attributed to the differences in the structure of the metal complexes. As mentioned above in Topic 5.2.1, RAPTAs stabilized the wild-type protein structure with an increase in melting temperature, in contrast, the melting temperature of both D67Y and D67E proteins decreased as a result of RAPTAs binding. The results are consistent with previous studies that the zinc finger domain of the wild-type BRCA1 protein forms the thermostable structure, while that of the mutant BRCA1 protein is slightly less thermostable structure (Atipairin *et al.*, 2011a; Atipairin *et al.*, 2011b; Matthews *et al.*, 2000). However, the interactions between surface residues and solvent appeared to be altered as the variant proteins were slightly less thermostable compared to the wild-type protein (Atipairin *et al.*, 2011b; Pjura and Matthews, 1993). This difference may also reflect an altered microenvironment around the mutation site.

#### **5.3.2 RAPTA complexes dismissed the zinc ions from the zinc binding sites of mutant BRCA1 RING domain protein**

It is notable that the zinc ejection by RAPTA-EA1 is markedly greater than that estimated for the other compounds, and more easier in D67Y than D67E or wild-type protein. A change in amino acid from aspartic acid (D, acidic amino acid) to tyrosine (Y, polar amino acid) could result in environment properties in Zn<sup>2+</sup> binding site and leading to weak binding with zinc atom. Platinum complexes have been reported to interact with the C-terminus of the HIV nucleocapsid NCp7 zinc finger domain, and leading to the ejection of Zn<sup>2+</sup> ions (Anzellotti *et al.*, 2006).

### 5.3.3 Inactivation of the mutant BRCA1 E3 ligase activity by the RAPTAs

Surprisingly, the D67E and D67Y proteins showed hypersensitivity to the RAPTA complexes, especially the D67Y, than wild-type BRCA1 proteins, consistent with the previous study showing that platination of the wild-type BRCA1 protein hardly affects the native structure and function of the protein whereas platination of the D67E BRCA1 results in distinct changes on structure and function (Atipairin *et al.*, 2011b). Previous preclinical and clinical studies have demonstrated that mutations in the BRCA1 RING domain (C61G mutation) disrupt an E3 ligase activity confers hypersensitivity to DNA-damaging chemotherapy and  $\gamma$ -irradiation (Atipairin *et al.*, 2011b; Ohta *et al.*, 2009; Ransburgh *et al.*, 2010; Ruffner *et al.*, 2001; Wei *et al.*, 2008). Recently, the substitution of serine 36 by tyrosine (S36Y) disrupts the  $\beta$ -helix of the BRCA1 RING domain has been shown to alter the protein conformation that affects interactions with BARD1 as well as with E2 enzyme, resulting in abrogated protein function (Christou *et al.*, 2014). It suggested that this variant affects the BRCA1 structure and BARD1 binding that exhibits the defective ubiquitin ligase activity. However, some evidences reported that the mutations at L51W and K65R of BRCA1 RING domains result in an increase in E3 ligase activity and rescue the E3 ligase activity of C61G and C64G cancer-associated mutations (Stewart *et al.*, 2016).

## 5.4 Cellular response to RAPTA complexes in human breast cancer cell lines

### 5.4.1 Antiproliferative effects of RAPTA complexes

RAPTA-EA1 appears to be more active against the human breast cancer cells (MCF-7, HCC1937, and MDA-MB-231) than cisplatin, RAPTA-C and RAPTA-T. Considering chemical structure, RAPTA-EA1 contains a ethacrynic (EA) ligand, having a higher hydrophobicity and bigger surface area than other complexes. It enhances cellular uptake of cancer cells to selectively bind to glutathione S-transferase (GST) and inhibits GST activity overcoming metallodrug resistance mechanisms with an increasing cytotoxic activity (Ang *et al.*, 2007; Angonigi *et al.*, 2015; Carter *et al.*, 2016). From earlier observations (protein binding affinity, protein conformation, and zinc ejection section), it has been shown that RAPTA-EA1 exerts stronger effect to interfere with the zinc finger pocket of the BRCA1 protein than other metal-based drugs, especially in the mutant protein, resulting in a loss of BRCA1 E3 ligase activity. It might explain why RAPTA-EA1 has a high efficiency to kill breast cancer cells than cisplatin or other RAPTA compounds. An increased sensitivity in *BRCA1*-mutated breast cancer cells might be related to a dysfunction of BRCA1 that is incapable to repair DNA damage induced by treatment with the complexes, eventually leading to cell death (Alli *et al.*, 2011; Tassone *et al.*, 2009).

Triple-negative breast cancer (TNBC) cells, lacking estrogen receptor (ER), progesterone receptor (PR) and human epidermal receptor 2-amplified (HER2-amplified) are extremely difficult to treat as the tumor is aggressive and targeted therapies are not effective (Cleator *et al.*, 2007; Liedtke *et al.*, 2008; Anders and

Carey, 2009). The treatment is further complicated if the tumor type produces enough functional BRCA1 protein. One of a novel biomarker to predict the response of treatment among breast cancer patients is the BRCA1 expression level. Over the years, the *BRCA1* gene and its encoded product have expected much attention as a potential molecular target for the anticancer based drugs (Atipairin *et al.*, 2010; Atipairin *et al.*, 2011a; Atipairin *et al.*, 2011b; Atipairin *et al.*, 2011c; Chakree *et al.*, 2012; Ratanaphan *et al.*, 2005; Ratanaphan *et al.*, 2009; Ratanaphan *et al.*, 2012; Ratanaphan *et al.*, 2014; Ratanaphan *et al.*, 2017). Recently, some RAPTA complexes exhibited a differential cellular response for breast cancer cell line depending on the BRCA1 status (Ratanaphan *et al.*, 2017). The present studies revealed that both MTT assay and real time analysis showed that all of these ruthenium(II) complexes, both RAPTA types and ruthenium(II) polypyridyl (Ru-bpy and Ru-phen), were more sensitive to HCC1937 cells (*BRCA1* mutant, TNBC) than MCF-7 (*BRCA1* wild-type, ER positive) or MDA-MB-231 cells (*BRCA1* wild-type, TNBC). Preclinical and clinical studies have recently reported a specific chemosensitivity profile of *BRCA1*-defective cells *in vitro* depending on BRCA1 protein expression (Ashworth, 2008; Quinn *et al.*, 2009; Tassone *et al.*, 2009). It has been reported that an increased resistance to cisplatin occurred when overexpression of BRCA1 in the MCF-7 cells was occurred (Husain *et al.*, 1998; Powell, 2016). On contrary, HCC1937 cells, which are derived from a patient with a *BRCA1* mutation (5382insC), have been found significantly more sensitive to cisplatin (Tassone *et al.*, 2009). These observations indicate that an increase in chemosensitivity are attributed to *BRCA1*-deficient breast cancer cells.

## **5.5 Effect of the RAPTA complexes on cells viability and protein function**

### **5.5.1 The combination treatment of RAPTA-EA1 and olaparib exhibited a synergistic effect on cell growth inhibition in *BRCA1*-associated breast cancer cell lines**

Olaparib is a potent oral PARP1 inhibitor that causes synthetic lethality in *BRCA1*-deficient or *BRCA2*-deficient cancer cells (Evers *et al.*, 2008). This lethality is a possible explanation by the cancer cells with defects in the *BRCA1* gene are defective in homologous recombinant repair (Hosoya and Miyagawa, 2014). However, recently evidences revealed that resistance to PARP1 inhibitor and cisplatin developed in cells derived from a tumor of a *BRCA1* (185delAG) mutation carrier (Drost *et al.*, 2016; Wang *et al.*, 2016). Recent trials assessing olaparib in combination with chemotherapy in patients with advanced ovarian, breast, and other solid tumors have shown encouraging efficacy (Lee *et al.*, 2014; Murray *et al.*, 2016). The excellent sensitivity of these cancers to olaparib, alone or in combination with platinum-containing drugs, provides strong support for olaparib in combination with metal-based drug as a novel targeted therapeutic against *BRCA*-deficient cancers (Balmaa *et al.*, 2014; Evers *et al.*, 2008; Lee *et al.*, 2014). RAPTA-EA1 showed significantly more effective against the *BRCA1*-deficient breast cancer cells than cisplatin. The combination treatment of RAPTA-EA1 and olaparib showed a synergistic effect of inhibiting cell proliferation than RAPTA-EA1 or olaparib alone in all three cell lines in a dose-dependent manner. The 5382insC mutation was

founded in a *BRCA1*-defective HCC1937 cell line (Neve *et al.*, 2006). It is likely that drug sensitivity in the *BRCA1*-mutated cells might be related to dysfunction of BRCA1 that is incapable to repair DNA damage induced by RAPTA-EA1 or olaparib treatment, eventually leading to cell death. Recently, preclinical and clinical studies have revealed a specific chemosensitivity profile of *BRCA1*-defective cells, depending on expression of the BRCA1 protein (Alli *et al.*, 2011; Ashworth, 2008; Quinn *et al.*, 2009; Tassone *et al.*, 2009). HCC1937 cells were more sensitive to olaparib in combination with cisplatin (Hastak *et al.*, 2010; Hosoya and Miyagawa, 2014). Furthermore, clinical study revealed that the progression-free survival was significantly improved after combination treatment of olaparib with carboplatin followed by maintenance monotherapy, with the greatest clinical benefit in *BRCA*-mutated patients, and had an acceptable and manageable tolerability profile (Oza *et al.*, 2016). Our results clearly show that PARP1 inhibitor in combination with metal-based drugs have the potential to improve therapeutic strategies for breast cancer. Therefore, the application of olaparib with combination of RAPTA-EA1 is a new therapeutic strategy for breast cancer cell.

### **5.5.2 The combination treatment of RAPTA-EA1 and olaparib exhibited a synergistic effect on inhibition of BRCA1-mediated E3 ligase activity**

We further investigated the inhibition of BRCA1 E3 ligase activity by RAPTA-EA1 in the presence of the PARP1 inhibitor, olaparib. The combination treatment on the BRCA1 RING protein exhibited a 5-fold higher ability to inhibit E3 ligase activity than RAPTA-EA1 alone, suggesting a synergistic effect. It is apparent that RAPTA-EA1 is able to efficiently interact with the BRCA1 RING zinc-finger protein, possibly interfering with the Zn<sup>2+</sup> binding site. Indeed, RAPTA-EA1 has a high proficiency to bind to the *N*-terminus of the BRCA1 RING protein in the absence or presence of a Zn<sup>2+</sup> ion. Olaparib has been reported to preferentially interact with the zinc-finger of PARP-1 protein, leading to zinc ejection (Mendes *et al.*, 2011). Therefore, RAPTA-EA1 and olaparib might cooperatively perturb the BRCA1-mediated E3 ligase activity by ejecting the Zn<sup>2+</sup> from native BRCA1 protein, leading to loss of E3 ligase activity. Therefore, targeting the BRCA1 RING domain protein through the disruption of the BRCA1 E3 ligase activity by RAPTA-EA1 or in combination with olaparib might be an effective method to treat breast cancers. Nevertheless, recent studies, in mice, have recommended that mutations in the *N*-terminal of BRCA1, such as the relatively common C61G, may not confer hypersensitivity to PARP inhibitor (Drost *et al.* 2011).

## CHAPTER 6

### CONCLUSION

The RAPTA complexes induced the conformational change of the plasmid DNA. The degree of unwinding of the plasmid induced by RAPTA-C was similar to that by RAPTA-EA1, but two-fold higher than carboRAPTA-C and two-fold smaller than cisplatin. Both RAPTA-C and carboRAPTA-C formed Ru-*BRCA1* interstrand adducts. However, the interstrand crosslinks of RAPTA-C treated-DNA showed more rapidly compared to carboRAPTA-C. The activity of two restriction enzymes, *PvuII* and *EcoO1019I*, was affected about two fold more than by treatment with RAPTA-C compared to treatment with carboRAPTA-C. Both RAPTA-C and carboRAPTA-C preferentially attacked at A, C and G (and not T), which differed from RAPTA-EA1 that preferentially attacked at A, G, T, C in the order. The *BRCA1* amplification was reduced in the presence of RAPTA complexes that compared to the untreated DNA control. RAPTA-C was more effective at blocking DNA replication, completely preventing amplification at a concentration of 600  $\mu\text{M}$ , while the amplification of carboRAPTA-C-treated *BRCA1* fragments was still observed at concentrations exceeding 1000  $\mu\text{M}$ . The amounts of lesions were established as 3 lesions/*BRCA1* fragment and 1 lesions/*BRCA1* fragment for RAPTA-C and carboRAPTA-C, respectively. Furthermore, we have investigated *in vitro* interaction of the RAPTA complexes and others complexes, including ruthenium(II) polypyridyl, gold(III) complexes, with the *N*-terminal region of the BRCA1 RING domain proteins, both wild-type and mutant proteins (D67E and D67Y) with respect to Ru-BRCA1 adducts, protein conformation and thermal denaturation. RAPTA-EA1, RAPTA-C and RAPTA-T, induced intermolecular crosslinks, resulting in dimers or larger aggregates. RAPTA-EA1 was found to exhibit a 5-fold higher binding affinity to the wild type BRCA1 RING domain than RAPTA-C and RAPTA-T, and more than thousand-fold than both gold(III) complexes, however similar to cisplatin. Furthermore, the CD spectra of the apo and holo form of BRCA1 RING domain proteins (without and with  $\text{Zn}^{2+}$  bound, respectively) changed upon RAPTA binding in a concentration-dependent manner. The RAPTA complexes disrupted the secondary structure of the BRCA1 RING proteins leading to an increase in  $\alpha$ -helical content and a decrease in  $\beta$ -sheets forms. However, only RAPTA-EA1-induced BRCA1 RING strongly interfered both apo and holo form of BRCA1, compared with cisplatin-, RAPTA-C-, and RAPTA-T. The RAPTA complexes stabilized the BRCA1 protein structure with an associated increase in melting temperatures ( $T_m$ ). The  $T_m$  of the BRCA1 RING domains were  $>95$   $^{\circ}\text{C}$ ,  $>95$   $^{\circ}\text{C}$ , 83.1  $^{\circ}\text{C}$ , and 85.2  $^{\circ}\text{C}$  after treated with cisplatin, RAPTA-EA1, RAPTA-C and RAPTA-T, respectively whereas the  $T_m$  of wild-type BRCA1 is 76  $^{\circ}\text{C}$ . In addition, both Ru-bpy-, Ru-phen-, Au-phen- and Au-terpy-treated holo form of BRCA1 protein showed strongly change in CD profiles, and gave the binding constant and the free energy of binding at the same level to both RAPTA-EA1-treated apo and holo form of BRCA1 proteins but contrast with cisplatin, RAPTA-C and RAPTA-T. The binding of RAPTAs or gold(III) complexes to the BRCA1 proteins resulted in a release of zinc ions in a dose- and time-dependent manner as well as thermal alteration of ruthenated-BRCA1 proteins. Zinc ejection by

gold(III) complexes, cisplatin and RAPTA-EA1 were similarly and slightly greater than that estimated for the RAPTA-C and RAPTA-T. The BRCA1-mediated ubiquitin E3 ligase activity was inversely proportional to the concentration of the RAPTA complexes, ruthenium(II) polypyridyl complexes, and gold(III) complexes. In addition, the reactivity of metal complexes towards the BRCA1 RING domain was decreased in the following order: Auterpy > Auphen > Ru-phen > RAPTA-EA1 > cisplatin > Ru-bpy > RAPTA-T > RAPTA-C. Furthermore, the RAPTA-mutant BRCA1 adducts exhibited similar profile binding affinity to the RAPTA-treated wild-type BRCA1 adducts. As founded in RAPTA-treated wild-type BRCA1 adducts, RAPTA-EA1 predominantly exhibited a higher binding affinity to the mutant proteins, both D67E and D67Y, BRCA1 RING domain than RAPTA-C and RAPTA-T. The CD spectra of the holo form of mutant BRCA1 RING showed some different profiles in shape with some differences in their amplitudes after exposure to RAPTA complexes. The D67Y protein was maintained and underwent more folded structural rearrangement after increasing metal complexes concentrations, whereas, the D67E protein was slightly changed in the secondary structure. In addition, the RAPTA complexes and cisplatin have higher binding constants and lower free energies for the D67Y protein than for the D67E or wild-type proteins. Moreover, it is notable that the structure of the D67Y protein is more susceptible towards binding the RAPTA complexes than the D67E or wild-type proteins. Interestingly, the RAPTA complexes stabilized the wild-type protein structure with an associated increase in melting temperatures, in contrast, the  $T_m$  in both the D67Y and D67E proteins decreased as a result RAPTA binding. RAPTA complexes disrupted the conformation of mutant BRCA1 RING domain protein and released the zinc ion from the binding site in a dose-dependent manner. Furthermore, the rate of zinc ejection by RAPTA-EA1 was markedly greater than that estimated for the other compounds. In addition, the rate of ejection by RAPTA complexes in D67Y protein was easier than D67E or wild-type protein. Interestingly, the D67Y BRCA1 RING domain protein exhibited the reduced ubiquitination function, and was more susceptible to the RAPTAs than D67E or wild-type BRCA1 RING domain protein. We further investigated the effect of RAPTA complexes on breast cancer cell viability. Both MTT assay and real time analysis showed that all of these ruthenium(II) complexes, both RAPTA types and ruthenium(II) polypyridyl (Ru-bpy and Ru-phen), were more sensitive to HCC1937 cells (*BRCA1* mutant, TNBC) than MCF-7 (*BRCA1* and p53 wild-type, ER positive) or MDA-MB-231 cells (*BRCA1* wild-type, p53 mutant, TNBC). Furthermore, the combination of RAPTA-EA1 and olaparib exhibited a synergistic effect and showed a higher ability of inhibiting cell proliferation than RAPTA-EA1 or olaparib alone. Indeed, it is an order of magnitude more effective in *BRCA1*-deficient (HCC1937) than *BRCA1*-proficient (MCF-7 and MDA-MB231) cells. We further investigated the inhibition of BRCA1 E3 ligase activity by RAPTA-EA1 in the presence olaparib. The combination on the BRCA1 RING protein exhibited a 5-fold higher ability to inhibit E3 ligase activity than RAPTA-EA1 alone.

To the best of our knowledge, the effect of RAPTA complexes on DNA-damaging ability did not correlate with the observed anticancer activity on breast cancer cells, but the BRCA1 protein structure and function were correlated with their anticancer activity, suggesting a protein-based mechanism of cytotoxicity.

Taken together the results from these study allow us to construct a functional model of RAPTA effects on the BRCA1 protein, where uptake and binding of RAPTA complexes to zinc finger of the RING domain of BRCA1 results in zinc displacement, disrupting the secondary structure of protein and leading to loss of protein function and ultimately led cancer cell death (Fig. 6.1). Therefore, targeting the BRCA1 RING domain protein through the disruption of the BRCA1 E3 ligase activity by RAPTA-EA1 might be an effective approach to treat breast cancers, especially if used in combination with DNA damaging agents.

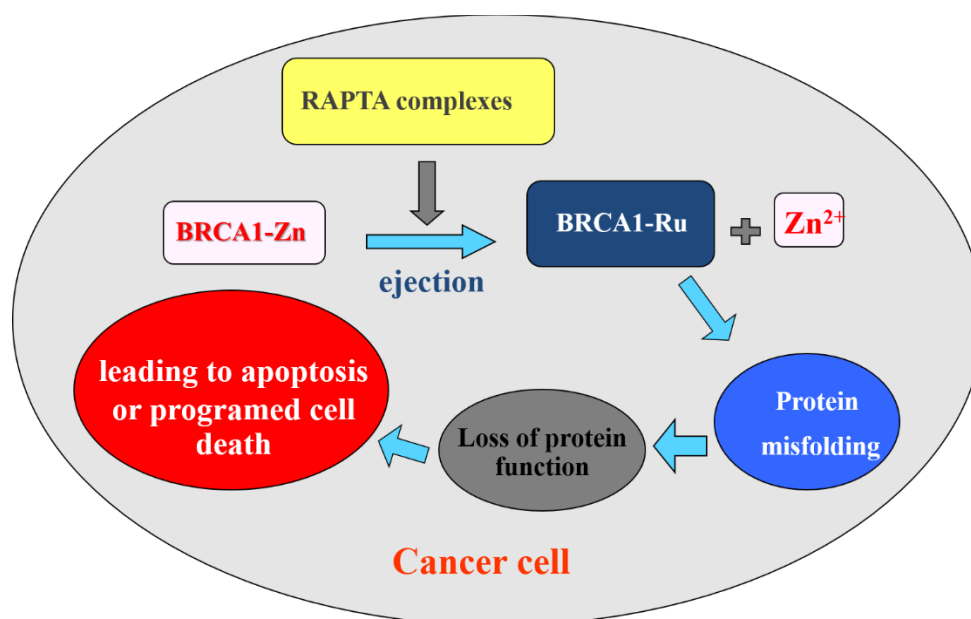


**Figure 6.1.** Following uptake RAPTA-EA1 interferes with the zinc finger motif of the BRCA1 RING domain protein resulting in zinc ion ejection and inactivation of the protein.

## REFERENCES

- Abbehausen C, Manzano CM, Corbi PP, Farrell NP. Effects of coordination mode of 2-mercaptothiazoline on reactivity of Au(I) compounds with thiols and sulfur-containing proteins. *J Inorg Biochem.* 2016; 165: 136-5.
- Abbehausen C, Peterson EJ, de Paiva REF, Corbi PP, Formiga AFB, Qu Y, et al. Gold(I)-phosphine-N-heterocycles: Biological activity and specific (ligand) interactions on the c-terminal HIV NCp7 zinc finger. *Inorg Chem.* 2013; 52: 1280-7.
- Adhireksan Z, Davey GE, Campomanes P, Groessl M, Clavel CM, Yu H. et al. Ligand substitutions between ruthenium-cymene compounds can control protein versus DNA targeting and anticancer activity. *Nat Commun.* 2014; 18: 3462.
- Afghahi A, Timms KM, Vinayak S, Jensen KC, Kurian AW, Carlson RW. Tumor BRCA1 reversion mutation arising during neoadjuvant platinum-based Chemotherapy in triple-negative breast cancer is associated with therapy resistance. *Clin Cancer Res.* 2017; 23: 3365-70.
- Agonigi G, Riedel T, Zacchini S, Păunescu E, Pampaloni G, Bartalucci N. Synthesis and antiproliferative activity of new ruthenium complexes with ethacrynic-acid-modified pyridine and triphenylphosphine ligands. *Inorg Chem.* 2015; 54: 6504-12.
- Aird RE, Cummings J, Ritchie AA, Muir M, Morris RE, Chen H. In vitro and in vivo activity and cross resistance profiles of novel ruthenium (II) organometallic arene complexes in human ovarian cancer. *Br J Cancer.* 2002; 86: 1652-7.
- Allardyce CS, Dyson P J. Ruthenium in medicine: Current clinical uses and future prospects. *Platinum Metals Rev.* 2001; 45: 62-9.
- Allardyce CS, Dyson PJ, Ellis DJ, Salter PA, Scopelliti R. Synthesis and characterisation of some water soluble ruthenium(II)-arene complexes and an investigation of their antibiotic and antiviral properties. *J Organomet Chem.* 2003; 668: 35-42.
- Allen NE, Beral V, Casabonne D, Kan SW, Reeves GK, Brown A, Green J. Moderate alcohol intake and cancer incidence in women. *J Natl Cancer Inst.* 2009; 101: 296-305.
- Alli E, Ford JM. BRCA1: Beyond double-strand break repair. *DNA Repair (Amst).* 2015; 32: 165-71.
- Alli E, Sharma VB, Hartman AR, et al. Enhanced sensitivity to cisplatin and gemcitabine in Brca1-deficient murine mammary epithelial cells. *BMC Pharmacol.* 2011; 11: 7.
- Anders CK, Carey LA. Biology, metastatic patterns, and treatment of patients with triple-negative breast cancer. *Clin Breast Cancer.* 2009; 9: S73-81.
- Anderson DE, Badzioch MD. Familial effects of prostate and other cancers on lifetime breast cancer risk. *Breast Cancer Res Treat.* 1993; 28: 107-13.
- Andreini, C.; Bertini, I.; Cavallaro, G. Minimal functional sites allow a classification of zinc sites in proteins *PloS One.* 2011, 6, e26325.
- Ang WH. Development of organometallic ruthenium(II) anticancer (RAPTA) drugs. *CHIMIA.* 2007; 61: 140-2.
- Ang WH. Novel strategies for overcoming drug resistance in transition metal-based



- anticancer compounds. Lausanne, Ecole Polytechnique Fédérale de Lausanne. **Ph.D. Dissertation**: 2007; 222.
- Ang WH, Dyson PJ. Classical and non-classical ruthenium-based anticancer drugs: Towards targeted chemotherapy. *Eur J Inorg Chem*. 2006; 20: 4003-18.
- Ang WH, Casini A, Sava G, Dyson PJ. Organometallic ruthenium-based antitumor compounds with novel modes of action. *J Organomet Chem*. 2011; 696: 989-98.
- Anzellotti AI, Farrell NP. Zinc metalloproteins as medicinal targets. *Chem Soc Rev*. 2008; 37: 1629-51.
- Apostolou P, Fostira F. Hereditary Breast Cancer: The Era of New Susceptibility Genes. *Biomed Res Int*. 2013; 2013:747318.
- Appleman LJ, Beumer JH, Jiang Y, et al. A phase 1 study of veliparib (ABT-888) in combination with carboplatin and paclitaxel in advanced solid malignancies. *J Clin Oncol Suppl*. 2014; Abstract 3049.
- Archev1 WB, Arrick BA. Transactivation of the estrogen receptor promoter by BRCA1. *Cancer Cell Int*. 2017; 17: 33.
- Arnold FH, Zhang JH. Metal-mediated protein stabilization. *Trends Biotechnol*. 1994; 12: 189-92.
- Ashworth A. A synthetic lethal therapeutic approach: Poly(ADP) ribose polymerase inhibitors for the treatment of cancers deficient in DNA doublestrand break repair. *J Clin Oncol*. 2008; 26:3785-90.
- Atipairin A, Canyuk B, Ratanaphan A. Cisplatin affects the conformation of apo form, not holo form, of BRCA1 RING finger domain and confers thermal stability. *Chem. Biodivers*. 2010; 7: 1949-67.
- Atipairin A, Canyuk B, Ratanaphan A. Substitution of aspartic acid with glutamic acid at position 67 of the BRCA1 RING domain retains ubiquitin ligase activity and zinc(II) binding with a reduced transition temperature. *J Biol Inorg Chem*. 2011a; 16: 217-26.
- Atipairin A, Canyuk B, Ratanaphan A. The RING heterodimer BRCA1-BARD1 is a ubiquitin ligase inactivated by the platinum-based anticancer drugs. *Breast Cancer Res Treat*. 2011b; 126: 203-9.
- Atipairin A, Ratanaphan A. *In vitro* enhanced sensitivity to cisplatin in D67Y BRCA1 RING domain protein. *Breast Cancer (Auckl)*. 2011c; 5: 201-208.
- Awada A, Campone M, Varga A, Aftimos P, Frenel JS, Bahleda R. An open-label, dose-escalation study to evaluate the safety and pharmacokinetics of CEP-9722 (a PARP-1 and PARP-2 inhibitor) in combination with gemcitabine and cisplatin in patients with advanced solid tumors. *Anticancer Drugs*. 2016; 27: 342-8.
- Audeh MW, Carmichael J, Penson RT, Friedlander M, Powell B, Bell-McGuinn KM, et al. Oral poly(ADP-ribose) polymerase inhibitor olaparib in patients with BRCA1 or BRCA2 mutations and recurrent ovarian cancer: a proof-of-concept trial. *Lancet*. 2010; 376: 245-51.
- Babak MV, Meier SM, Huber KVM, Reynisson J, Legin AA, Jakupec MA. et al. Target profiling of an antimetastatic RAPTA agent by chemical proteomics: relevance to the mode of action. *Chem Sci*. 2015; 6: 2449.
- Baer, R. Ludwig, T. The BRCA1/BARD1 heterodimer, a tumor suppressor complex with ubiquitin E3 ligase activity. *Curr Opin Genet Dev*. 2002; 278: 86-91.

- Balmana J, Tung NM, Isakoff SJ, Grana B, Ryan PD, Saura C, et al. Phase I trial of olaparib in combination with cisplatin for the treatment of patients with advanced breast ovarian and other solid tumors. *Ann Oncol.* 2014; 25: 1656-63.
- Bang YJ, Im SA, Lee KW, Cho JY, Song EK2, Lee KH. et al. Randomized, double-blind phase II trial with prospective classification by ATM protein level to evaluate the efficacy and tolerability of olaparib plus paclitaxel in patients With recurrent or metastatic gastric cancer.
- Battistin F, Scaletti F, Balducci G, Pillozzi S, Arcangeli A, Messori L. et al. Water-soluble Ru(II)- and Ru(III)-halide-PTA complexes (PTA=1,3,5-triaza-7-phosphaadamantane): Chemical and biological properties. *J Inorg Biochem.* 2016; 160: 180-8.
- Bau D.T., Fu YP, Chen ST, Cheng TC, Yu JC, Wu PE. et al. Breast cancer risk and the DNA double-strand break end-joining capacity of nonhomologous end-joining genes are affected by BRCA1. *Cancer Res.* 2004; 64: 5013-9.
- Bau D.T., Mau Y.C. and Shen C.Y. The role of BRCA1 in non-homologous end-joining. *Cancer Lett.* 2006; 240: 1-8.
- Baumann P, West SC. The human Rad51 protein: polarity of strand transfer and stimulation by hRP-A. *EMBO J.* 1997; 16(17): 5198-206.
- Beckford L., Lowe J., Dick L.R., Mayer R.J., Brownell J.E., Ubiquitin-like protein conjugation and the ubiquitin–proteasome system as drug targets, *Nat. Rev. Drug Discov.* 2011; 10: 29-46.
- Bell-McGuinn KM, Brady WE, Schilder RJ, Fracasso PM, Moore KN, Walker JL, et al. A phase I study of continuous veliparib in combination with IV carboplatin/paclitaxel or IV/IP paclitaxel/cisplatin and bevacizumab in newly diagnosed patients with previously untreated epithelial ovarian, fallopian tube, or primary peritoneal cancer: an NRG Oncology/Gynecologic Oncology Group study. In: *ASCO Annual Meeting Proceedings*; 2015.
- Benafif S, Hall M, An update on PARP inhibitors for the treatment of cancer. *Onco Targets Ther.* 2015; 8: 519-28.
- Bergamini P, Marvelli L, Marchi A, Vassanelli F, Fogagnolo M, Formaglio P. et al. Platinum and ruthenium complexes of new long-tail derivatives of PTA (1,3,5-triaza-7-phosphaadamantane): Synthesis, characterization and antiproliferative activity on human tumoral cell lines. *Inorg Chim Acta.* 2012; 391: 162-70.
- Bergamo A, Gava B, Alessio E, Mestroni G, Serli B, Cocchietto M, et al. Ruthenium-based NAMI-A type complexes with *in vivo* selective metastasis reduction and *in vitro* invasion inhibition unrelated to cell cytotoxicity. *Int J Oncol.* 2002; 21: 1331-8.
- Bergamo A, Gagliardi R, Scarzia V, Furlani A, Alessio E, Mestroni G, et al. *In vitro* cell cycle arrest, *in vivo* action on solid metastasizing tumors, and host toxicity of the antimetastatic drug NAMI-A and cisplatin. *J Pharmacol Exp Ther.* 1999; 289: 559-64.
- Bergamo A, Masi A, Dyson PJ, Sava G. Modulation of the metastatic progression of breast cancer with an organometallic ruthenium compound. *Int J Oncol.* 2008; 33: 1281-9.
- Bergink S, Jentsch S. Principles of ubiquitin and SUMO modifications in DNA repair.

- Nature. 2009; 458: 461-7.
- Bernardes VH, Qu Y, Du Z, Beaton J, Vargas MD, Farrell NP. Interaction of the HIV NCp7 Protein with Platinum(II) and Gold(III) Complexes Containing Tridentate Ligands. *Inorg Chem.* 2016; 55(21): 11396-407.
- Berners-Price SJ, Filipovska. Gold compounds as therapeutic agents for human diseases. *Metallomics.* 2011; 3: 863-73.
- Bettencourt-Dias M, Glover DM. Centrosome biogenesis and function: centrosomes brings new understanding. *Nat Rev Mol Cell Biol.* 2007; 8: 451-63.
- Biela A, Coste F, Culard F, Guerin M, Goffinont S, Gasteiger K, et al. Zinc finger oxidation of Fpg/Nei DNA glycosylases by 2-thioxanthine: biochemical and X-ray structural characterization. *Nucl Acids Res.* 2014; 42(16): 10748-61.
- Bielskienė K, Bagdonienė L, Mozūraitienė J, Kazbarienė B, Janulionis E. E3 ubiquitin ligases as drug targets and prognostic biomarkers in melanoma. *Medicina.* 2015; 51: 1-9.
- Bindoli A, Rigobello MP, Scutari G, Gabbiani C, Casini A, Messori L. Thioredoxin reductase: a target for gold compounds acting as potential anticancer drugs. *Coord Chem Rev.* 2009; 253: 1692-707.
- Bhattacharyya A, Ear US, Koller BH, Weichselbaum RR, Bishop DK. The breast cancer susceptibility gene BRCA1 is required for subnuclear assembly of Rad51 and survival following treatment with the DNA cross-linking agent cisplatin. *J Biol Chem.* 2000; 275: 23899-903.
- Biswas DK, Iglehart JD. Linkage between EGFR family receptors and nuclear factor kappaB (NF-kappaB) signaling in breast cancer. *J Cell Physiol.* 2006; 209: 645-52.
- Blees JS, Bokesch HR, Rubsamén D, Schulz K, Milke L, Bajer MM, et al. Erioflorin stabilizes the tumor suppressor Pcd4 by inhibiting its interaction with the E3-ligase beta-TrCP1. *PLoS One.* 2012; 7: e46567.
- Bork P, Hofmann K, Bucher P, Neuwald AF, Altschul SF, Koonin EV. A superfamily of conserved domains in DNA damage-responsive cell cycle checkpoint proteins. *FASEB J.* 1997; 11: 68-76.
- Brabec V, and Novakova O. DNA binding mode of ruthenium complexes and relationship to tumor cell toxicity. *Drug Resist. Update.* 2006; 9: 111-22.
- Brahemi G, Kona FR, Fiasella A, Buac D, Soukupov J, Brancale A, et al. Exploring the structural requirements for inhibition of the ubiquitin E3 ligase breast cancer associated protein 2 (BCA2) as a treatment for breast cancer. *J Med Chem.* 2010; 53: 2757-65.
- Brandt J, Garne JP, Tengrup I, Manjer J. Age at diagnosis in relation to survival following breast cancer: a cohort study. *World J Surg Oncol.* 2015; 13: 33.
- Brenton JD, Carey LA, Ahmed AA, Caldas C. Molecular classification and molecular forecasting of breast cancer: ready for clinical application? *J Clin Oncol.* 2005; 23: 7350-60.
- Brody JG, Moysich KB, Humblet O, Attfield KR, Beehler GP, Rudel RA. Environmental pollutants and breast cancer: epidemiologic studies. *Cancer.* 2007; 109: 2667-711.
- Brown JS, Jackson SP. Ubiquitylation, neddylation and the DNA damage response. *Open Biol.* 2015; 5:150018.
- Brzovic PS, Keefe JR, Nishikawa H, Miyamoto K, III DF, Fukuda M, et al. Binding

- and recognition in the assembly of an active BRCA1-BARD1 ubiquitin-ligase complex. *Proc Natl Acad Sci USA*. 2003; 100: 5646-51.
- Brzovic PS, Meza J, King MC, Klevit RE. The cancer-predisposing mutation C61G disrupts homodimer formation in the NH<sub>2</sub>-terminal BRCA1 RING finger domain. *J Biol Chem*. 1998; 273: 7795-99.
- Brzovic PS, Rajagopal P, Hoyt DW, King MC, Klevit RE. Structure of a BRCA1-BARD1 heterodimeric RING-RING complex. *Nat Struct Biol*. 2001; 8: 833-37.
- Busschots S, O'Toole S, O'Leary JJ, Stordal B. Carboplatin and taxol resistance develops more rapidly in functional BRCA1 compared to dysfunctional BRCA1 ovarian cancer cells. *Exp Cell Res*. 2015; 336: 1-14.
- Byrne MP, Stites WE. Chemically crosslinked protein dimers: stability and denaturation effects. *Protein Sci*. 1995; 4: 2545-58.
- Byrski T, Gronwald J, Huzarski T, Dent RA, Zuziak D, Wiśniowski R, et al. Neoadjuvant therapy with cisplatin in BRCA1-positive breast cancer patients. *Hered Cancer Clin Pract*. 2011; 9: A4.
- Byrski T, Gronwald J, Huzarski T, Grzybowska E, Budryk M, Stawicka M, et al. Pathologic complete response rates in young women with BRCA1-positive breast cancers after neoadjuvant chemotherapy. *J Clin Oncol*. 2010; 28: 375-9.
- Byrski T, Huzarski T, Dent R, Gronwald J, Zuziak D, Cybulski C, Response to neoadjuvant therapy with cisplatin in BRCA1-positive breast cancer patients. *Breast Cancer Res Treat*. 2009; 115: 359-63.
- Carey LA. Targeted chemotherapy? Platinum in BRCA1-dysfunctional breast cancer. *J Clin Oncol*. 2010; 28: 361-3.
- Carey LA, Perou CM, Livasy CA, Dressler LG, Cowan D, Conway K et al., Race, breast cancer subtypes, and survival in the Carolina Breast Cancer Study. *JAMA*. 2006; 295: 2492-502.
- Carter DA, Blair SE, Cokcetin NN, Bouzo D, Brooks P, Schothauer R. Therapeutic manuka honey: No longer so alternative. *Front Microbiol*. 2016; 7: 569.
- Casarsa C, Mischis MT, Sava G. TGF[ $\beta$ ]1 regulation and collagen-release-independent connective tissue re-modelling by the ruthenium complex NAMI-A in solid tumours. *J Inorg Biochem*. 2004; 98: 1648-54.
- Casini A, Gabbiani C, Michelucci E, Pieraccini G, Moneti G, Dyson PJ, et al. Exploring metallodrug-protein interactions by mass spectrometry: comparisons between platinum coordination complexes and an organometallic ruthenium compound. *J Biol Inorg Chem*. 2009; 14: 761-70.
- Casini A, Gabbiani C, Sorrentino F, Rigobello MP, Bindoli A, Geldbach TJ, et al. Emerging protein targets for anticancer metallodrugs: Inhibition of thioredoxin reductase and cathepsin B by antitumor ruthenium(II)-arene compounds. *J Med Chem*. 2008; 51: 6773-81.
- Casini A, Mastrobuoni G, Ang WH, Gabbiani C, Pieraccini G, Moneti G, et al. ESI-MS characterisation of protein adducts of anticancer ruthenium(II)-arene PTA (RAPTA) complexes. *ChemMedChem*. 2007; 2: 631-5.
- Catsburg C, Miller AB, Rohan TE. Active cigarette smoking and risk of breast cancer. *Int J Cancer*. 2015; 136: 2204-9.
- Ceccarelli DF, Tang X, Pelletier B, Orlicky S, Xie W, Plantevin V, et al. An allosteric

- inhibitor of the human Cdc34 ubiquitin-conjugating enzyme, *Cell*. 2011; 145: 1075-87.
- Chakree K, Ovatlarnporn C, Dyson PJ, Ratanaphan A, Altered DNA binding and amplification of human breast cancer suppressor gene BRCA1 induced by a novel antitumor compound, [Ru( $\eta^6$ -*p*-phenylethacrylate)Cl<sub>2</sub>(pta)]. *Int J Mol Sci*. 2012; 13: 13183-202.
- Chan CH, Morrow JK, Zhang S, Lin HK. Skp2: a dream target in the coming age of cancer therapy. *Cell Cycle*. 2014; 13: 679-80.
- Chan CH, Morrow JK, Li CF, Gao Y, Jin G, Moten A, et al. Pharmacological inactivation of Skp2 SCF ubiquitin ligase restricts cancer stem cell traits and cancer progression. *Cell*. 2013; 154: 556-68.
- Chandrasekharan S, Kandasamy KK, Dayalan P, Ramamurthy V. Estrogen induced concentration dependent differential gene expression in human breast cancer (MCF7) cells: role of transcription factors. *Biochem Biophys Res Commun*. 2013; 437: 475-81.
- Chang ET, Milne RL, Phillips KA, Figueiredo JC, Sangaramoorthy M, Keegan TH, et al. Family history of breast cancer and all-cause mortality after breast cancer diagnosis in the Breast Cancer Family Registry. *Breast Cancer Res Treat*. 2009; 117: 167-76.
- Chatterjee S, Kundu S, Bhattacharyya A, Hartinger CG, Dyson PJ. The ruthenium(II)-arene compound RAPTA-C induces apoptosis in EAC cells through mitochondrial and p53-JNK pathways. *J Biol Inorg Chem*. 2008; 13: 1149-55.
- Chatterjee D, Mitra A. Ru-edta induced cleavage of DNA. *J Coord Chem*. 2009; 62: 1719-24.
- Chen ZJ. Ubiquitin signalling in the NF-kappaB pathway. *Nat Cell Biol*. 2005; 7: 758-65.
- Chen D, Frezza M, Schmitt S, Kanwar J, Dou QP. Bortezomib as the first proteasome inhibitor anticancer drug: Current status and future perspectives. *Curr Cancer Drug Targets*. 2011; 11: 239-53.
- Chen A, Kleiman FE, Manley JL, Ouchi T, Pan ZQ. Autoubiquitination of the BRCA1/BARD1 RING ubiquitin ligase. *J Biol Chem*. 2002; 277: 22085-92.
- Chen CF, Li S, Chen Y, Chen PL, Sharp ZD, Lee WH. The nuclear localization sequences of the BRCA1 protein interact with the importin-alpha subunit of the nuclear transport signal receptor. *J Biol Chem*. 1996; 271: 32863-8.
- Chen JJ, Tsu CA, Gavin JM, Milhollen MA, Bruzzese FJ, Mallender WD, et al. Mechanistic studies of substrate-assisted inhibition of ubiquitinactivating enzyme by adenosine sulfamate analogues. *J Biol Chem*. 2011; 286: 40867-77.
- Chen LM, Mundt AJ, Powers C, Halpern HJ, Weichselbaum RR. Significance of family history in breast cancer treated with breast conservation therapy. *Breast J*. 1996; 2: 238-45.
- Chen H, Parkinson JA, Parsons S, Coxall RA, Gould RO, Sadler PJ. Organometallic ruthenium(II) diamine anticancer complexes: arene-nucleobase stacking and stereospecific hydrogen-bonding in guanine adducts. *J Am Chem Soc*. 2002; 124: 3064-82.

- Chen WY, Rosner B, Hankinson SE, Colditz GA, Willett WC. Moderate alcohol consumption during adult life, drinking patterns, and breast cancer risk. *JAMA*. 2011; 306: 1884–90.
- Chen Q, Xie W, Kuhn DJ, Voorhees PM, Lopez-Girona A, Mendy D, et al. Targeting the p27 E3 ligase SCF(Skp2) results in p27- and Skp2-mediated cell-cycle arrest and activation of autophagy. *Blood*. 2008; 111: 4690-99.
- Cheang MC, Voduc D, Bajdik C, Leung S, McKinney S, Chia SK, et al. Basal-like breast cancer defined by five biomarkers has superior prognostic value than triple-negative phenotype. *Clin Cancer Res*. 2008; 14: 1368-76.
- Chiba N, Parvin JD. Redistribution of BRCA1 among four different protein complexes following replication blockage. *J Biol Chem*. 2001; 276: 38549-54.
- Chlebowski RT, Kuller LH, Prentice RL, Stefanick ML, Manson JE, Gass M, et al., Breast cancer after use of estrogen plus progestin in postmenopausal women. *N Engl J Med*. 2009; 360: 573-87.
- Choi JR, Shin KS, Choi CY, Kang SJ. PARP1 regulates the protein stability and proapoptotic function of HIPK2. *Cell Death Dis*. 2016; 7: e2438.
- Chou TC, Talalay P. Quantitative analysis of dose-effect relationships: the combined effects of multiple drugs or enzyme inhibitors. *Adv Enzyme Regul*. 1984; 22: 27-55.
- Christou CM, Hadjisavvas A, Kyratzi M, Flouri C, Neophytou I, Anastasiadou V. The BRCA1 variant p.Ser36Tyr abrogates BRCA1 protein function and potentially confers a moderate risk of breast cancer. *PLoS One*. 2014; 9: e93400.
- Christou CM, Kyriacou K. BRCA1 and its network of interacting partners. *Biology*. 2013; 2: 40-63.
- Cibula D, Gompel A, Mueck AO, Vecchia CL, Hannaford PC, Skouby SO, et al. Hormonal contraception and risk of cancer. *Hum Reprod Update*. 2010; 16: 631-50.
- Cleator S, Heller W, Coombes RC. Triple-negative breast cancer: therapeutic options. *Lancet Oncol*. 2007; 8: 235-44.
- Coleman KA, Greenberg RA. The BRCA1-RAP80 complex regulates DNA repair mechanism utilization by restricting end resection. *J Biol Chem*. 2011; 286: 13669-80.
- Coleman RL, Sill MW, Bell-McGuinn K, Aghajanian C, Gray HJ, Tewari KS, et al. A phase II evaluation of the potent, highly selective PARP inhibitor veliparib in the treatment of persistent or recurrent epithelial ovarian, fallopian tube, or primary peritoneal cancer in patients who carry a germline BRCA1 or BRCA2 mutation. *Gynecol Oncol*. 2015; 137: 386-91.
- Cortez D, Wang Y, Qin J, Elledge SJ. Requirement of ATM-dependent phosphorylation of brca1 in the DNA damage response to double-strand breaks. *Science*. 1999; 286: 1162-6.
- Cui Y, Deming-Halverson SL, Shrubsole MJ, Beeghly-Fadiel A, Fair AM, Sanderson M. Associations of hormone-related factors with breast cancer risk according to hormone receptor status among white and African-American women. *Clin Breast Cancer*. 2014; 14: 417-25.
- Cun. S. Sun. H. A zinc-binding site by negative selection induces metallodrug

- susceptibility in an essential chaperonin. *Proc Natl Acad Sci.* 2010; 107: 4943-8.
- Dasari S, Tchounwou PB. Cisplatin in cancer therapy: molecular mechanisms of action. *Eur J Pharmacol.* 2014; 740: 364-78.
- de Almeida A, Oliveira BL, Correia JDG, Soveral G, Casinia A. Emerging protein targets for metal-based pharmaceutical agents: An update. *Coord Chem Rev.* 2013; 257: 2689-2704.
- de Bono JS, Mina LA, Gonzalez M, Curtin NJ, Wang E, Henshaw JW, et al. First-in-human trial of novel oral PARP inhibitor BMN 673 in patients with solid tumors. *J Clin Oncol.* 2013; 31: 2580.
- de Luca A, Hartinger CG, Dyson PJ, Lo Bello M, Casini A. A new target for gold(I) compounds: glutathione-S-transferase inhibition by auranofin.. *J Inorg Biochem.* 2013; 119: 38-42.
- de Paula QA, Mangrum JB, Farrell NP. Zinc finger proteins as templates for metal ion exchange: Substitution effects on the C-finger of HIV nucleocapsid NCp7 using M(chelate) species (M=Pt, Pd, Au). *J Inorg Biochem.* 2009; 103: 1347-54.
- Deegan BJ, Bona AM, Bhat V, Mikles DC, McDonald CB, Seldeen KL. Structural and thermodynamic consequences of the replacement of zinc with environmental metals on ER $\alpha$ -DNA interactions. *J Mol Recognit.* 2011; 24: 1007-1017.
- Del Conte G, Sessa C, von Moos R, Vigano L, Digena T, Locatelli A, et al. Phase I study of olaparib in combination with liposomal doxorubicin in patients with advanced solid tumours. *Br J Cancer.* 2014; 111: 651-659.
- Dent RA, Lindeman GJ, Clemons M, Wildiers H, Chan A, McCarthy NJ, et al. Phase I trial of the oral PARP inhibitor olaparib in combination with paclitaxel for first- or second-line treatment of patients with metastatic triplenegative breast cancer. *Breast Cancer Res.* 2013; 15: R88.
- Deng L, Wang C, Spencer E, Yang L, Braun A, You J, et al. Activation of the IkappaB kinase complex by TRAF6 requires a dimeric ubiquitin-conjugating enzyme complex and a unique polyubiquitin chain. *Cell.* 2000; 103: 351-361.
- Densham RM, Garvin AJ, Stone HR, Strachan J, Baldock RA, Daza-Martin M, et al. Human BRCA1-BARD1 ubiquitin ligase activity counteracts chromatin barriers to DNA resection. *Nat Struct Mol Biol.* 2016; 23: 647-55.
- DeSantis CE, Fedewa SA, Sauer AG, Kramer JL, Smith RA, Jemal A. Breast cancer statistics, 2015: Convergence of incidence rates between black and white women. *CA Cancer J Clin.* 2016; 66: 31-42.
- Díez O, Osorio A, Durán M, Martínez-Ferrandis JI, de la Hoya M, Salazar R, et al. "Analysis of BRCA1 and BRCA2 genes in Spanish breast/ovarian cancer patients: a high proportion of mutations unique to Spain and evidence of founder effects. *Hum Mutat.* 2003; 22: 301-12.
- Dilruba S, Kalayda GV. Platinum-based drugs: past, present and future. *Cancer Chemother Pharmacol.* 2016; 77: 1103-24.
- Ding K, Lu Y, Nikolovska-Coleska Z, Wang G, Qiu S, Shangary S, et al. Structure-based design of spiro-oxindoles as potent, specific small-molecule inhibitors of the MDM2-p53 interaction. *J Med Chem.* 2006; 49: 3432-5.
- Dizin E, Irminger-Finger I. Negative feedback loop of BRCA1-BARD1 ubiquitin

- ligase on estrogen receptor alpha stability and activity antagonized by cancer-associated isoform of BARD1. *Biochem Cell Biol.* 2010; 42: 693-700.
- Domagala P, Hybiak J, Rys J, Byrski T, Cybulski C, Lubinski, Pathological complete response after cisplatin neoadjuvant therapy is associated with the downregulation of DNA repair genes in BRCA1-associated triple-negative breast cancers. *Oncotarget.* 2016; 7: 68662-73.
- Dorcier A, Dyson PJ, Gossens C, Rothlisberger U, Scopelliti R, Tavernelli I. Binding of organometallic ruthenium(II) and osmium(II) complexes to an oligonucleotide: A combined mass spectrometric and theoretical study. *Organometallics.* 2005; 24: 2114-23.
- Dorcier A, Hartinger CG, Scopelliti R, Fish RH, Keppler BK, Dyson PJ. Studies on the reactivity of organometallic Ru-, Rh- and Os-pta complexes with DNA model compounds. *J Inorg Biochem.* 2008; 102: 1066-76.
- Dossus L, Boutron-Ruault MC, Kaaks R, Gram IT, Vilier A, Fervers B. et al. Active and passive cigarette smoking and breast cancer risk: Results from the EPIC cohort. *Int J Cancer.* 2014; 134: 1871-88.
- Downey M, Durocher D. Chromatin and DNA repair: the benefits of relaxation. *Nat Cell Biol.* 2006; 8: 9-10.
- Dougan SJ, Sadler PJ. The design of organometallic ruthenium arene anticancer agents. *CHIMIA.* 2007; 61: 704-15.
- Drew Y, Ledermann J, Hall G, Rea D, Glasspool R, Highley MS, et al. Phase 2 multicentre trial investigating intermittent and continuous dosing schedules of the poly(ADP-ribose) polymerase inhibitor rucaparib in germline BRCA mutation carriers with advanced ovarian and breast cancer. *Br J Cancer.* 2016; 114: 723-30.
- Drost R, Bouwman P, Rottenberg S, Boon U, Schut E, Klarenbeek S, et al. BRCA1 RING function is essential for tumor suppression but dispensable for therapy resistance. *Cancer Cell.* 2011; 20: 797-809.
- Drost R, Dhillon KK, van der Gulden H, van der Heijden I, Brandsma I, Cruz C. et al. BRCA1185delAG tumors may acquire therapy resistance through expression of RING-less BRCA1. *J Clin Invest.* 2016; 126: 2903-18.
- Dubarle-Offner J, Clavel CM, Gontard G, Dyson PJ, Amouri H. Selenoquinones stabilized by ruthenium(II) arene complexes: synthesis, structure, and cytotoxicity. *Chemistry.* 2014; 20: 5795-801.
- Dudgeon DD, Shinde S, Hua Y, Shun TY, Lazo JS, Strock CJ, et al. Implementation of a 220,000-compound HCS campaign to identify disruptors of the interaction between p53 and hDM2 and characterization of the confirmed hits. *J Biomol Screen.* 2010; 15: 766-82.
- Dumitrescu RG, Shields PG. The etiology of alcohol-induced breast cancer. *Alcohol.* 2005; 35: 213-25.
- Dwadasi S, Tong Y, Walsh T, Danso MA, Ma CX, Silverman P, et al. Cisplatin with or without rucaparib after preoperative chemotherapy in patients with triple-negative breast cancer (TNBC): Hoosier Oncology Group BRE09-146. *J Clin Oncol.* 2014; 32: 1019.
- Dyson PJ, Sava G. Metal-based antitumour drugs in the post genomic era. *Dalton Trans.* 2006; 1929-33.



- Eakin CM, Maccoss MJ, Finney GL, Klevit RE. Estrogen receptor alpha is a putative substrate for the BRCA1 ubiquitin ligase. *Proc Natl Acad Sci USA*. 2007; 104: 5794-9.
- Egger A, Hartinger C, Renfrew A, Dyson PJ. Metabolization of [Ru( $\eta^6$ -C<sub>6</sub>H<sub>5</sub>CF<sub>3</sub>)(pta)Cl<sub>2</sub>]: a cytotoxic RAPTA-type complex with a strongly electron withdrawing arene ligand. *J Biol Inorg Chem*. 2010; 15: 919-27.
- Ellison RC, Zhang Y, McLennan CE, Rothman KJ. Exploring the relation of alcohol consumption to risk of breast cancer. *Am J Epidemiol*. 2001; 154: 740-7.
- Escribano-Díaz C, Orthwein A, Fradet-Turcotte A, Xing M, Young JT, Tkác J, et al. A cell cycle-dependent regulatory circuit composed of 53BP1-RIF1 and BRCA1-CtIP controls DNA repair pathway choice. *Mol Cell*. 2013; 49: 872-83.
- Evans DGR, Lalloo F. Risk assessment and management of high risk familial breast cancer. *J Med Genet*. 2002; 39: 865-71.
- Evans DGR, Shenton A, Woodward E, Lalloo F, Howell A, Maher ER. Penetrance estimates for BRCA1 and BRCA2 based on genetic testing in a Clinical Cancer Genetics service setting: risks of breast/ovarian cancer quoted should reflect the cancer burden in the family. *BMC Cancer*. 2008; 8: 155.
- Evers B, Drost R, Schut E, de Bruin M, van der Burg E, Derksen PW. Selective inhibition of BRCA2-deficient mammary tumor cell growth by AZD2281 and cisplatin. *Clin Cancer Res*. 2008; 14: 3916-25.
- Fabbro M, Savage K, Hobson K, Deans AJ, Powell SN, McArthur GA, et al. BRCA1-BARD1 complexes are required for p53Ser-15 phosphorylation and a G1/S arrest following ionizing radiation-induced DNA damage. *J Biol Chem*. 2004; 279: 31251-58.
- Farmer H, McCabe N, Lord CJ, Tutt AN, Johnson DA, Richardson TB, et al. Targeting the DNA repair defect in BRCA mutant cells as a therapeutic strategy. *Nature*. 2005; 434: 917-21.
- Fan L, Goss PE, Strasser-Weippl K. Current Status and Future Projections of Breast Cancer in Asia. *Breast Care (Basel)*. 2015; 10:372-8.
- Fan S, Wang J, Yuan R, Ma Y, Meng Q, Erdos MR, et al. BRCA1 inhibition of estrogen receptor signaling in transfected cells. *Science*. 1999; 284: 1354-6.
- Fan S, Ma YX, Wang C, Yuan RQ, Meng Q, Wang JA. Role of direct interaction in BRCA1 inhibition of estrogen receptor activity. *Oncogene*. 2001; 20: 77-87.
- Fan S, Ma YX, Wang C, Yuan RQ, Meng Q, Wang JA. p300 Modulates the BRCA1 inhibition of estrogen receptor activity. *Cancer Res*. 2002 62: 141-151.
- Fedier A, Steiner RA, Schwarz VA, Lenherr L, Haller U, Fink D. The effect of loss of Brcal on the sensitivity to anticancer agents in p53-deficient cells. *Int J Oncol*. 2003; 22: 1169-73.
- Fenga C. Occupational exposure and risk of breast cancer (Review). *Biomed Rep*. 2016; 4: 282-92.
- Ferlay J, Steliarova-Foucher E, Lortet-Tieulent J, Rosso S, Coebergh JWW, Comber H, et al. Cancer incidence and mortality patterns in Europe: Estimates for 40 countries in 2012. *Eur J Cancer*. 2015; 49: 1374-403.
- Flugel D, Gorlach A, Kietzmann T. GSK-3beta regulates cell growth, migration, and angiogenesis via Fbw7 and USP28-dependent degradation of HIF-1alpha. *Blood*. 2012; 119: 1292-301.

- Fong PC, Boss DS, Yap TA, Tutt A, Wu P, Mergui-Roelvink M, et al. Inhibition of poly(ADP-ribose) polymerase in tumors from BRCA mutation carriers. *N. Engl J Med.* 2009; 361: 123-34.
- Font A, Taron M, Gago JL, Costa C, Sánchez JJ, Carrato C, et al. BRCA1 mRNA expression and outcome to neoadjuvant cisplatin-based chemotherapy in bladder cancer. *Ann Oncol.* 2011; 22: 139-44.
- Foulkes WD. Traffic control of BRCA1. *N. Engl J Med.* 2010; 362: 755-6.
- Frankel AD, Berg JM, Pabo CO. Metal-dependent folding of a single zinc finger from transcription factor IIIA. *Proc Natl Acad Sci U S A.* 1987; 84: 4841-5.
- Frasca DR, Gehrig LE, Clarke MJ. Cellular effects of transferrin coordinated to. *J Inorg Biochem.* 2001; 83: 139-49.
- Freneau P, Stoppa-Lyonnet D, Mouret E, Kambouchner M, Nicolas A, Zafrani B, et al. Low expression of bcl-2 in Brca1-associated breast cancers. *Br J Cancer.* 2000; 83: 1318-22.
- Fu XJ, Shi XJ, Lin K, Lin H, Huang WH, Zhang GJ, et al. Environmental and DNA repair risk factors for breast cancer in South China. *Int J Hyg Environ Health.* 2015; 218(3): 313-8.
- Fu YP, Yu JC, Cheng TC, Lou MA, Hsu GC, Wu CY, et al. Breast cancer risk associated with genotypic polymorphism of the nonhomologous end-joining genes: a multigenic study on cancer susceptibility. *Cancer Res.* 2003; 63: 2440-6.
- Fricker SP. The therapeutic application of lanthanides. *Chem Soc Rev.* 2006; 35: 524-33.
- Fukushima H, Matsumoto A, Inuzuka H, Zhai B, Lau AW, Wan L, et al. SCF(Fbw7) modulates the NF $\kappa$ B signaling pathway by targeting NF $\kappa$ B2 for ubiquitination and destruction. *Cell Rep.* 2012; 1: 434-43.
- Gaiddon C, Jeannequin P, Bischoff P, Pfeffer M, Sirlin C, Loeffler JP. Ruthenium (II)-derived organometallic compounds induce cytostatic and cytotoxic effects on mammalian cancer cell lines through p53-dependent and p53-independent mechanisms. *J Pharmacol Exp Ther.* 2005; 315: 1403-11.
- Galanski M, Arion VB, Jakupec MA, Keppler BK. Recent developments in the field of tumor-inhibiting metal complexes. *Curr Pharm Des.* 2003; 9: 2078-89.
- Gamsjaeger R, Liew CK, Loughlin FE, Crossley M, Mackay JP. Sticky fingers: zinc-fingers as protein-recognition motifs. *Trends Biochem Sci.* 2007; 32: 63-70.
- Ganeshpandian M, Loganathan R, Suresh E, Riyasdeen A, Akbarsha MA, Palaniandavar M. New ruthenium(II) arene complexes of anthracenyl-appended diazacycloalkanes: effect of ligand intercalation and hydrophobicity on DNA and protein binding and cleavage and cytotoxicity. *Dalton Trans.* 2014; 43: 1203-19.
- Garcia-Closas M, Brinton LA, Lissowska J, Chatterjee N, Peplonska B, Anderson WF et al. Established breast cancer risk factors by clinically important tumour characteristics. *Br J Cancer.* 2006; 95: 123-9.
- Gava B, Zorzet S, Spessotto P, Cocchietto M, Sava G. Inhibition of B16 melanoma metastases with the ruthenium complex imidazolium trans-imidazoledimethylsulfoxide-tetrachlororuthenate and down-regulation of tumor cell invasion. *J Pharmacol Exp Ther.* 2006; 317: 284-91.
- Gaynor D, Griffith DM. The prevalence of metal-based drugs as therapeutic or

- diagnostic agents: beyond platinum. *Dalton Trans.* 2012; 41: 13239-57.
- Goka ET, Lippman ME. Loss of the E3 ubiquitin ligase HACE1 results in enhanced Rac1 signaling contributing to breast cancer progression. *Oncogene.* 2015; 34: 5395-405.
- Gelmon KA, Tischkowitz M, Mackay H, Swenerton K, Robidoux A, Tonkin K, et al. Olaparib in patients with recurrent high-grade serous or poorly differentiated ovarian carcinoma or triple-negative breast cancer: a phase 2, multicentre, open-label, non-randomised study. *Lancet Oncol.* 2011; 12: 852-61.
- Gnerlich JL, Deshpande AD, Jeffe DB, Sweet A, White N, Margenthaler JA. Elevated breast cancer mortality in women younger than age 40 years compared with older women is attributed to poorer survival in early-stage disease. *J Am Coll Surg.* 2009; 208: 341-7.
- Gopal YN, Chanchorn E, VanDyke MW. Parthenolide promotes the ubiquitination of MDM2 and activates p53 cellular functions. *Mol Cancer Ther.* 2009; 8: 552-62.
- Gough CA, Gojobori T, Imanishi T. Cancer-related mutations in BRCA1-BRCT cause long-range structural changes in protein-protein binding sites: a molecular dynamics study. *Proteins.* 2007; 66: 69-86.
- Grasberger BL, Lu T, Schubert C, Parks DJ, Carver TE, Koblish HK, et al. Discovery and cocrystal structure of benzodiazepinedione HDM2 antagonists that activate p53 in cells. *J Med Chem.* 2005; 48: 909-12.
- Greenfield NJ. Using circular dichroism spectra to estimate protein secondary structure. *Nat Protoc.* 2006; 1: 2876-90.
- Groessl M, Hartinger CG, Połec-Pawlak K, Jarosz M, Dyson PJ, Keppler BK. Elucidation of the Interactions of an anticancer ruthenium complex in clinical trials with biomolecules utilizing capillary electrophoresis hyphenated to inductively coupled plasma-mass spectrometry. Short communication. *Chem Biodiver.* 2008; 5: 1609-14.
- Groessl M, Terenghi M, Casini A, Elvir L, Lobinski R, Dyson PJ. Reactivity of anticancer metallodrugs with serum proteins: new insights from size exclusion chromatography-ICP-MS and ESI-MS. *J Anal At Spectrom.* 2010; 25: 305-13.
- Guidi F, Modesti A, Landini I, Nobili S, Mini E, Bini L. et al. The molecular mechanisms of antimetastatic ruthenium compounds explored through DIGE proteomics. *J Inorg Biochem.* 2013; 118: 94-9.
- Gudmundsdottir K, Ashworth A. The roles of BRCA1 and BRCA2 and associated proteins in the maintenance of genomic stability. *Oncogene.* 2006; 25: 5864-74.
- Guo W, Zheng W, Luo Q, Li X, Zhao Y, Xiong S. et al. Transferrin serves as a mediator to deliver organometallic ruthenium(II) anticancer complexes into cells. *Inorg Chem.* 2013; 52: 5328-38.
- Hall J, Lee M, Newman B, Morrow J, Anderson L, Huey B, King M. Linkage of early-onset familial breast cancer to chromosome 17q21. *Science.* 1990; 250: 1684-9.
- Hajji L, Jara-Pérez V, Saraiba-Bello C, Segovia-Torrente G, Serrano-Ruiz M, Romerosa A. Synthesis, characterization, X-ray structural determination and theoretical study of the complexes [RuCp(8MTT-κS)LL'] (8MTT = 8-

- methylthio-theophyllinate; L,L' = PTA, mPTA; L = mPTA, L' = PPh<sub>3</sub>; PTA = 1,3,5-triaza-7-phosphaadamantane, mPTA = N-methyl-1,3,5-triaza-7-phosphaadamantane). *Inorg Chim Acta*. 2017; 455: 557-67.
- Hardcastle IR, Ahmed SU, Atkins H, Calvert AH, Curtin NJ, Farnie G, et al. Isoindolinone-based inhibitors of the MDM2-p53 protein-protein interaction. *Bioorg Med Chem Lett*. 2005; 15: 1515-20.
- Harkin DP, Bean JM, Miklos D, Song YH, Truong VB, Englert C. Induction of GADD45 and JNK/SAPK-dependent apoptosis following inducible expression of BRCA1. *Cell*. 1999; 97: 575-86.
- Harper JW, King RW. Stuck in the middle: drugging the ubiquitin system at the e2 step. *Cell*. 2011; 145: 1007-9.
- Harte MT, Gorski JJ, Savage KI, Purcell JW, Barros EM, Burn PM. NF- $\kappa$ B is a Critical Mediator of BRCA1 induced Chemoresistance. *Oncogene*. 2014; 33: 713-23.
- Hartinger CG, Casini A, Duhot C, Tsybin YO, Messori L, Dyson PJ. Stability of an organometallic ruthenium-ubiquitin adduct in the presence of glutathione: relevance to antitumour activity. *J Inorg Biochem*. 2008; 102: 2136-41.
- Hartinger CG, Zorbas-Seifried S, Jakupec MA, Kynast B, Zorbas H. From bench to bedside-preclinical and early clinical development of the anticancer agent indazolium *trans*-[tetrachloro-bis(1*H*-indazole)ruthenate(III)] (KP1019 or FFC<sub>14</sub>A). *J Inorg Biochem*. 2006; 100: 891-904.
- Hartwig A, Blessing H, Schwerdtle T, Walter I. Modulation of DNA repair processes by arsenic and selenium compounds. *Toxicology*. 2003; 193: 161-9.
- Hashizume R, Fukuda M, Maeda I, Nishikawa H, Oyake D, Yabuki Y, Ogata H, Ohta T. The RING heterodimer BRCA1-BARD1 is a ubiquitin ligase inactivated by a breast cancer-derived mutation. *EMBO J*. 2001; 276: 14537-40.
- Hastak K, Alli E, Ford JM. Synergistic chemosensitivity of triple-negative breast cancer cell lines to poly(ADP-Ribose) polymerase inhibition, gemcitabine, and cisplatin. *Cancer Res*. 2010; 70: 7970-80.
- Haupt Y, Maya R, Kazaz A, Oren M. Mdm2 promotes the rapid degradation of p53. *Nature*. 1997; 387: 296-9.
- Hecht SS. Tobacco smoke carcinogens and breast cancer. *Environ Mol Mutagen*. 2002; 39: 119-26.
- Herman AG, Hayano M, Poyurovsky MV, Shimada K, Skouta R, Prives C. Discovery of Mdm2-MdmX E3 Ligase Inhibitors Using a Cell-Based Ubiquitination Assay. *Cancer Discov*. 2011; 1: 312-25.
- Hicke L, Dunn R. Regulation of membrane protein transport by ubiquitin and ubiquitin-binding proteins. *Annu Rev Cell Dev Biol*. 2003; 19: 141-72.
- Hochstrasser M. Origin and function of ubiquitin-like proteins. *Nature*. 2009; 458: 422-9.
- Hoeller D, Dikic I. Targeting the ubiquitin system in cancer therapy. *Nature*. 2009; 458: 438-44.
- Hongthong K, Ratanaphan A. BRCA1-Associated Triple-Negative Breast Cancer and Potential Treatment for Ruthenium-Based Compounds. *Curr Cancer Drug Targets*. 2016; 16: 606-617.

- Honma M, Hayashi M, Hackman P, Sofuni T. Chlorambucil-induced structural changes in the gpt gene of AS 52 cells. *Mutat Res Toxicol Environ Mutagen*. 1997; 389: 199-205.
- Horwitz AA, Affar EB, Heine GF, Shi Y, Parvin JD. A mechanism for transcriptional repression dependent on the BRCA1 E3 ubiquitin ligase. *Proc Natl Acad Sci USA*. 2007; 104: 6614-9.
- Hosoya N, Miyagawa K. Targeting DNA damage response in cancer therapy. *Cancer Sci*. 2014; 105: 370-88.
- Howlander N, Noone AM, Krapcho M, Garshell J, Miller D, Altekruse SF, et al. SEER Cancer Statistics Review, 1975-2012. April 2015. Bethesda, MD: National Cancer Institute, 2015. [https://seer.cancer.gov/archive/csr/1975\\_2012/](https://seer.cancer.gov/archive/csr/1975_2012/)
- Hu C, Li X, Wang W, Zhang L, Tao L, Dong X, et al. Design, synthesis, and biological evaluation of imidazoline derivatives as p53-MDM2 binding inhibitors. *Bioorg Med Chem*. 2011; 19: 5454-61.
- Huang HC, Way TD, Lin CL, Lin JK. EGCG stabilizes p27kip1 in E2 stimulated MCF-7 cells through down-regulation of the Skp2 protein. *Endocrinology*. 2008; 149: 5972-83.
- Huang HL, Weng HY, Wang LQ, Yu CH, Huang QJ, Zhao PP, et al. Triggering Fbw7-mediated proteasomal degradation of c-Myc by oridonin induces cell growth inhibition and apoptosis. *Mol Cancer Ther*. 2012; 11: 1155-65.
- Huestis J, Zhou X, Chen L, Feng C, Hudson LG, Liu KJ. Kinetics and thermodynamics of zinc (II) and arsenic (III) binding to XPA and PARP-1 zinc finger peptides. *J Inorg Biochem*. 2016; 163: 45-52.
- Husain A, He G, Venkatraman ES, Spriggs DR. BRCA1 up-regulation is associated with repair-mediated resistance to cis-diamminedichloroplatinum (II). *Cancer Res*. 1998; 58: 1120-3.
- Hussain M, Carducci MA, Slovin S, Cetnar J, Qian J, Mc Keegan EM, et al. Targeting DNA repair with combination veliparib (ABT-888) and temozolomide in patients with metastatic castration-resistant prostate cancer. *Invest New Drugs*. 2014; 32: 904-12.
- Hutchins JR, Clarke PR. Many fingers on the mitotic trigger: post-translational regulation of the Cdc25C phosphatase. *Cell Cycle*. 2004; 3: 41-5.
- Ibrahim YH, Garcia-Garcia C, Serra V, He L, Torres-Lockhart K, Prat A, et al. PI3K inhibition impairs BRCA1/2 expression and sensitizes BRCA-proficient triple-negative breast cancer to PARP inhibition. *Cancer Discov*. 2012; 2: 1036-47.
- Ilari A, Baiocco P, Messori L, Fiorillo A, Boffi A, Gramiccia M. A gold-containing drug against parasitic polyamine metabolism: the X-ray structure of trypanothione reductase from *Leishmania infantum* in complex with auranofin reveals a dual mechanism of enzyme inhibition. *Amino Acids*. 2012; 42: 803-11.
- Inuzuka H, Shaik S, Onoyama I, Gao D, Tseng A, Maser RS, et al. SCF(FBW7) regulates cellular apoptosis by targeting MCL1 for ubiquitylation and destruction. *Nature*. 2011; 471(7336): 104-9.
- Irminger-Finger I, Leung WC, Li J, Dubois-Dauphin M, Harb J, Feki A. et al. Identification of BARD1 as mediator between proapoptotic stress and p53-dependent apoptosis. *Mol Cell*. 2001; 8:1255-66.

- Irminger-Finger I, Ratajska M, Pilyugin M. New concepts on BARD1: Regulator of BRCA pathways and beyond. *Int J Biochem Cell Biol.* 2016; 72:1-17.
- Irminger-Finger I, Siegel BD, Leung WC. The functions of breast cancer susceptibility gene 1 (BRCA1) product and its associated proteins. *Biol Chem.* 1999; 380: 117-28.
- Isakoff S, Mayer EL, He L, Traina TA, Carey LA, Krag KJ, et al. TBCRC009: A multicenter phase II clinical trial of platinum monotherapy with biomarker assessment in metastatic triple-negative breast cancer. *J Clin Oncol.* 2015; 33: 1902-9.
- Isakoff SJ, Overmoyer B, Tung NM, Gelman RS, Giranda VL, Bernhard KM, et al. A phase II trial of the PARP inhibitor veliparib (ABT888) and temozolomide for metastatic breast cancer. *J Clin Oncol.* 2010; 28: 1019.
- Issaeva N, Bozko P, Enge M, Protopopova M, Verhoef LG, Masucci M, et al. Selivanova, Small molecule RITA binds to p53, blocks p53-HDM-2 interaction and activates p53 function in tumors. *Nat Med.* 2004; 10: 1321-8.
- Jacques A, Lebrun C, Casini A, Kieffer I, Proux O, Latour JM. Reactivity of Cys4 zinc finger domains with gold (III) complexes: insights into the formation of "gold fingers". *Inorg Chem.* 2015; 54: 4104-13.
- Jakupec MA, Galanski M, Arion VB, Hartinger CG, Keppler BK. Antitumour metal compounds: More than theme and variations. *Dalton Trans.* 2008; 14: 183-94.
- Jakupec MA, Reisner E, Eichinger A, Pongratz M, Arion VB, Galanski M, et al. Redox-active antineoplastic ruthenium complexes with indazole: correlation of *in vitro* potency and reduction potential. *J Med Chem.* 2005; 48: 2831-7.
- Jayatunga MK, Thompson S, McKee TC, Chan MC, Reece KM, Hardy AP, et al. Inhibition of the HIF1 $\alpha$ -p300 interaction by quinone- and indandione-mediated ejection of structural Zn(II). *Eur J Med Chem.* 2015; 94: 509-16.
- Jenkins LM, Byrd JC, Hara T, Srivastava P, Mazur SJ, Stahl SJ, et al. 2005. Studies on the mechanism of inactivation of the HIV-1 nucleocapsid protein NCp7 with 2-mercaptobenzamide thioesters. *J Med Chem.* 48: 2847-58.
- Jennerwein MM, Eastman A. A polymerase chain reaction-based method to detect cisplatin adducts in specific genes. *Nucleic Acids Res.* 1991; 19: 6209-14.
- Jézéquel P, Loussouarn D, Guérin-Charbonnel C, Campion L, Vanier A, Gouraud W. Gene-expression molecular subtyping of triple-negative breast cancer tumours: importance of immune response. *Breast Cancer Res.* 2015; 17: 43.
- Jiang J, Thyagarajan-Sahu A, Krchnak V, Jedinak A, Sandusky GE, Sliva D. NAHA, a novel hydroxamic acid-derivative, inhibits growth and angiogenesis of breast cancer in vitro and in vivo. *PLoS One.* 2012; 7: e34283.
- Jiang J, Sliva D. Novel medicinal mushroom blend suppresses growth and invasiveness of human breast cancer cells. *Int J Oncol.* 2010; 37: 1529-36.
- Jiang J, Jedinak A, Sliva D. Ganodermanontriol (GDNT) exerts its effect on growth and invasiveness of breast cancer cells through the down-regulation of CDC20 and uPA. *Biochem Biophys Res Commun.* 2011; 415: 325-9.
- Johannsson O, Ostermeyer EA, Hakansson S, Friedman LS, Johannsson U, Sellberg G, et al. Founding BRCA1 mutations in hereditary breast and ovarian cancer in southern Sweden. *Am J Hum Genet.* 1996; 58: 441-50.

- Johnson N, Cai D, Kennedy RD, Pathania S, Arora M, Li YC, et al. Cdk1 participates in BRCA1-dependent S phase checkpoint control in response to DNA damage. *Mol Cell*. 2009; 35: 327-39.
- Jordan P, Carmo-Fonseca M. Molecular mechanisms involved in cisplatin cytotoxicity. *Cell Mol Life Sci*. 2000; 57: 1229-35.
- Joukov V, Groen AC, Prokhorova T, Gerson R, White E, Rodriguez A. et al. The BRCA1/BARD1 heterodimer modulates ran-dependent mitotic spindle assembly. *Cell*. 2006; 127: 539-52.
- Kalb R, Mallery DL, Larkin C, Huang JT, Hiom K. BRCA1 is a histone-H2A-specific ubiquitin ligase. *Cell Rep*. 2014; 8: 999-1005.
- Kalinowski DP, Illenye S, Van Houten B. Analysis of DNA damage and repair in murine leukemia L1210 cells using a quantitative polymerase chain reaction assay. *Nucleic Acids Res*. 1992; 20: 3485-94.
- Kaluđerovic GN, Krajnovic T, Momcilovic M, Stosic-Grujicic S, Mijatovic S, Maksimović-Ivanić D. et al. Ruthenium (II) p-cymene complex bearing 2,2'-dipyridylamine targets caspase 3 deficient MCF-7 breast cancer cells without disruption of antitumor immune response. *J Inorg Biochem*. 2015; 153: 315-21.
- Kaminska M, Ciszewski T, Lopacka-Szatan K, Miotła P, Starosławska E. Breast cancer risk factors. *Prz Menopauzalny*. 2015; 14: 196-202.
- Kapitza S, Pongratz M, Jakupec MA, Heffeter P, Berger W, Lackinger L, Keppler B. K. and Marian, B. Heterocyclic complexes of ruthenium (III) induce apoptosis in colorectal carcinoma cells. *J Cancer Res Clin Oncol*. 2005; 131: 101-10.
- Kang B, Sun XH. Regulation of cancer stem cells by RING finger ubiquitin ligases. *Stem Cell Investig*. 2014; 1: 5.
- Katiyar P, Ma Y, Riegel A, Fan S, Rosen EM. Mechanism of BRCA1-Mediated Inhibition of Progesterone Receptor Transcriptional Activity. *Mol Endocrinol*. 2009; 23: 1135-46.
- Kaufman B, Shapira-Frommer R, Schmutzler RK, Audeh MW, Friedlander M, Balmana J, et al. Olaparib monotherapy in patients with advanced cancer and a germline BRCA1/2 mutation. *J Clin Oncol*. 2015; 33: 244-50.
- Kaye SB, Lubinski J, Matulonis U, Ang JE, Gourley C, Karlan BY, et al. Phase II, openlabel, randomized, multicenter study comparing the efficacy and safety of olaparib, a poly (ADP-ribose) polymerase inhibitor, and pegylated liposomal doxorubicin in patients with BRCA1 or BRCA2 mutations and recurrent ovarian cancer. *J Clin Oncol*. 2012; 30: 372-9.
- Kelley MR, Fishel ML. DNA repair proteins as molecular targets for cancer therapeutics. *Anticancer Agents Med Chem*. 2008; 8: 417-25.
- Kelley TJ, Moghaddas S, Bose R, Basu S. Inhibition of immunopurified DNA polymerase-alpha from PA-3 prostate tumor cells by platinum (II) antitumor drugs. *Cancer Biochem Biophys*. 1993; 13: 135-46.
- Kerr P, Ashworth A. New complexities for BRCA1 and BRCA2. *Curr Biol*. 2001; 11: R668-76.
- Key TJ, Verkasalo PK, Banks E. Epidemiology of breast cancer. *Lancet Oncol*. 2001; 2: 133-40.

- Khan OA, Gore M, Lorigan P, Stone J, Greystoke A, Burke W, et al. A phase I study of the safety and tolerability of olaparib (AZD2281, KU0059436) and dacarbazine in patients with advanced solid tumours. *Br J Cancer*. 2011; 104: 750-5.
- Khoury K, Domling A. P53 mdm2 inhibitors. *Curr Pharm Des*. 2012; 18: 4668-78.
- Kilpina KJ, Dyson PJ. Enzyme inhibition by metal complexes: concepts, strategies and applications. *Chem Sci*. 2013; 4: 1410-9.
- Kim H, Huang J, Chen J. CCDC98 is a BRCA1-BRCT domain-binding protein involved in the DNA damage response. *Nat Struct Mol Biol*. 2007; 14: 710-5.
- Kim HS, Li H, Cevher M, Parmelee A, Fonseca D, Kleiman FE et al. DNA damage-induced BARD1 phosphorylation is critical for the inhibition of messenger RNA processing by BRCA1/BARD1 complex. *Cancer Res*. 2006; 66: 4561-5.
- Kim MY, Woo EM, Chong YT, Homenko DR, Kraus WL. Acetylation of estrogen receptor alpha by p300 at lysines 266 and 268 enhances the deoxyribonucleic acid binding and transactivation activities of the receptor. *Mol Endocrinol*. 2006; 20: 1479-93.
- Koepp DM, Schaefer LK, Ye X, Keyomarsi K, Chu C, Harper JW, et al. Phosphorylation-dependent ubiquitination of cyclin E by the SCFFbw7 ubiquitin ligase. *Science*. 2001; 294: 173-7.
- Kristeleit R, Shapira-Frommer R, Burris H, Patel MR, Lorusso P, Oza AM, et al. Phase 1/2 study of oral rucaparib: updated phase 1 and preliminary phase 2 results. *Ann Oncol*. 2014; 25: iv307-8.
- Kristeleit R, Swisher E, Oza A, Coleman R, Scott C, Konecny G, et al. Final results of ARIEL2 (Part 1): a phase 2 trial to prospectively identify ovarian cancer (OC) responders to rucaparib using tumor genetic analysis. *Eur Cancer Congr*. 2015; 51: s531.
- Krum SA, la Rosa Dalugdugan Ed, Miranda-Carboni GA, Lane TF. BRCA1 Forms a Functional Complex with -H2AX as a Late Response to Genotoxic Stress. *J Nucleic Acids*. 2010; pii: 801594.
- Kummar S, Chen A, Ji J, Zhang Y, Reid JM, Ames M, et al. Phase I study of PARP inhibitor ABT-888 in combination with topotecan in adults with refractory solid tumors and lymphomas. *Cancer Res*. 2011; 71: 5626-34.
- Kummar S, Ji J, Morgan R, Lenz HJ, Puhalla SL, Belani CP, et al. A phase I study of veliparib in combination with metronomic cyclophosphamide in adults with refractory solid tumors and lymphomas. *Clin Cancer Res*. 2012; 18: 1726-34.
- Lane TF. BRCA1 and transcription. *Cancer Biol Ther*. 2004; 3: 528-33.
- Ledermann J, Harter P, Gourley C, Friedlander M, Vergote I, Rustin G, et al. Olaparib maintenance therapy in patients with platinum-sensitive relapsed serous ovarian cancer: a preplanned retrospective analysis of outcomes by BRCA status in a randomised phase 2 trial. *Lancet Oncol*. 2014; 15: 852-61.
- Lee JM, Hays JL, Annunziata CM, Noonan AM, Minasian L, Zujewski JA, et al. Phase I/Ib study of olaparib and carboplatin in BRCA1 or BRCA2 mutation-associated breast or ovarian cancer with biomarker analyses. *J Natl Cancer Inst*. 2014; 106: dju089.



- Lee JS, Collins KM, Brown AL, Lee CH, Chung JH. hCds1-mediated phosphorylation of BRCA1 regulates the DNA damage response. *Nature*. 2000; 404: 201-4.
- Lee SY, Kim MT, Kim SW, Song MS, Yoon SJ. Effect of lifetime lactation on breast cancer risk: a Korean women's cohort study. *Int J Cancer*. 2003; 105: 390-3.
- Lei X, Johnson RP, Porco JA. Total synthesis of the ubiquitin-activating enzyme inhibitor (+)-panepophenanthrin, *Angew Chem Int Ed Engl*. 2003; 42:3913-7.
- Liedtke C, Mazouni C, Hess KR, André F, Tordai A, Mejia JA. et al. Response to neoadjuvant therapy and long-term survival in patients with triple-negative breast cancer. *J Clin Oncol*. 2008; 26: 1275-81.
- Leijen S, Burgers SA, Baas P, Pluim D, Tibben M, van Werkhoven E, et al. Phase I/II study with ruthenium compound NAMI-A and gemcitabine in patients with non-small cell lung cancer after first line therapy. *Invest New Drugs*. 2015; 33: 201-14.
- Levina A, Lay PA, Metal-based anti-diabetic drugs: advances and challenges. *Dalton Trans*. 2011; 40: 11675-86.
- Lew JQ, Freedman ND, Leitzmann MF, Brinton LA, Hoover RN, Hollenbeck AR, et al. Alcohol and risk of breast cancer by histologic type and hormone receptor status in postmenopausal women: the NIH-AARP Diet and Health Study. *Am J Epidemiol*. 2009; 170: 308-17.
- Li CI, Chlebowski RT, Freiberg M, Johnson KC, Kuller L, Lane D, et al. Alcohol consumption and risk of postmenopausal breast cancer by subtype: the women's health initiative observational study. *J Natl Cancer Inst*. 2010; 102: 1422-31.
- Li ML, Greenberg RA. Links between genome integrity and BRCA1 tumor suppression. *Trends Biochem Sci*. 2012; 37: 418-24.
- Li J, Lee D, Application of a tandem metathesis to the synthesis of (+)-panepophenanthrin, *Chem Asian J*. 2010; 5: 1298-302.
- Li D, Wang M, Firozi PF, Chang P, Zhang W, Baer-Dubowska W, et al. Characterization of a major aromatic DNA adduct detected in human breast tissues. *Environ Mol Mutagen*. 2002; 39: 193-200.
- Lips EH, Mulder L, Oonk A, van der Kolk LE, Hogervorst FBL, Imholz ALT. Triple-negative breast cancer: BRCAness and concordance of clinical features with BRCA1-mutation carriers. *Br J Cancer*. 2013; 108: 2172-7.
- Litton JK, Blum JL, Im YH, Martin M, Mina LA, Roche HH, et al. A phase 3, open-label, randomized, parallel, 2-arm international study of the oral PARP inhibitor talazoparib (BMN 673) in BRCA mutation subjects with locally advanced and/or metastatic breast cancer (EMBRACA). *J Clin Oncol*. 2015; 33: 15.
- Liu JF, Barry WT, Birrer M, Lee JM, Buckanovich RJ, Fleming GF, et al. Combination cediranib and olaparib versus olaparib alone for women with recurrent platinum-sensitive ovarian cancer: a randomised phase 2 study. *Lancet Oncol*. 2014; 15: 1207-14.
- Liu J, Pan Y, Ma B, Nussinov R. "Similarity trap" in protein-protein interactions could be carcinogenic: simulations of p53 core domain complexed with 53BP1 and BRCA1 BRCT domains. *Structure* 2006; 14: 1811-21.

- Liu J, Shaik S, Dai X, Wu Q, Zhou X, Wang Z, et al. Targeting the ubiquitin pathway for cancer treatment. *Biochim Biophys Acta*. 2015; 1855: 50-60.
- Liu JF, Tolaney SM, Birrer M, Fleming GF, Buss MK, Dahlberg SE, et al. A Phase 1 trial of the poly[ADP-ribose] polymerase inhibitor olaparib [DAZD2281] in combination with the anti-angiogenic cediranib [DAZD2171] in recurrent epithelial ovarian or triplenegative breast cancer. *Eur J Cancer*. 2013; 49: 2972-8.
- Lingle WL, Lutz WH, Ingle JN, Maihle NJ, Salisbury JL. Centrosome hypertrophy in human breast tumors: implications for genomic stability and cell polarity. *Proc Natl Acad Sci USA*. 1998; 95: 2950-5.
- Lochab S, Pal P, Kapoor I, Kanaujya JK, Sanyal S, Behre G, et al. E3 ubiquitin ligase Fbw7 negatively regulates granulocytic differentiation by targeting G-CSFR for degradation, *Biochim Biophys Acta*. 2013; 1833: 2639-52.
- Loo JA, Holler TP, Sanchez J, Gogliotti R, Maloney L, Reilly MD. Biophysical characterization of zinc ejection from HIV nucleocapsid protein by anti-HIV 2, 2-dithiobis [benzamides] and benzisothiazolones. *J Med Chem*. 1996; 39: 4313-20.
- Lord CJ, Ashworth A. BRCAness revisited. *Nat Rev Cancer*. 2016; 16: 110-20.
- LoRusso PM, Li J, Burger A, Heilbrun LK, Sausville EA, Boerner SA, et al. Phase I safety, pharmacokinetic, and pharmacodynamic study of the poly (ADP-ribose) polymerase (PARP) inhibitor veliparib (ABT-888) in combination with irinotecan in patients with advanced solid tumors. *Clin Cancer Res*. 2016; 22: 3227-37.
- Lotti LV, Ottini L, D'Amico C, Gradini R, Cama A, Belleudi F. et al. Subcellular localization of the BRCA1 gene product in mitotic cells. *Genes Chromosomes Cancer*. 2002; 35: 193-203.
- Liu Y, Colditz GA, Rosner B, Berkey CS, Collins LC, Schnitt SJ, et al. Alcohol intake between menarche and first pregnancy: a prospective study of breast cancer risk. *J Natl Cancer Inst*. 2013; 105: 1571-8.
- Liu Y, Mallampalli RK. Small molecule therapeutics targeting F-box proteins in cancer. *Semin Cancer Biol*. 2016; 36: 105-19.
- Liu G, Yang D, Sun Y, Shmulevich I, Xue F, Sood AK. et al. Differing clinical impact of BRCA1 and BRCA2 mutations in serous ovarian cancer. *Pharmacogenomics*. 2012; 13: 1523-35.
- Lu SY, Jiang YJ, Zou JW, Wu TX. Molecular modeling and molecular dynamics simulation studies on pyrrolopyrimidine-based alpha-helix mimetic as dual inhibitors of MDM2 and MDMX. *J Mol Graph Model*. 2011; 30: 167-78.
- Lub S, Maes K, Menu E, De Bruyne E, Vanderkerken D, van Valckenborgh V. Novel strategies to target the ubiquitin proteasome system in multiple myeloma. *Oncotarget*. 2016; 7: 6521-37.
- Ma J, Cheng L, Liu H, Zhang J, Shi Y, Zeng F, et al. Genistein down-regulates miR-223 expression in pancreatic cancer cells. *Curr Drug Targets*. 2013; 14: 1150-6.
- Ma Y, Fan S, Hu C, Meng Q, Fuqua SA, Pestell RG, et al. BRCA1 regulates acetylation and ubiquitination of estrogen receptor-alpha. *Mol endocrinol*. 2010 24: 76-90.
- Ma Y, Katiyar P, Jones LP, Fan S, Zhang Y, Furth PA, et al. The breast cancer

- susceptibility gene BRCA1 regulates progesterone receptor signaling in mammary epithelial cells. *Mol endocrinol.* 2006; 20: 14-34.
- MacLachlan TK, Somasundaram K, Sgagias M, Shifman Y, Muschel RJ, Cowan KH, et al. BRCA1 effects on the cell cycle and the DNA damage response are linked to altered gene expression. *J Biol Chem.* 2000; 275: 2777-85.
- Maksimenko J, Irmejs A, Nakazawa-Miklasevica M, Mebard-Gorkusa I, Trofimovics G, Gardovskis J, et al. Prognostic role of BRCA1 mutation in patients with triple-negative breast cancer. *Onco Lett.* 2014; 7: 278-84.
- Mallampalli RK, Coon TA, Glasser JR, Wang C, Dunn SR, Weathington NM, et al. Targeting F box protein Fbxo3 to control cytokine-driven inflammation. *J Immunol.* 2013; 191: 5247-55.
- Mallery DLJ, Vandenberg C, Hiom K. Activation of the E3 ligase function of the BRCA1/BARD1 complex by polyubiquitin chains. *EMBO J.* 2002; 21: 6755- 62.
- Mao JH, Kim IJ, Wu D, Climent J, Kang HC, DelRosario R, et al. FBXW7 targets mTOR for degradation and cooperates with PTEN in tumor suppression, *Science.* 2008; 321: 1499-502.
- Manisto S, Virtanen M, Kataja V, Uusitupa M, Pietinen P. Lifetime alcohol consumption and breast cancer: a case-control study in Finland. *Public Health Nutr.* 2000; 3: 11-8.
- Martin AM, Blackwood MA, Antin-Ozerkis D, Shih HA, Calzone K, Colligon TA, et al. Germline mutations in BRCA1 and BRCA2 in breast-ovarian families from a breast cancer risk evaluation clinic. *J Clin Oncol.* 2001 19: 2247-53.
- Mark WY, Jack C. C. Liao, Ying Lu, Ayeda Ayed, Rob Laister et al. Characterization of Segments from the Central Region of BRCA1: An Intrinsically Disordered Scaffold for Multiple Protein-Protein and Protein-DNA Interactions? *J Mol Biol.* 2005; 345: 275-87.
- Masutani M, Nozaki T, Nakamoto K, Nakagama H, Suzuki H, Kusuoka O, et al. The response of Parp knockout mice against DNA damaging agents. *Mutat Res.* 2000; 462: 159-66.
- Matthews JM, Kowalski K, Liew CK, Sharpe BK, Fox AH, Crossley M. A class of zinc fingers involved in protein-protein interactions biophysical characterization of CCHC fingers from fog and U-shaped. *Eur J Biochem.* 2000; 267: 1030-8.
- Matthews JM, Sunde M. Zinc fingers-folds for many occasions *IUBMB Life.* 2002; 54, 351-5.
- Mateo J, Carreira S, Sandhu S, Miranda S, Mossop H, Perez-Lopez R, et al. DNA-repair defects and olaparib in metastatic prostate cancer. *N Engl J Med.* 2015; 373: 1697-708.
- Matsuzawa M, Kakeya H, Yamaguchi J, Shoji M, Onose R, Osada H, et al. Enantio- and diastereoselective total synthesis of (+)-panepophenanthrin, a ubiquitin-activating enzyme inhibitor, and biological properties of its new derivatives. *Chem Asian J.* 2006; 1: 845-51.
- Maurmann L, Bose RN. Unwinding of zinc finger domain of DNA polymerase I by cis-diamminedichloroplatinum (II). *Dalton Trans.* 2010; 39: 7968-79.
- Mavaddat N, Antoniou AC, Easton DF, Garcia-Closas M. Genetic susceptibility to breast cancer. *Mol Oncol.* 2010; 4: 174-91.

- McNeish IA, Oza AM, Coleman RL, Scott CL, Konecny GE, Tinker A, et al. Results of ARIEL2: a phase 2 trial to prospectively identify ovarian cancer patients likely to respond to rucaparib using tumor genetic analysis. *J Clin Oncol*. 2015; 33: 5508.
- Medici S, Peana M, Nurchi VM, Lachowicz JI, Crisponi G, Zoroddu MA. Noble metals in medicine: Latest advances. *Coord Chem Rev*. 2015; 284: 329-50.
- Mehmood RK. Review of Cisplatin and Oxaliplatin in Current Immunogenic and Monoclonal Antibody Treatments. *Oncol Rev*. 2014; 8: 256.
- Melchart M, Habtemariam A, Parsons S, Sadler PJ. Chlorido-, aqua-, 9-ethylguanine- and 9-ethyladenine-adducts of cytotoxic ruthenium arene complexes containing O,O-chelating ligands. *J Inorg Biochem*. 2007; 101: 1903-12.
- Mendes F, Groessl M, Nazarov AA, Tsybin YO, Sava G, Santos I, et al. Metal-based inhibition of poly(ADP-ribose) polymerase, the guardian angel of DNA. *J Med Chem*. 2011; 54: 2196-206.
- Merlino A. Interactions between proteins and Ru compounds of medicinal interest: A structural perspective. *Coord Chem Rev*. 2016; 326: 111-34.
- Messick TE, Greenberg RG. The ubiquitin landscape at DNA double-strand breaks. *J Cell Biol*. 2009; 187: 319-26.
- Messori L, Orioli P, Vullo D, Alessio E, Lengo E. A spectroscopic study of the reaction of NAMI, a novel ruthenium (III) anti-neoplastic complex, with bovine serum albumin. *Eur J Biochem*. 2000; 267: 1206-13.
- Michalek JL, Besold AN, Michel SL. Cysteine and histidine shuffling: mixing and matching cysteine and histidine residues in zinc finger proteins to afford different folds and function. *Dalton Trans*. 2011; 40: 12619-32.
- Michels J, Vitale I, Saparbaev M, Castedo M, Kroemer G. Predictive biomarkers for cancer therapy with PARP inhibitors. *Oncogene*. 2014; 33: 3894-907.
- Michelucci E, Pieraccini G, Moneti G, Gabbiani C, Pratesi A, Messori L. Mass spectrometry and metallomics: A general protocol to assess stability of metallodrug-protein adducts in bottom-up MS experiments. *Talanta*. 2017; 167: 30-38.
- Miki Y, Swensen J, Shattuck-Eidens D, Futreal PA, Harshman K, Tavtigian S, et al. A strong candidate for the breast and ovarian cancer susceptibility gene BRCA1. *Science*. 1994; 266: 66-71.
- Miller RE, Ledermann JA. The Status of poly (adenosine diphosphateRibose) polymerase (PARP) inhibitors in ovarian cancer, Part 2: extending the scope beyond olaparib and BRCA1/2 mutations. *Clin Adv Hematol Oncol*. 2016; 14: 704-11.
- Mirza MR, Monk BJ, Herrstedt J, Oza AM, Mahner S, Redondo A. Niraparib maintenance therapy in platinum-sensitive, recurrent ovarian cancer. *N Engl J Med*. 2016; 375: 2154-64.
- Moberg K, Mukherjee A, Veraksa A, Artavanis-Tsakonas S, Hariharan IK. The *Drosophila* F box protein archipelago regulates dMyc protein levels in vivo. *Curr Biol*. 2004; 14: 965-74.
- Molife LR, Roxburgh P, Wilson RH, Gupta A, Middleton MR, Evans TRJ, et al. A phase I study of oral rucaparib in combination with carboplatin. *J Clin Oncol*. 2013; 31: 2586.
- Monteiro ANA, BRCA1: exploring the links to transcription. *Trends Biochem Sci*.

- 2000; 25: 469-74.
- Montani M, Pazmay GV, Hysi A, Lupidi G, Pettinari R, Gambini V. The water soluble ruthenium(II) organometallic compound [Ru(p-cymene)(bis(3,5 dimethylpyrazol-1-yl)methane)Cl]Cl suppresses triple negative breast cancer growth by inhibiting tumor infiltration of regulatory T cells. *Pharmacol Res.* 2016; 107: 282-90.
- Moore KN, Zhang ZY, Agarwal S, Patel MR, Burris HA, Martell RE, et al. Food effect substudy of a phase 3 randomized double-blind trial of maintenance with niraparib (MK4827), a poly(ADP)ribose polymerase (PARP) inhibitor versus placebo in patients with platinum-sensitive ovarian cancer. *ASCO Annual Meeting. Chicago, Illinois. J Clin Oncol.* 2014; 32: e16531.
- Morelli CMA, Ostuni A, Cristinziano PL, Tesaro D, Bavoso A. Interaction of cisplatin with a CCHC zinc finger motif. *J Pept Sci.* 2013; 19: 227-32.
- Morelli MAC, Ostuni A, Matassi G, Minichino C, Flagiello A, Pucci P. et al. Spectroscopic investigation of auranofin binding to zinc finger HIV-2 nucleocapsid peptides. *Inorganica Chim Acta.* 2016; 453: 330-8.
- Morris JR, Pangon L, Boutell C, Katagiri T, Keep NH, Solomon E. Genetic analysis of BRCA1 ubiquitin ligase activity and its relationship to breast cancer susceptibility. *Hum Mol Genet.* 2006; 15: 599-606.
- Moses JE, Commeiras L, Baldwin JE, Adlington RM. Total synthesis of panepophenanthrin. *Org Lett.* 2003; 5: 2987-8.
- Moynahan ME, Cui TY, Jasin M. Homology-directed DNA repair, mitomycin-c resistance, and chromosome stability is restored with correction of a Brcal mutation. *Cancer Res.* 2001; 61: 4842-50.
- Muggia F. Platinum compounds 30 years after the introduction of cisplatin: Implications for the treatment of ovarian cancer. *Gynecol Oncol.* 2009; 112: 275-81.
- Muggia F, Safra T, 'BRCAness' and its implications for platinum action in gynecologic cancer. *Anticancer Res.* 2014; 34: 551-6.
- Muhammad N, Guo Z. Metal-based anticancer chemotherapeutic agents. *Curr Opin Chem Biol.* 2014; 19: 144-53.
- Mullan PB, Quinn JE, Harkin DP. The role of BRCA1 in transcriptional regulation and cell cycle control. *Oncogene.* 2006; 25: 5854-63.
- Murray BS, Babak MV, Hartinger CG, Dyson PJ. The development of RAPTA compounds for the treatment of tumors. *Coord Chem Review.* 2016 306: 86-114.
- Naik R, Veldore VH, Gopinath KH. Genetics and breast cancer-oncologists perspectives. *Indian J Surg Oncol.* 2015; 6: 415-9.
- Namdarghanbari MA, Bertling J, Krezoski S, Petering DH. Toxic metal proteomics: Reaction of the mammalian zinc. *J Inorg Biochem.* 2014; 136: 115-21.
- Nangle S, Xing W, Zheng N. Crystal structure of mammalian cryptochrome in complex with a small molecule competitor of its ubiquitin ligase. *Cell Res.* 2013; 23: 1417-9.
- Naseem R, Sturdy A, Finch D, Jowitt T, Webb M. Mapping and conformational characterization of the DNA-binding region of the breast cancer susceptibility protein BRCA1. *Biochem J.* 2006; 395: 529-35.
- Nateri AS, Riera-Sans L, Da Costa C, Behrens A. The ubiquitin ligase SCFFbw7

- antagonizes apoptotic JNK signaling. *Science*. 2004; 303: 1374-8.
- Nazarov AA, Hartinger CG, Dyson PJ. Opening the lid on piano-stool complexes: An account of ruthenium (II)-arene complexes with medicinal applications. *J Organomet Chem*. 2014; 751: 251-60.
- Ndagi U, Mhlongo N, Soliman ME. Metal complexes in cancer therapy - an update from drug design perspective. *Drug Des Devel Ther*. 2017; 11: 599-616.
- Neve RM, Chin K, Fridlyand J, Yeh J, Baehner FL, Fevr T. A collection of breast cancer cell lines for the study of functionally distinct cancer subtypes. *Cancer Cell*. 2006; 10: 515-27.
- Nhukeaw T, Temboot P, Hansongnern K, Ratanaphan A. Cellular responses of BRCA1-defective and triple-negative breast cancer cells and in vitro BRCA1 interactions induced by metallo-intercalator ruthenium(II) complexes containing chloro-substituted phenylazopyridine, *BMC Cancer*. 2014; 7: 73.
- Nielsen TO, Hsu FD, Jensen K, Cheang M, Karaca G, Hu Z. et al. Immunohistochemical and clinical characterization of the basal-like subtype of invasive breast carcinoma. *Clin Cancer Res*. 2004; 10: 5367-74.
- Nichols HB, Trentham-Dietz A, Newcomb PA, Egan KM, Titus LJ, Hampton JM, et al. Pre-diagnosis oophorectomy, estrogen therapy and mortality in a cohort of women diagnosed with breast cancer. *Breast Cancer Res*. 2013; 15: R99.
- Nishikawa H, Ooka S, Sato K, Arima, K, Okamoto J, Klevit RE, et al. Mass spectrometric and mutational analyses reveal Lys-6-linked polyubiquitin chains catalyzed by BRCA1-BARD1 ubiquitin ligase. *J Biol Chem*. 2004; 279: 3916-24.
- Nishikawa H, Wu W, Koike A, Kojima R, Gomi H, Fukuda M. et al. BRCA1-associated protein 1 interferes with BRCA1/BARD1 RING heterodimer activity. *Cancer Res*. 2009; 69: 111-9.
- Novakova O, Chen H, Vrana O, Rodger A, Sadler PJ, Brabec V. DNA interactions of monofunctional organometallic ruthenium(II) antitumor complexes in cell-free media. *Biochemistry*. 2003; 42: 11544-54.
- O'Brien KA, Lemke SJ, Cocke KS, Rao RN, Beckmann RP. Casein kinase 2 binds to and phosphorylates BRCA1. *Biochem Biophys Res Commun*. 1999; 260: 658-64.
- O'Donovan PJ, Livingston DM. BRCA1 and BRCA2: breast/ovarian cancer susceptibility gene products and participants in DNA double-strand break repair. *Carcinogenesis*. 2010; 31: 961-7.
- Ogiwara H, Kohno T. CBP and p300 Histone Acetyltransferases Contribute to Homologous Recombination by Transcriptionally Activating the BRCA1 and RAD51 Genes. *PLoS One*. 2012; 7: e52810.
- Ohta T, Fukuda M. Ubiquitin and breast cancer. *Oncogene*. 2004; 23: 2079-88.
- Ohta T, Sato K, Wu W. The BRCA1 ubiquitin ligase and homologous recombination repair. *FEBS Lett*. 2011; 585: 2836-44.
- Ohta T, Wu W, Koike A, Asakawa H, Koizumi H, Fukuda M. Contemplating chemosensitivity of basal-like breast cancer based on BRCA1 dysfunction. *Breast Cancer*. 2009; 16: 268-74.
- Oommen D, Yiannakis D, Jha AN. BRCA1 deficiency increases the sensitivity of ovarian cancer cells to auranofin. *Mutat Res*. 2016; 784-785: 8-15.
- Orlicky S, Tang X, Neduva V, Elowe N, Brown ED, Sicheri F, et al. An allosteric

- inhibitor of substrate recognition by the SCF(Cdc4) ubiquitin ligase. *Nat Biotechnol.* 2010; 28: 733-7.
- Orelli BJ, Logsdon Jr JM Jr, Bishop DK. Bishop, Nine novel conserved motifs in BRCA1 identified by the chicken orthologue. *Oncogene.* 2001; 20: 4433-8.
- O'Shaughnessy J, Osborne C, Pippen JE, Yoffe M, Patt D, Rocha C, et al. Iniparib plus chemotherapy in metastatic triple-negative breast cancer. *N Engl J Med.* 2011; 364: 205-14.
- O'Shaughnessy J, Schwartzberg L, Danso MA, Miller KD, Rugo HS, Neubauer M, et al. Phase III study of iniparib plus gemcitabine and carboplatin versus gemcitabine and carboplatin in patients with metastatic triple-negative breast cancer. *J Clin Oncol.* 2014; 32: 3840-7.
- O'Sullivan Coyne G, Chen AP, Meehan R, Doroshow JH. PARP Inhibitors in Reproductive System Cancers: Current Use and Developments. *Drugs.* 2017; 77: 113-30.
- Ouchi M, Fujiuchi N, Sasai K, Katayama H, Minamishima YA, Ongusaha PP et al., BRCA1 phosphorylation by Aurora-A in the regulation of G2 to M transition. *J Biol Chem.* 2004; 279: 19643-8.
- Oza AM, Cibula D, Benzaquen AO, Poole C, Mathijssen RH, Sonke GS, et al. Olaparib combined with chemotherapy for recurrent platinum-sensitive ovarian cancer: a randomised phase 2 trial. *Lancet Oncol.* 2015; 16: 87-97.
- Pace NJ, Weerapana E. Zinc-Binding Cysteines: Diverse Functions and Structural Motifs. *Biomolecules.* 2014; 4: 419-34.
- Pageau GJ, Lawrence JB. BRCA1 foci in normal S-phase nuclei are linked to interphase centromeres and replication of pericentric heterochromatin. *J Cell Biol.* 2006; 175: 693-701.
- Palermo G, Magistrato A, Riedel T, von Erlach T, Davey CA, Dyson PJ. Fighting cancer with transition metal complexes: From naked DNA to protein and chromatin targeting strategies. *ChemMedChem.* 2016; 11: 1199-210.
- Pan Peng G, Hung WC, Lin SY. MRMonoubiquitination of H2AX protein regulates DNA damage response signaling. *J Biol Chem.* 2011; 286: 28599-607.
- Pannecouque C, Beata Szafarowicz, Natalia Volkova, Vasiliy Bakulev, Wim Dehaen, Yves Me'ly, Dirk Daelemans. Inhibition of HIV-1 Replication by a Bis-Thiadiazolbenzene-1, 2-Diamine That Chelates Zinc Ions from Retroviral Nucleocapsid Zinc Fingers. *Antimicrob Agents Chemother.* 2010; 54: 1461-8.
- Park SY, Kolonel LN, Lim U, White KK, Henderson BE, Wilkens LR. Alcohol consumption and breast cancer risk among women from five ethnic groups with light to moderate intakes: the Multiethnic Cohort Study. *Int J Cancer.* 2014; 134: 1504-10.
- Parvin JD. The BRCA1-dependent ubiquitin ligase,  $\gamma$ -tubulin, and centrosomes. *Environ Mol Mutagen.* 2009; 50: 649-53.
- Patel S, Player MR. Small-molecule inhibitors of the p53-HDM2 interaction for the treatment of cancer. *Expert Opin Invest Drugs.* 2008; 17: 1865-82.
- Patmasiriwat P, Bhothisuwan K, Sinilnikova OM, Chopin S, Methakijvaroon S, Badzioch M, et al. Analysis of breast cancer susceptibility genes BRCA1 and BRCA2 in Thai familial and isolated early-onset breast and ovarian cancer. *Human Mutat.* 2002; 20: 230-6.

- Paul TT, Cortez D, Bowers B, Elledge SJ, Gellert M. Direct DNA binding by Brca1. *Proc Natl Acad Sci USA*. 2001; 98: 6086-91.
- Peacock AFA, Sadler PJ. Medicinal organometallic chemistry: Designing metal arene complexes as anticancer agents. *Chem-Asian J*. 2008; 3: 1890-9
- Petroski MD, Zhou X, Dong G, Daniel-Issakani S, Payan DG, Huang J. Substrate modification with lysine 63-linked ubiquitin chains through the UBC13-UEV1A ubiquitin-conjugating enzyme. *J Biol Chem*. 2007; 282: 29936-45.
- Pettinari R, Marchetti F, Petrini A, Pettinari C, Lupidi G, Fernández B. et al. Ruthenium(II)-arene complexes with dibenzoylmethane induce apoptotic cell death in multiple myeloma cell lines. *Inorg Chim Acta*. 2017; 454: 139-48.
- Piccioli F, Sabatini S, Messori L, Orioli P, Hartinger CG, Keppler BK. A comparative study of adduct formation between the anticancer ruthenium(III) compound *HInd trans*-[RuCl<sub>4</sub>(Ind)<sub>2</sub>] and serum proteins. *J Inorg Biochem*. 2004; 98: 1135-42.
- Pishvaian MJ, Wang H, Zhuang T, He AR, Hwang JJ, Hankin A, et al. A phase I/II study of ABT-888 in combination with 5-fluorouracil (5-FU) and oxaliplatin (Ox) in patients with metastatic pancreatic cancer (MPC). *J Clin Oncol*. 2013; 31: 147.
- Pjura P, Matthews BW. Structures of randomly generated mutants of T4 lysozyme show that protein stability can be enhanced by relaxation of strain and by improved hydrogen bonding via bound solvent. *Protein Sci*. 1993; 2: 2226-32.
- Pluim D, van Waardenburg RC, Beijnen JH, Schellens JH. Cytotoxicity of the organic ruthenium anticancer drug NAMI-A is correlated with DNA binding in four different human tumor cell lines. *Cancer Chemother Pharmacol*. 2004; 54: 71-8.
- Plummer R, Jones C, Middleton M, Wilson R, Evans J, Olsen A, et al. Phase I. study of the poly (ADP-ribose) polymerase inhibitor, AG014699, in combination with temozolomide in patients with advanced solid tumors. *Clin Cancer Res*. 2008; 14: 7917-23.
- Plummer R, Lorigan P, Steven N, Scott L, Middleton MR, Wilson RH, et al. A phase II study of the potent PARP inhibitor, Rucaparib (PF-01367338, AG014699), with temozolomide in patients with metastatic melanoma demonstrating evidence of chemopotential. *Cancer Chemother Pharmacol*. 2013; 71:1191-9.
- Plummer R, Stephens P, Aissat-Daudigny L, Cambois A, Moachon G, Brown PD, et al. Phase 1 dose-escalation study of the PARP inhibitor CEP-9722 as monotherapy or in combination with temozolomide in patients with solid tumors. *Cancer Chemother Pharmacol*. 2014 74: 257-65.
- Polec-Pawlak K, Abramski JK, Semenova O, Hartinger CG, Timerbaev AR, Keppler BK, Jarosz M. Platinum group metallodrug-protein binding studies by capillary electrophoresis - inductively coupled plasma-mass spectrometry: A further insight into the reactivity of a novel antitumor ruthenium(III) complex toward human serum proteins. *Electrophoresis*. 2006; 27: 1128-35.
- Pongratz M, Schluga P, Jakupec MA, Arion VB, Hartinger CG, Allmaier G. et al. Transferrin binding and transferrin-mediated cellular uptake of the ruthenium coordination compound KP1019, studied by means of AAS, ESI-MS and CD



- spectroscopy. *J Anal At Spectrom.* 2004; 19: 46-51.
- Powell SN. BRCA1 loses the ring but lords over resistance. *J Clin Invest.* 2016; 126: 2802-4.
- Pourteimoor V, Mohammadi-Yeganeh S, Paryan M. Breast cancer classification and prognostication through diverse systems along with recent emerging findings in this respect; the dawn of new perspectives in the clinical applications. *Tumour Biol.* 2016; 37: 14479-99.
- Prat A, Perou CM. Deconstructing the molecular portraits of breast cancer. *Mol Oncol.* 2011; 5: 5-23.
- Provencher SW, Glöckner J. Estimation of globular protein secondary structure from circular dichroism. *Biochemistry.* 1981; 20: 33-7.
- Puhalla S, Beumer JH, Pahuja S, Appleman LJ, Abdul-Hassan Tawbi H, et al. Final results of a phase 1 study of single-agent veliparib (V) in patients (pts) with either BRCA1/2-mutated cancer (BRCA<sub>p</sub>), platinum-refractory ovarian, or basal-like breast cancer (BRCA-wt). ASCO Annual Meeting. 2014; Abstract Meeting Library. Available at <http://meetinglibrary.asco.org/content/129661-144>.
- Pulvino M, Liang Y, Oleksyn D, DeRan M, Van Pelt E, Shapiro J, et al. Inhibition of proliferation and survival of diffuse large B-cell lymphoma cells by a small-molecule inhibitor of the ubiquitin-conjugating enzyme Ubc13-Uev1A. *Blood.* 2012; 120:1668-77.
- Pysz MA, Gambhir SS, Willmann JK. Molecular imaging: current status and emerging strategies. *Clin Radiol.* 2010; 65: 500-16.
- Quinn JE, Carser JE, James CR, Kennedy RD, Harkin DP. BRCA1 and implications for response to chemotherapy in ovarian cancer. *Gynecol Oncol.* 2009; 113: 134-42.
- Quinn JE, James CR, Stewart GE, Mulligan JM, White P, Chang GK, et al. BRCA1 mRNA expression levels predict for overall survival in ovarian cancer after chemotherapy. *Clin Cancer Res.* 2007; 13: 7413-20.
- Quinn JE, Kennedy RD, Mullan PB, Gilmore PM, Carty M, Johnston PG, et al. BRCA1 functions as a differential modulator of chemotherapy-induced apoptosis. *Cancer Res.* 2003; 63: 6221-8.
- Quintal SM, dePaula QA, Farrell NP. Zinc finger proteins as templates for metal ion exchange and ligand reactivity. Chemical and biological consequences. *Metallomics.* 2011; 3: 121-39.
- Rademaker-Lakhai JM, van den BD, Pluim D, Beijnen JH, Schellens JHM. A phase I and pharmacological study with imidazolium-*trans*-DMSO-imidazole-tetrachlororuthenate, a novel ruthenium anticancer agent. *Clin Cancer Res.* 2004; 10: 3717-27.
- Rahman N, Seal S, Thompson D, Kelly P, Renwick A, Elliott A, et al. PALB2, which encodes a BRCA2-interacting protein, is a breast cancer susceptibility gene. *Nat Genet.* 2007; 39: 165-7.
- Rajan A, Carter CA, Kelly RJ, Gutierrez M, Kummar S, Szabo E, et al. A phase I combination study of olaparib with cisplatin and gemcitabine in adults with solid tumors. *Clin Cancer Res.* 2012; 18: 2344-51.
- Rakha EA, Reis-Filho JS, Ellis IO. Basal-like breast cancer: a critical review. *J Clin Oncol.* 2008; 26: 2568-81.

- Ramadevi P, Singh R, Jana SS, Devkar R, Chakraborty D. Mixed ligand ruthenium arene complexes containing N-ferrocenyl amino acids: Biomolecular interactions and cytotoxicity against MCF7 cell line. *J Organomet Chem.* 2017; 833: 80-7.
- Ransburgh DJ, Chiba N, Ishioka C, Toland AE, Parvin JD. Identification of breast tumor mutations in BRCA1 that abolish its function in homologous DNA recombination. *Cancer Res.* 2010; 70: 988-95.
- Ratanaphan A. A DNA repair BRCA1 estrogen receptor and targeted therapy in breast cancer. *Int J Mol Sci.* 2012; 13: 14898-916.
- Ratanaphan A, Canyuk B. Host Cell Reactivation and Transcriptional Activation of Carboplatin-Modified BRCA1. *Breast Cancer (Auckl).* 2014; 8: 51-6.
- Ratanaphan A, Canyuk B, Wasiksiri S, Mahasawat P. In vitro platination of human breast cancer suppressor gene1 (BRCA1) by the anticancer drug carboplatin. *Biochim Biophys Acta.* 2005; 1725: 145-51.
- Ratanaphan A, Nhukeyaw T, Hongthong H, Dyson PJ. Differential Cytotoxicity, Cellular Uptake, Apoptosis and Inhibition of BRCA1 Expression of BRCA1-Defective and Sporadic Breast Cancer Cells Induced by an Anticancer Ruthenium(II)-Arene Compound, RAPTA-EA1. 2017; 17: 212-20.
- Ratanaphan A, Nhukeyaw T, Temboot P, Hansongnern K. DNA-binding properties of ruthenium(II) complexes with the bidentate ligand 5-chloro-2-(phenylazo)pyridine. *Transition Met Chem.* 2012; 37: 207.
- Ratanaphan A, Panomwan P, Canyuk B, Maipang T. Identification of novel intronic BRCA1 variants of uncertain significance in a Thai hereditary breast cancer family. *J Genet.* 2011; 90: 327-31.
- Ratanaphan A, Wasiksiri S, Canyuk B, Prasertsan P. Cisplatin-damaged BRCA1 exhibits altered thermostability and transcriptional transactivation. *Cancer Biol Ther.* 2009; 8: 890-8.
- Reiss KA, Herman JM, Zahurak M, Brade A, Dawson LA, Scardina A, et al. A phase I study of veliparib (ABT-888) in combination with low-dose fractionated whole abdominal radiation therapy in patients with advanced solid malignancies and peritoneal carcinomatosis. *Clin Cancer Res.* 2015; 21: 68-76.
- Rice WG, Baker DC, Schaeffer CA, Graham L, Bu M, Terpening S, et al. Inhibition of multiple phases of human immunodeficiency virus type 1 replication by a dithiane compound that attacks the conserved zinc fingers of retroviral nucleocapsid proteins. *Antimicrob Agents Chemother.* 1997; 41: 419-26.
- Rice WG, Schaeffer CA, Harten B, Villinger F, South TL, Summers MF, et al. Inhibition of HIV-1 infectivity by zinc-ejecting aromatic C-nitroso compounds. *Nature.* 1993; 361: 473-5.
- Rice WG, Supko JG, Malspeis L, Buckheit RW, Clanton D, Bu M, et al. Inhibitors of HIV nucleocapsid protein zinc fingers as candidates for the treatment of AIDS. *Science.* 1995; 270: 1194-7.
- Rice WG, Turpin JA, Huang M, Clanton D, Buckheit RW, Covell DG, Wallqvist A, et al. Azodicarbonamide inhibits HIV-1 replication by targeting the nucleocapsid protein. *Nat Med.* 1997; 3: 341-5.
- Rico-Bautista E, Yang CC, Lu L, Roth GP, Wolf DA. Chemical genetics approach to restoring p27Kip1 reveals novel compounds with antiproliferative activity in

- prostate cancer cells. *BMC Biol.* 2010; 8: 153.
- Rich TA, Woodson AH, Litton J, Arun B. Hereditary breast cancer syndromes and genetic testing. *J Surg Oncol.* 2015; 111: 66-80.
- Ries LAG, Eisner MP, Kosary CL, Hankey BF, Miller BA, Clegg L, et al, SEER cancer statistics review, 1975–2000. National Cancer Institute. Bethesda, MD, [http://seer.cancer.gov/csr/1975\\_2000/](http://seer.cancer.gov/csr/1975_2000/), 2003. Access on 16 June 2017.
- Roddam AW, Pirie K, Pike MC, Chilvers C, Crossley B, Hermon C, et al. Active and passive smoking and the risk of breast cancer in women aged 36–45 years: a population based case–control study in the UK. *Br J Cancer.* 2007; 97: 434-9.
- Rodriguez JA, Henderson BR. Identification of a functional nuclear export sequence in BRCA1. *J Biol Chem.* 2000; 275: 38589-96.
- Ronconi L, Sadler PJ. Using coordination chemistry to design new medicines. *Coordin Chem Rev.* 2007; 251: 1633-48.
- Rosen EM. BRCA1 in the DNA damage response and at telomeres. *Front Genet.* 2013; 4: 85.
- Rosen EM, Fan S, Ma Y. BRCA1 regulation of transcription. *Cancer Lett.* 2006; 236: 175-85.
- Roswall N, Weiderpass E. Alcohol as a risk factor for cancer: existing evidence in a global perspective. *J Prev Med Public Health.* 2015; 48: 1-9.
- Rowling PJ, Cook R, Itzhaki LS. Toward classification of BRCA1 missense variants using a biophysical approach. *J Biol Chem.* 2010; 285: 20080-7.
- Roy S, Kaur M, Agarwal C, Tecklenburg M, Sclafani RA, Agarwal R. p21 and p27 induction by silibinin is essential for its cell cycle arrest effect in prostate carcinoma cells. *Mol Cancer Ther.* 2007; 6: 2696-707.
- Rubin R, Strayer DS. Rubin's pathology: Clinicopathology foundations of medicine. Lippincott Williams and Wilkins, Philadelphia, 2005.
- Ruffner H, Jaozeiro CA, Hemmati D, Hunter T, Verma IM. Cancer-predisposing mutations within the RING domain of BRCA1: loss of ubiquitin protein ligase activity and protection from radiation hypersensitivity. *Proc Natl Acad Sci USA.* 2001; 98: 5134-9.
- Rugo H, Olopade O, DeMichele A, Veer L, Buxton M, Hylton N, et al. Veliparib/carboplatin plus standard neoadjuvant therapy for high-risk breast cancer: first efficacy results from the I-SPY 2 Trial. *Cancer Res.* 2013; 73(24 Suppl): Abstract nr S5-02.
- Russo A, Herd-Smith A, Gestri D, Bianchi S, Vezzosi V, Del Turco MR. et al. Does family history influence survival in breast cancer cases? *Int J Cancer.* 2002; 99: 427-30.
- Rydzik AM, Brem J, Struwe WB, Kochan GT, Benesch JLP, Schofield CJ. Ejection of structural zinc leads to inhibition of  $\gamma$ -butyrobetaine hydroxylase. *Bioorg Med Chem Lett.* 2014; 24: 4954-57.
- Saha T, Rih JK, Roy R, Ballal R, Rosen EM. Transcriptional regulation of the base excision repair pathway by BRCA1. *J Biol Chem.* 2010; 285: 19092-105.
- Sackton KL, Dimova N, Zeng X, Tian W, Zhang M, Sackton TB, et al. Synergistic blockade of mitotic exit by two chemical inhibitors of the APC/C. *Nature.* 2014; 514: 646-9.

- Sambrook J, Russell DW. Molecular cloning: a laboratory manual 3<sup>rd</sup> ed. New York, USA: Cold Spring Harbor Laboratory Press; 2001.
- Samol J, Ranson M, Scott E, Macpherson E, Carmichael J, Thomas A, et al. Safety and tolerability of the poly (ADP-ribose) polymerase (PARP) inhibitor, olaparib (AZD2281) in combination with topotecan for the treatment of patients with advanced solid tumors: a phase I study. *Invest New Drugs*. 2012; 30: 1493-500.
- Sandhu SK, Schelman WR, Wilding G, Moreno V, Baird RD, Miranda S, et al. Poly(ADP-ribose) polymerase (PARP) inhibitors for the treatment of advanced germline BRCA2 mutant prostate cancer. *Ann Oncol*. 2013; 24: 1416-8.
- Sankaran S, Starita LM, Groen AC, Ko MJ, Parvin JD. Centrosomal microtubule nucleation activity is inhibited by BRCA1-dependent ubiquitination. *Mol Cell Biol*. 2005; 25: 8656-68.
- Sato K, Hayami R, Wu W, Nishikawa T, Nishikawa H, Okuda Y, et al. Nucleophosmin/B23 is a candidate substrate for the BRCA1-BARD1 ubiquitin ligase. *J Biol Chem*. 2004; 279: 30919-22.
- Sato K, Sundaramoorthy E, Rajendra E, Hattori H, Jeyasekharan AD, Ayoub N, et al. A DNA-damage selective role for BRCA1 E3 ligase in claspin ubiquitylation, CHK1 activation, and DNA repair. *Curr Biol*. 2012; 22: 1659-66.
- Sava G, Bergamo A. Ruthenium-based compounds and tumor growth control (review). *Int J Oncol*. 2000; 17: 353-65.
- Sava G, Gagliardi R, Bergamo A, Alessio E, Mestroni G. Treatment of metastases of solid mouse tumors by NAMI-A: comparison with cisplatin, cyclophosphamide and dacarbazine. *Anticancer Res*. 1999; 19: 969-72.
- Sava G, Frausin F, Cocchietto M, Vita F, Podda E, Spessotto P, et al. Actin-dependent tumour cell adhesion after short-term exposure to the antimetastasis ruthenium complex NAMI-A. *Eur J Cancer*. 2004; 40: 1383-96.
- Sava G, Zorzet S, Turrin C, Vita F, Soranzo M, Zabucchi G, et al. Dual action of NAMI-A in inhibition of solid tumor metastasis: selective targeting of metastatic cells and binding to collagen. *Clin Cancer Res*. 2003; 9: 1898-1905.
- Savage KI, Harkin DP. BRCA1, a 'complex' protein involved in the maintenance of genomic stability. *FEBS J*. 2015; 282: 630-46.
- Schlegel BP, Starita LM, Parvin JD. Overexpression of a protein fragment of RNA helicase A causes inhibition of endogenous BRCA1 function and defects in ploidy and cytokinesis in mammary epithelial cells. *Oncogene*. 2003; 22: 983-91.
- Scolaro C, Bergamo A, Brescacin L, Delfino R, Cocchietto M, Laurenczy G, et al. *In vitro* and *in vivo* evaluation of ruthenium (II) arene PTA complexes. *J Med Chem*. 2005; 48: 4161-71.
- Scolaro C, Chaplin AB, Hartinger CG, Bergamo A, Cocchietto M, Keppler BK, et al. Tuning the hydrophobicity of ruthenium(II)-arene (RAPTA) drugs to modify uptake, biomolecular interactions and efficacy. *Dalton Trans*. 2007; 43: 5065-72.
- Scolaro C, Geldbach TJ, Rochat S, Dorcier A, Gossens C, Bergamo A, et al. Influence

- of hydrogen-bonding substituents on the cytotoxicity of RAPTA compounds. *Organometallics*. 2006; 25: 756-65.
- Siegel RL, Miller KD, Jemal A. Cancer Statistics, 2016. *CA Cancer J Clin*. 2016; 66: 7-30.
- Siegel RL, Miller KD, Jemal A. Cancer Statistics, 2017. *CA Cancer J Clin*. 2017; 67: 7-30.
- Sikov W, Berry D, Perou C, Singh B, Cirrincione C, Tolaney S, et al. Impact of the addition of carboplatin and/or bevacizumab to neoadjuvant once-per-week paclitaxel followed by dose-dense doxorubicin and cyclophosphamide on pathologic complete response rates in stage II to III triple-negative breast cancer: Calgb 40603 (Alliance). *J Clin Oncol*. 2015; 33: 13-21.
- Sekirnik R, Rose NR, Thalhammer A, Seden PT, Mecinovic J, Schofield CJ. Inhibition of the histone demethylase JMJD2A by ejection of structural Zn(II). *Chem Commun (Camb)*. 2009; 14: 6376-8.
- Sekizawa R, Ikeno S, Nakamura H, Naganawa H, Matsui S, Iinuma H, et al. Panepophenanthrin, from a mushroom strain, a novel inhibitor of the ubiquitinactivating enzyme. *J Nat Prod*. 2002; 65: 1491-93.
- Serrano-Ruiz M, Lorenzo-Luis P, Romerosa A. Easy synthesis and water solubility of ruthenium complexes containing PPh<sub>3</sub>, mTPPMS, PTA and mPTA, (mTPPMS = meta-triphenylphosphine monosulfonate, PTA = 1,3,5-triaza-7-phosphaadamantane, mPTA = N-methyl-1,3,5-triaza-7-phosphaadamantane). *Inorg Chim Acta*. 2017; 455: 528-34.
- Shen SX, Weaver Z, Xu X, Li C, Weinstein M, Chen L, et al. A targeted disruption of the murine *Brcal* gene causes gamma-irradiation hypersensitivity and genetic instability. *Oncogene*. 1998; 17: 3115-24.
- Silver DP, Richardson AL, Eklund AC, Wang ZC, Szallasi Z, Li Q, et al. Efficacy of neoadjuvant Cisplatin in triple-negative breast cancer. *J Clin Oncol*. 2010; 28: 1145-53.
- Snouwaert JN, Gowen LC, Latour AM, Mohn AR, Xiao A, DiBiase L. BRCA1 deficient embryonic stem cells display a decreased homologous recombination frequency and an increased frequency of non-homologous recombination that is corrected by expression of a *brcal* transgene. *Oncogene*. 1999; 18: 7900-7.
- Sobhian B, Shao G, Lilli DR, Culhane AC, Moreau LA, Xia B. RAP80 targets BRCA1 to specific ubiquitin structures at DNA damage sites. *Science*. 2007; 316: 1198-202.
- Sokratous K, Hadjisavvas A, Diamandis EP, Kyriacou K. The role of ubiquitin-binding domains in human pathophysiology. *Crit Rev Clin Lab Sci*. 2014; 51: 280-90.
- Sorlie T, Wang Y, Xiao C, Johnsen H, Naume B, Samaha RR, et al. Distinct molecular mechanisms underlying clinically relevant subtypes of breast cancer: gene expression analyses across three different platforms. *BMC Genomics*. 2006; 7: 127.
- Sorlie T, Perou CM, Tibshirani R, Aas T, Geisler S, Johnsen H, et al. Gene expression patterns of breast carcinomas distinguish tumor subclasses with clinical implications. *Proc Natl Acad Sci USA*. 2001; 98: 10869-74.

- Sotiriou C, Neo SY, McShane LM, Korn EL, Long PM, Jazaeri A, et al. Breast cancer classification and prognosis based on gene expression profiles from a population-based study. *Proc Natl Acad Sci USA*. 2003; 100: 10393-8.
- Sousa GF, Wlodarczyk SR, Monteiro G. Carboplatin: molecular mechanisms of action associated with chemoresistance. *Braz J Pharm Sci*. 2014; 50: 693-701.
- Spell SR, Farrell NP. [Au(dien)(N-heterocycle)](3+): reactivity with biomolecules and zinc finger peptides. *Inorg Chem*. 2015; 54: 79-86.
- Spence J, Gali RR, Dittmar G, Sherman F, Karin M, Finley D. Cell cycle-regulated modification of the ribosome by a variant multiubiquitin chain. *Cell*. 2000; 102: 67-76.
- Starita LM, Horwitz AA, Keogh MC, Ishioka C, Parvin JD, Chiba N. BRCA1/BARD1 ubiquitinate phosphorylated RNA polymerase II. *J Biol Chem*. 2005; 280: 24498-505.
- Starita LM, Parvin JD. The multiple nuclear functions of BRCA1: transcription, ubiquitination and DNA repair. *Curr Opin Cell Biol*. 2003; 15: 345-50.
- Starita LM, Parvin JD. Substrates of the BRCA1-dependent ubiquitin ligase. *Cancer Biol Ther*. 2006; 5: 137-41.
- Starita LM, Machida Y, Sankaran S, Elias JE, Griffin K, Schlegel BP, et al. BRCA1-dependent ubiquitination of gamma-tubulin regulates centrosome number. *Mol Cell Biol*. 2004; 24: 8457-66.
- Starita LM, Young DL, Islam M, Kitzman JO, Gullingsrud J, Hause RJ. et al. Massively parallel functional analysis of BRCA1 RING domain variants. *Genetics*. 2015; 200: 413-22.
- Stewart MD, Duncan ED, Coronado E, DaRosa PA, Pruneda JN, Brzovic PS. Tuning BRCA1 and BARD1 activity to investigate RING ubiquitin ligase mechanisms. *Protein Sci*. 2017; 26: 475-83.
- Stratton MR and Rahman N. The emerging landscape of breast cancer susceptibility. *Nat Genet*. 2007; 40: 17-22.
- Sun LJ, Chen ZJ. The novel functions of ubiquitination in signaling. *Curr Opin Cell Biol*. 2004; 16: 119-26.
- Sun X, Zhou X, Du L, Liu W, Liu Y, Hudson LG. et al. Arsenite binding-induced zinc loss from PARP-1 is equivalent to zinc deficiency in reducing PARP-1 activity, leading to inhibition of DNA repair. *Toxicol Appl Pharmacol*. 2014; 274: 313-8.
- Suzuki R, Orsini N, Mignone L, Saji S, Wolk A. Alcohol intake and risk of breast cancer defined by estrogen and progesterone receptor status--a meta-analysis of epidemiological studies. *Int J Cancer*. 2008; 122: 1832-41.
- Swisher EM, Lin KK, Oza AM, Scott CL, Giordano H, Sun J, et al. Rucaparib in relapsed, platinum-sensitive high-grade ovarian carcinoma (ARIEL2 Part 1): an international, multicentre, openlabel, phase 2 trial. *Lancet Oncol*. 2017; 18: 75-87.
- Sy SM, Huen MS, Chen J. PALB2 is an integral component of the BRCA complex required for homologous recombination repair. *Proc Natl Acad Sci USA*. 2009; 106: 7155-60.
- Tabrizi L, Chiniforoshan H. Ruthenium (II) p-cymene complexes of naphthoquinone derivatives as antitumor agents: A structure-activity relationship study. *J*

- Organomet Chem. 2016; 822: 211-20.
- Tan MH, Mester JL, Ngeow J, Rybicki LA, Orloff MS, Eng C. Lifetime cancer risks in individuals with germline PTEN mutations. *Clin Cancer Res.* 2012; 18:400-7.
- Tanino H, Kosaka Y, Nishimiya H, Tanaka Y, Minatani N, Kikuchi M, et al. BRCAness and prognosis in triple-negative breast cancer patients treated with neoadjuvant chemotherapy. *PLoS One.* 2016; 11: e0165721.
- Taron M, Rosell R, Felip E, Mendez P, Souglakos J, Ronco MS, et al. BRCA1 mRNA expression levels as an indicator of chemoresistance in lung cancer. *Hum Mol Genet.* 2004; 13: 2443-9.
- Tassone P, Di Martino MT, Ventura M, Pietragalla A, Cucinotto I, Calimeri T, et al. Loss of BRCA1 function increases the antitumor activity of cisplatin against human breast cancer xenografts in vivo. *Cancer Biol Ther.* 2009; 8: 648-53.
- Thalib L, Wedrén S, Granath F, Adami HO, Rydh B, Magnusson M, et al. Breast cancer prognosis in relation to family history of breast and ovarian cancer. *Br J Cancer.* 2004; 90: 1378-81.
- Telli ML, Timms K, Reid JE, Hennessy B, Mills GB, Jensen KC, et al. Homologous recombination deficiency (HRD) score predicts response to platinum-containing neoadjuvant chemotherapy in patients with triple-negative breast cancer. *Clin Cancer Res.* 2016; 22: 3764-73.
- Thompson D, Easton DF. Cancer incidence in BRCA1 mutation carriers. *J Natl Cancer Inst.* 2002; 94: 1358-65.
- Trondl R, Heffeter P, Kowol CR, Jakupec MA, Berger W, Keppler BK. NKP-1339, the first ruthenium-based anticancer drug on the edge to clinical application. *Chem Sci.* 2014; 5: 2925-32.
- Torres-Mejía G, Cupul-Uicab LA, Allen B, Galal O, Salazar-Martínez E, Lazcano-Ponce EC. Comparative study of correlates of early age at menarche among Mexican and Egyptian adolescents. *Am J Hum Biol.* 2005; 17: 654-8.
- Travis RC, Key TJ. Oestrogen exposure and breast cancer risk. *Breast Cancer Res.* 2003; 5: 239-47.
- Trudu F, Amato F, Vaňhara P, Pivetta T, Peña-Méndez EM, Havel J. Coordination compounds in cancer: Past, present and perspectives. *J Appl Biomed.* 2015; 13: 79-103.
- Tryggvadottir L, Tulinius H, Eyfjord JE, Sigurvinsson T. Breastfeeding and reduced risk of breast cancer in an Icelandic cohort study. *Am J Epidemiol.* 2001; 154: 37-42.
- Trynda-Lemiesz L. Interaction of an anticancer ruthenium complex *HInd*[RuInd<sub>2</sub>Cl<sub>4</sub>] with cytochrome C. *Acta Biochim Pol.* 2004; 51: 199-205.
- Tsotsoros SD, Bate AB, Dows MG, Spell SR, Bayse CA, Farrell NP. Modulation of the stacking interaction of MN<sub>4</sub> (M=Pt, Pd, Au) complexes with tryptophan through N-heterocyclic ligands. *J Inorg Biochem.* 2014; 132: 2-5.
- Tsotsoros SD, Qu Y, Farrell NP. The reaction of dichlorodiammineplatinum (II), [PtCl<sub>2</sub>(NH<sub>3</sub>)<sub>2</sub>], isomers with zinc fingers. *J Inorg Biochem.* 2015; 143: 117-22.
- Tsotsoros SD, Lutz PB, Daniel AG, Peterson EJ, de Paiva REF, Rivera E. et al. Enhancement of the physicochemical properties of [Pt(dien)(nucleobase)]<sup>2+</sup> for HIVNCp7 targeting. *Chem Sci.* 2017; 8: 1269.

- Tsukamoto S, Hirota H, Imachi M, Fujimuro M, Onuki H, Ohta T, et al. Himeic acid A: a new ubiquitin-activating enzyme inhibitor isolated from a marine-derived fungus, *Aspergillus* sp. *Bioorg Med Chem Lett*. 2005; 15: 191-4.
- Tsukamoto S, Takeuchi T, Rotinsulu H, Mangindaan RE, van Soest W, Ukai K, et al. Leucettamol A: a new inhibitor of Ubc13–Uev1A interaction isolated from a marine sponge, *Leucetta aff. microrhaphis*. *Bioorg Med Chem Lett*. 2008; 18: 6319-20.
- Turnbull C, Ahmed S, Morrison J, Pernet D, Renwick A, Maranian M, et al. Genome-wide association study identifies five new breast cancer susceptibility loci. *Nat Genet*. 2010; 42: 504-7.
- Turner N, Tutt A, Ashworth A. Hallmarks of 'BRCAness' in sporadic cancers. *Nat Rev Cancer*. 2004; 4: 814-9.
- Turpin JA, Song Y, Inman JK, Huang M, Wallqvist A, Maynard A, et al. Synthesis and biological properties of novel pyridinioalkanoyl thioesters (PATE) as anti-HIV-1 agents that target the viral nucleocapsid protein zinc fingers. *J Med Chem*. 1999; 42: 67-86.
- Tutt A, Ellis P, Kilburn L, Gilett C, Pinder S, Abraham J. et al. TNT trial: a randomized phase III trial of carboplatin compared with docetaxel for patients with metastatic or recurrent locally advanced triple negative or BRCA 1/2 breast cancer. *Cancer Res*. 2015; 75(9 Supplement): S3-01-S3-01.
- US mortality data, National Center for Health Statistics, Centers for Disease Control and Prevention. American Cancer Society, Inc., Surveillance Research, 2015.
- Vacca A, Bruno M, Boccarelli A, Coluccia M, Ribatti D, Bergamo A, Garbisa S, Sartor L, Sava G. Inhibition of endothelial cell functions and of angiogenesis by the metastasis inhibitor NAMI-A. *Br J Cancer*. 2002; 86: 993-8.
- Ungermannova D, Parker SJ, Nasveschuk CG, Wang W, Quade B, Zhang G, et al. Largazole and its derivatives selectively inhibit ubiquitin activating enzyme (e1). *PLoS One*. 2012; 7: e29208.
- Ushiyama S, Umaoka H, Kato H, Suwa Y, Morioka H, Rotinsulu H, et al. Manadosterols A and B, sulfonated sterol dimers inhibiting the Ubc13–Uev1A interaction, isolated from the marine sponge *Lissodendryx fibrosa*. *J Nat Prod* 2012; 75: 1495-9.
- van der Noll R, Marchetti S, Steeghs N, Beijnen JH, Mergui-Roelvink MW, Harms E, et al. Long-term safety and anti-tumour activity of olaparib monotherapy after combination with carboplatin and paclitaxel in patients with advanced breast ovarian or fallopian tube cancer. *Br J Cancer*. 2015; 113: 396-402.
- van Lier MG, Wagner A, Mathus-Vliegen EM, Kuipers EJ, Steyerberg EW, van Leerdam ME. High cancer risk in Peutz-Jeghers syndrome: a systematic review and surveillance recommendations. *Am J Gastroenterol*. 2010; 105: 1258-64.
- Vassilev LT, Vu BT, Graves B, Carvajal D, Podlaski F, Filipovic Z, et al. In vivo activation of the p53 pathway by small-molecule antagonists of MDM2. *Science*. 2004; 303: 844-8.
- Velkova A, Carvalho MA, Johnson JO, Tavtigian SV, Monteiro AN. Identification of Filamin A as a BRCA1-interacting protein required for efficient DNA repair. *Cell Cycle*. 2010; 9: 1421-33.



- Vencken PM, Kriege M, Hoogwerf D, et al. Chemosensitivity and outcome of BRCA1- and BRCA2-associated ovarian cancer patients after first-line chemotherapy compared with sporadic ovarian cancer patients. *Ann Oncol.* 2011; 22: 1346-52.
- Venkitaraman AR. Cancer suppression by the chromosome custodians, BRCA1 and BRCA2. *Science.* 2014; 343: 1470-5.
- Vercruyse T, Basta B, Dehaen W, Humbert N, Balzarini J, Debaen F, et al. A phenyl-thiadiazolylidene-amine derivative ejects zinc from retroviral nucleocapsid zinc fingers and inactivates HIV virions. *Retrovirology.* 2012; 9: 95.
- Vergara A, D'Errico G, Montesarchio D, Mangiapia G, Paduano L, Merlino A. Interaction of anticancer ruthenium compounds with proteins: high-resolution X-ray structures and raman microscopy studies of the adduct between hen egg white lysozyme and AziRu. *Inorg Chem.* 2013; 52:4157-9.
- Vierstra RD. The ubiquitin/26S proteasome pathway, the complex last chapter in the life of many plant proteins. *Trends Plant Sci.* 2003; 8: 135-42.
- Villalona-Calero MA, Duan W, Zhao W, Shilo K, Schaaf LJ, Thurmond J. et al. Veliparib alone or in combination with mitomycin C in patients with solid tumors with functional deficiency in homologous recombination repair. *J Natl Cancer Inst.* 2016; 108.
- Voltan R, Secchiero P, Ruozi B, Forni F, Agostinis C, Caruso L, et al. Nanoparticles engineered with rituximab and loaded with Nutlin-3 show promising therapeutic activity in B-leukemic xenografts. *Clin Cancer Res.* 2013; 19: 3871-80.
- Von Minckwitz G, Loibl S, Schneeweiss A, Salat C, Rezai M, Zahm DM, et al. Early survival analysis of the randomized phase II trial investigating the addition of carboplatin to neoadjuvant therapy for triple-negative and HER2-positive early breast cancer (Geparsixto). *Cancer Res.* 2015; 76; abstract S2-04.
- Wainberg ZA, Rafii S, Ramanathan RK, Mina LA, Averett Byers L, Chugh R, et al. Safety and antitumor activity of the PARP inhibitor BMN673 in a phase 1 trial recruiting metastatic small-cell lung cancer (SCLC) and germline BRCA-mutation carrier cancer patients. 2014 ASCO Annual Meeting. (2014) Abstracts Meeting Library. Available at <http://meetinglibrary.asco.org/content/128953-144>.
- Walter I, Schwerdtle T, Thuy C, Parsons JL, Dianov GL. Hartwig, Impact of arsenite and its methylated metabolites on PARP-1 activity, PARP-1 gene expression and poly(ADP-ribosyl)ation in cultured human cells. *DNA Repair (Amst.).* 2007; 6: 61-70.
- Wang B, Elledge SJ. Ubc13/Rnf8 ubiquitin ligases control foci formation of the Rap80/Abraxas/Brc1/Brcc36 complex in response to DNA damage. *Proc Natl Acad Sci USA.* 2007; 104: 20759-63.
- Wang Z, Gao D, Fukushima H, Inuzuka H, Liu P, Wan L, et al. Skp2: a novel potential therapeutic target for prostate cancer. *Biochim Biophys Acta.* 2012; 1825: 11-7.
- Wang Y, Kraiss JJ, Bernhardt AJ, Nicolas E, Cai KQ, Harrell MI. et al. RING domain-deficient BRCA1 promotes PARP inhibitor and platinum resistance. *J Clin Invest.* 2016; 126: 3145-57.

- Wang Z, Liu P, Inuzuka H, Wei W. Roles of F-box proteins in cancer. *Nat Rev Cancer*. 2014; 14: 233-47.
- Wang YL, Wang B, Zhang H, Li N, Tanaka K, Zhou X, et al. BRCA1 involved in regulation of Bcl-2 expression and apoptosis susceptibility to ionizing radiation. *Sci China Phys Mech Astron*. 2011 54: 916.
- Wang LH, Yang XY, Zhang X, Mihalic K, Fan YX, Xiao W, et al. Suppression of breast cancer by chemical modulation of vulnerable zinc fingers in estrogen receptor. *Nat Medicine*. 2004 10: 40-7.
- Wang LH, Yang XY, Zhang X, An P, Kim HJ, Huang J, et al. Disruption of estrogen receptor DNA-binding domain and related intramolecular communication restores tamoxifen sensitivity in resistant breast cancer. *Cancer Cell*. 2006; 10: 487-99.
- Wang W, Zhang X, Qin JJ, Voruganti S, Nag SA, Wang MH, et al. Natural product ginsenoside 25-OCH<sub>3</sub>-PPD inhibits breast cancer growth and metastasis through down-regulating MDM2. *PLoS One*. 2012; 7: e41586.
- Wang F, Zhou X, Liu W, Sun X, Chen C, Hudson LG. et al. Arsenite-induced ROS/RNS generation causes zinc loss and inhibits the activity of poly(ADP-ribose) polymerase-1. *Free Radic Biol Med*. 2013; 61: 249-56.
- Watts FZ, Brissett NC. Linking up and interacting with BRCT domains. *DNA Repair (Amst)*. 2010; 9: 103-108.
- Wei W, Jin J, Schlisio S, Harper JW, Kaelin WG. The v-Jun point mutation allows c-Jun to escape GSK3-dependent recognition and destruction by the Fbw7 ubiquitin ligase. *Cancer Cell*. 2005; 8: 25-33.
- Wei L, Lan L, Hong Z, Yasui A, Ishioka C, Chiba N. Rapid recruitment of BRCA1 to DNA double-strand breaks is dependent on its association with Ku80. *Mol Cell Biol*. 2008; 28: 7380-93.
- Weiderpass E, Meo M, Vainio H. Risk Factors for Breast Cancer, Including Occupational Exposures. *Saf Health Work*. 2011; 2: 1-8.
- Weissleder R, Pittet MJ. Imaging in the era of molecular oncology. *Nature*. 2008; 452: 580-9.
- Welcker M, Orian A, Jin J, Grim JE, Harper JW, Eisenman RN, et al. The Fbw7 tumor suppressor regulates glycogen synthase kinase 3 phosphorylation-dependent c-Myc protein degradation. *Proc Natl Acad Sci USA*. 2004; 101: 9085-90.
- Wesolowski R, Zhao M, Geyer SM, Lustberg MB, Mrozek E, Layman RM, et al. Phase I trial of the PARP inhibitor veliparib (V) in combination with carboplatin (C) in metastatic breast cancer (MBC) *J Clin Oncol*. 2014; 32: 1075.
- Wester HJ. Nuclear imaging probes: from bench to bedside. *Clin Cancer Res*. 2007; 13: 3470-81.
- Wexselblatt E, Gibson D. What do we know about the reduction of Pt (IV) pro-drugs? *J Inorg Biochem*. 2012; 117: 220-9.
- Wheate NJ, Walker S, Craig GE, Oun R. The status of platinum anticancer drugs in the clinic and in clinical trials. *Dalton Trans*. 2010; 39: 8113-27.
- Williams RS, Green R, Mark Glover JN. Crystal structure of the BRCT repeat region from the breast cancer associated protein BRCA1. *Nat Struct Biol*. 2001; 8: 838-42.

- Williamson EA, Dadmanesh F, Koeffler HP. BRCA1 transactivates the cyclin-dependent kinase inhibitor p27<sup>Kip1</sup>. *Oncogene*. 2002; 21: 3199-206.
- Wilson R, Evans TJ, Middleton MR, Molife LR, Spicer J, Dieras V, et al. A phase I study of intravenous and oral rucaparib in combination with chemotherapy in patients with advanced solid tumours. *Br J Cancer*. 2017; 116: 884-92.
- Witvrouw M, Balzarini J, Pannecouque C, Jhaumeer-Laulloo S, Este JA, Schols D, et al. SRR-SB3, a disulfide-containing macrolide that inhibits a late stage of the replicative cycle of human immunodeficiency virus. *Antimicrob. Agents Chemother*. 1997; 41: 262-8.
- Wolff MS, Britton JA, Wilson VP. Environmental Risk Factors for Breast Cancer among African-American Women. *Cancer*. 2003; 97: 289-310.
- Wong E, Giandomenico CM. Current status of platinum-based antitumor drugs. *Chem Rev*. 1999; 99: 2451-66.
- Wong-Brown MW, Meldrum CJ, Carpenter JE, Clarke CL, Narod SA, Jakubowska A. Prevalence of BRCA1 and BRCA2 germline mutations in patients with triple-negative breast cancer. *Breast Cancer Res Treat*. 2015; 150: 71-80.
- Woynarowski JM, Faivre S, Herzig MC, Arnett B, Chapman WG, Trevino AV, et al. Oxaliplatin-induced damage of cellular DNA. *Mol Pharmacol*. 2000; 58: 920-7.
- Wu K, Hu W, Luo Q, Li X, Xiong S, Sadler PJ, et al. Competitive binding sites of a ruthenium arene anticancer complex on oligonucleotides studied by mass spectrometry: ladder-sequencing versus top-down. *J Am Soc Mass Spectrom*. 2013; 24: 410-20.
- Wu K, Liu S, Luo Q, Hu W, Li X, Wang F. Thymines in single-stranded oligonucleotides and G-quadruplex DNA are competitive with guanines for binding to an organoruthenium anticancer complex. *Inorg Chem*. 2013; 52: 11332-42.
- Wu G, Lyapina S, Das I, Li J, Gurney M, Pauley A, et al. SEL-10 is an inhibitor of notch signaling that targets notch for ubiquitin-mediated protein degradation. *Mol Cell Biol*. 2001; 21: 7403-15.
- Wu LC, Wen ZS, Qiu YT, Chen XQ, Chen HB, Wei MM, et al. Largazole arrests cell cycle at G1 phase and triggers proteasomal degradation of E2F1 in lung cancer cells. *ACS Med Chem Lett*. 2013 4: 921-6.
- Wu-Bear F, Lagazon K, Yuan W, Bear R. The BRCA1/BARD1 heterodimer assembles polyubiquitin chains through an unconventional linkage involving lysine residues K6 of ubiquitin. *J Biol Chem*. 2003; 278: 34743-6.
- Wu W, Xu C, Ling X, Fan C, Buckley BP, Chernov MV, et al. Targeting RING domains of Mdm2-MdmX E3 complex activates apoptotic arm of the p53 pathway in leukemia/lymphoma cells. *Cell Death Dis*. 2015; 6: e2035.
- Xia Y, Pao GM, Chen HW, Verma IM, Hunter T. Enhancement of BRCA1 E3 ubiquitin ligase activity through direct interaction with the BARD1 protein. *J Biol Chem*. 2003; 278: 5255-63.
- Xie J, Peng M, Guillemette S, Quan S, Maniatis S, Wu Y, et al. FANCI/BACH1 acetylation at lysine 1249 regulates the DNA damage response. *PLoS Genet*. 2012; 8: e1002786.
- Xu GW, Ali M, Wood TE, Wong D, Maclean N, Wang X, et al. The ubiquitin-activating enzyme E1 as a therapeutic target for the treatment of leukemia

- and multiple myeloma. *Blood*. 2010; 115: 2251-9.
- Xu B, Kim S, Kastan MB. Involvement of BRCA1 in S-phase and G(2)-phase checkpoints after ionizing irradiation. *Mol Cell Biol*. 2001; 21(10): 3445-50.
- Xu X, Weaver Z, Linke SP, Li C, Gotay J, Wang XW, et al. Centrosome amplification and a defective G2-M cell cycle checkpoint induce genetic instability in BRCA1 exon 11 isoform-deficient cells. *Mol Cell*. 1999; 3: 389-95.
- Yada M, Hatakeyama S, Kamura T, Nishiyama M, Tsunematsu R, Imaki H, et al. Phosphorylation-dependent degradation of c-Myc is mediated by the F-box protein Fbw7. *EMBO J*. 2004; 23: 2116-25.
- Yamane K, Katayama E, Tsuruo T. The BRCT regions of tumor suppressor BRCA1 and of XRCC1 show DNA end binding activity with a multimerizing feature. *Biochem Biophys Res Commun*. 2000; 279: 678-84.
- Yamanokuchi R, Imada K, Miyazaki M, Kato H, Watanabe T, Fujimuro M, et al. Hyrtioreticulins A-E, indole alkaloids inhibiting the ubiquitin-activating enzyme, from the marine sponge *Hyrtios reticulatus*. *Bioorg Med Chem*. 2012; 20: 4437-42.
- Yan YK, Melchart M, Habtemariam A, Sadler PJ. Organometallic chemistry, biology and medicine: ruthenium arene anticancer complexes. *Chem Commun*. 2005; 14: 4764-76.
- Yang Y, Kitagaki J, Dai RM, Tsai YC, Lorick KL, Ludwig RL, et al. Inhibitors of ubiquitin-activating enzyme (E1), a new class of potential cancer therapeutics, *Cancer Res*. 2007; 67: 9472-81
- Yang Y, Ludwig RL, Jensen JP, Pierre SA, Medaglia MV, Davydov IV, et al. Small molecule inhibitors of HDM2 ubiquitin ligase activity stabilize and activate p53 in cells. *Cancer Cell*. 2005; 7: 547-59.
- Yang Q, Yoshimura G, Nakamura M, Nakamura Y, Suzuma T, Umemura T, et al. Correlation between BRCA1 expression and apoptosis-related biological parameters in sporadic breast carcinomas. *Anticancer Res*. 2002; 22: 3615-9.
- Yarden RI, Brody LC. BRCA1 interacts with components of the histone deacetylase complex. *Proc Natl Acad Sci USA*. 1999; 96: 4983-8.
- Yarden RI, Papa MZ. BRCA1 at the crossroad of multiple cellular pathways: approaches for therapeutic interventions. *Mol Cancer Ther*. 2006; 5: 1396-404.
- Yarden RI, Pardo-Reoyo S, Sgagias M, Cowan KH, Brody LC. BRCA1 regulates the G2/M checkpoint by activating Chk1 kinase upon DNA damage. *Nat Genet*. 2002; 30: 285-9.
- Youlden DR, Cramb SM, Yip CH, Baade PD. Incidence and mortality of female breast cancer in the Asia-Pacific region. *Cancer Biol Med*. 2014; 11: 101-15.
- Yu X, Chen J. DNA damage-induced cell cycle checkpoint control requires CtIP, a phosphorylation-dependent binding partner of BRCA1 C-terminal domains. *Mol Cell Biol*. 2004; 24: 9478-86.
- Yu X, Chini CC, He M, Mer G, Chen J. The BRCT domain is a phospho-protein binding domain. *Science*. 2003; 302: 639-42.
- Yu X, Fu S, Lai M, Baer R, Chen J. BRCA1 ubiquitinates its phosphorylation-dependent binding partner CtIP. *Genes Dev*. 2006; 20: 1721-6.

- Yuh SH, Tibudan M, Hentosh P. Analysis of 2-chloro-2'-deoxy-adenosine incorporation into cellular DNA by quantitative polymerase chain reaction. *Anal Biochem.* 1998; 262: 1-8.
- Zagouri F, Sergentanis TN, Tsigginou A, Dimitrakakis C, Zografos GC, Dimopoulos MA, et al. Female breast cancer in Europe: statistics, diagnosis and treatment modalities. *J Thorac Dis.* 2014; 6: 589-90.
- Zeng X, King RW. An APC/C inhibitor stabilizes cyclin B1 by prematurely terminating ubiquitination. *Nat Chem Biol.* 2012; 8: 383-92.
- Zhang X, Gu L, Li J, Shah N, He J, Yang L, et al. Degradation of MDM2 by the interaction between berberine and DAXX leads to potent apoptosis in MDM2-overexpressing cancer cells. *Cancer Res.* 2010; 70: 9895-904.
- Zhang W, Luo J, Chen F, Yang F, Song W, Zhu A, et al. BRCA1 regulates PIG3-mediated apoptosis in a p53-dependent manner. *Oncotarget.* 2015; 6: 7608-18.
- Zhang J, Powell SN. The role of the BRCA1 tumor suppressor in DNA doublestrand break repair. *Mol Cancer Res.* 2005; 3: 531-9.
- Zhao D, Zheng HQ, Zhou Z, Chen C. The Fbw7 tumor suppressor targets KLF5 for ubiquitin-mediated degradation and suppresses breast cell proliferation. *Cancer Res.* 2010; 70: 4728-38.
- Zhong Q, Boyer TG, Chen P, Lee W. Deficient nonhomologous end-joining activity in cell-free extracts from Brca1-null fibroblasts. *Cancer Res.* 2002; 62: 3966-70.
- Zhou XX, Cooper KL, Huestis J, Xu H, Burchiel SW, Hudson LG, et al. S-nitrosation on zinc finger motif of PARP-1 as a mechanism of DNA repair inhibition by arsenite. *Oncotarget.* 2016; 7: 80482-92.
- Zhou W, Slingerland JM. Links between oestrogen receptor activation and proteolysis: relevance to hormone-regulated cancer therapy. *Nat Rev Cancer.* 2014; 14: 26-38.
- Zhou X, Sun X, Mobarak C, Gandolfi AJ, Burchiel SW, Hudson LG. Differential binding of monomethylarsonous acid compared to arsenite and arsenic trioxide with zinc finger peptides and proteins. *Chem Res Toxicol.* 2014; 27:690-8.
- Zhu Q, Pao GM, Huynh AM, Suh H, Tonnu N, Nederlof PM, et al. BRCA1 tumour suppression occurs via heterochromatin-mediated silencing. *Nature.* 2011; 477: 179-184.
- Zorzet S, Bergamo A, Cocchietto M, Sorc A, Gava B, Alessio E, et al. Lack of *in vitro* cytotoxicity, associated to increased G(2)-M cell fraction and inhibition of matrigel invasion, may predict *in vivo*-selective antimetastasis activity of ruthenium complexes. *J Pharmacol Exp Ther.* 2000; 295: 927-33.

**APPENDIX**

## Experimental

For clarity and contextual understanding, the following results, MS top down experiments, are presented here that were performed in the laboratory of Professor Paul Joseph Dyson, LCOM, EPFL, Lausanne, Switzerland.

### Mass spectrometry studies with model peptide

The BRCA1 peptide (10  $\mu$ M) was incubated with RAPTA-C or RAPTA-EA1) at a 1:1 and 1:5 protein:complex ratios at 4° C for 24 h. All incubations were performed in sterile MilliQ water. Incubated proteins were stored at -20 °C until analysis. Electron-Transfer Dissociation (ETD) peptide fragmentation studies were performed on an ETD enabled hybrid linear ion trap (LTQ) Orbitrap Elite mass spectrometer (Thermo Scientific, Bremen, Germany) coupled to a Triversa Nanomate (Advion) chip-based electrospray system. The samples were infused using a spray voltage of 1.6 kV. The automatic gain control (AGC) target was set to  $1 \times 10^6$  for full scans in the Orbitrap mass analyzer. ETD experiments used fluoranthene as the reagent anion and the target for fluoranthene anions was set to  $5 \times 10^5$ . Precursor ions for MS/MS were detected in the Orbitrap mass analyzer at a resolving power of 120,000 (at 400  $m/z$ ) with an isolation width of 3, and product ions were transferred to the FTMS operated with an AGC of  $5 \times 10^4$  over a  $m/z$  range of 200-2000. The reaction time with the fluoranthene radical anions into the LTQ was set from 50 to 100 ms. A minimum of 100 scans were averaged for each ETD fragmentation spectra. The Orbitrap FTMS was calibrated for the normal mass range keeping a mass accuracy in the 1-3 ppm level. Data were analyzed using the tool available at <http://www.cheminfo.org>. (Patiny and Borel, 2013)

## Results and Discussion

To determine the preferential binding sites of the RAPTA complexes on the BRCA1 ZF region, Electron Transfer Dissociation (ETD) fragmentation mass spectrometry was performed on a 50 amino acid synthetic peptide mimicking the ZF region of BRCA1 incubated with RAPTA-EA1 and RAPTA-C. ETD fragmentation is a well-established technique used to probe the localization of post-translational modifications (Zhurov *et al.*, 2013) (such as glycosylation and phosphorylation) and drug metalation sites on peptides (Murray *et al.*, 2014; Williams *et al.*, 2010) and proteins (Meier *et al.*, 2012). ETD causes fragmentation of the N-C $\alpha$  bonds of the peptide backbone generating C and Z type peptide fragments which can be used to identify modified amino acid residues on a peptide.

Initially full scans mass spectra of the 1:5 peptide:complex incubations were analyzed and showed adducts with a 1:1 stoichiometry for RAPTA-C, and up to 1:3 adducts with RAPTA-EA1 (Fig. A1, Fig. A2). Adducts corresponding to RAPTA species that are consistent with previous MS studies were observed (Nhukeaw *et al.*, 2014). Further ETD fragmentation was performed on suitable drug peptide adducts; for RAPTA-C the most intense adducts [Peptide +

RAPTA-C -2Cl] at +7 and +9 charge states and for RAPTA-EA1 [Peptide + RAPTA-EA1 -3Cl +2OH] at +8 and +9 charge states were selected for ETD fragmentation. Analysis of C-type ETD fragments (fragments from the amino terminus) of RAPTA-C peptide adduct showed an absence of any metallated fragments before residue Cys<sup>24</sup> (C<sup>24</sup>) and the first metallated fragment at residue Leu<sup>29</sup> (C<sup>29</sup>) indicating that binding takes place along a short peptide stretch, Lys<sup>25</sup>Phe<sup>26</sup>Cys<sup>27</sup>Met<sup>28</sup>Leu<sup>29</sup> (residues 45-49 on full length BRCA1). Analysis of Z fragments (fragments from the carboxyl terminus) showed no metallated fragments until Lys<sup>34</sup> (Z<sup>15</sup>), with a first metallated fragment at Lys<sup>35</sup> (Z<sup>16</sup>), narrowing down to a binding site on Lys<sup>35</sup> (residue 55 on full length BRCA1). For RAPTA-EA1, similar analysis of C-type fragments showed the absence of metallated fragments until Phe<sup>23</sup> (C<sup>23</sup>), and the first metallated fragment at Met<sup>28</sup> (C<sup>28</sup>), narrowing down the binding site to a short peptide stretch Cys<sup>24</sup>Lys<sup>25</sup>Phe<sup>26</sup>Cys<sup>27</sup>Met<sup>28</sup> (residues 44-48 on full length BRCA1). Z fragment analysis showed that similarly, RAPTA- EA1 binds at Lys<sup>35</sup>. (see Tables A1-3 for further information). The binding sites of the RAPTA complexes on the BRCA1 RING domain are different to those reported for cisplatin, where binding was found at the His<sup>117</sup> residue (Atipairin *et al.*, 2010).

The similar binding sites observed for both RAPTA complexes suggest that the different arene ligands have little impact on the localization of binding, although it does significantly affect stoichiometry and kinetics. As mentioned above, RAPTA binding leads to zinc ion displacement, which is not surprising based on the close proximity of the binding regions to site I of the RING domain of BRCA1 (Cys<sup>24</sup>, Cys<sup>27</sup> and Cys<sup>44</sup>, Cys<sup>47</sup>), which would also lead to conformational changes on this region and loss of protein function.



ILECPICLELIKEPVSTKCDHIFC\*K\*F\*C\*M\*LKLLNQKKGPSQCPLCKNDITK  
 ILECPICLELIKEPVSTKCDHIFCKFCMLKLLNQK\*KGPSQCPLCKNDITK

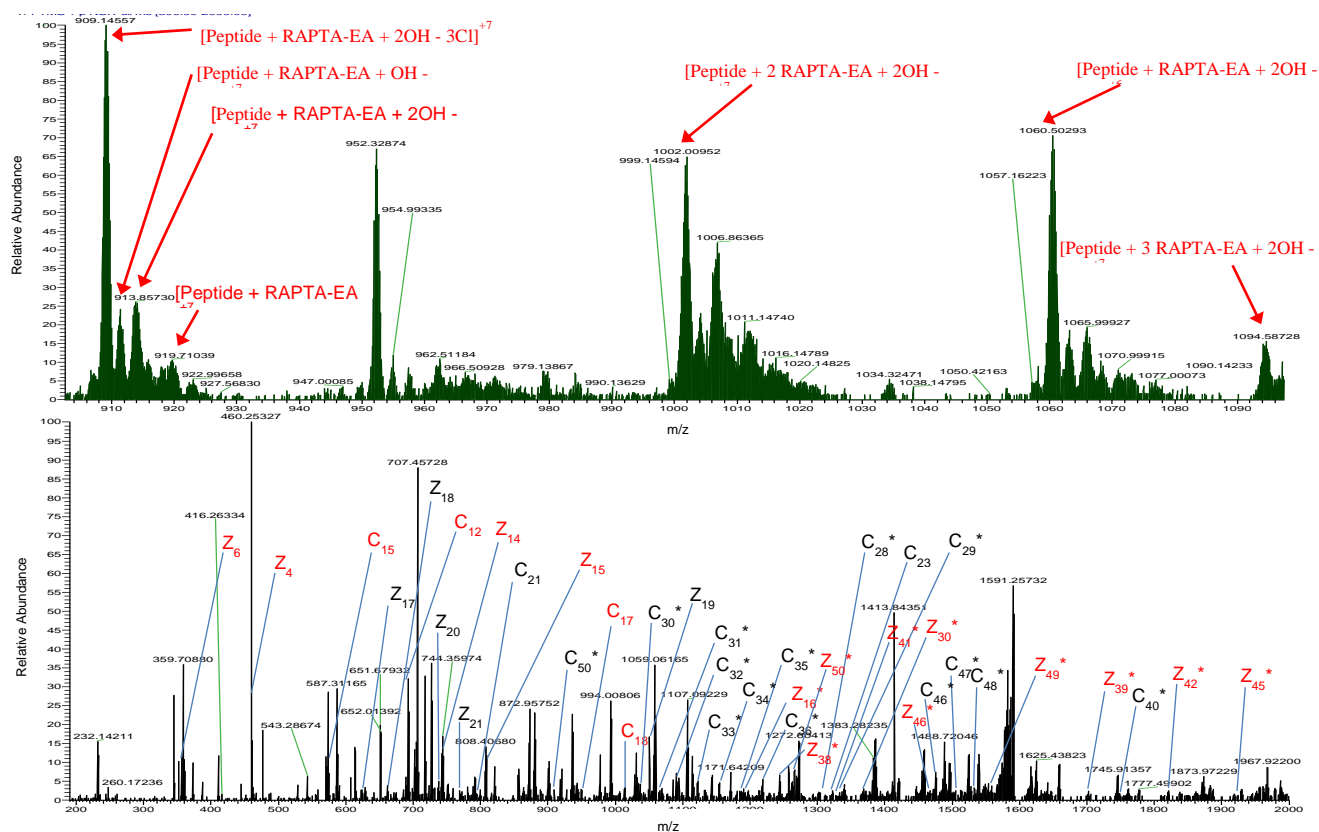


**Figure A1.** LTQ Orbitrap FTMS of RAPTA-EA after incubation with the BRCA1 peptide. Top: full scan 900-1100 m/z mass spectra of the 1:5 peptide:complex ratio showing the formation of up to 3 adduct peaks at different charge states (+6 and +7). The ion at m/z 951.82 (+6) corresponds to the native BRCA1 peptide. Bottom: ETD spectra of the [BRCA1peptide + RAPTA-EA -3Cl +2OH]<sup>9+</sup> adduct after a 100 ms interaction period with the fluoroanthene radical anions showing metallation at the peptide fragment Cys<sup>24</sup> Lys<sup>25</sup> Phe<sup>26</sup> Cys<sup>27</sup> Met<sup>28</sup> (corresponding fragments in black) and Lys<sup>35</sup>

(corresponding fragments in red). Fragments labelled with \* correspond to a metallated fragment. Residues in bold correspond to zinc binding residues on the peptide.

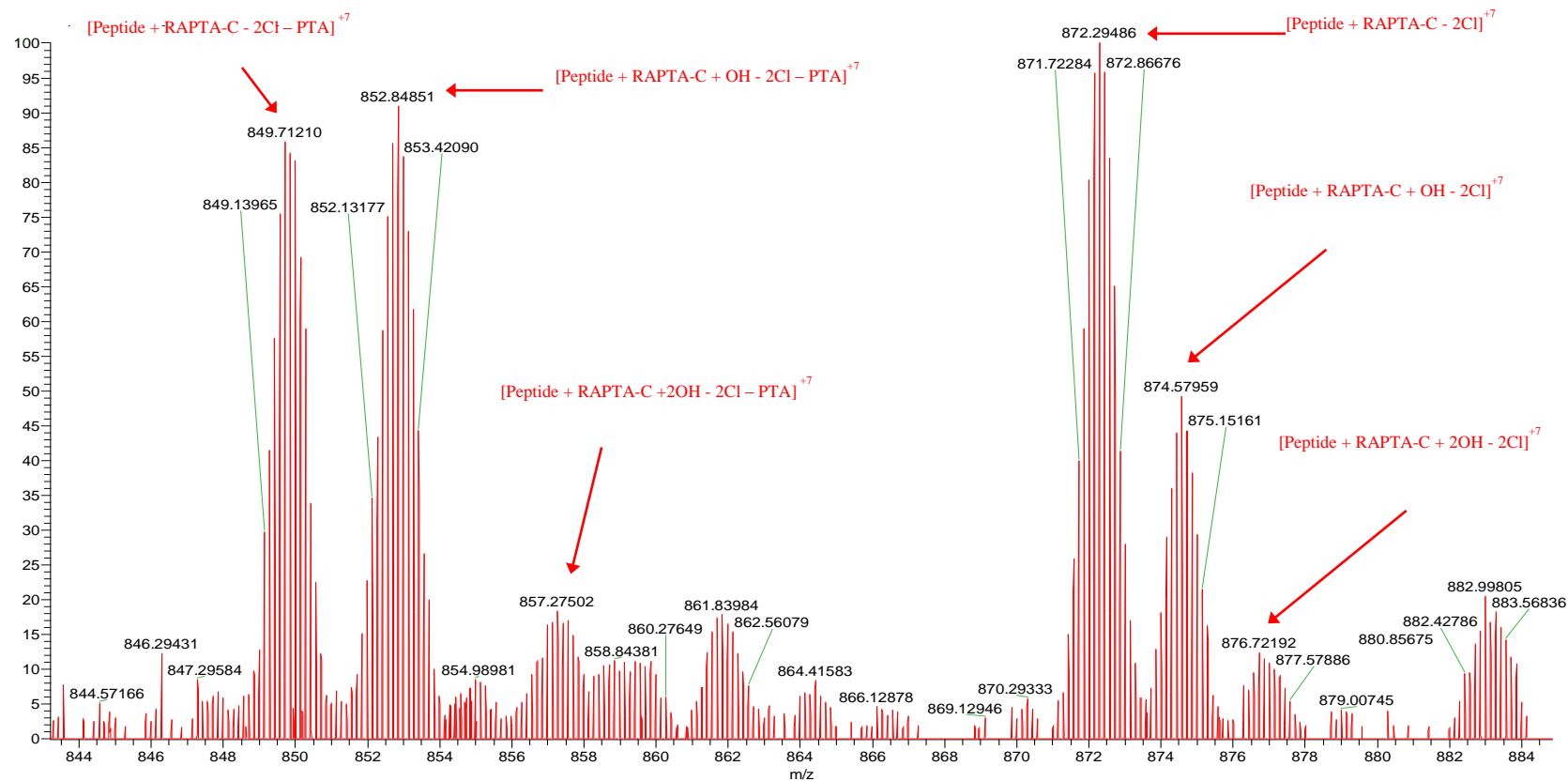


**Figure A2.** Full scan mass spectra (zoom in the mass range 840-884 *m/z*) acquired on the LTQ Orbitrap of RAPTA-C after incubation with the BRCA1 peptide (1:5 (peptide:drug) ratio), showing the formation of single adduct peaks with RAPTA-C.

**Table A1.** Most important C and Z fragments obtained by ETD fragmentation of the adduct [BRCA1 +7H + RAPTA-C -2Cl]<sup>9+</sup> (m/z 678.3411) detected when BRCA1

Ion Type (Fragment from ETD)	Theoretical m/z	Experimental m/z	Mass Error (ppm)
C <sub>11</sub> <sup>+</sup>	1257.69453	1257.69508	-0.44
C <sub>12</sub> <sup>+</sup>	1385.78949	1385.79004	-0.40
[C <sub>15</sub> +2H] <sup>3+</sup>	570.98927	570.98982	-0.96
[C <sub>17</sub> +H] <sup>2+</sup>	950.02012	950.02067	-0.58
[C <sub>22</sub> +H] <sup>2+</sup>	1248.15716	1248.157705	-0.44
[C <sub>29</sub> + RAPTA-C -2Cl ] <sup>3+</sup>	1253.59048	1253.591027	-0.44
[C <sub>30</sub> + RAPTA-C -2Cl ] <sup>3+</sup>	1296.2888	1296.289347	-0.42
[C <sub>32</sub> + RAPTA-C -2Cl ] <sup>3+</sup>	1371.67817	1371.678723	-0.40
[C <sub>33</sub> + RAPTA-C -2Cl ] <sup>4+</sup>	1057.26923	1057.269775	-0.52
[C <sub>34</sub> + RAPTA-C -2Cl ] <sup>3+</sup>	1452.37868	1452.379223	-0.37
[C <sub>35</sub> + RAPTA-C -2Cl ] <sup>3+</sup>	1495.077	1495.077547	-0.37
[C <sub>36</sub> + RAPTA-C -2Cl ] <sup>4+</sup>	1153.33135	1153.3319	-0.48
[C <sub>46</sub> + H + RAPTA-C -2Cl ] <sup>3+</sup>	1880.59723	1880.597783	-0.29
[C <sub>50</sub> + 3H + RAPTA-C -2Cl ] <sup>4+</sup>	1525.26511	1525.26566	-0.36
[Z <sub>6</sub> + H] <sup>2+</sup>	702.39066	702.3912	-0.77
[Z <sub>14</sub> + 2H] <sup>2+</sup>	744.35898	744.35953	-0.74
[Z <sub>15</sub> + 2H] <sup>2+</sup>	808.40646	808.40701	-0.68
[Z <sub>16</sub> + RAPTA-C -2Cl ] <sup>2+</sup>	1067.99151	1067.99206	-0.51
[Z <sub>17</sub> + RAPTA-C -2Cl ] <sup>2+</sup>	1132.0208	1132.02135	-0.49
[Z <sub>20</sub> + RAPTA-C -2Cl ] <sup>2+</sup>	1302.12633	1302.126875	-0.42
[Z <sub>34</sub> + RAPTA-C -2Cl ] <sup>4+</sup>	1077.77835	1077.7789	-0.51
[Z <sub>38</sub> + RAPTA-C -2Cl ] <sup>4+</sup>	1179.06361	1179.064155	-0.46
[Z <sub>50</sub> + 2H + RAPTA-C -2Cl ] <sup>5+</sup>	1217.00347	1217.004022	-0.45

peptide was incubated with RAPTA-C (1:5, protein:drug ratio)

**Table A2.** Most important C and Z fragments obtained by ETD fragmentation of the adduct [BRCA1 +5H + RAPTA-C -2Cl]<sup>7+</sup> (m/z 871.8649) after incubation of BRCA1 peptide with RAPTA-C (1:5, protein:drug ratio).

Ion Type (Fragment from ETD)	Theoretical m/z	Experimental m/z	Mass Error (ppm)
C <sub>12</sub> <sup>+</sup>	1385.78949	1385.79004	-0.40
[C <sub>15</sub> + H] <sup>2+</sup>	855.98027	855.98082	-0.64
[C <sub>24</sub> + H] <sup>2+</sup>	1373.69987	1373.700415	-0.40
[C <sub>29</sub> + RAPTA-C -2Cl] <sup>3+</sup>	1253.59048	1253.591027	-0.44
[C <sub>30</sub> + RAPTA-C -2Cl] <sup>3+</sup>	1296.2888	1296.289347	-0.42
[C <sub>32</sub> + RAPTA-C -2Cl] <sup>3+</sup>	1371.67817	1371.678723	-0.40
[C <sub>33</sub> + H + RAPTA-C -2Cl] <sup>4+</sup>	1057.52118	1057.52173	-0.52
[C <sub>34</sub> + RAPTA-C -2Cl] <sup>3+</sup>	1452.37868	1452.379223	-0.37
[C <sub>36</sub> + RAPTA-C -2Cl] <sup>3+</sup>	1537.77532	1537.775867	-0.36
[C <sub>39</sub> + H + RAPTA-C -2Cl] <sup>3+</sup>	1618.48001	1618.48056	-0.34
[C <sub>45</sub> + H + RAPTA-C -2Cl] <sup>3+</sup>	1842.58292	1842.583473	-0.30
[C <sub>48</sub> + H + RAPTA-C -2Cl] <sup>4+</sup>	1467.22358	1467.224133	-0.38
[Z <sub>6</sub> + H] <sup>+</sup>	702.39066	702.3912	-0.77
[Z <sub>14</sub> + H] <sup>2+</sup>	744.35898	744.35953	-0.74
[Z <sub>15</sub> + H] <sup>2+</sup>	808.40646	808.40701	-0.68
[Z <sub>16</sub> + RAPTA-C -2Cl] <sup>2+</sup>	1067.99151	1067.99206	-0.51
[Z <sub>17</sub> + RAPTA-C -2Cl] <sup>2+</sup>	1132.0208	1132.02135	-0.49
[Z <sub>18</sub> + RAPTA-C -2Cl] <sup>3+</sup>	792.69466	792.69521	-0.69
[Z <sub>20</sub> + RAPTA-C -2Cl] <sup>2+</sup>	1302.12633	1302.126875	-0.42
[Z <sub>26</sub> + H + RAPTA-C -2Cl] <sup>3+</sup>	1118.55067	1118.551217	-0.49
[Z <sub>30</sub> + H + RAPTA-C -2Cl] <sup>3+</sup>	1285.29086	1285.29141	-0.43
[Z <sub>38</sub> + 2H + RAPTA-C -2Cl] <sup>4+</sup>	1179.06361	1179.064155	-0.46
[Z <sub>45</sub> + H + RAPTA-C -2Cl] <sup>4+</sup>	1381.9324	1381.932948	-0.40
[Z <sub>49</sub> + RAPTA-C -2Cl] <sup>4+</sup>	1492.22759	1492.228143	-0.37
[Z <sub>50</sub> + 2H + RAPTA-C -2Cl] <sup>5+</sup>	1217.00347	1217.004022	-0.45

**Table A3.** Most important C and Z fragments obtained by ETD fragmentation of the adduct [BRCA1 +7H + RAPTA-EA1 +2OH -3Cl]<sup>8+</sup> (m/z 795.1339) after incubation of BRCA1 peptide with RAPTA-EA1 (1:5, protein:drug ratio).

Ion Type (Fragment from ETD)	Theoretical m/z	Experimental m/z	Mass Error (ppm)
C <sub>12</sub> <sup>+</sup>	1385.78949	1385.79004	-0.40
[C <sub>15</sub> + H] <sup>2+</sup>	855.98027	855.98082	-0.64
[C <sub>18</sub> + H] <sup>2+</sup>	1014.0676	1014.068155	-0.55
[C <sub>20</sub> + H] <sup>2+</sup>	1123.08567	1123.086215	-0.49
[C <sub>29</sub> + 3H + RAPTA-EA +2OH -3Cl] <sup>3+</sup>	1339.93206	1339.93261	-0.41
[C <sub>31</sub> + 2H + RAPTA-EA +2OH -3Cl] <sup>3+</sup>	1419.98913	1419.989677	-0.39
[C <sub>32</sub> + H + RAPTA-EA +2OH -3Cl] <sup>3+</sup>	1457.34787	1457.348423	-0.38
[C <sub>34</sub> + 2H + RAPTA-EA +2OH -3Cl] <sup>4+</sup>	1153.7881	1153.78865	-0.48
[C <sub>36</sub> + H + RAPTA-EA +2OH -3Cl] <sup>4+</sup>	1217.58363	1217.584175	-0.45
[C <sub>39</sub> + H + RAPTA-EA +2OH -3Cl] <sup>3+</sup>	1703.81377	1703.81432	-0.32
[C <sub>46</sub> + 2H + RAPTA-EA +2OH -3Cl] <sup>4+</sup>	1474.70006	1474.700613	-0.37
[C <sub>47</sub> + H + RAPTA-EA +2OH -3Cl] <sup>4+</sup>	1503.20484	1503.20539	-0.37
[C <sub>50</sub> + 5H + RAPTA-EA +2OH -3Cl] <sup>5+</sup>	1271.81537	1271.815914	-0.43
Z <sub>14</sub> <sup>2+</sup>	743.35116	743.351705	-0.73
Z <sub>15</sub> <sup>2+</sup>	807.39864	807.399185	-0.68
[Z <sub>16</sub> + H + RAPTA-EA +2OH -3Cl] <sup>2+</sup>	1196.49606	1196.49661	-0.46
[Z <sub>16</sub> + 2H + RAPTA-EA +2OH -3Cl] <sup>3+</sup>	797.9998	798.00035	-0.69
[Z <sub>18</sub> + RAPTA-EA +2OH -3Cl] <sup>2+</sup>	1317.0429	1317.04345	-0.42
[Z <sub>20</sub> + 2H + RAPTA-EA +2OH -3Cl] <sup>3+</sup>	954.08968	954.0902267	-0.57
[Z <sub>38</sub> + 3H + RAPTA-EA +2OH -3Cl] <sup>3+</sup>	1657.75469	1657.75524	-0.33
[Z <sub>38</sub> + 3H + RAPTA-EA +2OH -3Cl] <sup>4+</sup>	1243.31588	1243.31643	-0.44
[Z <sub>41</sub> + 4H + RAPTA-EA +2OH -3Cl] <sup>4+</sup>	1332.13361	1332.13416	-0.41
[Z <sub>45</sub> + 2H + RAPTA-EA +2OH -3Cl] <sup>3+</sup>	1928.24642	1928.246963	-0.28
[Z <sub>5</sub> + H] <sup>+</sup>	574.29569	574.29624	-0.96
[Z <sub>50</sub> + 3H + RAPTA-EA +2OH -3Cl] <sup>4+</sup>	1585.50675	1585.507303	-0.35

## Conclusions

In summary, Electron Transfer Dissociation (ETD) fragmentation mass spectrometry revealed the preferential binding sites of the RAPTA complexes on the BRCA1 zinc finger RING domain at a similar short peptide stretch, Cys<sup>24</sup>Lys<sup>25</sup>Phe<sup>26</sup>Cys<sup>27</sup>Met<sup>28</sup>Leu<sup>29</sup> and Lys<sup>35</sup> (residues 44-49 and 55 on full length BRCA1).

## References

- Atipairin A, Canyuk B, Ratanaphan A. Cisplatin affects the conformation of apo form, not holo form, of BRCA1 RING finger domain and confers thermal stability. *Chem Biodivers*. 2010; 7:1949-67.
- Nhukeaw T, Temboot P, Hansongnern K, Ratanaphan A. Cellular responses of BRCA1-defective and triple-negative breast cancer cells and in vitro BRCA1 interactions induced by metallo-intercalator ruthenium(II) complexes containing chloro-substituted phenylazopyridine, *BMC Cancer*. 2014; 7: 73.
- Meier SM, Tsybin YO, Dyson PJ, Keppler BK, Hartinger CG. Fragmentation methods on the balance: unambiguous top-down mass spectrometric characterization of oxaliplatin-ubiquitin binding sites. *Anal Bioanal Chem*. 2012; 402: 2655-62.
- Murray BS, Menin L, Scopelliti R, Dyson PJ. Conformational control of anticancer activity: the application of arene-linked dinuclear ruthenium(II) organometallics. *Chem Sci*. 2014; 5: 2536-2545.
- Patiny L, Borel A. ChemCalc: A Building Block for Tomorrow's Chemical Infrastructure. *J Chem Inf Model*. 2013, 53: 1223–1228.
- Williams JP, Brown JM, Campuzano I, Sadler PJ. Identifying drug metallation sites on peptides using electron transfer dissociation (ETD), collision induced dissociation (CID) and ion mobility-mass spectrometry (IM-MS). *Chem Commun Camb Engl*. 2010; 46: 5458–5460.
- Zhurov KO, Fornelli L, Wodrich MD, Laskay ÚA, Tsybin YO. Principles of electron capture and transfer dissociation mass spectrometry applied to peptide and protein structure analysis. *Chem Soc Rev*. 2013; 42: 5014-30.

## VITAE

**Name** Mr. Pornvichai Temboot

**Student ID** 5810730005

### **Educational Attainment**

Degree	Name of Institution	Year of Graduation
Bachelor of Science (Second-Class Honors)	Faculty of Science, Thaksin University	2007

### **Scholarship Awards during Enrolment**

Human Resource Development in Science Project (Science Achievement scholarship of Thailand, SAST). 2004-2007, Thaksin University.

The Royal Golden Jubilee Ph.D. Program, the Thailand research fund, 2007 to present, Prince of Songkla University.

### **Academics Award during Enrollment**

The best poster presentation award, entitled: The effect of RAPTA-EA1 on secondary structure of familial D67E and D67Y mutations in the BRCA1 RING protein. The 3<sup>rd</sup> Current Drug Development International Conference (CDD 2014), May 1-3, 2014. Pavilion Queen's Bay Krabi, Ao Nang Beach, Thailand.

The outstanding oral presentation award, entitled: Human breast cancer susceptibility gene 1 (BRCA1) damaged by the ruthenium(II)-arene pta (RAPTA) complexes. The RGJ-Ph.D. Congress X. April 3-5 2009, Jomtein Palm Beach Resort, Pattaya, Chonburi, Thailand.

### **List of Publications**

**Temboot P**, Lee RFS, Menin L, Patiny L, Dyson PJ, Ratanaphan A. Biochemical and biophysical characterization of ruthenation of BRCA1 RING protein by RAPTA complexes and its E3 ubiquitin ligase activity. *Biochem Biophys Res Commun* 2017; 488(2): 355-361.

Nhukeaw T, **Temboot P**, Hansongnern K, Ratanaphan A. Cellular responses of BRCA1-defective and triple-negative breast cancer cells and in vitro BRCA1 interactions induced by metallo-intercalator ruthenium(II)

complexes containing chloro-substituted phenylazopyridine. *BMC Cancer*. 2014; 14: 73.

Ratanaphan A, Nhukeaw T, **Temboot P**, Hansongnern K. DNA-binding properties of ruthenium(II) complexes with the bidentate ligand 5-chloro-2-(phenylazo)pyridine. *Transit Metal Chem*. 2012; 37: 207-214.

Ratanaphan A, **Temboot P**, Dyson P. J. In vitro ruthenation of human breast cancer suppressor gene 1 (*BRCA1*) by the antimetastasis compound RAPTA-C and its analogue CarboRAPTA-C. *Chem Biodivers*. 2010; 7: 1290-1302.

**Temboot P**, Hongthong K, Nhukeaw T, Casini A, Ratanaphan A. Inhibiting effect of gold(III) polypyridyl complexes on BRCA1 expression in BRCA1 associated and sporadic breast cancer cells and in vitro conformational and functional analysis of BRCA1 RING domain protein. *Exp Ther Med*. 2017. Submitted.

**Temboot P**, Hongthong K, Nhukeaw T, Casini A, Ratanaphan A. Inhibiting effect of gold(III) polypyridyl complexes on BRCA1 expression in BRCA1 associated and sporadic breast cancer cells and in vitro conformational and functional analysis of BRCA1 RING domain protein. *Exp Ther Med*. 2017. Submitted.

**Temboot P**, Dyson PJ, Ratanaphan A. In vitro enhanced sensitivity to RAPTA complexes in D67Y BRCA1 RING domain protein. Submitted.

Hongthong K, **Temboot P**, Nhukeaw T, Dyson PJ, Ratanaphan A. RAPTA-EA1 induces formation of nuclear BRCA1 foci, p53-independent p21/RAD51 and CK8 expression in triple-negative BRCA1-associated breast cancer cells. *Biochem Biophys Res Commun*. 2017. Submitted.

### List of Proceedings

**Temboot P**, Dyson PJ, Ratanaphan A. Synergistic effects of combined olaparib and RAPTA-EA1 in BRCA1-associated breast cancer cell lines. The 4<sup>th</sup> Current Drug Development International Conference. June 1-3 2016. Phuket Graceland, Patong Beach, Phuket, Thailand.

**Temboot P**, Dyson PJ, Ratanaphan A. BRCA1-mediated E3 ubiquitin ligase activity is inactivated by RAPTA-EA1 alone or in combination with olaparib. The 4<sup>th</sup> International Biochemistry and Molecular Biology Conference. May 26-27 2016. BP Samila Beach Hotel, Songkhla, Thailand.

**Temboot P**, Dyson PJ, Ratanaphan A. The effect of RAPTA-EA1 on secondary structure of familial D67E and D67Y mutations in the BRCA1 RING protein. The 3<sup>rd</sup> Current Drug Development International Conference. May 1-3 2014. Pavilion Queen's Bay, Ao Nang Beach, Krabi, Thailand.



- Temboot P**, Dyson PJ, Ratanaphan A. Real-time monitoring of growth profile and cellular recovery of breast cancer cell towards ruthenium(II)-arene (pta) complexes treatments. The 4<sup>th</sup> International Biochemistry and Molecular Biology Conference. April 2-3 2014. Rama Gardens Hotel & Resort, Bangkok, Thailand.
- Temboot P**, Dyson PJ, Ratanaphan A. Effect of ruthenium(II)-arene (PTA) on secondary structure of the BRCA1 RING protein. The 7<sup>th</sup> Princess Chulabhorn International Sciences Congress. November 29- December 3 2012, Shangri-Lar hotel, Bangkok, Thailand.
- Temboot P**, Dyson PJ, Ratanaphan A. Human breast cancer susceptibility gene 1 (*BRCA1*) damaged by the ruthenium(II)-arene pta (RAPTA) complexes. The RGJ-Ph.D. Congress X. April 3-5 2009, Jomtein Palm Beach Resort, Pattaya, Chonburi, Thailand.